Calmodulin As a Regulator of Circadian Clock Function and Photoperiodic Flowering in *Arabidopsis thaliana*.

Andrew James Murphy

Submitted by Andrew James Murphy, to the University of Exeter as a thesis for the degree of Doctor of Philosophy Biological Sciences, December, 2009.

I certify that all material in this thesis which is not my own work has been identified and that no material has previously been submitted and approved for the award of a degree by this or any other University.

(Signature).....

To my wonderful parents, no words are sufficient to describe how grateful I am for your unwavering belief and support.

ACKNOWLEDGEMENTS

From the first days of my study to the binding of this thesis, I am immensely grateful for the continued guidance and direction of my supervisor, Dr John Love.

I would also very much like to thank all those who have offered advice, support and assistance throughout the course of my work. In particular, I would like to thank George Littlejohn for being such a wonderful sounding board for ideas and Karen Moore for setting such a good example in how to undertake experimentalism.

TABLE OF CONTENTS

ABBREVIATIONS

$\Delta \angle$	Change in angle as measured in degrees
35S	The constitutive strong promoter of the Cauliflower mosaic virus
35S::aequorin$_{(cyt)}$	*Arabidopsis thaliana* ecotype Columbia 0 expressing cytosolic *Victoria aquoria* aequorin under the control of the 35S promoter
7-AAD	7-Aminoactinomycin D
apoCaM	Calmodulin which is not bound to Ca^{2+}
atHAP5	*ARABIDOPSIS HAEM ACTIVATION PROTEIN 5*
ATP	Adenosine trisphosphate
A. thaliana	*Arabidopsis thaliana*
Ca^{2+}-CaM	Calcium bound calmodulin
Ca^{2+}_{chlo}	Chloroplastic free calcium
Ca^{2+}_{cyt}	Cytosolic free calcium
cADPR	Cyclic adenosine diphosphate ribose
CaM	Calmodulin
CAM1	*CALMODULIN 1*
CAB2	*CHLOROPHYLL A/B BINDING PROTEIN 2*
CaMBP	Calmodulin-binding protein
CaMKIV	Ca^{2+}-CaM-dependent protein kinase IV
CCA1	*CIRCADIAN CLOCK ASSOCIATED 1*
CICR	Calcium induced calcium release
CMZ	Calmidazolium
CO	*CONSTANS*
Col 0	*Arabidopsis thaliana* ecotype Columbia 0
COP1	*CONSTITUTIVE PHOTOMORPHOGENIC 1*
CRY1 / 2 / 3	*CRYPTOCHROME 1 / 2 / 3*
DACC	Depolarisation-activated calcium channel
EDTA	Ethylene diamine tetra-acetic acid
EGTA	Ethylene glycol tetra-acetic acid
ELF3	*EARLY FLOWERING 3*
EtBr	Ethidium bromide

FRET	Förster resonance energy transfer
FRP	The ‘free running period’ of a circadian oscillator
FRQ	*FREQUENCY*
FT	*FLOWERING LOCUS T*
GAPC	*GLYCERALDEHYDE-3-PHOSPHATE DEHYDROGENASE C SUBUNIT*
GI	*GIGANTEA*
GVG	A chimaeric transcription factor.
HACC	Hyperpolarisation-activated calcium channel
HCA	Hydrophobic cluster analysis
HEPES	4-(2-hydroxyethyl)-1-piperazineethanesulphonic acid
HY5	*ELONGATED HYPOCOTYL 5*
K_D	The dissociation equilibrium constant
Ler	Arabidopsis thaliana ecotype Lansberg erecta
LDS	Lithium dodecyl sulphate
MOPS	3-(N-morpholino)propansulphonic acid
MS media	Murashage and Skoog media
NaAc	Sodium acetate
NAADP	Nicotinic acid adenine dinucleotide phosphate
Nos 0	Arabidopsis thaliana ecotype Nossen 0
NTC	No-Template Control
PAGE	Polyacrylamide gel electrophoresis
PBS	Phosphate buffered saline
PBST	Phosphate buffered saline -Tween 20
PDF	Pigment Dispersing Factor
PEB buffer	Protein extraction buffer
Pfr	The active ‘far red’ form of phytochrome which absorbs most strongly at 730 nm
PHYA / B / C / D / E	*PHYTOCHROME A / B / C/ D / E*
pI	Isoelectric point
PPE buffer	Plant protein elution buffer
Pr	The inactive ‘red’ form of phytochrome which absorbs most strongly at 660 nm

PRC	Phase response curve
PRR	*PSEUDO-RESPONSE REGULATOR*
qRT-PCR	Quantitative Real Time-PCR
RLN	Rosette leaf number at flowering
SAP	Shrimp Alkaline Phosphatase
SCN	Suprachiasmatic nucleus
smGFP	Soluble-modified green fluorescent protein
smGN	*soluble-modified GFP/calspermin*
SOC1	*SUPPRESSOR OF OVEREXPRESSION OF CONSTANS 1*
SPA1	*SUPPRESSOR OF PHYA-105*
SPY	*SPINDLY*
TAE	Tris/acetate/EDTA buffer
TOC1	*TIMING OF CAB EXPRESSION 1*
TOE1	*TARGET OF EAT 1*
VICC	Voltage-independent calcium/cation channel
VLFR	Very low fluence responses
W5	N-(6-Aminohexyl)-1-naphthalenesulphonamide
W7	N-(6-aminohexyl)-5-chloro-1-naphthalenesulphonamide
WC-1	*WHITE COLLAR-1*
Ws	*Arabidopsis thaliana* ecotype Wassilewskija
'X'	A hypothetical component of the *Arabidopsis thaliana* circadian clock
'Y'	A hypothetical component of the Arabidopsis thaliana circadian clock putatively identified as GIGANTEA
ZTL	*ZEITLUPE*

ABSTRACT

Discrete changes in the amplitude, frequency, and cellular localisation of calcium ion (Ca^{2+}) transients encode information about numerous stimuli and function to mediate stimulus-specific responses. Cytoplasmic Ca^{2+} (Ca^{2+}_{cyt}) undergoes circadian oscillations in concentration that appear to be under the control of the same endogenous oscillator that regulates expression of genes in the photoperiodic-flowering pathway. It is currently not known whether these circadian [Ca^{2+}_{cyt}] oscillations are biochemical artefacts or are decoded and function to transduce clock dependent responses. Calmodulin (CaM) is a primary node in Ca^{2+} signalling in plants and as such is a promising target for investigating the role of Ca^{2+} in clock-controlled processes. In this study, *Arabidopsis thaliana* were treated with experimentally validated concentrations of pharmacological CaM inhibitors. Under inductive photoperiods (16 h light : 8 h dark), CaM inhibition was found to increase developmental flowering time, whilst under non-inductive photoperiods no such changes were evident. Inhibition of CaM led to changes in expression of the key clock gene *TIMING OF CAB EXPRESSION 1* and flowering time genes, *CONSTANS* and *FLOWERING LOCUS T* and removed repression of flowering in darkness. These observations are consistent with CaM modulating the activity of the putative clock component GIGANTEA and the proteasomal targeting protein SUPPRESSOR OF PHYA-105.

Due to the unwanted side effects often generated by chemical CaM inhibitors, a peptide inhibitor of CaM comprising a green fluorescent protein / calspermin fusion and labelled smGN was developed. Surface plasmon resonance analysis and affinity chromatography showed smGN to have extremely high selectivity for, and affinity to, CaM and to function as a powerful inhibitor of CaM *in vitro*.

Further work on the methodology used to deploy smGN as a recombinant alternative to chemical CaM inhibitors *in planta* is also described.

CHAPTER 1: INTRODUCTION

1.1 Circadian Clocks

1.1.1 Early investigations into biological rhythms.

Daily biological rhythms are an almost ubiquitous feature of life on Earth and are even observed in organisms inhabiting apparently constant environments such as caves or the deep ocean (Sharma & Chandrashekaran, 2005). Biological clocks were first empirically investigated in the early XVIIIth century by the astronomer de Marian. De Marian's observations centred on *Mimosa pudica* (Sensitive Plant), which showed daily cycles of leaf movement; in the morning *M. pudica* leaves unfolded and tracked the movement of the sun during the day before folding shut again, at dusk. Crucially, de Marian discovered that the movements of the *M. pudica* leaf continued when the plants were transferred to constant darkness, thereby displaying an endogenous rhythm (Sharma & Chandrashekaran, 2005).

1.1.2 The characteristics of circadian rhythms.

Franz Halberg distinguished self-sustaining endogenous rhythms from diurnal rhythms that were not maintained without continual external input. Such endogenous rhythms were termed 'circadian', from the Latin *circa* meaning "approximately" and *dias* meaning "day" (Halberg, 1959).

Circadian rhythms have three principle features. The first of these features is a period of oscillation which continues to behave rhythmically in the absence of external stimuli and displays a free running period (FRP) approximating 24 hours.

Although FRPs cluster around 24 hours, variations in FRP exist between, and within species (Edwards *et al.*, 2005; Sharma & Chandrashekaran, 2005). Recent studies have shown that the stability of the continuing phase-relationship, defined as *"*the time interval between a well defined phase of a biological rhythm and a phase of the light-dark cycle when the biological rhythm is synchronised by the periodic time-cue*"*, is dependent upon the length of the FRP. Under a 24 hour photoperiod, clocks with FRPs, close to but not equal to, 24-hours display greater stability than those with FRPs of exactly 24 hours (Sharma & Chandrashekaran, 2005).

The second principle feature displayed by circadian clocks is the ability for endogenous rhythms to entrain to environmental periodicities (also known as zeitgebers), including temperature, nutrient availability, humidity, predation and social cycles (Johnson, 1992; Stokkan *et al.*, 2001). Entrainment is observed when, upon the removal of the driving rhythm, the driven rhythm maintains broadly the same oscillatory features as would be expected were the driving rhythm still present. Whilst the endogenous clock adjusts its phase and period to entrain to a driving rhythm, the clock and the driving rhythm do not, however, necessarily attain synchrony. Although notionally similar, it is important to distinguish between "synchronisation" and "entrainment". Synchronisation implies that a driven rhythm matches that of the driving rhythm. Synchronisation does not however, imply permanent entrainment.

Perhaps the most powerful, and certainly the most studied zeitgeber, is the daily oscillation between light and dark which acts as the dominant entraining force in species as diverse as cyanobacteria and mammals (Sharma & Chandrashekaran, 2005). Two models of circadian entrainment have been proposed. The "discrete entrainment model" postulates that only discrete, repetitive time-cues such as dawn and dusk are responsible for clock adjustment (Daan, 1977; Pittendrigh, 1981). Earlier discrete entrainment models required a fixed FRP, however more recent versions allow a degree of FRP modulation (Johnson *et al.*, 2003; Johnson *et al.*, 2004).

Conversely, in the "continuous entrainment model" (Daan, 2000; Johnson *et al.*, 2003), entraining stimuli continuously modulate the clock through changes in the angular velocity of a clock's FRP (*i.e.* its acceleration or deceleration), in order to adapt its period to that of the environment. Sensitivity to entrainment, however may vary throughout the day (a phase-dependent entrainment response) (Pittendrigh & Daan, 1976a). The continuous entrainment model is supported by an observation known as "Aschoff's Rule" whereby diurnal organisms exhibit a faster clock (shorter FRP), in higher rather than lower light intensities. In nocturnal organisms, such as *Mus booduga* (Field Mouse), this situation is reversed (Elvin, 2005).

Phase-dependent entrainment responses are often described by means of a 'phase response curve' (PRC) (figure 1.1). A PRC is defined as *"*a plot of phase shifts of a circadian rhythm as a function of the circadian phase where a stimulus or zeitgeber is applied*"* (Johnson *et al.*, 2003). When organisms are transferred from an entraining light / dark photoperiod to constant darkness, a pulse of light administered during the subjective day has minimal influence on the phase of the rhythm on following days (Johnson, 1999). This period of minimal effect is known as 'the dead zone' and is characteristic of PRCs. However, when a light pulse is administered during the subjective night, a phase shift in the circadian rhythm is induced. Applying a light stimulus during early subjective night generally results in a delay in the phase of the rhythm, mimicking the effects of a later dusk. When light is given during the latter part of the subjective night, the phase of the circadian rhythm is normally advanced as if the organism were tracking an earlier dawn (Johnson, 1990; Johnson *et al.*, 2003). It has been proposed that such phase-dependent entrainment responses serve to buffer minor variations inherent in the FRP (Pittendrigh & Daan, 1976a).

Organisms are normally considered to either have 'type 0' or 'type 1' PRCs (figure 1.1). When plotted, type-0 PRCs are characterised by a 'breakpoint' at the interface between the region where a stimulus induces a delay and that where the stimulus propagates an advance in the clock. Type-1 PRCs exhibit smaller maximum shifts than type-0 curves (less than six hours) and have a smooth, unbroken transition between delays and advancements of the clock. However it is often the strength of a stimulus which is the deciding factor regarding which form of PRC is elicited. A jump in intensity of light or temperature can therefore often convert a type-1 PRC to a type-0 PRC (Johnson, 1999; Johnson *et al.*, 2003; Peterson & Saunders, 1980).

Observations of differential phase-resetting have tended to support the discrete 'evening / morning' (dusk / dawn), model of entrainment (Daan *et al.*, 2001; Johnson *et al.*, 2003; Pittendrigh & Daan, 1976a, 1976b). However, unlike in natural environments where changes in light levels at dusk and dawn occur gradually, experiments have generally utilised a sudden 'lights-on / lights-off' strategy at dawn and dusk. Further investigation has shown that under conditions mimicking natural dawn / dusk transitions, organisms including

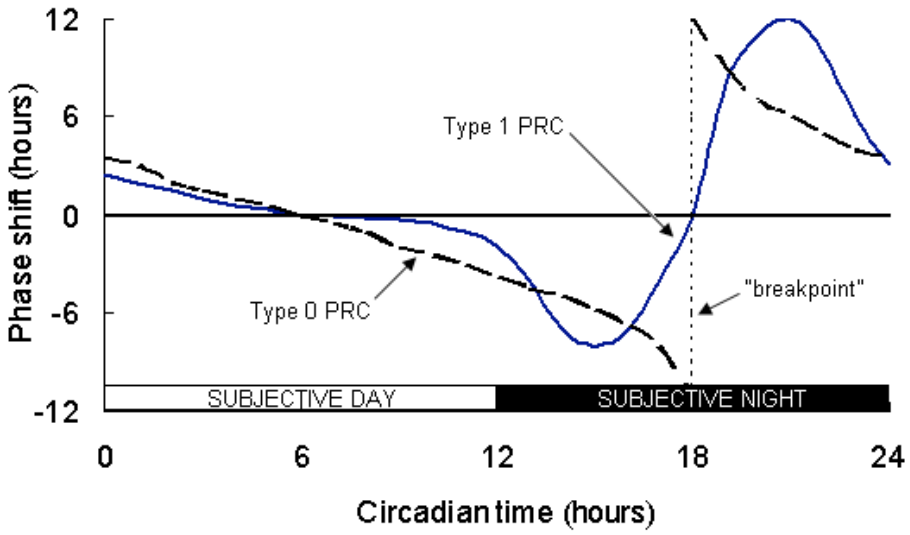

Figure 1.1: Characteristic phase response curves (adapted from Devlin, 2002 and Johnson *et al*., 2003).

Phase response curves (PRCs) are plots of the phase shifts generated in circadian rhythms when a stimulus is applied.
Following the transfer of an organism from a light / dark photoperiod to constant darkness, administration of a light stimulus during the subjective day has minimal effect on the phase of the rhythm on subsequent days. Application of a similar stimulus during early subjective night delays the phase of the rhythm, mimicking a later dusk. When the stimulus is applied during the latter part of subjective night, the phase of the rhythm is normally advanced mimicking an earlier dawn (Johnson, 1990; Johnson 2003).
Organisms normally display either 'type-0' or 'type-1' PRCs. Type-0 PRCs (shown as black dashed line), are characterised by a 'breakpoint' (vertical dotted line), between the region where a stimulus induces a delay and that where the stimulus stimulates a phase advance. In contrast, type-1 PRCs (shown as blue continuous line), display an unbroken transition between phase delays and advancements.

Mesocricetus auratus (Syrian Hamster) and *Drosophila melanogaster* (Fruit Fly) can entrain to a much wider range of day-lengths than when day / night transitions are abrupt (Boulos *et al.*, 1996, 2002). These experiments point to an important role for continuous entrainment in natural environments and are supported by the observation that even under conditions of constant light it is possible to entrain a range of organisms to a simple sine-wave of light intensity (Swade, 1969). It appears likely that, in the future, our understanding of entrainment will therefore move beyond the simple categories of “discrete” and “continuous”.

The third principle feature of circadian oscillators is the ability to maintain a robust FRP over a physiological range of temperatures (‘temperature compensation’) and is required for maintenance of the phase relationship between an organism and its environment (Pittendrigh, 1954).

Despite circadian oscillators being temperature compensated, it is not implied that individual components within the oscillator remain unaffected by temperature shifts, rather that, as a closed system, the oscillator is capable of self-regulation.

In addition to the three principle features of circadian clocks, a number of secondary features have also been described (Roenneberg & Merrow, 2005).

- FRPs show little variance across an extended number of cycles.
- Clear variations exist between species in the range of FRPs to which an organism may entrain.
- Circadian rhythms are entrainable by restricted classes of environmental periodicities.
- In clocks entrained by light, FRPs are fluence-dependent.
- Transients are always observed, prior to achievement of a new steady-state.
- Circadian rhythms show great robustness to chemical perturbation.

1.1.3 The architecture of circadian clocks in model systems.

Circadian clocks are key feature of a diverse range of organisms including plants, animals, fungi, and cyanobacteria and have arisen multiple times, most probably as a "phylogenetic improvement" of existing systems which were driven solely by external stimuli (Roenneberg & Merrow, 2002). Two hypotheses have been proposed to explain the selective advantage of circadian systems. The "internal synchronisation hypothesis" postulates that endogenous biological clocks enable synchrony between physiological and metabolic processes in an organism, having become intrinsically intertwined with other traits involved in reproductive fitness (Woelfle *et al.*, 2004). The "external synchronisation hypothesis" proposes a more direct link between the environment and the circadian clock. This hypothesis states that circadian oscillations have arisen and been selected for as a means of enabling organisms to better co-ordinate their physiology and biochemistry with daily changes in the external environment (Sharma, 2003). These hypotheses are complementary, with both the temporal segregation of incompatible metabolic processes and the ability to synchronise light-sensitive metabolic processes to hours of darkness being distinctly advantageous.

All endogenous clocks can essentially be described by means of a "three division framework" comprising entraining-inputs, a central pacemaker and discrete clock outputs (Kuhlman *et al.*, 2007). Whilst this basic architecture is common throughout living organisms, phylogenetic analyses of key clock genes show that that circadian clocks have evolved independently in each biological kingdom (Berger, 2004; Brunner & Merrow, 2008). The biological clocks of certain species have been intensely studied and have become the model for each group. These species include *Arabidopsis thaliana* for plants, *Neurospora crassa* for fungi, *Drosophila melanogaster* for invertebrates and *Cricetulus griseus* (hamster) for vertebrates.

The major functional distinction between different circadian systems is the location of the circadian oscillator. Due to the decentralised organisation of the body plan in plants and fungi, each cell contains its own individual circadian oscillator and can be independently entrained to different circadian periods than its neighbours (Thain, 2000). The molecular architecture of the core oscillator in

the model plant *Arabidopsis thaliana*, which is the focus of this thesis, is discussed in depth in section 1.2.

The relative ease of culture and non-pathogenic nature of *N. crassa* has led to it becoming a favoured organism for the study of circadian phenomena in fungi.

The most overt output of the *N. crassa* clock is mycelial development and conidiation which occur with a wild-type FRP of approximately 21.5 hours (Correa & Bell-Pederson, 2002). Light input in to the clock is mediated by the PAS-domain containing transcription factor WHITE COLLAR-1 (WC-1) which, when bound to flavin adenine dinucleotide, acts as a blue-light responsive photoreceptor (Mackey, 2007). As well as being responsible for light input to the clock, WC-1 acts as a component of the core circadian oscillator. The 'light-responsive WC complex', composed of WC-1 and WHITE COLLAR-2 activates transcription of *FREQUENCY* (*FRQ*), which also forms a central component of the circadian oscillator. FRQ forms kinase-regulated homodimers which translocate to the nucleus and in-turn target the WC complex for degradation via phosphorylation (Mackey, 2007). Intriguingly, even though the oscillator is composed of only a single phosphorylation-regulated loop, it remains robustly temperature compensated. Circadian oscillations in superoxide dismutase expression lead to rhythmic abundance of reactive oxygen species, which in turn serve to regulate the activity of numerous morphogenic enzymes and modulate the timing of conidiation (Yoshida & Hasunuma, 2003).

Higher animals possess a central nervous system capable of rapid transduction and integration of environmental information, and circadian control is projected from a centralised primary pacemaker comprising distinct groupings of neural cells.

Drosophila melanogaster has a long history as a model organism and has contributed greatly to the study of circadian phenomena in higher animals. Circadian rhythmicity in *D. melanogaster* is commonly assessed by measurement of activity patterns, with wild-type flies showing show an FRP of approximately 24.6 h and a bimodal rhythm of activity consisting of a short peak around dawn and a longer peak either side of dusk (Rieger *et al*., 2007).

As well as a primary neural oscillator responsible for such patterns of activity, *D. melanogaster* possesses numerous brain-independent, autonomous regional oscillators including those located in the wing margin, prothorasic gland and

proboscis. However, of all the peripheral oscillators, only the antennal clock has been shown to generate functional output (Andretic & Hirsch, 2002). For brevity, discussion of the *D. melanogaster* circadian system will therefore centre on the primary neural oscillator. Circadian photoperceception to this system is mediated via the compound eye. Each eye consists of roughly 800 ommatidia which contain specialised photoreceptor cells expressing numerous photosensitive rhodopsins (Helfrich-Forster, 2002). Projections from the optic nerve enable photoperiod specific information to entrain approximately 150 specialised clock neurons in a process dependent upon transmembrane Ca^{2+} flux (Block, 2006).

Two major groups of clock-neurons have been identified in *D. melanogaster*; the dorsal lateral neurons which lie in the superior brain, and the ventral lateral neurons which lie in the anterior brain and are necessary and sufficient for generation of rhythmic behaviour (Helfrich-Forster et al., 2007). Of the approximately 75 ventral lateral neurons, a subgroup of five secrete the neuropeptide 'pigment dispersing factor' (PDF). PDF acts to co-ordinate the synchronisation of all the clock neurons and enhances the robustness of the *D. melanogaster* clock against perturbation. Indeed, only a single PDF secreting neuron is sufficient to ensure robust circadian rhythms (Helfrich-Forster *et al*., 2007). Both the ventral and lateral dorsal neurons form projections to the accessory medulla, which acts as the circadian pacemaker controlling locomotor activity rhythms, and to the dorsal brain which acts as the primary regulator of hormonal secretion. Circadian signals are therefore transduced to effector organs in both an electrical and hormonal manner (Helfrich-Forster, 2002).

Of all the animals where circadian clocks have been intensively investigated, rodents have the greatest relevance to understanding circadian phenomena in humans, and are therefore of significant interest. Circadian locomotor activity in rodents is most commonly measured by rhythms in wheel running and drinking activity and the availability of mutants has made studying arrhythmic activity comparatively simple (Block & Zucker, 1976). The mammalian pacemaker is located in the suprachiasmatic nucleus (SCN) within the anterior hypothalamus, dorsal to the optic chiasma (Johnson, 1992). It has been hypothesised that mammals rely on a completely centralised pacemaker because, unlike plants,

the retina is the only efficient mechanism by which light can reach the molecular clock (Johnson, 1992). In mammals retinal ganglion cells form projections to the SCN via the retinohypothalamic tract (Miyamoto, 1998). Approximately three-percent of these ganglion cells express the photopigment melanopsin. When melanopsin is excited by light, ganglion cells discharge to the SCN leading to depolarisation and eventual entrainment (Berger, 2004; Kuhlman, 2007) The SCN regulates multiple down-stream targets including metabolism and thermoregulation, however the primary target of SCN outputs appears to be the pineal gland.

The pineal hormone melatonin is synthesised and released in a circadian manner, peaking during subjective night and remaining basal throughout the subjective day. Melatonin regulates daily patterns of rest and activity Kuhlman, 2007. Consequently, a single neural lesion in the SCN is capable of entirely deregulating mammalian sleep / wake rhythms and inducing arrhythmia (Sharma and Chandrashekaran 2005). If acting as a mere signal transducer between the eye and oscillators elsewhere, destruction of the SCN should eliminate synchronisation between the environment and locomotor activity. A rhythmic free run would, however, remain. The presence of arrhythmia upon removal of the SCN is therefore a clear demonstration that this group of cells does not act upstream of an oscillator but rather acts as a physical timekeeper itself (Bjorn, 2002).

1.2 The Circadian Clock in *Arabidopsis thaliana*

1.2.1 The diversity of circadian controlled processes in Arabidopsis thaliana.

In plants, circadian clocks control the timing of numerous processes including flower opening in species such as *Nymphea stellata* (Water Lily) and *Mesembryanthemum crystallinum* (Common Iceplant), leaf folding in *Mimosa pudica* (Sensitive Plant) and scent emission in *Antirrhinum majus* (Snapdragon) (Dodd *et al*., 2005a; Kolosova, 2001).

In *Arabidopsis thaliana*, which due to its ease of propagation and manipulation has become the plant system of choice in which to study circadian rhythms, a number of circadian controlled outputs have been investigated. These processes include regulation of transcript levels, stomatal opening, CO_2 fixation, leaf movement and pulsatile root elongation (Hubbard *et al*., 2007; Dodd *et al*.,

2005a; Salomé *et al.*, 2008; Gardner *et al.*, 2006; Schafer & Bowler, 2002). The most investigated circadian-controlled response in *A. thaliana* is the induction of accelerated flowering.

1.2.2 The core circadian oscillator.

The core of the *A. thaliana* circadian clock is a molecular oscillator that is at least partially controlled by self sustaining positive and negative feedbacks, and in turn generates rhythmic oscillations in the abundance of clock component transcripts and protein.

At the heart of the *A. thaliana* oscillator lies TIMING OF CAB EXPRESSION 1 (TOC1), CIRCADIAN CLOCK ASSOCIATED 1 (CCA1) and LATE ELONGATED HYPOCOTYL (LHY). Two further core components termed 'X' and 'Y' are believed to exist. Whilst there is currently no strong candidate for X, GIGANTEA (GI) is a strong candidate for component Y (figure 1.2). (Park *et al.*, 1999; Harmer *et al.*, 2000; Mizoguchi *et al.*, 2005).

TOC1 is a histidine kinase and was the first described member of a family of proteins known as PSEUDO-RESPONSE REGULATORs (Makino *et al.*, 2001; McClung *et al.*, 2002; Strayer *et al.*, 2000). Although sharing no known common biochemical function, the PRR family contains a C-terminal domain akin to those of the CONSTANS (CO) family transcriptional activators, together with an acidic amino-acid motif also often found in transcriptional activators (Kawamura *et al.*, 2008; McClung *et al.*, 2002; Putterill *et al.*, 1995). TOC1 is believed to activate transcription of component *X*, the protein product of which induces transcription of *CCA1* and *LHY*. CCA1 and LHY are DNA binding, MYB-like transcription factors first identified by their interaction with the promoter of the morning peaking, circadian cycling, *CHLOROPHYLL A/B BINDING PROTEIN* 2 (*CAB2*) gene (Carré, 1995). However, LHY and CCA1 also interact with genes whose expression peaks in the evening (Harmer *et al.*, 2000; Kawamura *et al.*, 2008). Due to the homology between CCA1 and LHY these proteins are consistently modelled as a single component within the circadian clock (CCA1/LHY), and act to repress TOC1 expression.

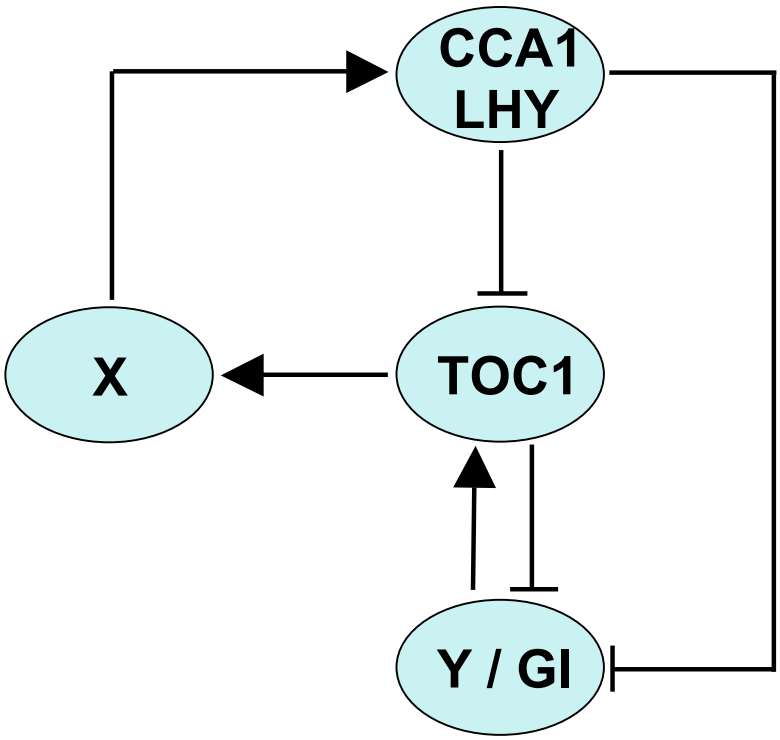

Figure 1.2: Schematic representation of the feedbacks believed to form the core of the *Arabidopsis thaliana* circadian clock.

The core circadian oscillator of *A. thaliana* is believed to be formed by feedbacks between the histidine kinase TIMING OF CAB EXPRESSION 1 (TOC1), the transcription factors CIRCADIAN CLOCK ASSOCIATED 1 (CCA1) and LATE ELONGATED HYPOCOTYL (LHY) and two further components termed 'X' and 'Y'. Although there is no clear candidate for X, the nuclear localised protein GIGANTEA (GI) is believed to fulfil the role of Y.
TOC1 is believed to activate transcription of *X*, which, when translated, induces transcription of *CCA1*/*LHY*. Due to their homology, CCA1 and LHY are treated as a single component, which acts to repress TOC1 expression. Y/GI is believed to act antagonistically to CCA1/LHY and activate transcription of TOC1, whilst both TOC1 and CCA1/LHY are believed to repress expression of *Y*/*GI*.

In addition, both TOC1 and CCA1/LHY repress expression of *Y*/*GI*. GI is a nuclear localised protein containing no domains of recognised biochemical function and has no close sequence similarity to other *A. thaliana* proteins, (David *et al*., 2006; Huq *et al.*, 2000). Y/GI is believed to act antagonistically to CCA1/LHY and activate transcription of TOC1 (Harmer *et al.*, 2000; Locke *et al.*, 2005b).

1.2.3 Stimulus perception and entrainment of the circadian clock.

In *A. thaliana*, light input to the clock is principally mediated by five phytochromes (PHYTOCHROME A to E) and three cryptochromes (CRYPTOCHROME 1 to 3) (Devlin & Kay, 2000; Somers *et al.*, 1998a).

Phytochromes are dimeric phosphoproteins (monomer size 124 kDa) (Kim *et al.*, 2005a) that are predominately involved in red and far-red light perception (Clack *et al.*, 1994; Hirschfeld *et al.*, 1998). The globular N-terminal domain of the phytochrome is both necessary and sufficient for photoperception and the C-terminal domain is believed responsible for interacting with downstream signalling elements (Kim *et al.*, 2005a; Schafer & Bowler, 2002). Phytochromes exhibit at least two separate and photoconvertible spectral sensitivities (Kim *et al.*, 2005a; Schafer & Bowler, 2002). The inactive red form of phytochrome (Pr) absorbs most strongly at 660 nm whilst the active far red (Pfr), absorbs at maximally 730 nm (Quail et al., 1995; Reed, 1999). Overlapping absorption spectra of the Pr and Pfr forms however ensure that photoconversion is never absolute but merely results in wavelength-dependent equilibrium between the two forms of phytochrome (Genoud *et al.*, 2008). Although much less pronounced, phytochromes have also show absorption (abs) in the blue region of the spectrum (λabs Pfr = approximately 370 nm, (λabs Pr = approximately 400 nm) (Hartmann, 1966), which may mediate some blue-light-dependent responses such as phototropism (Whippo & Hangarter, 2004).

Mutant analysis has demonstrated a role for PHYA, PHYB, PHYD and PHYE in regulating clock period (McClung *et al.*, 2002; Somers *et al.*, 1998a). PHYA is highly light labile and is the primary receptor mediating both far-red and very low fluence responses (VLFR) and is involved in FRP length and re-entrainment (Johnson *et al.*, 1994). PHYB is non light-labile and acts as the dominant receptor for red light at fluences greater than those transduced by PHYA

(Hirschfeld *et al.*, 1998; Devlin & Kay, 2000; Gardner *et al.*, 2006). Both *PHYD* and *PHYE* are recent duplications of, and show partial redundancy to, *PHYB*. Although *PHYD* and *PHYE* show similar gene expression patterns to *PHYB* across all tissues, total transcript levels are much reduced (Goosey *et al.*, 1997; Mathews & Sharrock, 1997).

The *A. thaliana* cryptochrome family consists of two highly similar members *CRYPTOCHROME 1* (*CRY1*) and *CRYPTOCHROME 2* (*CRY2*) and a third divergent member, *CRYPTOCHROME 3* (*CRY3*). Cryptochromes have homology to DNA-lyases involved in blue / UV light-dependent DNA repair (Devlin, 2002; Pokorny *et al.*, 2005) and are activated by non-covalent linkage to pterin and flavin chromophores (Ahmad *et al.*, 1998a; Ahmad *et al.*, 1998b; Devlin & Kay, 2000; Mockler *et al.*, 1999). Both CRY1 CRY2 have been shown to have roles in circadian input (Somers *et al.*, 1998b), with CRY1 acting as the principal receptor of high intensity blue light (Somers *et al.*, 1998a). CRY2 acts additively and partially redundantly to CRY1 and is rapidly degraded under green, blue and UV light (Ahmad *et al.*, 1998a; Devlin & Kay, 2000).

1.2.4 Gating and modulation of light inputs to the circadian clock.

Transcription of phytochromes and cryptochromes shows circadian regulation. Rhythmic modulation of photoreceptor levels is believed to enable restriction of light signalling in to the clock to selected periods of the day, a system of clock fine-tuning called ‘gating’ (Millar & Kay, 1996). *PHYB*, *PHYD* and *CRY1* expression peaks following subjective dawn whilst transcription of *PHYA* and *CRY2* peaks at dusk (Bognár *et al.*, 1999; Tóth *et al.*, 2001; Fankhauser & Staiger, 2002). Oscillations in photoreceptor mRNA appear to be reflected at the protein level. CRY2 oscillates in a circadian manner and levels of nuclear phytochrome vary throughout the day (Fankhauser & Staiger, 2002). Oscillations of photoreceptor proteins are insufficient to fully regulate timing of light input in to the clock and the action of a number of secondary components has also been observed (Fankhauser & Staiger, 2002; Millar & Kay, 1996). These components act via the rhythmic activation or repression of photoreceptors or their signalling intermediates (Carre, 2002)

EARLY FLOWERING 3 (ELF3) is a PHYB interacting protein, believed to inhibit the PHYB-mediated induction of clock-controlled genes. (Liu *et al.*, 2001; Carre,

2002). Although having no functionally identified domains, ELF3 shows nuclear localisation and contains acidic regions similar to those found in some transcription factors (Carre, 2002). Peaks in *ELF3* transcript and nuclear-localised protein occur in the evening in a manner consistent with a function related to gating of light inputs. Once established, these oscillations are maintained under constant darkness, indicating that transcription of *ELF3* is clock rather than light regulated (Hicks *et al.*, 2001; Liu *et al.*, 2001).

Unlike for mutants of the core components *lhy* and *cca1* which display arrhythmia under normal photoperiods and constant darkness, *elf3* mutants display arrhythmic *CAB2* expression only under constant light. Such photoperiod-dependent arrhythmicity is a strong indicator that ELF3 acts solely in light input and not as a core component of the central oscillator (McClung *et al.*, 2002; Searle & Coupland, 2004).

Although a strong candidate for a core clock component, GI is also implicated in the transduction of light signals to the clock. Decreasing light fluence results in clock period lengthening in wild-type seedlings (Somers *et al.*, 1998a; Somers *et al.*, 1998b). When grown in red light, *gi* mutants only show a similar period lengthening at fluences below 1 μmol m^{-2} s^{-1}, indicating that GI acts downstream of non light-labile photoreceptors, most likely PHYB. As GI is nuclear localised, it is likely to act in early PHYB signal transduction. (Park *et al.*, 1999).

ZEITLUPE (ZTL), is a ubiquitin-protein ligase believed to play a role in mediating signalling to, and regulation of, the *A. thaliana* central oscillator (Kim *et al.*, 2005b). The C-terminus of ZTL interacts with PHYB and CRY1, ZTL therefore acts directly downstream of these photoreceptors (Jarillo *et al.*, 2001; Kim *et al.*, 2005b). ZTL undergoes light induced conformational changes and it has been proposed that such changes may occur due to interactions with light stimulated photoreceptors (Fankhauser & Staiger, 2002; Gardner *et al.*, 2006). ZTL has, however, been observed to be stabilised by direct interaction with GI, *in vitro*, in the absence of phytochromes or cryptochromes. Consquently light activation of ZTL may not require further co-factors, as GI is already regulated by light (Kim *et al.*, 2007). As well as playing a possible role in light signal transduction, ZTL is believed to directly interact with and regulate core clock components. ZTL contains a LIGHT OXYGEN VOLTAGE domain and multiple

Kelch repeats, both of which are motifs that are commonly involved in protein-protein interaction (Kim *et al.*, 2007). Overexpressing *ZTL* leads to a reduction in levels of *TOC1* and a subsequent period shortening of the clock. It has been proposed that TOC1 is targeted for degradation via an F-box domain in ZTL. These domains are involved in recruiting proteins for proteosome-based degradation via E3 ligase-dependent ubiquitination (Kim *et al.*, 2005b). This hypothesis is supported by the observation that TOC1 degradation requires functional ZTL, and that proteasome inhibitors prevent destruction of TOC1 (Más *et al*., 2003a).

Unlike ELF3, GI and ZTL, which primarily mediate signalling from PHYB to the clock, SUPPRESSOR OF PHYA-105 (SPA1) negatively regulates PHYA-dependent very low fluence responses (VLFR) and far-red responses (Johnson *et al.*, 1994; Hoecker, 1999; Casal *et al.*, 2003). SPA1 is a member of a family of four 114 kD nuclear localised proteins which act with partial redundancy (Hoecker, 1999; Laubinger, 2004). Similarity to known proteins suggests that SPA1 may act as an atypical protein kinase (Hoecker, 1999). Both PHYA and PHYB are required for accumulation of *SPA1* transcript, however only functional PHYA is required for SPA1 function (Hoecker, 1999; Casal *et al.*, 2003). It now appears likely that, upon complexing with the E3 ligase CONSTITUTIVE PHOTOMORPHOGENIC 1 (COP1), SPA1 targets both PHYA and a number of its signalling intermediates for proteasomal degradation (Ishikawa *et al.*, 2006; Saijo *et al.*, 2008; Seo *et al.*, 2004).

1.2.5 A model of the circadian clock in Arabidopsis thaliana.

Mathematical modelling has been invaluable in resolving the architecture of complex gene networks. In *A. thaliana*, the greatest success in simulating the circadian oscillator has been achieved using a model composed of three interlocking feedback loops (Locke *et al*, 2006; Zeilinger *et al.*, 2006) (figure 1.3) One particular advantage of such a model is its ability to closely simulate circadian phenomena observed in different mutant lines. Additionally the three-loop model is unique in its ability to describe both the discrete and continuous aspects of circadian entrainment, with simulated PRCs closely follow experimental findings (Zeilinger *et al.*, 2006).

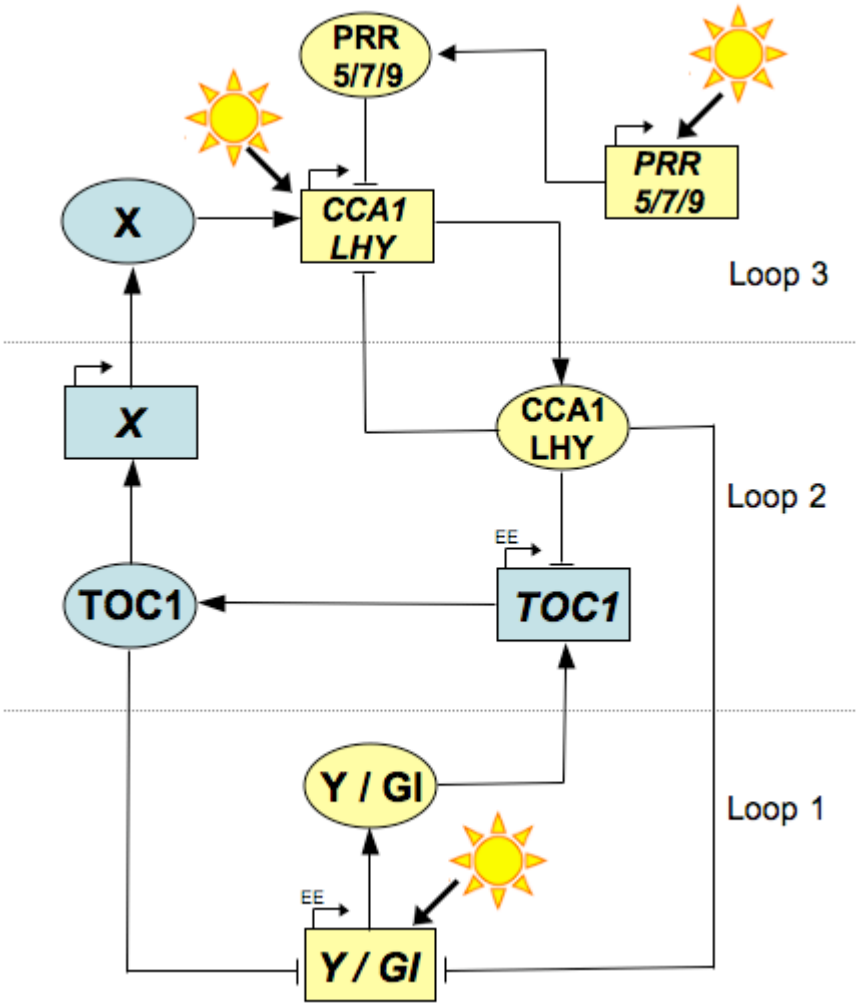

Figure 1.3: The 'three loop' model of the *A. thaliana* circadian oscillator (adapted from Locke *et al*., 2005b and Zeilinger *et al*., 2006).

Under the three-loop model of the *A. thaliana* circadian oscillator, light stimuli activate expression of hypothetical component '*Y*', for which *GIGANTEA* (*GI*) is a strong candidate. 'Y'/GI protein product then activates expression of *TOC1*. TOC1 is proposed to act via the hypothetical component 'X', to increase light-stimulated expression of both *CCA1/LHY*. Simultaneously TOC1 is modelled as suppressing further expression of *'Y'*. Further Expression of *CCA1/LHY* is proposed to be limited both by direct negative-feedback and by the light induced pseudo response regulators PRR5, PRR7 and PRR9. Elements showing peak expression during the morning / day-time are displayed in yellow. Elements showing peak expression during the evening / night-time are displayed in blue.

In the most current iteration of the three-loop model, expression of hypothetical component '*Y*' is upregulated in response to light stimuli. GI is a strong candidate for this component as its transcript abundance increases from approximately four-hours post-dawn and peaks prior to dusk in a manner similar to that modelled for *Y* (figure 1.4). Additionally, a modelled mutation in *Y* (which reduces translation by 70%) generates a one-hour decrease in the FRP of *LHY*/*CCA1* oscillations similar to that observed in *gi* mutants, whilst the shortened period observed in the *lhy/cca1* double mutants is absent in models in which *Y* is not included (Park *et al*., 1999; Locke *et al*., 2006; Ueda, 2006). Y/GI protein product is modelled as activating transcription of *TOC1* which shows peak abundance approximately two-hours after *GI*. Experimental data have previously indicated that *TOC1* transcription is light responsive. However there is no experimental evidence that *TOC1* is directly regulated by light (Makino *et al.*, 2001). The activation of *TOC1* transcription by GI, as proposed in this model, therefore offers a mechanism by which light stimuli are able to modulate expression of *TOC1* (Ueda, 2006). Following transcription, TOC1 is modelled as suppressing further expression of *'Y'*. Simultaneously, it is proposed that TOC1 serves as a transcriptional activator, acting via the hypothetical, night peaking, component 'X', to induce expression of *CCA1/LHY* (Locke *et al*., 2006; Ueda, 2006). A modelled mutation in *TOC1* (which reduces translation by 94%), leads to markedly reduced levels of *CCA1*/*LHY* which show a short-period rhythm; correctly mimicking *CCA1*/*LHY* expression patterns observed in the strong *toc1-2* mutant (Harmer & Kay, 2005; Locke, 2006; McClung, 2006). *CCA1/LHY* is further modelled as being regulated by auto-repression, light stimuli and the action of PSEUDO-RESPONSE REGULATORs (PRRs) (Wang and Tobin, 1998; Martinez-Garcia *et al*., 2000). Daybreak acts to both stimulate *CCA1*/*LHY* expression and initiate an expression cascade consisting of *PRR5*, *PRR7*, and *PRR9.* PRR protein product is then modelled as acting to repress further *CCA1*/*LHY* expression. The combination of clock-regulation, light responsiveness, down-regulation by PRRs and auto-repression leads to a *CCA1/LHY* profile whereby transcript abundance peaks immediately following dawn before rapidly returning to basal levels (Wang & Tobin, 2005; Locke, 2006).

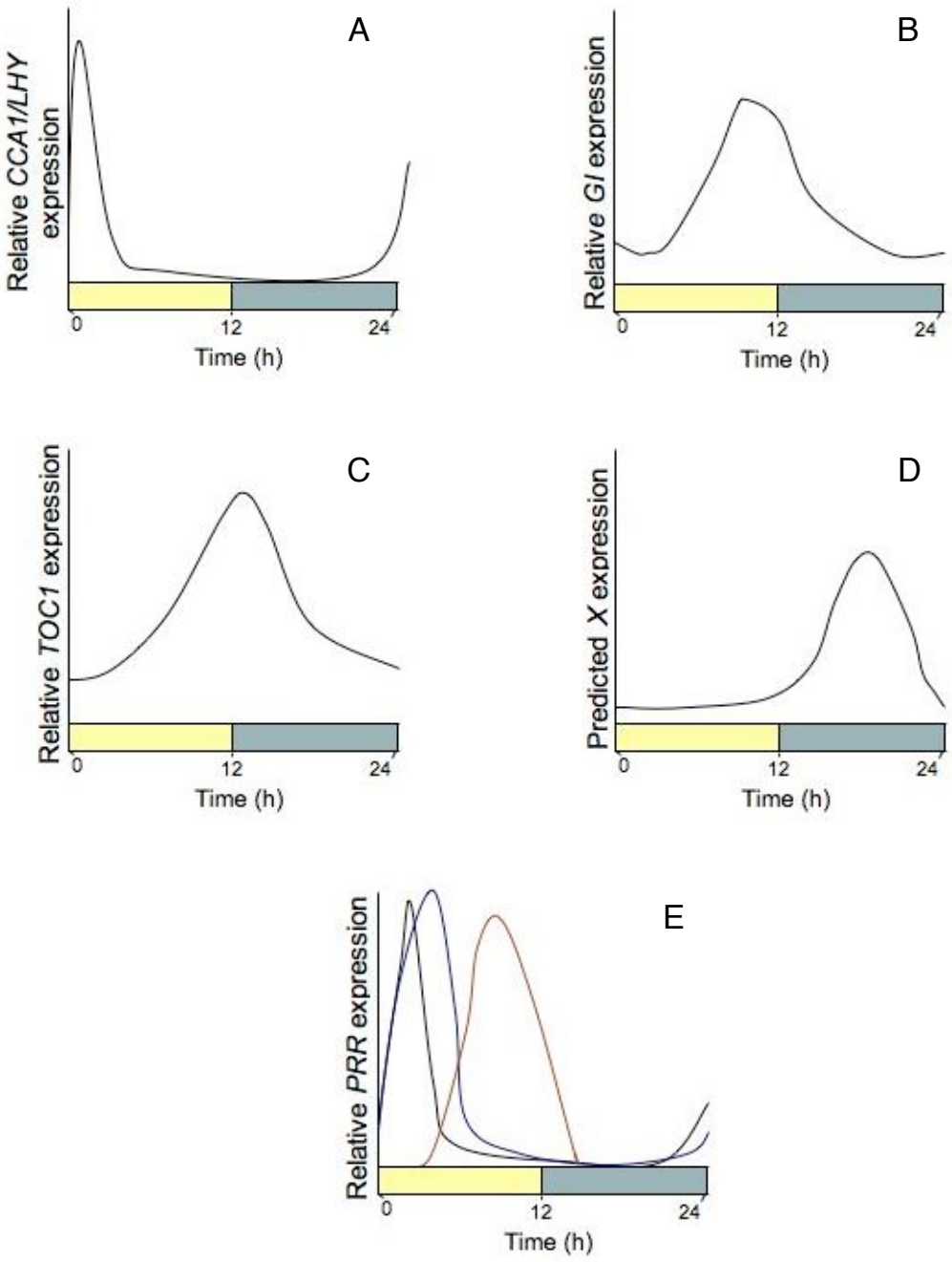

Figure 1.4: A schematic representation of the rhythms in abundance of core *A. thaliana* clock gene transcripts following entrainment under a neutral 12L : 12D photoperiod.

(A) *CCA1/LHY* transcript abundance peaks soon after subjective dawn before rapidly diminishing.
(B) *GI* mRNA increases from four hours post subjective-dawn, peaking at approximately ten hours and declining throughout the night.
(C) *TOC1* expression follows *GI*, peaking at subjective-dusk.
(D) Expression of hypothetical clock component 'X' is predicted to peak during the night.
(E) Expression of the *PSEUDO-RESPONSE REGULATORs* occurs sequentially with *PRR9* transcript (shown in black) peaking at two to three hours post subjective-dawn, *PRR7* (in blue) peaking at approximately five hours and *PRR5* (in red) peaking at nine to ten hours after subjective-dawn.

CCA1/LHY functions predominantly, and perhaps exclusively, as a transcriptional repressor in circadian associated events (Kawamura *et al.*, 2008), and is also modelled as repressing *GI* and *TOC1* expression via binding to highly specific *AAAATATCT* 'evening elements' in their promoters (Harmer *et al.*, 2000; Locke, 2006; Kawamura *et al.*, 2008). As with experimental data, models simulating a *cca1*/*lhy* double-null mutation result in a shortened clock period and a phase-advance in both *GI* and *TOC1* expression (Mizoguchi *et al.*, 2002; Locke, 2006). Additionally, when *CCA1/LHY* is modelled as constitutively high, '*Y/GI*' is expressed arrhythmically in a manner consistent with experimental data (Fowler *et al.*, 1999; Makino *et al.*, 2002; Mizoguchi *et al.*, 2005).

1.3 Flowering and Photoperiodism in *Arabidopsis thaliana*

1.3.1 Models of photoperiodism in plants.

Throughout nature, changes in physiology and behaviour tend to occur in synchrony with the passing of the seasons. The first researchers to definitively show that such changes can occur as a direct result of alterations in day length were Garner and Allard (1920), who coined the term photoperiodism to describe this phenomenon. Photoperiodic responses are common in plants, fungi and animals and, and are most commonly directly involved with survival and reproduction (table 1.1). Of the many photoperiodic responses described in plants, induction of flowering has been the most intensively studied. It is on this basis that flowering plants have been divided in to three classifications. Long-day plants are those displaying transition to flowering when the length of the photophase (illuminated part of the photoperiod) exceeds a critical threshold. Short-day plants are those which flower when the photophase lasts less than a critical threshold. Day-neutral plants do not initiate flowering as a response to photoperiod (Garner & Allard, 1920). Within the long-day and short-day classifications are 'obligate' species which require a critical threshold to be reached in order to flower and 'facultative' species which will show eventual, though delayed, flowering even if the threshold is not breached (table 1.2).

Table 1.1: *The diversity of photoperiodic responses.*

Group	Photoperiodic Response
Higher plants	Germination Hypocotyl elongation Storage organ formation Branching Vegetative reproduction Floral induction Floral sex determination Winter hardiness Dormancy
Insects	Migration Mating Sex determination of progeny Oviposition Pupal eclosion Diapause
Birds	Gonad development Fat deposition Migration Mating
Mammals	Gonad development Antler formation Migration Food hoarding Hibernation

Table modified and extended from Koukkari & Sothern (2006).

Table 1.2: *Photoperiodic-flowering responses in plants.*

Flowering Response type	Species
Long-day (facultative)	*Arabidopsis thaliana* (Arabidopsis) *Brassica rapa* (Turnip) *Hordeum vulgare* (Barley) *Pisum sativum* (Pea)
Long-day (obligate)	*Avena sativa* (Oat) *Catananche caerulea* (Cupid's dart) *Hibiscus syriacus* (Hibiscus) *Hyoscyamus niger* (Henbane) *Lolium temulentum* (Rye grass)
Short-day (facultative)	*Cannabis sativa* (Hemp) *Gossypium hirsutum* (Cotton) *Oryza sativa* (Rice) *Solidago shortii* (Goldenrod)
Short-day (obligate)	*Coffea* sp. (Coffee) *Stevia rebaudiana* (Sugar leaf) *Tagetes erecta* (Mexican marigold) *Xanthium strumarium* (Cocklebur)
Day-neutral	*Allium cepa* (Onion) *Cucumis sativus* (Cucumber) *Poa annua* (Meadow grass) *Solanum lycopersicum* (Tomato)

Table modified and extended from Koukkari & Sothern (2006).

However, it is important to note that, due to the extensive array of photoperiodism-controlled responses, an organism may display long-day type responses for one photoperiodic output whilst it may display day-neutral or short-day types for others (McGraw-Hill, 2009).

The earliest and simplest model to describe photoperiodic responses is known as the 'hourglass' model and argues against the involvement of the circadian clock. In this model, light directly induces alterations in the levels or activities of regulatory molecules, which begin to return to basal levels during the night. A photoperiodic response is only elicited once levels of these effectors reach a critical threshold. (Hall & McWatters, 2006; Kendrick, 1994). Further studies however, have made it clear that the circadian clock plays an integral role in

photoperiodism, as night breaks generate alterations in photoperiodic responses in a circadian manner matching that of PRCs (Koukkari & Sothern, 2006).

Two models have been proposed to explain the mechanism by which the circadian clock regulates photoperiodism. The 'external coincidence' model requires a temporal coincidence between circadian-clock controlled rhythms of photosensitivity and incident light in order for the elicitation of photoperiodic responses (Brady, 1982). In this model, light plays dual roles, both to entrain the clock -and by extension the rhythms of photosensitivity seen in PRCs- (section 1.1.2) and to act as the external signal that promotes a photoperiodic response (figure 1.5). During the winter, photosensitive periods are confined to the night. As days lengthen however, there is a lag in clock re-entrainment and photosensitive periods begin to extend in to daylight hours enabling responses to be elicited. By comparison, in the alternative 'internal coincidence model' (Pittendrigh & Minnis, 1964) the only role played by light is the entrainment of an endogenous oscillator or oscillators (figure 1.5). In this model, changes in day length induce alterations in the phase-relationship of two or more circadian-regulated components of a signalling pathway. A response is triggered as a direct result of the establishment of a favourable 'coincidence' between the two rhythms, for example the secretion of a hormone release and the coincidental expression of its receptor (Hall & McWatters, 2006).

For the majority of photoperiodic responses, it has proved difficult to discriminate which of the two 'coincidence' models are at play (Zivkovic, 2009). Experiments have typically involved night-break light pulses and light/dark cycles lasting other than 24 hours and have often returned inconclusive results. However more recent molecular data indicates that, at least some photoperiodic responses may be governed by the coincidence of both internal and external cues (Nozue, 2007; Sawa *et al.,* 2008). The prevailing evidence suggests that in *A. thaliana* photoperiodic flowering is primarily governed by the external coincidence model (section 1.3.2).

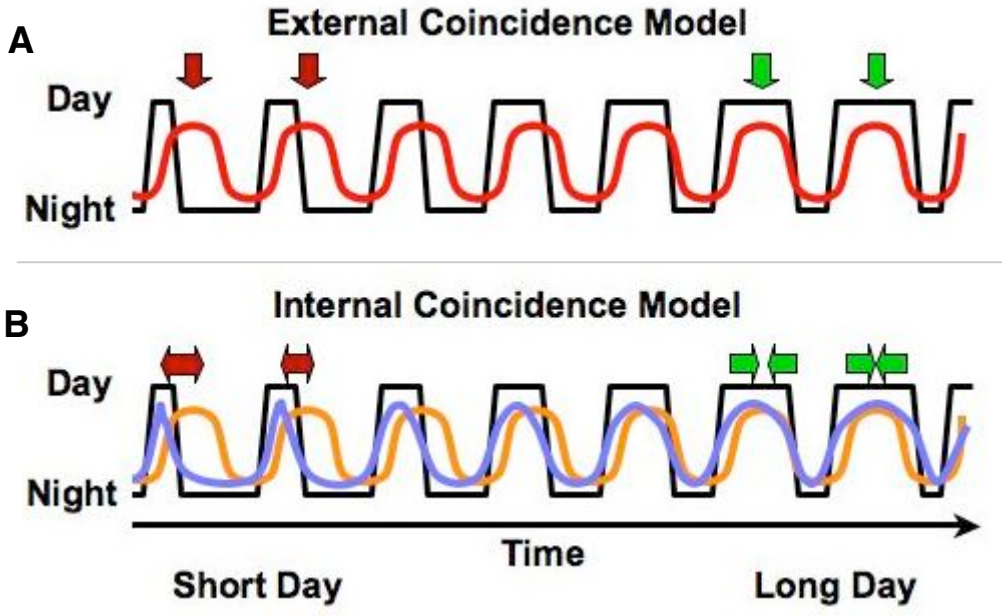

Figure 1.5: Two models by which the circadian clock may regulate photoperiodism.

Fig 1.5 A: In the 'external coincidence' model, light plays a dual role, both in entrainment of the clock and as the external signal that promotes a photoperiodic response. During winter months, the photosensitive period of the circadian rhythm is confined to the night. As days lengthen the photosensitive period extends in to the hours of illumination enabling the induction of photoperiodic responses.

Fig 1.5 B: In the 'internal coincidence' model light only acts to entrain the circadian clock. In this model, changing day length leads to altered phase-relationships between two or more rhythms (displayed in orange and purple). A photoperiodic response is inhibited until a favourable 'coincidence' between the two rhythms is established.

1.3.2 Flowering pathways in Arabidopsis thaliana.

In *A. thaliana* four distinct flowering pathways have been recognised (table 1.3). These pathways integrate powerful endogenous and exogenous signals in order that flowering is initiated at the most opportune moment for reproduction (Anthony, 2006). Flowering pathways converge upon an overlapping group of targets known as "floral pathway integrators" (FPIs). FPIs are common nodes that modulate expression of the floral meristem identity genes which control the transition of a vegetative to a floral meristem (Yu *et al*., 2004).

Table 1.3: *Characteristics of the four main flowering pathways in* A. thaliana.

		Origin of pathway activating stimulus	
Pathway type		Exogenous	Endogenous
	Enabling	Vernalisation	Autonomous
	Promoting	Photoperiodic	Giberellin

Flowering pathways are divided in to 'enabling' pathways, which regulate the competence of the meristem to act upon floral signals and 'promoting' pathways, which activate the genes involved in floral differentiation (Boss *et al*., 2004). The enabling pathways are composed of the age-dependent 'autonomous' pathway and the 'vernalisation' pathway which lifts repression of flowering following extended periods of cold (Henderson & Dean, 2004). The promoting pathways consist of the giberellin pathway, which is responsive to levels of endogenous gibberellins and the photoperiodic pathway which regulates flowering in a day-length-dependent manner (Henderson & Dean, 2004). The photoperiodic pathway is under the control of the circadian oscillator and is therefore the pathway with the most direct relevance to the work presented in this thesis.

1.3.3 The photoperiodic flowering pathway in Arabidopsis thaliana.

In addition to its roles as a modulator of the light input pathway and a core oscillator component, GI is the first output in the molecular cascade that leads to photoperiodic flowering (Martin-Tryon *et al.*, 2007; Simpson, 2003). *gi* mutants are late flowering under long days, whilst plants constitutively

expressing *GI* are early flowering under all photoperiods (Mizoguchi *et al.*, 2005; Casal, 2007). GI is believed promote photoperiodic flowering through interaction with the N-acetylglucosamine transferase SPINDLY (SPY) (Gardner *et al.*, 2006; Mizoguchi *et al.*, 2005; Tseng *et al.*, 2004). SPY acts as floral repressor within the giberellin-dependent flowering pathway and is believed to act in a similar fashion in photoperiodic flowering (Tseng *et al.*, 2004). Following interaction between SPY and GI, floral repression is released and expression of CONSTANS is initiated. CO is a zinc-finger transcription factor that is not involved in circadian timekeeping. The only phenotype displayed in *co* mutants is late flowering under long days, whilst plants misexpressing *CO* flower early in a dose-dependent manner (Suárez-López *et al.*, 2001; Komeda, 2004). As well as absolute expression levels, the phase of *CO* transcription is critical to the induction of flowering. Although transcribed under both short day and long day conditions, *CO* only induces flowering once a critical daylength threshold is reached. Under short days, *CO* transcription occurs exclusively during the night (figure 1.6). As the length of day increases this peak widens and transcription of *CO* also occurs during late afternoon and early morning (Suárez-López *et al.*, 2001; Valverde *et al.*, 2004; Valverde, 2006).

CO protein also displays circadian regulation even when *CO* is misexpressed, increasing during hours of light and then undergoing rapid proteasomal degradation after transition to darkness, in a manner mediated by SPA1 (Valverde *et al.*, 2004; Valverde, 2006). SPA1 primarily mediates destruction of target proteins via heterodimerisation with COP1 (section 1.2.3). (Lin & Wang, 2007; Parks *et al.*, 2001). In the absence of light, COP1 accumulates in the nucleus where it dimerises with SPA1 and initiates degradation of CO. In the presence of light, COP1 translocates to the cytosol and SPA1 is no longer able to target CO to the proteasome and flowering can be initiated (Seo *et al.*, 2004). The necessity of the coincidence between entrained *CO* expression and incident light in order for CO to remain un-degraded is a convincing argument that photoperiodic flowering in *A. thaliana* is predominantly regulated by an 'external coincidence' system (Valverde, 2006; Yanovsky & Kay, 2002).

Although CO activates expression of a number of floral pathway integrator genes including *LEAFY* (*LFY*) and *SUPPRESSOR OF OVEREXPRESSION OF CONSTANS 1* (*SOC1*), its primary target is *FLOWERING LOCUS T* (*FT*)

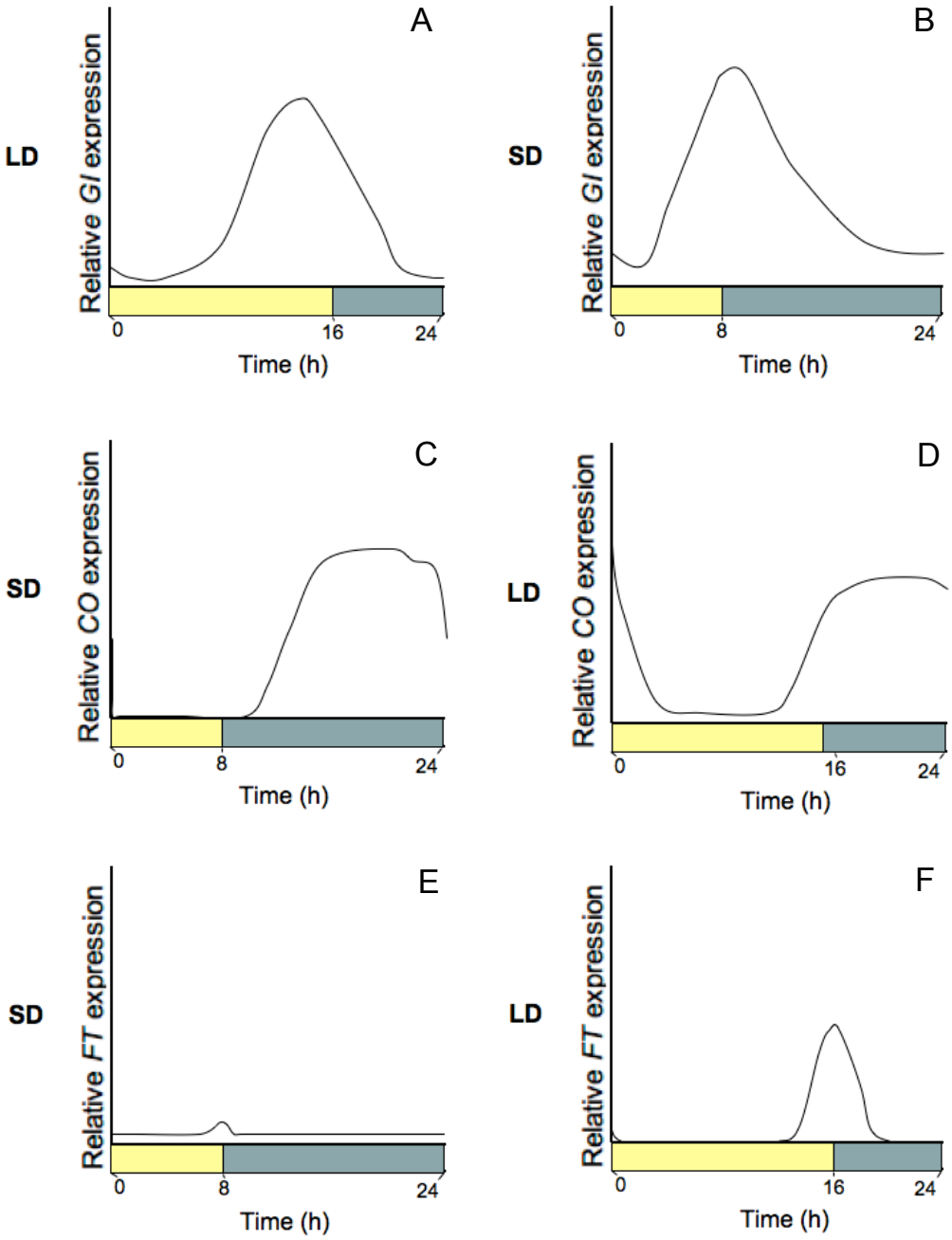

Figure 1.6: A schematic representation of the expression of flowering-time associated genes in *A. thaliana* grown under 8L : 16D and 16L : 8D photoperiods.

Daylength has a significant effect on the expression patterns of photoperiodic-flowering genes. *GI* acts as the first output of the photoperiodic flowering pathway. Under short days (A), *GI* transcript peaks at approximately dusk (eight to nine hours), whilst under long days maximal expression occurs at approximately thirteen to fourteen hours. Under short days, *CO* is expressed exclusively during the night (C). As daylength increases transcription of *CO* also extends in to early morning and late afternoon (D). Light stabilised CO is required for *FT* expression. *FT* is therefore minimal under short days (E). Under long days (F), a larger peak in *FT* mRNA is seen at dusk.

(Blázquez, 2005; Hepworth *et al*., 2002; Imaizumi & Kay, 2006). FT is a globular protein of 20 kDa with homology to mammalian Raf kinases and proposed phosphotidylethanolamine binding activity (Putterill *et al.*, 2004; Yanovsky & Kay, 2002). *FT* is the principal target of CO and *co* null mutants show no accumulation of *FT* (Valverde *et al.*, 2004; Yanovsky & Kay, 2002). CO activates transcription of *FT* by complexing with the transcription factor ARABIDOPSIS HAEM ACTIVATION PROTEIN 5 (AtHAP5), which recognises *CCAAT* multiple-repeats within the *FT* promoter (Imaizumi & Kay, 2006). FT is expressed in leaf phloem, however it translocates to the shoot apical meristem where it activates transcription of floral meristem identity genes and triggers floral transition (Wigge *et al.*, 2005; Corbesier *et al.*, 2007). FT induces flowering in a dose-dependent manner and *ft* mutants show extremely late flowering under long days, whilst plants constitutively expressing *FT* show dramatically accelerated flowering under short days (Simpson, 2003; Endo *et al.*, 2005).

Under short days, *FT* mRNA levels are barely detectable. Under long days however, a large peak in *FT* transcript follows the peak in *CO* transcript seen in late afternoon (Yanovsky & Kay, 2002). Mutations eliminating *SPA1* or phase shifting *CO* expression therefore modulate *FT* expression and abundance (Yanovsky & Kay, 2002).

Although CO is the dominant mechanism by which transcription of *FT* is controlled; it has been suggested that GI may be involved in the fine-tuning of *FT* expression in a manner independent of CO. GIGANTEA represses expression of the floral repressor *TARGET OF EAT 1* (*TOE1*) via *MicroRNA172* (*MiR172*). Whilst levels of *MiR172* are greater under long days than short days circadian oscillations in *MiR172* transcript abundance have not been demonstrated (Jung *et al.*, 2007). Whether a clock-dependent or clock-independent GI pathway regulates *MiR172* expression is yet to be established (Jung *et al.*, 2007).

Calcium-Mediated Signalling in Plants

1.4.1 Second messengers.

Cellular signal transduction can be divided in to extracellular and intracellular events. Extracellular stimuli trigger the formation or release of intracellular signalling molecules (second messengers), which lead to the activation of systems that modulate cellular functions (Hardie, 1991). Second messengers affect almost every aspect of cellular function. The process by which a signal is amplified above a detection threshold due to the binding of an extracellular ligand inducing release of a greater number of second messenger molecules is known as a temporal cascade. In such a cascade, the presence of a stimulus alone is insufficient for the elicitation of a response. Inhibitors of second messengers are therefore capable of blocking stimuli induced activity. Likewise, in the absence of a stimulus, the addition of a second messenger is capable of eliciting cellular responses (Hardie, 1991).

Only a relatively limited number of second messengers exist and these can be broadly grouped in to three main categories: Diffusible gases such as nitric oxide and carbon monoxide, hydrophobic molecules, such as diacylglycerols and phosphatidylinositols which are primarily associated with the plasma membrane, and hydrophilic molecules, which include cyclic adenosine monophosphate (cAMP), inositol trisphosphate (IP_3), and Ca^{2+}. (Plieth, 2001; Xue *et al*., 2004; Zalejski *et al*., 2005; Mathuis, 2006; Correa-Aragunde, 2006). Second messengers are activated in response to a wide range of stimuli and are required to modulate the activity of a diverse set of downstream targets. In order to convey information regarding different stimuli within short periods of time, it is necessary that second messenger signals are short lived and have low latency times. These properties are important determinants of why second messengers tend to be small molecules which can be rapidly synthesised, degraded, sequestered or released (Barbieri, 2003). The ability to rapidly and accurately modulate the concentration of second messengers enables tight control over the amplitude, frequency and waveform of the signal. By confining messenger molecules to specific subcellular locales such as the endoplasmic reticulum or plasma membrane, cells can target second messengers and create microdomains of elevated concentration, thus adding a spatial aspect to the temporal cascade (Hofer & Lefkimmiatis, 2007; Chen, 2008). Different stimuli

are therefore able to invoke differentiated patterns of second messenger release. Such patterns, which are also termed 'signatures', enable precise modulation of specific downstream targets (Hardie, 1991).

1.4.2 Calcium as an activator of physiological responses in plant cells.

Although Ca^{2+} has been accepted since the XVIIIIth century as one of a number of important macro and structural elements, the concept of Ca^{2+} as an intracellular regulator is comparatively modern (Hepler, 2005).

The first evidence that intracellular Ca^{2+} could activate specific cellular and physiological responses was established in *Rana pipiens* (Northern Leopard Frog). Heilbrunn (1940), demonstrated that individual skeletal muscle fibres, in which both ends had been removed, underwent accelerated contraction when placed in an isotonic solution of saline and $CaCl_2$ compared to those placed in saline alone.

Kamada and Kinoshita (1943) subsequently verified that microinjection of Ca^{2+} into intact nerve fibres also resulted in a similar reversible contraction.

Evidence that Ca^{2+} plays a role in signal transduction in plants was elucidated in the alga *Chara corallina* where intracellular cytoplasmic streaming was shown to be under the control of Ca^{2+} (Williamson & Ashley, 1982; Rudd & Franklin-Tong, 2001). It has since become clear that Ca^{2+} has more direct molecular targets than any other second messenger, binding to, and modulating the activity of an array of calcium binding proteins and anion channels (Dieter & Marme, 1983). This diversity of targets may be due to the length of evolutionary time for which Ca^{2+} has been employed as a second messenger. Sanders *et al*. (1999), have suggested that due to the low solubility product of Ca^{2+} and orthophosphate, mechanisms enabling maintenance of cytosolic free Ca^{2+} (Ca^{2+}_{cyt}) at concentrations well below that of seawater would be necessary to maintain energy metabolism. Elevation of [Ca^{2+}_{cyt}] due to external stresses is therefore presumed to be a primitive response, with the large homeostatic differential in Ca^{2+} concentration between seawater and the cytosol offering a clear niche for the evolution of mechanisms to rapidly signal environmental parameters (Sanders *et al*., 1999; Endo, 2006; White & Broadley, 2003).

1.4.3 Measuring changes in cytosolic free calcium.

Direct investigation of Ca^{2+} signalling and associated physiological responses requires the means to monitor [Ca^{2+}_{cyt}] in a non-destructive manner (Rudd & Franklin-Tong, 2001). Several distinct methodologies have been employed *in planta* to achieve such an end. Early studies employed calcium-selective microelectrodes to accurately monitor changes in [Ca^{2+}_{cyt}]. However, such electrodes are complicated to construct and operate and are limited to measuring [Ca^{2+}_{cyt}] at a single location within a cell. Given the low cytoplasmic diffusion co-efficient of Ca^{2+}, such limited spatial sensitivity is far from ideal (Gilroy *et al*., 1993).

The advent of calcium sensitive fluorescent dyes provided the ability to more accurately quantify the spatial and temporal aspects of changes in [Ca^{2+}_{cyt}]. Such Ca^{2+} sensitive dyes are generally divided in to two classes. Single wavelength dyes, such as calcium green, Fluo-3 and Rhod-2, show increased fluorescence in the presence of elevated [Ca^{2+}_{cyt}]. However, total fluorescence is dependent upon the amount of dye present thus making calibration of data difficult (Rudd & Franklin-Tong, 2001). Ratiometric dyes, such as Fura-2 and Indo-1, show a spectral shift upon binding Ca^{2+}. Determination of changes in [Ca^{2+}_{cyt}], is therefore independent of total dye concentration, instead relying upon the ratio of fluorescence at each wavelength (Gilroy *et al*., 1993; Rudd & Franklin-Tong, 2001). The large dynamic-range of the various calcium-sensitive dyes makes them useful for recording changes in [Ca^{2+}_{cyt}] elicited by a wide range of stimuli. However the use of fluorescent dyes in plant cells has been constrained by dye uptake. Unlike in animal cells where ester-loading protocols have proven effective, such techniques show reduced effectiveness in plant cells primarily due to extracellular hydrolysis of the applied ester-dye (Gilroy *et al*., 1993). Several techniques, including electroporation and protoplasting have been devised to circumvent such difficulties in dye loading, with the most widely used technique involving microinjection of the marker directly into the cell cytoplasm. However, whilst microinjection allows the simultaneous addition of various effector molecules, the technique is limited to individual cells and is therefore time-consuming (Gilroy *et al*., 1993). More recently, the use of biolistics to deliver Ca^{2+}-sensitive fluorescent dyes, such as fura-dextran, has shown promise as a method to circumvent the time constraints inherent with

microinjection (Bothwell *et al*., 2006; 2008). However, although such 'diolistic' methodology enables delivery of Ca^{2+} sensors in a relatively high-throughput manner, and has been used to successfully visualise events such as post-fertilisation [Ca^{2+}_{cyt}] elevations in *Fucus serratus*, the presence of the biolistic microcarriers can lead to imaging artifacts (Bothwell *et al*., 2008).

A significant advance in monitoring the dynamics of intracellular [Ca^{2+}], both in the cytosol and other cellular compartments, came through the development of recombinant Ca^{2+}-sensitive reporter proteins.

The photoprotein aequorin comprises a 22 kDa apoprotein together with a prosthetic group (coelentrazine) and has been used to investigate changes in [Ca^{2+}] induced by wide range of stimuli such as cold-shock, fungal elicitors and heat-stress (Knight *et al*., 1991; Knight, 1996; Larkindale & Knight 2002). Coelentrazine readily crosses the plant cell wall and is able to complex with the recombinant apoaequorin. Upon binding Ca^{2+}, the coelentrazine is oxidized to coelenteramide, and is accompanied by emission of a photon of blue light (approximately 470 nm). The wide dynamic range of aequorin, together with the ability to target it to desired subcellular compartments and the lack of photo-damage associated with fluorescent probes have made it a useful tool for monitoring intracellular [Ca^{2+}_{cyt}] *in planta.* The greatest impediment associated with aequorin is the extremely low signal intensity generated by oxidation of coelentrazine (less than one photon per molecule). Although this necessarily limits the use of aequorin for the study of the rapid kinetics of calcium signalling at a single cell level, it has become invaluable for the investigation of longer term changes in [Ca^{2+}] at the whole plant level and for the study of 'long range' signalling responses (Rudd & Franklin-Tong, 2001).

Unlike aequorin, recombinant Ca^{2+} sensors based upon green fluorescent protein (GFP) chimaeras, do not rely on the exogenous application of a prosthetic activator and can be selectively excited by a tuned external light source.

Three main classes of GFP-based sensors have been developed for the study of Ca^{2+} dynamics in living organisms. CaMgaroos were developed by the insertion of the Ca^{2+} binding protein calmodulin (CaM) in place of residue Tyr145 of an enhanced yellow fluorescent protein (eYFP) (Baird *et al*, 1999; Geddes, 2005). Upon binding Ca^{2+}, the eYFP chromophore of the CaMgaroo

deprotonates and its fluorescence increases several fold. PeriCaMs consist of a circularly permutated eYFP to which CaM is fused at the C-terminal and the M13 CaM-binding peptide at the N-terminal. Upon binding Ca^{2+}, CaM complexes with M13 and induces a conformational change in eYFP which can be tailored to either increase or decrease fluorescence (Nagai *et al*, 2001; Geddes, 2005). Of the GFP-based probes, the Ca^{2+} sensor CaMeleon has been most heavily utilised in plants (Allen *et al*., 1999; Demaurex & Frieden, 2003). The CaMeleon construct is based upon enhanced cyan fluorescent protein (eCFP) and eYFP acting as a donor-acceptor pair for non-radiative Förster resonance energy transfer (FRET). The CaMeleon construct consists of a CaM binding peptide such as M13 or CaM-dependent protein kinase kinase (CKKp) inserted between the terminal EF-hand Ca^{2+} binding domains of CaM. eCFP and eYFP are fused to either terminal of this module (Hoeflich, 2009). Upon binding Ca^{2+}, the CaM moiety complexes with the CaM-binding domain and undergoes a conformational change which brings the fluorescent proteins within 8 nm of each other and allows FRET to occur. A spectral shift in emitted light from approximately 480 nm to approximately 535 nm allows ratiometric determination of Ca^{2+} dynamics (Miyawaki et al 1997; Allen *et al*., 1999). Ongoing improvements to the spectral separation and quantum efficiency of CaMeleons (together with the ability to target such sensors to specific organelles and tissues), has ensured that over the last decade CaMeleons have played an increasingly important role in dissection of $[Ca^{2+}]$ signalling dynamics in plant tissues ranging from guard cells to root hairs and pollen tubes (Allan *et al*., 1999; Demaurex & Frieden., 2003; Demaurex, 2005; Iwano, 2009).

1.4.4 Calcium homeostasis, transporters and channels.

In order both to reduce toxicity and control signal specificity it is critical that, during signalling events, Ca^{2+} entry to the cytoplasm is tightly regulated via Ca^{2+}-permeable ion channels. It is equally important that cells are able to rapidly end $[Ca^{2+}_{cyt}]$ transients by efficiently removing calcium from the cytoplasm.

$[Ca^{2+}_{cyt}]$ is maintained at resting levels (100 to 200 nm) by the action of a series of high-capacity, low-affinity H^+/Ca^{2+} antiporters and low-affinity, high-capacity Ca^{2+}-ATPases which transport Ca^{2+} against the electrochemical gradient to the

apoplast or to the lumen of organelles including the ER, the nucleus and plastids where resting [Ca^{2+}] is in the region of 0.1 to 10 mM (White & Broadley, 2003).

Plant ATPases belong to two phylogenetic subgroups (Geisler *et al*. 2000). In *A. thaliana*, the P-type ATPase IIA subgroup has four members and have been identified in the plasma membrane and tonoplast (Sanders *et al*., 2002; White & Broadley, 2003) (figure 1.7). The P-type ATPase IIB family is activated by Ca^{2+}-CaM and bears structural similarity to animal ATPases (Sanders *et al*., 1999).

Unlike animals, where this subgroup of pumps is located exclusively in the plasma membrane, the ten members identified in *A. thaliana* are distributed between the plasmalemma, endoplasmic reticulum and tonoplast, with an additional plastid-localised member showing light-dependent Ca^{2+} uptake (Sanders *et al*., 1999; White & Broadley, 2003). It has been speculated that the diversity of P-type ATPase isoforms indicates that they are functionally distinct and show distinct responsivities to specific [Ca^{2+}] perturbations, with both Ca^{2+}-CaM-dependent and Ca^{2+}-CaM-independent regulation necessary to maintain finely balanced [Ca^{2+}_{cyt}] homeostasis (White & Broadley, 2003). This role for P-type ATPases as primarily acting in the maintenance of [Ca^{2+}_{cyt}] homeostasis is further supported by the observation that expression of at least some P-type ATPases is responsive to exogenous calcium levels (Hirschi, 1999).

Eleven genes have been identified that code for H^+/Ca^{2+} antiporters in *A. thaliana*. The transporters so far biochemically characterised localise to the plasmalemma or tonoplast and display varying transport capacity, cation specificity and autoinhibitory properties (Tuteja & Mahajan, 2007). Unlike Ca^{2+}-ATPases, the principal involvement of high-capacity H^+/Ca^{2+} antiporters does not appear to be the maintenance of [Ca^{2+}_{cyt}] homeostasis. Rather, these transporters are proposed to act in the removal of Ca^{2+} from the cytosol during signalling events thereby terminating a [Ca^{2+}_{cyt}] transient or modulating its form (Allen *et al*., 2000; White & Broadley, 2003).

Although Ca^{2+} stores act to prevent cytotoxicity they also serve other functions. For example Ca^{2+} is required for maturation of proteins in the ER secretory system (Nagata *et al*., 2004). The principal function of such stores however, is to serve as mobilisable sources of Ca^{2+} for the generation of [Ca^{2+}_{cyt}] signatures (White, 2000).

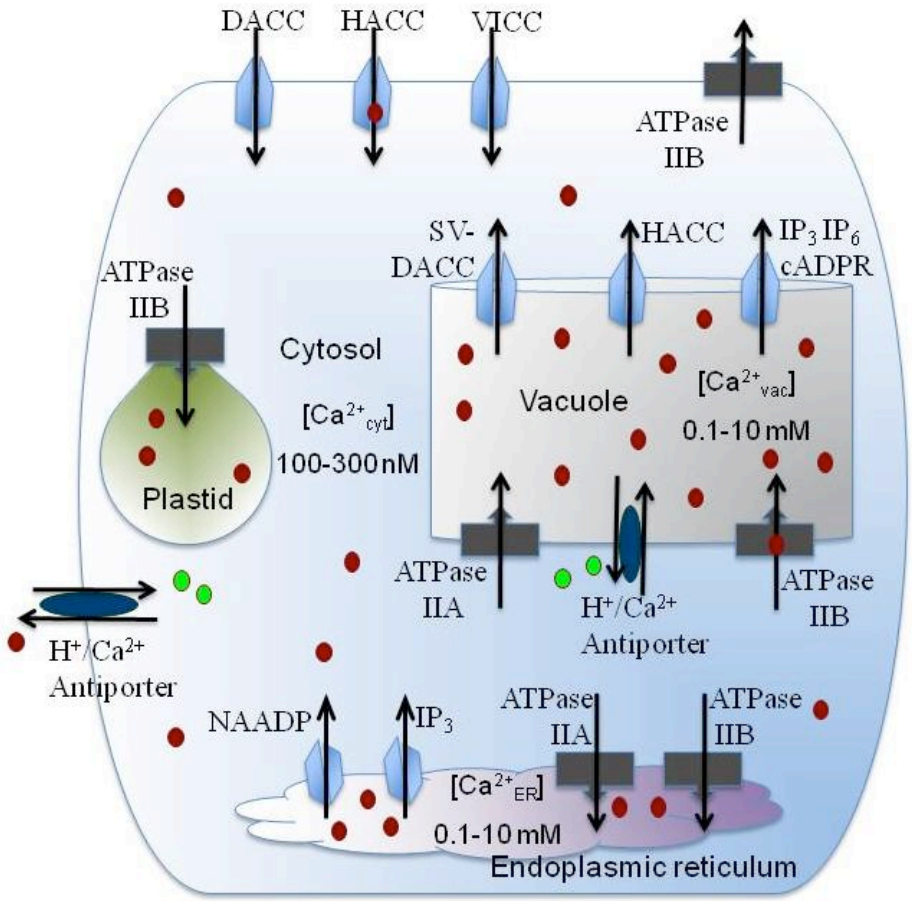

Figure 1.7: Diagram indicating the localisation of Ca^{2+} transporters in an *A. thaliana* cell (based on Broadley & White, 2003).

Numerous Ca^{2+}-permeable channels are localised in the *A. thaliana* plasma membrane. These include depolarisation-activated Ca^{2+} channels (DACCs), hyperpolarisation-activated Ca^{2+} channels (HACCs) and voltage-insensitive calcium/cation channels (VICCs). The plasma membrane is also incorporates pumps which remove Ca^{2+} to the apoplast against the prevailing electrochemical gradient. These pumps include H^+/Ca^{2+} antiporters and the P-type ATPase IIB.

Tonoplast Ca^{2+}-permeable channels comprise at least two ligand-gated channels, separately regulated by cADPR and IP_3, two HACCs and the depolarisation activated 'slowly activating vacuolar' channel which is the most abundant voltage-gated channel in the tonoplast. The tonoplast is also home to P-type ATPases IIA and IIB which remove Ca^{2+} from the cytosol to the vacuole against the prevailing electrochemical gradient.

The endoplasmic reticulum contains at least two types of ligand-gated Ca^{2+}-permeable channels, including an IP_3-gated channel and a channel gated by nicotinic acid adenine dinucleotide phosphate (NAADP); a molecule first identified as a calcium agonist in the eggs of marine invertebrates. Like the vacuole, the endoplasmic reticulum contains P-type ATPases IIA and IIB which use energised transport remove Ca^{2+} from the cytosol.

Ca^{2+} permeable channels which allow Ca^{2+} to enter the cytoplasm have been identified in all plant membranes and are classified by voltage dependence; they include voltage-independent calcium/cation channels (VICCs), depolarisation-activated calcium channels (DACCs) and hyperpolarisation-activated calcium channels (HACCs). Within these classifications, channel-specific biochemical regulation involving secondary effectors such as the interaction of ligands or mechanosensitivity generates 'physiological flexibility' to calcium influx (Thion *et al*., 1998; White & Broadley, 2003).

The plasmalemma has been most intensively studied membrane of the plant cell in regard to Ca^{2+}-permeable channels and so far is the only location where VICCs have been found. Of these, many biochemically-distinct VICC subtypes have been identified, all of which show permeability to a diversity of mono- and divalent cations (Demidchik *et al*., 2002; White & Davenport, 2002). VICCs are generally regarded as the only Ca^{2+} permeable channels with a moderate to high probability of being open at the resting potential of plant cell membranes (approximately -50 mV, where potential is measured on the cytoplasmic side of the membrane relative to the non-cytoplasmic side) (White & Davenport, 2002). Rather than playing a primary role in Ca^{2+} signalling, VICCs appear to be primarily involved in maintenance of calcium homeostasis and are believed to act as a counter to the continual Ca^{2+} efflux generated by ATPases and H^+/Ca^{2+} antiporters (White & Broadley, 2003). Although classed as voltage insensitive, at least some VICCs show weak voltage dependence. Some subtypes show reduced conductance at extreme negative potentials, whilst others show increased conductance. This spectrum of activity is again believed to contribute to the maintenance of calcium homeostasis (White & Davenport, 2002).

At least two classes of DACCs are believed to operate in the plasmalemma, and are activated by membrane potentials more positive than approximately -125 mV (White & Broadley, 2003). The maxi-cation class is relatively non-selective to cations, having a high single-channel conductance for a range of mono- and divalent cations (White, 1993). Unlike in animals, these relatively non-selective Ca^{2+}-permeable channels tend to dominate over more Ca^{2+}-selective channels within the plant plasma membrane such as the voltage-dependent cation channel 2 class (VDCC2) (Sanders *et al*., 1999). VDCC2s, whilst displaying a much greater selectivity for Ca^{2+} than maxi-cation channels,

show a much-reduced single channel conductance (Sanders *et al*., 1999; Sanders, 2002). As plasma membrane depolarisation is inducible via diverse processes and stimuli, it has been argued that DACCs most likely play a role in general stress signalling (White & Broadley, 2003).

Moreover, whilst all DACCs are responsive to membrane depolarisation, for a subset, depolarisation is not in itself sufficient to allow activation of the channel and subsequent Ca^{2+} influx. Characterisation of Ca^{2+}-permeable channels in *A. thaliana* protoplast cultures indicated that the predominant DACC of the plasma membrane is almost certainly co-regulated by cytoskeletal interaction (Thion *et al*., 1998)

Patch clamp electrophysiology has shown that plasma membrane HACCs are common across multiple cell types, typically activating at membrane potentials more negative than approximately -125 mV. HACCs generally show a low selectivity for Ca^{2+} and are permeable to many divalent cations, whilst being inhibited by moderate levels of trivalent cations (<100 μM Gd^{3+} / La^{3+}) (Véry & Davies, 2000; White & Broadley, 2003). Activation of at least a subset of plasma membrane HACCs is tunable by external factors. Increasing $[Ca^{2+}_{cyt}]$ results in root hair channels activating at more positive voltages, whilst in guard cells, similar increases in $[Ca^{2+}_{cyt}]$ lead to plasmalemma HACCs activating at increasingly negative membrane potentials (Véry & Davies, 2000). Abscisic acid (ABA), has also been found to drive the activation potential of guard cell HACCs towards more positive voltages. Increased ABA therefore promotes channel opening, entry of Ca^{2+} and stomatal closure (White, 2000).

Calcium permeable channels in the mitochondria, plastids and the nucleus are believed to play a comparatively small role in generation of specific calcium signals and for the most part await comprehensive biochemical classification; such channels will not therefore be described in depth here.

In mature plant cells, the vacuole acts as the dominant intracellular Ca^{2+} store and is capable of generating enduring elevations in $[Ca^{2+}_{cyt}]$. Tonoplast Ca^{2+}-permeable channels comprise at least one DACC, two HACCs and two ligand-gated channels, separately regulated by cyclic adenosine diphosphate ribose (cADPR) and IP_3. cADPR-gated vacuolar channels have been identified in root hairs and guard cells, display high selectivity for Ca^{2+} and a similar pharmacology to cADPR-gated endomembrane channels in animals where

activation is inhibited when [Ca^{2+}_{cyt}] is above 600 nm (White & Broadley 2003; Leckie *et al*., 1998). Unlike, cADPR-gated vacuolar channels, those regulated by IP_3 are insensitive to [Ca^{2+}_{cyt}]. However, activation is enhanced by extreme tonoplast hyperpolarisation or osmotic stress and these channels have been speculated to play a role in regulation of turgor pressure.

The depolarisation activated 'slowly activating vacuolar' (SV) channel is the most abundant and best characterised voltage-gated channel in the tonoplast, being found in multiple tissues and displaying moderate cation sensitivity. The SV channel is regulated by phosphorylation and shows greatly enhanced activity when [Ca^{2+}_{cyt}] is greater than 600 nm (Pei *et al*., 1999; White & Broadley, 2003). Like the IP_3-gated channel, the SV channel is implicated in the regulation of guard cell turgor pressure and stomatal closure. ABA-induced influx of Ca^{2+} to the cytoplasm via plasmalemma Ca^{2+}-permeable channels is believed to catalyse the synthesis of highly diffusible cADPR via activation of ADENSINE DIPHOSPHATE RIBOSE CYCLASE. Following activation of cADPR-gated channels in the tonoplast, local [Ca^{2+}] increases stimulate the opening of SV channels in a manner termed 'calcium induced calcium release' (CICR) (Ward & Schroeder, 1994; Pei *et al*., 1999; Krinke *et al*., 2007).

Unlike the SV channel, activation of tonoplast HACCs is not stimulated by elevated [Ca^{2+}_{cyt}], rather one subtype is insensitive to [Ca^{2+}_{cyt}], whilst a second is inhibited by [Ca^{2+}_{cyt}] above 1 µM. Additionally, vacuolar acidification has been found to inhibit opening of these HACCs. Such mechanisms are believed to act in curtailing channel activity before rises in [Ca^{2+}_{cyt}] induce cytotoxicity (White, 2000; White & Broadley, 2003). Although the vacuole serves as the dominant intracellular Ca^{2+} pool, such capacity does not guarantee that it acts alone in the release of internally mobilised Ca^{2+} during signalling events (Sanders *et al*., 1999). Indeed, intracellular Ca^{2+} mobilisation has been observed in regions of *Papaver rhoeas* (Common Poppy) pollen tubes spatially separated from the vacuole (Franklin-Tong *et al*., 1996). Furthermore, intracellular dye-injection in *Fucus serratus* rhizoids has demonstrated elemental Ca^{2+} release closely correlating with the distribution of the endoplasmic reticulum (ER) (Goddard *et al*., 2000). It is no surprise then that Ca^{2+}-permeable channels have also been identified in this organelle. As well as a DACC, which shows increased activity due to cytoplasmic alkalinisation, vesicular flux assays have indicated that the

ER membrane contains a Ca^{2+}-permeable channel gated by nicotinic acid adenine dinucleotide phosphate (NAADP); a molecule first identified as a calcium agonist in sea urchin eggs (Navazio *et al*., 2000). Recent studies in animals have indicated that NAADP initiated Ca^{2+} release is amplified by cADPR and IP_3-dependent mechanisms (Guse & Lee, 2008). Whether such a mechanism also occurs in plants is yet to be elucidated.

1.4.5 Encoding information in Ca^{2+}_{cyt} signatures.

The kinetics of Ca^{2+}_{cyt} signatures can be resolved by a number of factors (Trewavas & Malhó, 1998).

- The lag time between a stimulus and initiation of a change in $[Ca^{2+}_{cyt}]$.
- The time to reach peak $[Ca^{2+}_{cyt}]$ once a rise has been initiated.
- The amplitude of peak $[Ca^{2+}_{cyt}]$.
- The duration for which peak $[Ca^{2+}_{cyt}]$ persists.
- The time taken for $[Ca^{2+}_{cyt}]$ to return to basal levels.
- The number of repetitive peaks and troughs in a $[Ca^{2+}_{cyt}]$ signature.
- The spatial location of the elevation in $[Ca^{2+}_{cyt}]$.

The dynamics of $[Ca^{2+}_{cyt}]$ signatures, as induced by a range of biotic and abiotic stimuli, have been investigated in multiple cell and tissue types *in planta* including root hairs, rhizoid cells, pollen tubes and, generally, guard cells (McAinsh *et al*., 1995; Holdaway-Clarke *et al*., 1997; Allen *et al*., 2000; Rudd & Franklin-Tong, 2001). Whilst it is not in the scope of this thesis to explore the detailed kinetics of each of these signatures, reviews by Plieth (2001), Rudd & Franklin-Tong (2001) and Ng *et al.* (2003) cover this area comprehensively.

Ca^{2+}-signatures are believed to act via terminal Ca^{2+} sensors, such as anion channels or via signalling elements such as Ca^{2+}-binding proteins including calmodulins, Ca^{2+}-dependent protein kinases and calcineurin B-like proteins. These signalling elements proliferate further molecular interactions, which commonly include cascades of protein phosphorylation / dephosphorylation, and modulate the elicitation of numerous acute and chronic physiological responses including fertilisation, stomatal closure, gravitropism, fructan

synthesis and acclimation (Cousson & Vavasseur, 1998; Knight *et al*., 1998; Antoine *et al*., 2000; MacRobbie, 2000; Luan *et al*., 2002).

Although the 'molecular relays' triggered by elevations in [Ca^{2+}_{cyt}] trigger numerous physiological responses, proof that [Ca^{2+}_{cyt}] signatures end code information that is subsequently decoded has been difficult to obtain (Scrase-Field & Knight, 2003).

It has been speculated that [Ca^{2+}_{cyt}] transients may act merely as a switch, allowing a pre-programmed response to occur rather than directly encoding a specific response (Scrase-Field & Knight, 2003). A number of arguments have been put forward to support this hypothesis.

Firstly, whilst stimuli such as salt stress and osmotic stress generate [Ca^{2+}_{cyt}] signatures that appear spatially and temporally similar at the single cell and whole plant level, each challenge activates transcription of distinct sets of downstream genes (Knight *et al*., 1997; Kiegle *et al*., 2000; Scrase-Field & Knight, 2003). However, given that [Ca^{2+}_{cyt}] imaging techniques are never likely to be as sensitive as the Ca^{2+} responsive machinery of the cell, it appears certain that subtle variations in the [Ca^{2+}_{cyt}] signatures generated by each stimulus may go detected. Indeed, recent work in animals indicates that it is microdomain specific elevations of [Ca^{2+}_{cyt}] which are responsible for regulating changes in gene expression, whilst larger scale elevations merely serve to seed these spatially restricted phenomena (Di Capite *et al*., 2009).

Secondly, It has been argued that in a system where [Ca^{2+}_{cyt}] signatures truly encode information, distinct signatures should lead to distinct responses (Scrase-Field & Knight, 2003). However, although cold and osmotic stresses induce activation of a largely overlapping set of genes, the [Ca^{2+}_{cyt}] signatures generated by these stimuli are quite distinct, with cold stress leading to a biphasic peak in [Ca^{2+}_{cyt}] and osmotic stress inducing a root-specific single peak (Scrase-Field & Knight, 2003). Although the encoding of similar responses via broadly different signatures may appear counter-intuitive, no persuasive arguments have yet been put forward to suggest that plants cannot employ mechanisms whereby two very different, information containing signals cannot converge on similar downstream targets. Additionally, if it is the case that microdomain specific elevations of [Ca^{2+}_{cyt}] are responsible for regulating changes in gene expression (Di Capite *et al*., 2009), then similarities in [Ca^{2+}]

within these microdomains may easily be over shadowed by large changes in global [Ca^{2+}_{cyt}].

Thirdly, given that apparently subtle alterations in local [Ca^{2+}_{cyt}] may govern the elicitation of discrete downstream responses, it would appear logical that non-specific calcium release should not induce specific programmed responses. In guard cells, 'burst' release of caged Ca^{2+} or IP_3 produce [Ca^{2+}_{cyt}] transients highly dissimilar to those generated endogenously. However stomatal closure is still elicited (Gilroy *et al*., 1990). Indeed, burst release of calcium agonists have been shown to trigger a range of different responses dependent upon species and tissue type (Scrase-Field & Knight, 2003). Such an experiment would appear to show that an elevation in [Ca^{2+}_{cyt}] merely allows the activation of a response, rather than dictating the response itself (Scrase-Field & Knight, 2003). However, it is interesting that, within a species and cell type, burst release of calcium agonists are reported to consistently generate the same end response. This may indicate that disordered elevations in [Ca^{2+}_{cyt}] may signal a catastrophic or unexpected event, triggering a default response conferring the greatest likelihood of survival.

Given the ambiguity surrounding the true role of [Ca^{2+}_{cyt}] signatures Rushton & Knight (2006) have suggested that in order to attribute specific downstream responses entirely to the precise kinetics of a [Ca^{2+}_{cyt}] signature, it is necessary to artificially generate such signatures in the absence of their corresponding stimuli.

The relatively few reported attempts at imposing such artificial [Ca^{2+}_{cyt}] oscillations have focused on the guard cell as system of choice. In both *A. thaliana* and *Vicia faba*, artificial transients have been produced by repetitive incubation of epidermal strips in high-Ca^{2+} depolarising and low-Ca^{2+} hyperpolarising buffers and were found to trigger stomatal closure (Allen *et al*., 2000; 2001; Li *et al*., 2004b). Importantly, the amplitude, frequency and period of the transients directly corresponded with the degree of stomatal closure indicating that all three features encode information specific to the downstream process. Additionally, in *V. faba* the total number of transients was found to directly correspond to the length of time the stomata remained closed. Moreover, whilst the number of transients inducing the maximum period of stomatal closure remained unchanged across three different phases of stomatal

growth, the optimal period-length of transients varied for each growth stage (Li *et al*., 2004b).

These experiments clearly show that [Ca^{2+}_{cyt}] signatures encode specific information which can be decoded to activate and modulate fixed end responses. However, quantifying whether such signatures can encode information that determines fully segregated end responses (specificity), remains to be established (Scrase-Field & Knight, 2003).

External modulation of [Ca^{2+}_{cyt}] using depolarising and hyperpolarising buffers is unlikely to precisely mimic a [Ca^{2+}_{cyt}] signature elicited by an exogenous stimulus. It is likely therefore that future research to determine specificity in [Ca^{2+}_{cyt}] signalling will rely on more powerful methodologies such as intracellular Ca^{2+} release combined with increasingly sophisticated imaging techniques.

1.4.6 Circadian Ca^{2+}_{cyt} rhythms.

In addition to the multiple stimuli which initiate acute changes in [Ca^{2+}_{cyt}], 24-hour oscillations in [Ca^{2+}_{cyt}] have been observed in both *Nicotiana tabaccum* and *A. thaliana*. In *A. thaliana*, these daily [Ca^{2+}_{cyt}] oscillations occur in the 100 to 300 nM range and, following transfer to constant light, maintain phase, shape and amplitude characteristics comparable to those observed under diurnal conditions (Love *et al.*, 2004).

Although not yet having a defined role in circadian signalling, circadian [Ca^{2+}_{cyt}] oscillations encode information regarding both photoperiod and light-quality. Under short days, [Ca^{2+}_{cyt}] increases throughout the photophase, peaking just prior to dusk and falling sharply to a basal low throughout the night. Under long days, [Ca^{2+}_{cyt}] rises following dawn before plateauing and returning to basal levels prior to nightfall (Love *et al.*, 2004). Increasing fluence affects the amplitude and shape of the entrained oscillation, however period and phase remain unaffected (Love *et al.*, 2004; Xu *et al.*, 2007). Mutant analyses have indicated that the cryptochromes act to regulate basal [Ca^{2+}_{cyt}], whilst PHYB influences peak amplitude of the [Ca^{2+}_{cyt}] oscillations (Xu *et al.*, 2007).

Mathematical simulations suggest that, upon transition to light, photoreceptors trigger acute accumulation of Ca^{2+}_{cyt}, whilst the circadian oscillator provides longer acting regulation which acts to extend the period of increase (Robertson *et al*., 2007). The core oscillator may contribute to regulation of circadian

[Ca^{2+}_{cyt}] rhythms via rhythmic modulation of photoreceptor levels (Fankhauser & Staiger, 2002). However it is unlikely that this process accounts for the entirety of circadian control over [Ca^{2+}_{cyt}]. It is equally as unlikely that [Ca^{2+}_{cyt}] rhythms are generated via interactions between Ca^{2+}-permeable channels and the primarily nuclear components of the core-oscillator (Webb, 2003). It is therefore probable that the clock regulates expression of genes whose products or substrates function to modulate [Ca^{2+}_{cyt}] in a circadian manner. As described in section 1.4.4, cADPR stimulates influx of Ca^{2+} from internal stores to the cystosol. ADENSINE DIPHOSPHATE RIBOSE CYCLASE synthesises cADPR in a circadian manner and inhibition of this enzyme strongly reduces circadian [Ca^{2+}_{cyt}] rhythms. It has therefore been suggested cADPR is the principle means by which circadian Ca^{2+}_{cyt} release is orchestrated (Dodd *et al*., 2007). The role of internal stores as primary sites of mobilisation for circadian Ca^{2+}_{cyt} is also supported, as gadolinium chloride ($GdCl_3$), which disrupts extracellular Ca^{2+} influx, does not alter circadian oscillations of [Ca^{2+}_{cyt}] (Dodd *et al*., 2007).

In *A. thaliana*, circadian [Ca^{2+}_{cyt}] oscillations require functional *CCA/LHY* to retain rhythmicity and have FRPs approximating those of other circadian regulated outputs such as *CAB2*. These features strongly indicate that [Ca^{2+}_{cyt}] is modulated by the primary cellular oscillator (Xu *et al.*, 2007). The situation is complicated however; following transfer to constant darkness *CAB2* oscillations continue, whereas [Ca^{2+}_{cyt}] rhythms disappear (Xu *et al.*, 2007). Upon returning the seedlings to constant light, [Ca^{2+}_{cyt}] rhythms spontaneously reappear and show a circadian phase matching those observed before transfer to darkness. It appears therefore, that a light-dependent mechanism is necessary for the maintenance of [Ca^{2+}_{cyt}] rhythms but unnecessary for maintenance of *CAB2* oscillations (Xu *et al.*, 2007).

Additionally, clock regulated genes in *A. thaliana toc1* mutants display FRPs of 21 to 22 hours whereas [Ca^{2+}_{cyt}] rhythms retain wild-type periods. This rhythmic de-coupling between circadian transcripts and [Ca^{2+}_{cyt}] also occurs in *N. tabaccum* (Johnson *et al.*, 1995; Xu *et al.*, 2007). One implication of these observations is that rhythms of transcript and [Ca^{2+}_{cyt}] may be controlled by separate oscillators. However, as previously discussed, the proposed structure of the central oscillator is composed of multiple interlocking loops. It would therefore be interesting to determine if individual loops generate distinct outputs

which may contribute to any disparity between observed [Ca^{2+}_{cyt}] and transcript rhythmicities.

Circadian [Ca^{2+}_{cyt}] rhythms may encode photoperiodic information and may act as output from, or inputs back into, the central oscillator. Given the nuclear localisation of the known core clock components and absence of nuclear Ca^{2+} rhythms, it appears unlikely that [Ca^{2+}] rhythms play a role as a direct input to the clock (Dodd *et al.*, 2005a; Wood *et al.*, 2001). However, re-localisation of cytosolic signalling components to the nucleus resulting from circadian changes in [Ca^{2+}_{cyt}] have not been ruled out as a mechanism by which [Ca^{2+}_{cyt}] may regulate the clock (Dodd *et al.*, 2005a; Wood *et al.*, 2001). Even if acting as a feedback in to the clock, the [Ca^{2+}_{cyt}] signal may serve to transduce photoperiodic information to multiple downstream targets. The most obvious candidates for such targets are processes such as stomatal opening which are known to be regulated both by Ca^{2+} and the clock (Hubbard *et al*., 2007). However, any circadian regulated processes, including photoperiodic flowering, are potential targets of circadian [Ca^{2+}_{cyt}] oscillations.

In addition to changes in [Ca^{2+}_{cyt}], spikes in chloroplastic free calcium concentration ([Ca^{2+}_{chlo}]) occur approximately 15 to 30 minutes after nightfall in both *A. thaliana* and *Nicotiana plumbaginifolia*. It has been speculated that rather than acting as a determinant of day length, these spikes function to signal the transition to darkness (Love *et al.*, 2004; Sai & Johnson, 2002). An internal coincidence between the light-level-dependent [Ca^{2+}_{chlo}] spike and high levels of circadian regulated [Ca^{2+}_{cyt}] at dusk may act as a reinforcing signal that the plant is under short day conditions. In contrast, under long days, the [Ca^{2+}_{chlo}] spike occurs whilst [Ca^{2+}_{cyt}] is basal and may act to reinforce day-length-dependent processes such as photoperiodic flowering (Love *et al.*, 2004; Sai & Johnson, 2002).

Although, it is possible to modulate circadian [Ca^{2+}_{cyt}] signatures either by modifying the light regime under which plants are grown or by generating lesions in components of the circadian oscillator (Johnson *et al*., 1995; Love *et al*., 2004; Xu *et al*., 2007), generation of wholly artificial, plant-wide, circadian [Ca^{2+}_{cyt}] signatures has not yet proved viable. However, less discrete modulation of [Ca^{2+}] has been shown to affect clock-regulated processes including both rhythmic behaviour and photoperiodic-flowering time (Friedman

et al., 1989; Persson *et al.*, 2001). In *Robinia pseudoacacia* (Black Locust tree), the application of exogenous Ca^{2+} or calcium ionophore phase-shifts circadian regulated leaflet movement, whilst in *Pharbitis nil* (Morning Glory), application of the calcium-chelator EGTA directly preceding nightfall retards flowering. *P. nil* is a short-day plant, therefore any delay in flowering is likely explained by artificial depletion of $[Ca^{2+}_{cyt}]$ at nightfall mimicking the presence of long-day photoperiods (Friedman *et al.*, 1989; McClung *et al.*, 2002). In contrast, addition of Ca^{2+} or calcium ionophore before dusk appears to reinforce short-day conditions and results in accelerated flowering.

Modulation of $[Ca^{2+}_{chlo}]$ also affects photoperiodic flowering. Overexpression of the *Pisum sativum* Ca^{2+}_{chlo} transporter PPF1 in *A. thaliana* leads to increased $[Ca^{2+}_{chlo}]$ and a dose-dependent extension of flowering time. In contrast, plants carrying an antisense *PPF1* construct, and having reduced $[Ca^{2+}_{chlo}]$, show accelerated flowering (Li *et al.*, 2004a; Wang *et al.*, 2003). Whilst dramatic alterations in flowering time were associated with changes in $[Ca^{2+}_{chlo}]$, potential alterations in expression patterns of genes coding for clock, flowering-time or calcium-binding proteins have not been examined.

1.4.7 Calmodulin.

Calmodulin (CaM) is both the most abundant and best characterised of the calcium-sensing proteins found in plants, acting as a principal node connecting $[Ca^{2+}]$ with numerous structural and enzymatic proteins (Hoeflich & Ikura, 2002; Popescu *et al.*, 2007).

CaM is a evolutionarily ancient and highly-conserved protein of approximately 148 residues that is essential for eukaryotic life. CaM has a dumbbell-like tertiary structure that contains a pair of globular domains connected by a seven-turn α-helix (figure 1.8). Each lobe contains a pair of linked domains called EF hands comprising a 12 amino-acid helix-turn-helix motif (Babu *et al.*, 1988). Each EF hand co-operatively binds Ca^{2+} with a 1:1 stoichiometry and an affinity (K_D) of approximately 10^{-7} M for the C-terminal Ca^{2+} binding sites and approximately 10^{-6} M for the N-terminal sites (Park *et al.*, 2008; White & Broadley, 2003).

CaM undergoes a conformational change upon binding Ca^{2+} whereby the interhelical angles in the EF hands are altered, inducing a transition from a

'closed' to an 'open' conformation. In the open conformation, conserved methionine residues are exposed, presenting hydrophobic surfaces capable of interacting with numerous target proteins (Nelson & Chazin, 1998; Yang & Poovaiah, 2003).

CaM is predominantly cytosolic, however it is also present at much lower concentrations in organelles including the nucleus, peroxisome and endoplasmic reticulum as well being found in the extracellular matrix (White & Broadley, 2003; Yang & Poovaiah, 2003). CaM is readily diffusible and therefore able to modulate the actions of other proteins, which may be confined to specific regions. CaM has been implicated in Ca^{2+}-dependent signalling for stimuli as diverse as illumination, gravity, oxidative stress and anoxia.

CaM mediated responses include cell proliferation, protein folding, acclimation and motility and occur in all plant organs (Park *et al.*, 2008; Snedden & Fromm, 2001; White & Broadley, 2003).

The *A. thaliana* genome contains seven true *CAM* genes coding for only four separate CaM isoforms. *A. thaliana* CaMs show remarkable sequence conservation, with between one and five conservative substitutions in mostly polar hydrophilic residues (table 1.4).

Table 1.4: *Number of amino acid substitutions between* A. thaliana *CaM isoforms.*

Number of amino acid substitutions between *A. thaliana* CaM isoforms				
Isoform	1/4	2/3/5	6	7
1/4	0	-	-	-
2/3/5	5	0	-	-
6	5	2	0	-
7	4	1	1	0

The maintenance of multiple conserved CaMs indicates strong selective pressure against sequence divergence and probable non-redundancy (McCormack *et al.*, 2005). The presence of single amino acid substitutions in otherwise conserved isoforms also appears to generate slightly altered affinities for Ca^{2+} and protein interaction partners thus offering increased flexibility in the decoding and transduction of Ca^{2+} signals (Rashid, 2004; McCormack *et al.*, 2005). Subtle differences in expression exist between *A. thaliana* CaM isoforms

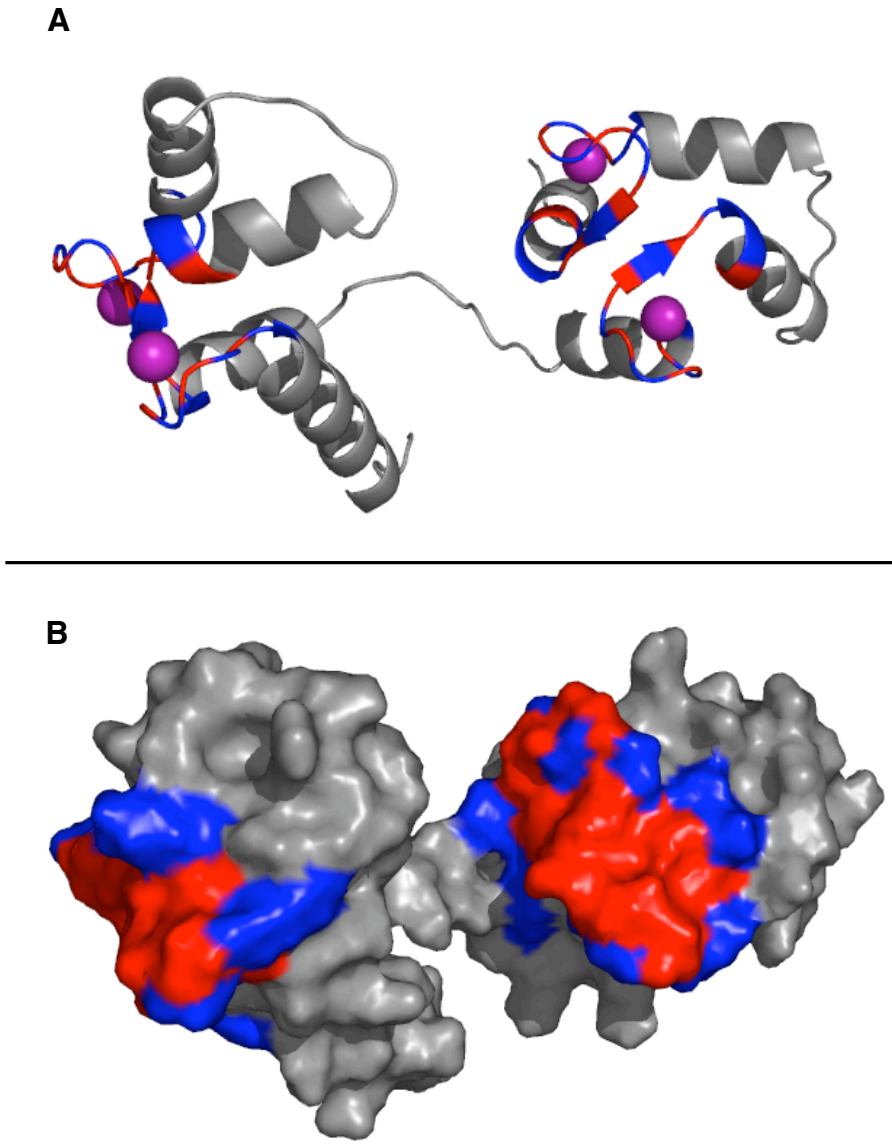

Figure 1.8: The structure of calmodulin.

The structure of calmodulin rendered as ribbon (A) and spacefill (B) diagrams. Residues within the EF-hand motifs contribute to an electronegative environment conducive to Ca^{2+} binding and are shown in blue. Residues within the EF-hands directly interacting with Ca^{2+} are shown in red. Upon binding Ca^{2+} (rendered as purple spheres (A)), CaM undergoes a conformational change resulting in increased α-helical content, inducing a transition from a 'closed' to an 'open' conformation. In the open conformation hydrophobic groups are exposed and present a binding surface to target proteins.

with the closest paralogs having the most similar expression profiles throughout development. Whilst CaMs 1 and 4 are identical in amino acid sequence, only *CAM1* has been observed to undergo circadian oscillation in transcript, probably due to divergence of upstream regulatory elements. Similarly, although CaMs 2, 3 and 5 are identical at the peptide level, *CAM2* is the only member of the family to show upregulated expression due to touch (McCormack & Braam, 2003).

CaM-binding proteins (CaMBPs) in plants show great diversity and have been identified in all compartments and extracellular spaces where CaM is found (Popescu *et al.*, 2007; Snedden & Fromm, 2001). Although apoCaM is one of the most abundant intracellular proteins (occurring at concentrations between 5 and 40 μM), Ca^{2+}-CaM is present only at 'sub-saturating' levels compared to total concentration of all available interaction partners. This sub-saturation, combined with the inherent diversity of interaction partners, leads to competition between CaMBPs for Ca^{2+}-CaM and is believed to act in fine-tuning transduction of Ca^{2+} signatures (Zielinski, 1998). Whilst the exact function of many CaMBPs remains to be elucidated, at least two CaMBPs have been identified as playing a role in the regulation of flowering time. In *P. nil* a Ca^{2+}-dependent protein kinase appears to be involved in transduction of Ca^{2+}-CaM-dependent flowering-time signals and in *N. tabaccum*, a CaM binding protein kinase (CBK) acts as a negative regulator of flowering (Hua *et al.*, 2003; Jaworski, 2003). The tobacco CBK has been shown to phosphorylate Histone IIIS and therefore may affect flowering by the alteration of chromatin condensation (Hua *et al.*, 2003).

In *P. nil,* application of the CaM inhibitors chloropromizine and W7 leads to a delay in photoperiodic flowering (Friedman *et al.*, 1989). As discussed previously, similarly delayed flowering occurs when *P. nil* are treated with the Ca^{2+}-chelator EGTA, strongly indicating that any role [Ca^{2+}] plays in the regulation of photoperiodic flowering is elicited via recruitment of CaM (Friedman *et al.*, 1989).

Whilst similar direct evidence for the involvement of CaMBPs in regulation of flowering time in *A. thaliana* has not been forthcoming, protein microarrays have shown *A. thaliana* CaMs to interact with at least 60 nuclear transcription factors (Popescu *et al.*, 2007). Increases in [Ca^{2+}_{cyt}] cause CaM to translocate in to the

nucleus where it interacts with these DNA-binding proteins to mediate Ca^{2+}_{cyt}-regulated gene expression (Popescu *et al.*, 2007; Snedden & Fromm, 2001). Such CaM mediated, Ca^{2+}_{cyt}-regulated gene expression extends to the self-regulation of *CAM* expression. This form of feedback has been proposed as a regulatory mechanism whereby the application of a particular stimulus leads to acclimation and enhanced transduction of signals generated by similar challenges (Popescu *et al.*, 2007; Snedden & Fromm, 2001).

Whether the stimuli of transition between the light and dark phases of a photoperiod affects expression of *CAM* via such a self-regulatory mechanism is unknown. If such an effect were to occur however, it could conceivably act to enhance the transduction of any signal encoded in the daylength-dependent circadian $[Ca^{2+}_{cyt}]$ oscillations discussed previously.

1.5 Hypothesis and Project Outline

This study was conducted to test the hypothesis that calmodulin (CaM) transduces photoperiodic information encoded within circadian regulated calcium signals, either as a feedback to the endogenous oscillator or directly in to the photoperiodic flowering pathway.

Cytoplasmic free calcium (Ca^{2+}_{cyt}) acts as a powerful second messenger, coupling stimulus-specific information to downstream targets and responses (Malhó, 1999). In addition to the acute changes induced by various stimuli, circadian, and day-length specific, oscillations in Ca^{2+}_{cyt} concentration $[Ca^{2+}_{cyt}]$ have also been characterised in *Arabidopsis thaliana*. Given their circadian nature, parsimony suggests that these daily $[Ca^{2+}_{cyt}]$ rhythms may be involved in regulation of, or signalling from, the circadian clock (Gómez and Simón, 1995; Love *et al*., 2004). In plants, the circadian clock regulates numerous seasonally-sensitive, or 'photoperiodic', responses including germination, hypocotyl elongation, branching and storage organ formation. However, the most obvious and most well investigated photoperiodic response is the transition to flowering (Koukkari and Sothern, 2006). Consequently, if photoperiodic information present in circadian $[Ca^{2+}_{cyt}]$ rhythms were decoded floral induction would be a likely target.

In plants, calmodulin (CaM) acts as the primary calcium sensing protein and connects $[Ca^{2+}_{cyt}]$ oscillations with numerous target proteins (Popescu *et al.*,

2007). Consequently, CaM is likely to be involved in any mechanism whereby circadian [Ca^{2+}_{cyt}] rhythms are decoded and act to modulate photoperiodic flowering. In the short-day plant *Pharbitis nil* (Morning Glory), inhibition of CaM delays flowering, apparently mimicking a long-day photoperiod. The molecular bases behind such changes remain unstudied however (Friedman *et al.*, 1989).

In *A. thaliana,* however, where photoperiod-dependent oscillations in [Ca^{2+}_{cyt}] have been observed, there is currently no published data addressing the involvement of CaM in the transduction of circadian signals and modulation of photoperiodic flowering. This study investigated several strategies to comprehensively address this question.

Firstly, a pharmacological approach to assess the effects of CaM inhibition on photoperiodic flowering was undertaken. *A. thaliana* were treated daily with inhibitors at concentrations which had been experimentally optimised in order to minimise secondary effects. mRNA was isolated from plants harvested over a 28-hour time-course and qRT-PCR was used to quantify changes in expression of genes of interest in the circadian clock and photoperiodic-flowering pathway. In order to connect the molecular effects of CaM inhibition recorded via qRT-PCR with the resultant physiological effects, flowering times in control and inhibitor treated plants was also analysed under long and short-day photoperiods.

Chemical inhibitors of CaM are difficult to apply evenly and are known to confer unwanted secondary effects even at relatively low concentrations (Jan & Tseng, 2000a, 2000b; Lin & Rydqvist, 2000). To counter these constraints, a second approach involving the development of a peptide inhibitor of calmodulin comprising a Green Fluorescent Protein / calspermin fusion and labelled smGN was pursued. Surface plasmon resonance and affinity chromatography studies were undertaken to determine the kinetics and specificity of the interaction between smGN and CaM.

Finally, *A. thaliana* was transformed with the *smGN* transgene under the control of a glucocorticoid inducible promoter in order to provide tightly controlled intracellular inhibition of CaM whilst negating the negative side effects inherent with pharmacological CaM inhibitors.

CHAPTER 2: MATERIALS AND METHODS

Materials

2.1.1 Antibiotics.

Antibiotics were obtained from several suppliers. Stock solutions were prepared to the given concentrations and stored as shown in table 2.1.

Table 2.1: *Antibiotics.*

Name	1000 X stock concentration	Solvent	Storage	Source
Ampicillin	100 mg ml^{-1}	ddH_2O	-20 °C	Roche
Cefotaxime	100 mg ml^{-1}	ddH_2O	-20 °C	Sigma
Hygromycin*	50 mg ml^{-1}	HEPES† pH 7.0	4 °C	Invitrogen
Kanamycin	50 mg ml^{-1}	ddH_2O	-20 °C	Sigma
Rifampicin	50 mg ml^{-1}	Dimethylsulphoxide (DMSO)	-20 °C	Sigma

* Purchased as pre-dissolved stock.
† 4-(2-hydroxyethyl)-1-piperazineethanesulphonic acid

2.1.2 Synthetic oligonucleotides.

Primers for amplification or verification of target DNA sequences were supplied by Invitrogen (table 2.2). Lyophilised primers were dissolved to 100 mM stock solution in nuclease free water.

Predesigned QuantiTect primers for quantitative Real Time-PCR (qRT-PCR) were obtained from Qiagen and made to 5 X stocks in nuclease free water following manufacturers recommendations. Sequences of Quantitect primers are not provided by the manufacturer.

Table 2.2: *Known primer sequences.*

Gene name	Direction	Primer sequence
smGN	5’	ACA GCC ATG GCA ATG AGT AAA GGA GAA CTT TTC ACT GG
smGN	3’	AAC CCC GGG TTA GTA CTC TGG CAG AAT AGC ATC CTG

2.1.3 Vectors.

The glucocorticoid-inducible, binary vector pINDEX3 (Ouwerkerk *et al.*, 2001) (figure 2.1), was used for all *in planta* expression studies.

2.1.4 Microbial strains.

2.1.4.1 Escherichia coli.

For propagation of plasmids, chemically competent *E. coli* MAX Efficiency DH5-α Competent Cells (Invitrogen) were used.

For transformation with ligation products, One Shot® OmniMAX^{TM} 2 T1 *E. coli* (Invitrogen), were used.

2.1.4.2 Agrobacterium tumefaciens.

Agrobacterium tumefaciens strain GV3101 was used for all transformations of *Arabidopsis thaliana*.

2.1.5 Arabidopsis thaliana *Ecotypes and Lines.*

Seed of *A. thaliana* Columbia 0 (Col 0) expressing cytosolic recombinant *Victoria aquoria* aequorin under the control of the constitutive strong Cauliflower mosaic virus 35S promoter (35S::*aequorin*$_{(cyt)}$) were a kind gift from Professor Marc Knight (School of Biological and Biomedical Sciences, Durham University, UK). Seed of *A. thaliana* Col 0 mutant *Spa1-3* (SUPPRESSOR OF PHYA-105) (AT2G46340) were generously donated by Professor Ute Höecker (Botanisches Institut, Universität zu Köln, Germany).

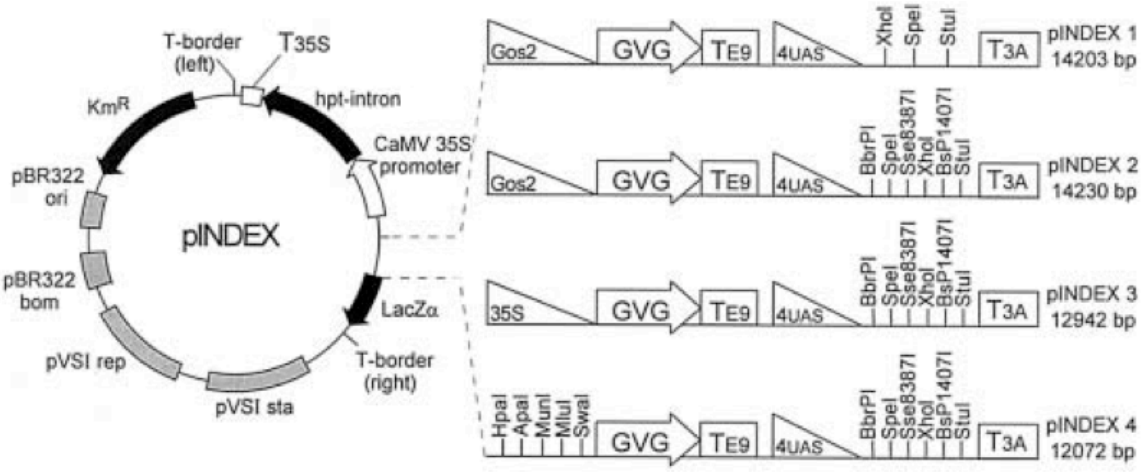

Figure 2.1: Map of the pINDEX family of vectors (from Ouwerkerk *et al.*, 2001).

pINDEX3 is a plant binary expression vector containing a chimaeric transcriptional activator (GVG) comprising the Gal4 DNA binding domain from yeast, the *Herpes simplex* VP16 transactivation domain and the rat Glucocorticoid receptor regulatory domain. The plasmid confers bacterial kanamycin and plant hygromycin resistance. Expression of a transgene is dependant upon the addition of a glucocorticoid such as dexamethasone. Unique restriction sites are labelled.

2.1 Methods

2.2.1 Polymerase Chain Reaction.

Taq DNA polymerase (Promega, UK), was used for diagnostic PCR. Reaction constituents and thermal cycling conditions are shown in tables 2.3 and 2.4. All reactions were prepared on ice and performed using a G-Storm GS1 thermocycler (Gene Technologies, UK).

Table 2.3: *Diagnostic PCR reactions.*

Constituent	µl per digest	Final concentration
5 X Reaction buffer	10	1
dNTPs (10 mM each)	0.8	200 µM each
Forward Primer (10 µM)	2	0.4 µM
Reverse Primer (10 µM)	2	0.4 µM
Taq polymerase (5 U μl^{-1})	0.5	2.5 U
Template (≈ 200 ng μl^{-1})	2	(≈ 4 ng μl^{-1})
ddH_2O	33.2	-
Total volume:	50	-

Table 2.4: *Thermal cycling conditions for diagnostic PCR reactions.*

Step	Temperature	Time	Number of cycles
Initial denaturation	95°C	60 seconds	1
Denaturation	95°C	30 seconds	
Annealing	2.5°C below primer T_m	40 seconds	30
Extension	72°C	1 minute per kb	
Final extension	72°C	2 minutes	1
Soak	4°C	-	1

2.2.2 Restriction endonuclease DNA digests.

All restriction digests involved enzymes with optimum activity at 37 °C and were incubated for two to five hours. Representative conditions for a digest using a single restriction endonuclease are shown in table 2.5.

Table 2.5: *DNA Digests.*

Constituent	µl per digest	Final concentration
Plasmid DNA or PCR product	4 - 10	1 µg
Restriction endonuclease	0.3 - 1	3 - 10 U
BSA 10 X (1 mg ml^{-1})	0 or 4*	0 or 4 µg
Buffer 10 X	4	1 X
ddH_2O	21 - 31.7	
Total volume:	40	-

* dependent on enzyme

For digests involving two restriction endonucleases, a single compatible buffer was selected. Where compatible buffers were not available, a digest utilising a single restriction endonuclease was performed. The DNA was then PCR-purified by ethanol precipitation (section 2.2.3) and a digestion with the second restriction endonuclease performed.

2.2.3 Ethanol precipitation of DNA.

0.1 volumes of 3 M sodium acetate (NaAc) (pH 5.2) and 2.5 volumes of ice cold 100% ethanol were added to DNA solutions and frozen in liquid nitrogen. DNA was precipitated by centrifugation at 16,000g for 30 minutes at 4 °C.

The supernatant was removed and 1 ml ice-cold 75% ethanol added. The solution was incubated on ice for five minutes and centrifuged at 16,000g for one minute at 4 °C. Pelleted DNA was re-dissolved in nuclease-free water.

2.2.4 Blunt-ending of DNA restriction fragments.

DNA digests were purified by ethanol precipitation and redissolved in 40 µl volumes containing 2 U Pfu DNA polymerase (Promega), 1 X (final volume) buffer and 800 µM dNTPs. Reactions were conducted for 20 minutes at 72 °C before DNA was recovered by ethanol precipitation.

2.2.5 Dephosphorylation of digested DNA.

1U Shrimp Alkaline Phosphatase (SAP) and 1 X dephosphorylation buffer (final concentration) was added to digested DNA with 5' protruding ends and left to incubate for ten minutes. For blunt end digests, 5 U SAP was added and the reaction allowed to proceed at 37 °C for 30 minutes.

SAP was heat inactivated by incubation at 65 °C for 15 minutes.

2.2.6 DNA ligations

Typical ligation reactions were prepared on ice as shown in table 2.6. Ligations involving cohesive ends were incubated at 15 °C overnight. Ligations involving blunt-end inserts were incubated at 4 °C for 24 to 36 hours.

Table 2.6: *Ligation reactions.*

Constituent	µl per digest	Final concentration
T4 DNA ligase (1 U μl^{-1})	1	1 U
10 X ligase buffer	1	1 X
Cut vector	0.5	5 ng μl^{-1}
Insert	0.3 - 0.6	3:1 / 6:1 molar ratio to vector
ddH_2O	7	-
Total volume:	10	-

2.2.7 Agarose gel electrophoresis of DNA.

50 X Tris/acetate/EDTA (TAE) buffer for DNA gel electrophoresis

2 M Tris(hydroxymethyl)aminomethane (Tris base), pH 8.0
50 mM ethylenediaminetetraaceticacid (EDTA) -sodium-salt
1 M acetic acid
In ddH_2O

TAE was filtered, autoclaved and stored at room temperature.

6 X DNA loading buffer for gel electrophoresis

0.25% (w/v) bromophenol blue
0.25% (w/v) xylene cyanol FF
15% (v/v) Ficol™ (Pharmacia, UK)
In ddH_2O

DNA loading buffer was stored at 4 °C.

0.35g of agarose was added to 50 ml 1 X TAE, dissolved by boiling and 0.2 µg of ethidium bromide added when the solution had sufficiently cooled. DNA samples were diluted with 20% (v/v) DNA loading buffer before loading on to the gel. For analytical gels, 5 µl of HYPERLADDER I (Bioline, UK) was loaded as a DNA standard. Gels were run in 1 X TAE at 50 mA for approximately 40 to 60 minutes. DNA bands were visualised under ultraviolet (UV) light.

2.2.8 DNA purification from TAE-agarose gels.

DNA was recovered from agarose gel slices using a QIAquick gel extraction kit (Qiagen, UK) or a Wizard SV Gel and PCR Cleanup Kit (Promega) according to manufacturers directions.

2.2.9 Agarose gel electrophoresis of RNA.

50 X MOPS buffer for RNA gel electrophoresis

1 M 3-(N-morpholino)propansulphonic acid (MOPS), pH 7.0
0.25 M sodium citrate
50 mM EDTA-sodium-salt
In ddH_2O

50 X MOPS was filtered and autoclaved and stored at 4 ^oC.

2 X RNA Sample loading buffer

1X MOPS buffer
60% (v/v) formamide
6.6% (v/v) formaldehyde
0.02% (v/v) xylene cyanol F
0.02% (v/v) bromophenol blue
50 $\mu g \cdot ml^{-1}$ ethidium bromide

Sample loading buffer was stored at 4 ^oC.

1.3 g / 100 ml of agarose was added to 40 ml (80% final gel volume) 1 X MOPS and dissolved by boiling. When solutions had cooled sufficiently 6.6% final gel volume formaldehyde was added to the gel and made up to 50 ml with nuclease free ddH_2O.

2 µg of RNA per sample was added to 10 µl 2 X RNA sample loading buffer and the final volume made up to 20 µl. Samples were incubated at 65 ^oC for ten minutes before loading on to the gel.

Gels were run under 1 X MOPS buffer, at 30 mA for approximately three hours. RNA bands were visualised under UV light.

2.2.10 Polyacrylamide gel electrophoresis (PAGE) of proteins.

NUPAGE® 4 - 12% Bis-Tris gels, 4 X LDS protein loading buffer, 20 X MOPS running buffer, 400 X antioxidant 10 X protein reducing agent and SimplyBlue SafeStain were purchased from Invitrogen.

SDS-PAGE gel destain.

12.5% (v/v) isopropanol
10% (v/v) acetic acid
In ddH_2O

Gel destain was stored at room temperature.

Protein samples were diluted with 40% (v/v) LDS loading buffer, and 16% (v/v) sample reducing agent and incubated for ten minutes at 65 ^{o}C before being loaded on to the gel. Gels were placed in a XCell SureLock® Mini-Cell (Invitrogen) under 1 X MOPS buffer at 100 V until the dye front had migrated in to the 12% acrylamide portion of the gel. Gels were removed and stained using SimplyBlue SafeStain (Invitrogen) according to the manufacturers staining protocol.

Gels were imaged with a VDS Image Master (Amersham Pharmacia Biotech, UK) or with a Canon LidoScan 600 (Canon, UK).

2.2.11 Protein immunodetection.

Transfer buffer for Western blot.

5% (v/v) 20 X NuPAGE® Transfer Buffer (Invitrogen, UK)
0.1% (v/v) NuPAGE® Antioxidant
20% (v/v) methanol
In ddH_2O

The solution was used immediately.

10 X phosphate buffered saline (PBS).

1.5 M NaCl
0.162 M Na_2HPO_4
0.038 M NaH_2PO_4
In ddH_2O

The pH was adjusted to 7.4 with 1.0 M hydrochloric acid (HCl)

PBS was autoclaved and stored at room temperature.

Phosphate buffered saline-Tween 20 (PBST).

1 X PBS
0.1% (v/v) Tween 20

PBST was used immediately.

Membrane blocking buffer.

10% (w/v) non-fat milk powder
In 1 x PBST

Membrane blocking buffer was used immediately.

Ponceau S staining solution.

0.1% (w/v) Ponceau S
5% (v/v) acetic acid
In ddH_2O

Staining solution was used immediately.

Chromogenic substrate solution for alkaline phosphatase detection.

100 mM Tris-HCl
5 mM $MgCl_2$
0.35 mM 5-bromo-4-chloro-3-indolyl phosphate (Pierce, UK)
0.35 mM nitro blue tetrazolium (Pierce, UK)
In ddH_2O

The pH was adjusted to 9.5 with 1.0 M Potassium Hydroxide (KOH) and the solution was used immediately.

Following electrophoresis, the SDS-PAGE gel was transferred to an XCell II blot module (Invitrogen) and run over night at 9 V and at 4 ^{o}C in order to transfer the protein to a PVDF membrane.

2.2.12 Reversible staining of PVDF membranes.

PVDF membrane was incubated in Ponceau S solution for five minutes and excess stain removed by brief immersion in ddH_2O. Temporary staining was reversed by washing the membrane in 7.5% (v/v) methanol and 10% (v/v) acetic acid.

2.2.13 Immunodetection.

PVDF membranes were transferred to blocking buffer for one hour and given two ten-minute washes in PBST. Membranes were then incubated for one hour in 0.5 X blocking buffer containing the primary antibody. Unbound antibody was removed by washing in PBST and membranes transferred to 0.5 X blocking buffer containing the secondary-antibody Alkaline Phosphatase Conjugate for one hour. Membranes were washed in PBST and transferred to 10 ml chromogenic substrate solution for ten minutes.

Membranes were imaged using a Canon LidoScan 600.

2.2.14 Growth of Escherichia coli.

Luria Bertani (LB) broth.

1% (w/v) bacto-tryptone
0.5% (w/v) yeast extract
0.5% (w/v) NaCl
In ddH_2O

LB broth was adjusted to pH 7.4 with 1.0 M KOH and autoclaved.

For solid medium 2% (w/v) Number 2 agar (Oxoid, UK) was added to the broth.

SOC medium for rescue of transformed *E. coli.*

2% (w/v) bacto-tryptone
0.5% (w/v) yeast extract
0.058% (w/v) NaCl
In ddH_2O

SOC was adjusted to pH 7.0 with 1.0 M KOH and the medium autoclaved.
Once the medium had cooled below 50 ^oC, 2% (by final volume) of sterile 1 M glucose was added.
0.5% (by final volume) of sterile 2 M $MgCl_2$ was added immediately prior to use,

2.2.14.1 Culture on solid medium.

E. coli were plated on to LB-agar containing appropriate antibiotics (table 2.1) and incubated overnight at 37 ^oC to allow development of colonies.

2.2.14.2 Culture in liquid medium.

Using sterile microbiological practice, an isolated bacterial colony was picked from solid culture an inoculated in to a 2 L flask of 400 ml LB broth containing appropriate antibiotics. Unless otherwise stated cultures were incubated at 37 ^oC with orbital shaking at 200 rpm overnight.

2.2.15 Transformation of Escherichia coli.

20 ng of plasmid DNA or 100 to 200 ng DNA from a ligation reaction was added to 40 µl aliquots of chemically competent *E. coli*. Samples were incubated on ice for 30 minutes before being placed in a water bath at 42 ^oC for 30 seconds and returned to ice for a further two minutes. 0.5 ml of SOC was added and the samples were incubated at 37 ^oC for 60 minutes. 50 to 150 µl of the cells were plated on LB-agar containing appropriate antibiotics and incubated overnight at 37 °C.

2.2.16 Purification of plasmids from Escherichia coli.

Small-scale purification (up to 15 µg) of plasmid DNA was performed using the QIAprep Spin Miniprep Kit (Qiagen) according to manufacturers recommendations. Plasmid purity was determined by standard spectrophotometric readings.

2.2.17 Cultivation of Arabidopsis thaliana.

2.2.17.1 Sterile growth medium.

0.5 X Murashage and Skoog (MS) medium for *A. thaliana* cultivation.
0.6% (w/v) Phytogel (Sigma)
0.215% (w/v) MS salts with B vitamins (Duchefa, NL)
0.5% (w/v) tryptone
0.5% (w/v) sucrose
In ddH_2O

MS medium was adjusted to pH 5.9 with 1.0 M KOH and autoclaved.

Appropriate antibiotics, inhibitors or control solutions were added immediately prior to pouring.

2.2.17.2 Routine plant growth conditions.

All *A. thaliana* were grown under cool fluorescent white light at 20 ^{o}C (L36W/30, Osram, Germany) at fluence rates of 30 or 60 µmol m^{-2} s^{-1}.

2.2.18 Transformation of Arabidopsis thaliana.

YEB medium for general *A. tumefaciens* growth.
0.5% (w/v) beef extract
0.5% (w/v) bacto-tryptone
0.5% (w/v) sucrose
0.1%(w/v) yeast extract
In ddH_2O

YEB was adjusted to pH 7.0 with 1.0 M KOH.

For solid medium, the recipe was supplemented 2.0% (w/v) Number 2 agar.

Appropriate antibiotics were added immediately prior to pouring.

Electrocompetence buffer for *Agrobacterium*.
1 mM HEPES (pH 7.5)
10% glycerol
The Buffer was filter sterilised and stored at room temperature.

Modified infiltration medium for inoculation of *A. thaliana.*
5% (w/v) sucrose
0.4% (w/v) ascorbic acid
0.215% (w/v) MS salts with B vitamins
0.044 M benzylamino purine (BAP)
0.02% Silwet L-77

2.2.18.1 Preparation of electrocompetent Agrobacterium.

A single colony of *A. tumefaciens* GV3101 was inoculated into 10 ml YEB containing 50 µg ml^{-1} rifampicin and shaken (200 rpm) for 36 hours. 250 ml YEB was inoculated with 2 ml of the starter culture and shaken at 28 °C until mid log phase (OD_{600} = 0.4 to 0.6). The culture was centrifuged for five minutes at 4,000g at 4 °C, supernatant removed and cells washed in 15 ml ice-cold electrocompetence buffer. Cells were re-centrifuged, resuspended in 2 ml electrocompetence buffer and dispensed in 50 µl aliquots for storage at -80 °C.

2.2.18.2 Transformation of electrocompetent Agrobacterium.

100ng plasmid DNA was added to aliquots of electrocompetent *A. tumefaciens* GV3101 and incubated for 15 minutes on ice. Aliquots were transferred to pre-chilled 2 mm electroporation cuvettes (Eppendorf, Germany) and electroporated at 2.5 kV, 25 µF and 400 Ω for 9 to 11 µs using an Eppendorf 2510 electroporator (Eppendorf, Germany). 1 ml of ice cold SOC was added and the cuvette was placed on ice for two minutes. The contents of the cuvette were incubated for two hours at 28 °C. 50 to 100 µl of the cells were plated on YEB-agar containing appropriate antibiotics and incubated for 48 hours at 28 °C.

2.2.18.3 Transformation of Arabidopsis thaliana *by floral dipping.*

Plants were sown in compost and grown under a 12L : 12D photoperiod until multiple inflorescences appeared.

400 ml of YEB medium containing the appropriate antibiotics was inoculated with 3 ml of pre-cultured *A. tumefaciens* GV3101 carrying the binary vector pINDEX3 and grown at 28 °C with 180 rpm orbital shaking to OD_{600} = 0.6 to 1.0. Cells were centrifuged at 2,500g for ten minutes and resuspended in 800 ml of modified infiltration medium.

A. thaliana were transformed by submerging the inflorescences for 15 to 40 seconds in the infiltration solution. Plants were placed in darkness overnight before being returned to a 12L : 12D photoperiod (fluence of 60 µmol m^{-2} s^{-1}), to set seed.

2.2.18.4 Selection of transformant Arabidopsis thaliana.

Seed harvested from florally dipped plants was surface sterilised and sown on to 0.5 X MS agar plates containing 50 mg ml^{-1} hygromycin and 100 mg ml^{-1} cefotaxime. Plates were wrapped in foil and left for four days. Seedlings were then transferred to a 12L : 12D photoperiod (60 µmol m^{-2} s^{-1}), for a further 48 hours. Hygromycin resistant seedlings were identified as those having hypocotyls greater than 6 mm and dark green cotyledons. The most vigorous seedlings from each line were transferred to compost and allowed to flower and set seed.

2.2.19 Extraction of proteins from Arabidopsis thaliana

Total-protein was extracted from five grams of ground *A. thaliana* seedlings using the Plant Total Protein Extraction Kit (Sigma). Manufacturers protocols were followed with the exception that the supplied protease inhibitor was substituted with EDTA-Free Halt Protease Inhibitor Cocktail (Pierce). Protein concentration was determined by means of the Bradford assay (Bradford, 1976).

2.2.20 Extraction of nucleic acids from Arabidopsis thaliana.

EB solution for isolation of plant genomic DNA.

100 mM Tris-HCL (pH 8.0)
500 mM NaCl
50 mM EDTA (pH 8.0)
In ddH_2O

EB solution was filter sterilised and stored at room temperature.

10 mM beta-Mercaptoethanol was added directly to the solution before each extraction.

Tris-EDTA buffer.

50mM Tris-HCL
10mM EDTA
In ddH_2O

The buffer was adjusted to pH 8.0 with 1.0 M HCl, filter sterilised and stored at room temperature.

2.2.20.1 Extraction of genomic DNA from Arabidopsis thaliana.

200 mg samples of *A. thaliana* leaf tissue were ground under liquid nitrogen, and placed in pre-chilled 1.5 ml microcentrifuge tubes containing 0.75 ml EB solution. 50 µl sodium dodecyl sulphate (SDS) was added, and the tubes were incubated at 60 °C for 15 minutes. 250 µl of 5 M NaAc (pH 5.2) was added and the tubes transferred to ice for 30 minutes. The samples were centrifuged at 20,000g at 4 °C, for 20 minutes and the supernatant transferred to fresh tubes containing 0.75 ml isopropanol. DNA was precipitated by incubation at -20 °C for one hour followed by centrifugation at 20,000g at 4 °C, for 20 minutes. The isopropanol was removed and the pellets were re-dissolved in 0.5 ml 2 M LiCl and incubated on ice for three hours. RNA was removed by centrifugation at 20,000g and 4 °C, for 20 minutes. DNA was recovered by ethanol precipitation (section 2.2.3).

2.2.20.2 RNA extraction from Arabidopsis thaliana.

Total RNA was extracted using Concert^{TM} Plant RNA Reagent (Invitrogen) according to the manufacturers protocol. RNA purity was determined by standard spectrophotometric readings.

2.2.21 cDNA synthesis from Arabidopsis thaliana *mRNA.*

The SuperScript III first strand cDNA synthesis kit (Invitrogen) was used for reverse transcription of isolated RNA following the manufacturers protocol. Synthesised cDNA was used immediately or stored at -20 °C.

2.2.22 Pharmacological calmodulin-inhibitor dose-response assays.

A dose-response assay was undertaken to determine optimal concentrations of the potent calmodulin (CaM) inhibitors N-(6-aminohexyl)-5-chloro-1-naphthalenesulphonamide (W7) and Calmidazolium (CMZ) for use in subsequent experiments. The less active analogue of W7, N-(6-Aminohexyl)-1-naphthalenesulphonamide (W5) was also utilised as a comparison to treatment with W7. All inhibitors were dissolved in DMSO and final concentrations of the DMSO solvent in each treatment were adjusted to be equal (0.1%).

The optimum concentration of W7 and CMZ was defined as the maximum concentration at which an inhibitor did not induce changes in gross root

morphology or growth. The initial concentration range of inhibitors (table 2.7) was determined by centring on commonly utilised concentrations as determined by a literature review (Gardner *et al.*, 2006; Jan & Tseng, 2000a, 2000b; Sengupta *et al.*, 2007; Si & Olds-Clarke, 2000). 0.5 X MS agar plates containing inhibitors or controls were prepared, and fifteen surface sterilised *A. thaliana* 35S::*aequorin*$_{(cyt)}$ seed were equidistantly placed. Seedlings were grown vertically for 14 days under 60 µmol m^{-2} s^{-1} white light in a 16L : 8D photoperiod. For each experimental population mean root length and mean lateral root number were calculated together with the standard error of the mean.

Table 2.7: *Calmodulin inhibitor dose-response assays*.

Inhibitor	Function	Concentrations utilised (µM)
W7	Napthalene-sulphonamide CaM Inhibitor	0, 10, 20, 30, 40, 50, 60, 80, 100, 125, 150, 200
W5	Reduced affinity analogue of W7	
Calmidazolium	Substituted imidazole CaM Inhibitor	0, 0.1, 0.25, 0.5, 1, 1.5, 2, 4, 5, 10

2.2.23 Confocal microscopy of Arabidopsis thaliana *roots.*

In order to determine whether differences in root development were due to changes in the gross morphology of the root elongation zone, five to eight primary roots from each treatment were examined using a LSM 510 Laser Confocal Scanning Microscope (Zeiss, Germany) and a 40 X oil immersion lens. Roots were incubated for ten minutes in 1.2 ml of the cell-wall stain calcofluor-white (350 µM) (Calbiochem, UK). Roots were transferred to 1.2 ml of the nuclear stain 7-Aminoactinomycin D (7-AAD) (75 µM) (Invitrogen) and stained for five minutes. Roots were rinsed in 1.2 ml ddH_2O, before being mounted in ddH_2O for imaging.

Calcofluor-white excitation was performed using a 405 nm laser diode. 7-AAD excitation was performed with an 8 mA 543 nm HeNe laser. Emission spectra

were recorded using a 420 to 480 nm band pass filter for calcofluor-white and with a 560 longpass filter for 7-AAD. The length of each visible cell in the root elongation zone was recorded using LSM510 image analysis software.

2.2.24 Determining acclimation of Arabidopsis thaliana to *calmodulin inhibitors.*

Surface sterile 35S::*aequorin*$_{(cyt)}$ seed were germinated under 60 µmol m^{-2} s^{-1} white light in a 12L : 12D photoperiod on 0.5 X MS medium containing either 50 µM W7, 50 µM W5, 1 µM CMZ or a DMSO carrier-solvent control and grown vertically for seven days. Plates were imaged at zero hours using a flat-bed scanner, then rotated 90° and replaced in to the growth cabinet. Plates were re-imaged at five hours, 12 hours and 24 hours. Changes in both mean root length and root angle were recorded.

To compare the acute and chronic effects of CaM inhibition on root gravitropism a further set of seeds were germinated on vertical plates containing only 0.5 X MS medium. After seven days, seedlings were carefully removed and transferred to new vertical 0.5 X MS plates containing 50 µM W7, 50 µM W5, 1 µM CMZ or a 0.1% DMSO control. Changes in root length and root angle were imaged at 5, 12, 24, 36 and 48 hours.

2.2.25 Application of pharmacological calmodulin *inhibitors.*

A. thaliana (35S::*aequorin*$_{(cyt)}$), were germinated on compost in either 16L : 8D or 8L : 16D photoperiods. Once a plant had developed ten true leaves it was sprayed daily at dawn with either 200 µl of H_2O plus 0.1% DMSO, 50 µM W7, 50 µM W5 or 1 µM CMZ using an Aztek-A4309 airbrush (Testors, USA). Aerial tissues of each plant were harvested on day 15, frozen in liquid nitrogen and stored at -80 °C. Harvesting was performed at dawn, and every four hours thereafter, for 28 hours. Three individual replicates consisting of four to seven pooled plants were collected for each treatment. Tissue was ground under liquid nitrogen and RNA extraction and cDNA synthesis performed as indicated previously (section 2.2.21).

2.2.26 Reaction conditions for quantitative Real Time-PCR.

A single-step quantitative Real Time-PCR (qRT-PCR) protocol, whereby mRNA was reverse transcribed immediately preceding the qRT-PCR reaction, was carried out using SensiMix One-Step mastermix (Quantace, UK) according to reaction and cycling conditions in tables 2.8 & 2.9.

A CAS 1200 liquid handling robot (Corbett Robotics, Australia) was used to prepare all reactions to a final volume of 20 µl. A Rotor-Gene 6000 (Corbett Robotics) was used for qRT-PCR cycling. Relative fluorescence was acquired during the extension steps.

Table 2.8: *qRT-PCR reactions.*

Constituent	µl per digest	Final concentration
2 X SensiMix One Step	10	1
5 X Quantitect primers	4	1 X
RNA template (100 ng μl^{-1})	1	5 ng μl^{-1}
50 X SYBR GREEN I	0.4	1 X
50 X RNase inhibitor (10 U μl^{-1})	0.4	0.2 U μl^{-1}
Nuclease free water	7	-
Total volume:	20 µl	

Table 2.9: *Thermal cycling conditions for qRT-PCR reactions.*

Step	Temperature	Time	Number of cycles
Heat activation	95°C	10 minutes	1
Denaturation	95°C	20 seconds	
Annealing	56 or 58°C	30 seconds	35
Extension	72°C	20 seconds	
Final extension	72°C	5 minutes	1
Melt	72 - 95°C	-	1

2.2.27 Verification and optimisation of primers.

Predesigned Quantitect primers (Qiagen, UK), were chosen for use in the qRT-PCR series due to closely matched amplification efficiencies. Sequences of Quantitect primers are however, not provided by the manufacturer.

Primers were tested for real time amplification across different annealing temperatures. The annealing temperatures selected were those that yielded the earliest amplification of the gene of interest in conjunction with a late rise in No-Template Controls (table 2.10).

Table 2.10: *qRT-PCR primer annealing temperatures.*

Primer set*	Optimised annealing temperature
CaM1 (AT5G37780) †	58°C
TOC1 (AT5G61380) †	56°C
CONSTANS (AT5G15840) †	56°C
FT (AT1G65480) †	56°C
GAPC (AT1G13440) ‡	56 / 58°C

* Primers were supplied by Qiagen as pre-designed pairs for which sequences were not provided.
† Target genes. ‡ Housekeeping gene.

Levels of *CaM1*, *TOC1*, *CO* and *FT* transcript were quantified for each harvested sample. Following each qRT-PCR run, end-point melt analysis was performed to ensure only a single amplicon was present. Data analysis was performed using the REST 2005 mathematical model for relative quantification in qRT-PCR (Pfaffl *et al.*, 2002) (http://www.corbettlifescience.com/shared/rotor-gene%203000/rest/SetupRest2005_1.9.10.zip). Data was collated and plotted using Prism software (GraphPad, USA).

2.2.28 Determining the effect of Pharmacological CaM inhibition on photoperiodic flowering time.

A. thaliana (35S::*aequorin*$_{(cyt)}$), were germinated on compost, under 60 µmol m^{-2} s^{-1} white light in either 16L : 8D or 8L : 16D photoperiods. Upon developing three true leaves, each plant was sprayed daily at dawn with either 50 µM W7, 50 µM W5, 1 µM CMZ or 0.1% DMSO carrier-solvent control (n = 35 to 45 plants per treatment). Upon flowering (primary bolt ≥ 1 cm), plants were harvested and flowering time recorded by chronological age and number of rosette leaves.

2.2.29 Bioinformatic identification of putative CaM interaction partners.

Amino acid sequences of proteins involved in the *A. thaliana* photoperiodic flowering pathway were analysed for putative CaM binding motifs using the CaM Target Database server hosted at the University of Toronto (http://calcium.uhnres.utoronto.ca/ctdb), (Yap *et al.*, 2000).

2.2.30 The effects of pharmacological CaM inhibitors on flowering in constant darkness.

0.5 X MS agar containing 5% sucrose (w/v) and either 50 μM W7, 50 μM W5, 1 μM CMZ or a 0.1 % DMSO carrier-solvent control was prepared and 100 ml aliquots added to sterile 500 ml flasks. Seed of wild-type *A. thaliana* or of *spa1-3* mutants (which contain a mutation in the gene coding for the potential CaM interaction partner SPA1) were surface sterilised and pipetted on to the surface of the agar before the flasks were transferred to darkness.

After 70 days, the flasks were removed and plants were examined for signs of floral induction using a MZ16 epifluorescence dissecting microscope (Leica, Germany). A GFP2 filter (480/40 nm excitation filter, 510 nm longpass barrier filter) was used for detection of autofluorescence.

2.2.31 Engineering an inducible peptide inhibitor of CaM in to A. thaliana.

A sequence verified fusion construct labelled *smGN* (soluble-modified GFP/calspermin), composed of a plant-expressible soluble *green fluorescent protein* (*smGFP*) upstream of the of *Rattus norvegicus calspermin* cDNA sequence had previously been cloned in to pBlueScript. *smGN* was isolated by primary digestion with XbaI, blunt ending, and secondary digestion with XhoI. The plant binary vector pINDEX3 was digested with StuI and Xho I and dephosphorylated with SAP. *smGN* was then ligated in to pINDEX3 downstream of the chimaeric GVG promoter.

Chemically competent *E. coli* were transformed with the *smGN*-pINDEX3 ligation product and selected by antibiotic resistance. Recombinant plasmid was isolated by Miniprep (section 2.2.16) and the orientation of *smGN* confirmed via diagnostic PstI and EcoRI digests.

A. tumefaciens GV3101 was transformed with the pINDEX3-*smGN* construct and used to transform *A. thaliana* 35S::*aequorin*$_{(cyt)}$ as described previously (section 2.2.18). The presence of *smGN* in transformed *A. thaliana* was confirmed by *smGN*-specific PCR on isolated genomic DNA.

2.2.32 Determining inducibility of smGN expression in Arabidopsis thaliana.

Plants at the ten-leaf stage from six individual transformant lines (together with untransformed controls) were sprayed daily for three days with 0 µM, 10 µM or 30 µM of the glucocorticoids dexamethasone or triamcinolone in order to induce expression of the *smGN* transgene. Leaves were removed and examined for signs of smGN expression by epifluorescence microscopy using a Leica GFP3 filter (70 nm/40 nm excitation filter, 525 nm/50 nm barrier filter) optimised for GFP expression in plants. A GFP2 long pass filter was also used to ensure that pigment autofluorescence was not incorrectly classified as native GFP.

Tissue from plants treated with 10 µM dexamethasone or a DMSO control was harvested for RNA extraction and subsequent cDNA synthesis. Synthesised cDNA was used as a template for *smGN*-specific PCR reactions (primer sequences previously shown in table 2.2), in order to examine the inducibility of transgene expression.

To validate translation of the chimaera, total protein extract was prepared from plants treated with 10 µM or 30 µM dexamethsone or triamcinolone or a 0.1% DMSO carrier-solvent control. Protein extract from a line lacking the smGN transgene served as a negative control. 100 µg total protein extract from each treatment was examined using polyacrylamide gel electrophoresis as per section 2.2.10.

Western blotting was used to further verify the presence of smGN (section 2.2.11). 250 ng GFP was loaded as a positive control for immunodetection. Transfer of the protein to the blotting membrane was confirmed by reversible Ponceau S stain and immunodetection accomplished using Mouse Anti-GFP and Anti Mouse-IgG Alkaline Phosphatase Conjugate.

CHAPTER 3: OPTIMISATION OF PHARMACOLOGICAL CALMODULIN INHIBITOR CONCENTRATIONS

3.1 Introduction

3.1.1 Modulating calmodulin inhibition.

Although a wide range of CaM-inhibitors exist, a limited number are routinely used in inhibition studies. Amongst these agents, the competitive inhibitors N-(6-aminohexyl)-5-chloro-1-naphthalenesulphonamide (W7), N-(6-Aminohexyl)-1-naphthalenesulphonamide (W5) and calmidazolium (CMZ), which have been used to dissect the roles CaM plays in numerous processes in plants and animals including mouse-sperm capacitation, gravisensing and viral infection responses (Si & Olds-Clarke, 2000; Sinclair *et al*., 1996; Nemerow & Cooper 1984). W7 sequesters CaM preferentially, but not exclusively, and W5 is routinely used as a pseudo-control. W5 is a dechlorinated structural analogue of W7 being approximately an order of magnitude less potent than W7 and is generally regarded as showing no effect at concentrations where W7 is deployed successfully (Garofalo *et al.*, 1983; Kaplan *et al.*, 2006; Love *et al.*, 1997b). The absence of a chlorine atom within the naphthalene ring of W5 causes the aromatic system to be more negatively charged. This charge redistribution translates to a reduction in the ability of W5 to effectively inhibit CaM due to weakened Van der Waals force interactions (Endo *et al.*, 1981; Hidaka *et al.*, 1981; Kaplan *et al.*, 2006) (figure 3.1). CMZ belongs to a different class of CaM inhibitors (substituted imidazoles), than W5 and W7 (naphthalene-sulphonamides), and is amongst the most selective pharmacological inhibitors of CaM (Williams *et al.*, 1996). There is however, no low affinity CMZ analogue available for CaM inhibition studies. Successful uses of inhibitors to dissect the involvement of CaM in signalling pathways is dependent upon them being utilised at levels sufficient to interfere with signalling, yet not great enough to induce gross morphological changes. However, CaM inhibitors are often utilised at widely varying concentrations depending on the experimental procedure being undertaken. Concentrations commonly range from 10 to 150 μM for W7 and W5 and from 0.1 to 30 μM for CMZ (Si & Olds-Clarke, 2000; Sengupta *et al*., 2007).

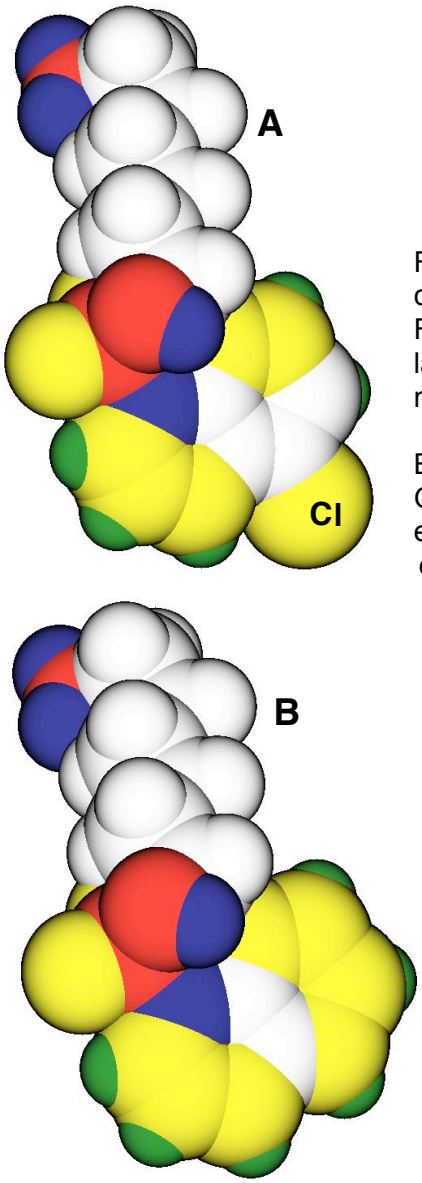

Figure 3.1: Structural and charge-distribution comparisons of W7 and W5.

Fig. 3.31 A: The naphthalene-sulphonamide calmodulin inhibitor W7.
Fig. 3.31 B: W5 is a reduced potency analogue of W7 lacking a chlorine atom (labelled 'Cl') within the naphthalene ring.

Blue: most positively charged (electron-deficient); Green: moderately positively charged; White: electrically neutral; Yellow: moderately negatively charged; Red: strongly negatively charged (electron-rich).

Currently no widely accepted method for determining the optimal concentrations of CaM inhibitors to use in plant-based studies exists. However, over-inhibition of CaM is likely to result in developmental abnormalities. As root growth is both sensitive to chemical perturbation and dependent upon the presence of CaM (Muto & Hirosawa, 1987; Rea *et al*., 1995; Kato *et al*., 2003), a dose-response curve recording the effects of increasing concentrations of W7, W5 and CMZ on root growth in *A. thaliana* seedlings was recorded. This curve enabled selection of the maximum concentration of the inhibitor which does not generate significant changes in root development and therefore indicates that secondary effects of the inhibitor compound were minimal.

CaM is involved in cell division and cell elongation, changes in which lead to disruption of root growth (Vos & Hepler, 1998; Sheremet *et al*., 2008). Roots were therefore isolated from inhibitor-treated *A. thaliana* seedlings and examined via confocal fluorescence microscopy to determine whether changes in morphology at the cellular level had occurred.

3.1.2 Phenotypic plasticity and acclimation in Arabidopsis thaliana.

A. thaliana is highly metabolically and phenotypically plastic, rapidly modifying gene expression as an early response to environmental challenges (Sachs & Ho, 1986). In turn, these changes in transcription lead to modulation of cellular and biochemical systems and enable the plant to compensate for these challenges. *Arabidopsis thaliana CAM*s are inducible by a number of stimuli and are implicated in adaptation to environmental stresses (Townley, 2002). Given the inducibility of *CAM* and its role in adaptive responses, precise up-regulation of its expression could negate the effects extended and chronic exposure to CaM inhibitors would otherwise generate (Hong *et al.*, 1997; Polisensky & Braam, 1996). Ca^{2+}-CaM signalling plays an important role in the gravitational orientation of roots (Moreau, 1987; Sinclair *et al.*, 1996; Zhang, 2003). Consequently, a root gravitropism assay was undertaken in order to determine the ability of *A. thaliana* to acclimate to sustained exposure to CaM inhibitors.

3.2 Results

3.2.1 The effects of increasing concentrations of pharmacological calmodulin inhibitors on root length.

Mean root length of seedlings grown on W7 and W5 did not begin to diverge until inhibitor concentrations greater than 50 μM were reached (figure 3.2 A). Above 50 μM, a rapid divergence in root lengths between plants grown on W7 and those grown on W5 was observed. Whilst the mean root lengths of seedlings grown on medium inoculated with 100 μM W5 remained similar to those of control plants, seedlings grown on 100 μM W7 showed dramatically reduced root lengths (approximately 10 mm) compared to controls (approximately 52 mm). At 200 μM, W7 seedlings no longer produced true roots; instead a mass of root hairs growing directly from the hypocotyl was observed. Mean roots lengths in seedlings grown on 200 μM W5 were approximately 40% as great as controls.

Between 1 μM and 1.5 μM CMZ, root lengths sharply decreased (figure 3.2 B). Increases in concentration to 2 μM CMZ resulted in a further moderate increase which plateaued to 10 μM.

3.2.2 The effects of increasing concentrations of pharmacological calmodulin inhibitors on root number.

Seedlings grown on 0.5 X MS agar containing 0 to 50 μM W7 or W5 displayed no significant alteration in root number as determined by Student's t-test ($P = 0.223$ at 50 μM; figure 3.3 A).

Between 50 to 80 μM, divergence in the number of roots in plants treated with W7 or W5 was observed. Whilst W5 treated plants had root lengths statistically similar to those of plants grown in the absence of inhibitor ($P = 0.455$ at 80 μM), plants grown on W7 exhibited a small but significant increase in total root number ($P = 0.046$ at 80 μM). At 100 to 120 μM, W5 treated plants had root numbers statistically similar to plants grown in the absence of inhibitor ($P = 0.800$ at 120 μM), whilst plants grown on W7 exhibited an approximate doubling in total root number compared to untreated plants ($P = 0.005$). This increase occurred at concentrations causing a rapid decrease in primary root length and may therefore form a compensatory mechanism. Higher concentrations of W7 (120 to 200 μM), resulted in a rapid decline in root number to zero.

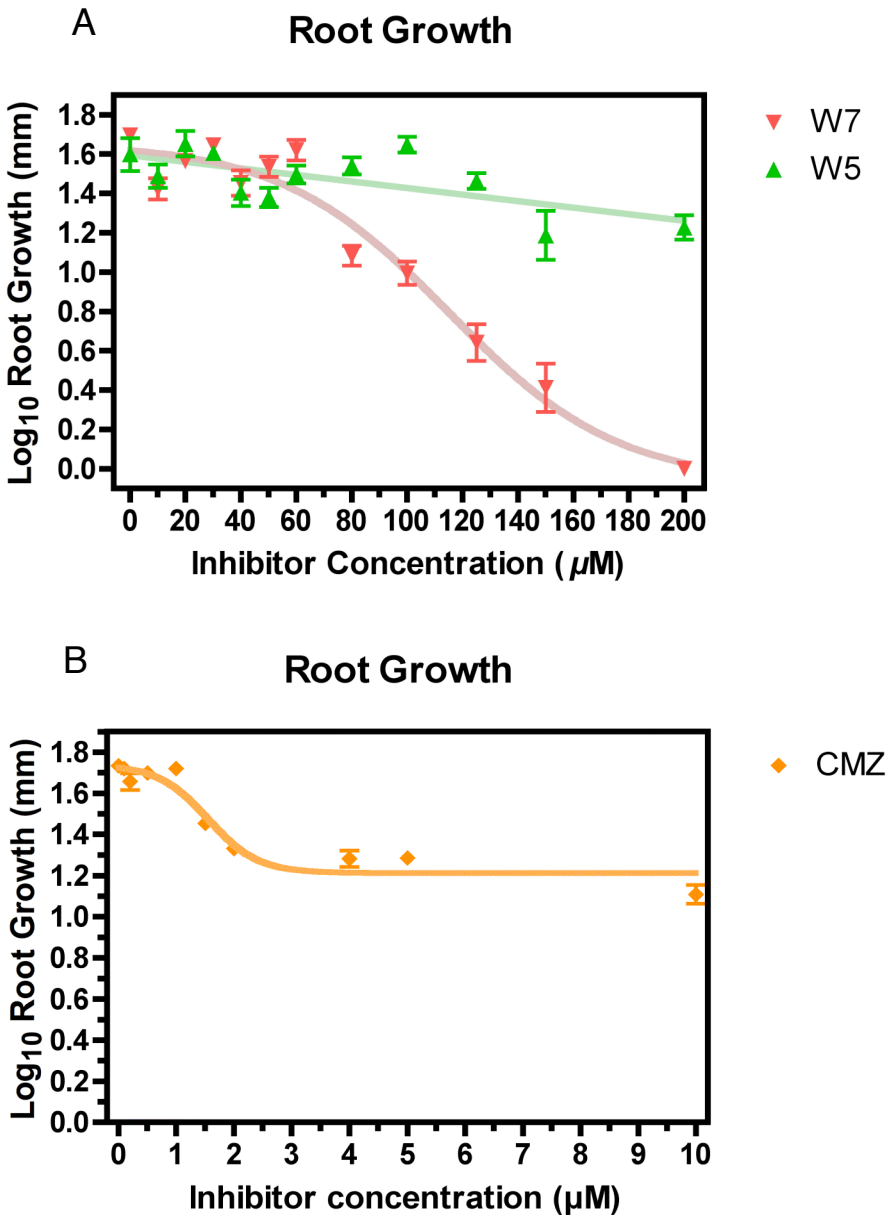

Figure 3.2: Dose response curves of inhibition of root growth in *A. thaliana* seedlings by the calmodulin inhibitors W7, W5 and calmidazolium.

Fifteen *A. thaliana* seedlings were germinated on vertically positioned plates containing 0.5 X MS agar and increasing concentrations of W7 or W5 (inverted red triangles and green triangles respectively; Fig. 3.2 A), or calmidazolium (CMZ) (orange diamonds; Fig 3.2 B). Mean root lengths were measured after 14 days. Vertical bars indicate the standard error of the mean.

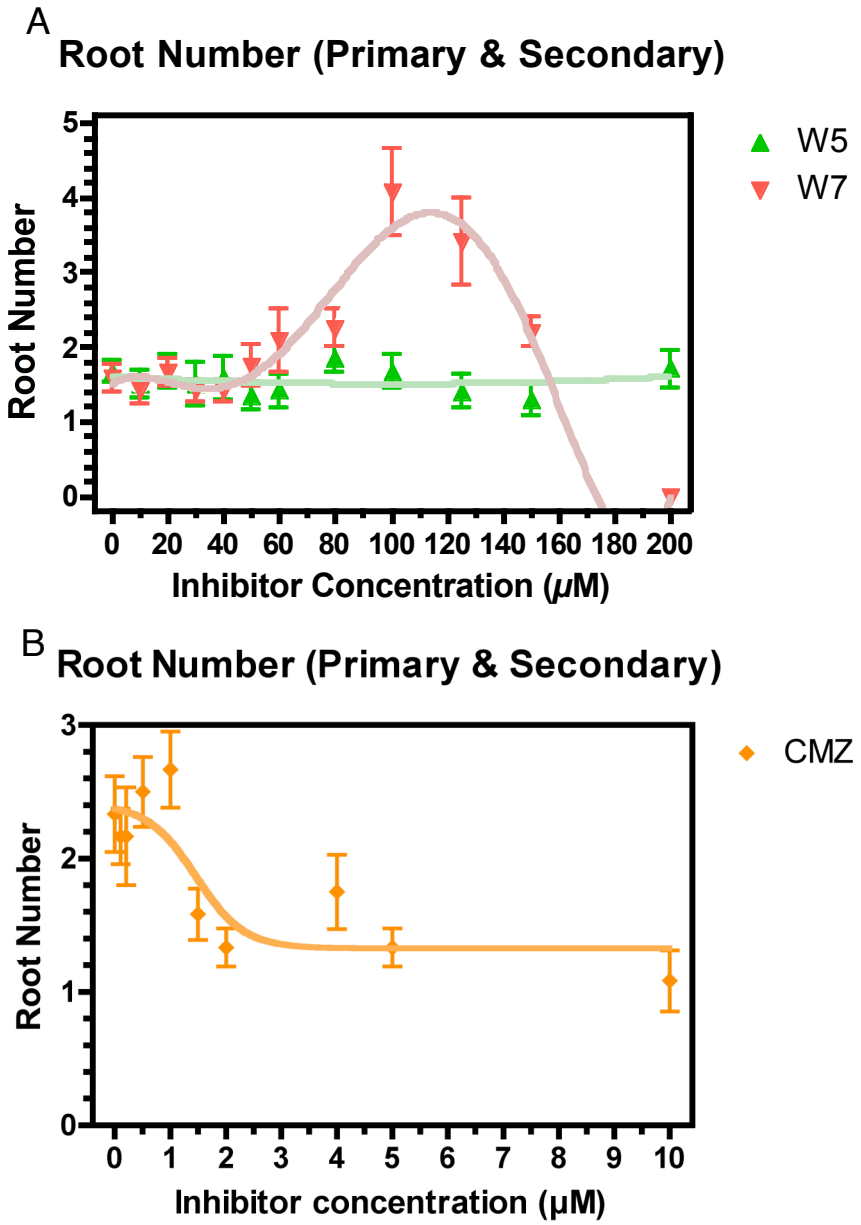

Figure 3.3: Dose response curves of the effect of the calmodulin inhibitors W7, W5 and calmidazolium on root number in *A. thaliana* seedlings.

Fifteen *A. thaliana* seedlings were germinated on vertically positioned 0.5 X MS agar plates containing increasing concentrations of W7 or W5 (inverted red triangles and green triangles respectively; Fig. 3.3 A), or calmidazolium (CMZ) (orange diamonds; Fig. 3.3 B). After 14 days the number of roots on each seedling was recorded. Vertical bars indicate standard error of the mean.

Seedlings grown on agar containing CMZ displayed a root number pattern similar to that of total root length (figure 3.3 B). At all concentrations up to 1 μM CMZ, root numbers were non-significantly different from untreated controls (P = 0.303 at 1 μM).

Between 1 μM and 1.5 μM CMZ, a significant reduction in lateral root number was observed compared to controls (P = 0.007 at 1.5 μM). Increases in inhibitor concentration from 1.5 to 10 μM did not generate further significant reductions in root number (P = 0.053).

3.2.3 Confocal microscopy of inhibitor treated roots.

Differences in root development caused by exposure to CaM inhibitors were examined by measuring cell length in the root elongation zone, using Laser Scanning Confocal Microscopy. The fluorescent stains 7-Aminoactinomycin D (7-AAD) and calcofluor-white were selected as nuclear and cell wall stains respectively. 7-AAD was found to bind the cell walls of stained *A. thaliana* roots as well as nuclear material, however, under some circumstances, this proved to aid visualisation as calcofluor-white proved less effective at staining cells bordering the root tip than it did cells in more mature regions of the root.

No significant differences in cell length, as determined by Dunnett's Multiple Comparison Test, were found between roots grown on control medium (6.7 μm (SE = ± 0.2)), and those grown on plates containing either 50 μM W5 (7.4 μm (SE = ± 0.2), P > 0.05)), or 100 μM W5 (7.8 μm (SE = ± 0.15), P > 0.05).

Root morphology also appeared unaffected at these levels of applied inhibitor (figures 3.4 and 3.5). 1 μM CMZ resulted in small but significant increases in cell length (8.3 μm (SE = ± 0.53), P < 0.05), 2 and 4 μM CMZ led to greater increases (2 μM CMZ = 13.2 μm (SE = ± 0.38), P < 0.01; 4 μM CMZ = 14.2 μm (SE = ± 0.35), P < 0.01), but otherwise roots appeared developmentally normal. Roots exposed to 50 μM W7 exhibited a small increase in mean cell length (9.0 μm (SE = ± 0.25), P < 0.01), with no other morphological changes apparent. Roots exposed to 100 μM or 200 μM W7 displayed much greater increases in cell length (100 μM W7 = 13.1 μm (SE = ± 0.54), P < 0.01; 200 μM W7 = 22 μm (SE = ± 0.9), P < 0.01) and altered root morphology. Root tips displayed highly variable cell shape and disrupted cell packing. Root diameter was variable across the length of the root and often bulbous around the elongation zone.

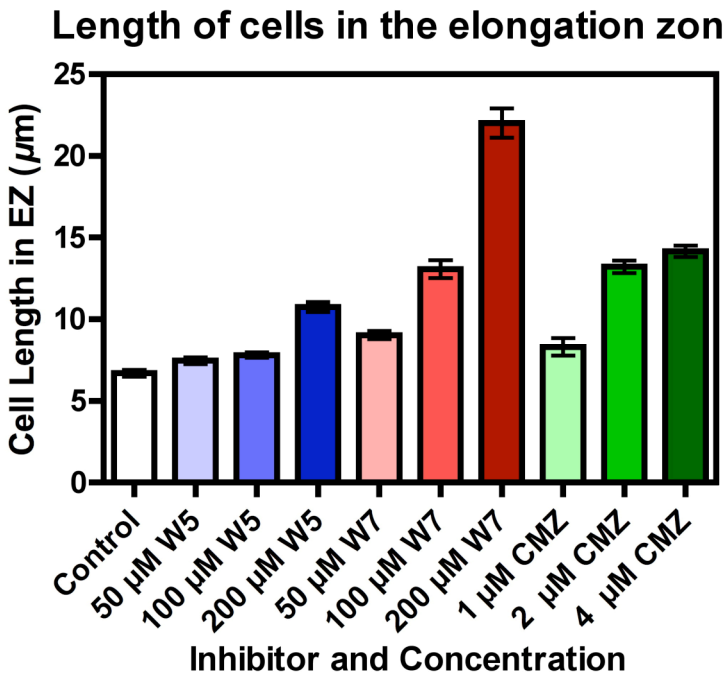

Figure 3.4: The effect of increasing concentrations of the calmodulin inhibitors W7, W5 or CMZ on the length of cells within the root elongation zone.

A. thaliana seedlings were germinated on vertically positioned 0.5 X MS agar plates containing increasing concentrations of the potent calmodulin inhibitors calmidazolium (CMZ) (green bars), W7 (pink and red bars) or the reduced potency analogue of W7, W5 (blue bars).
After 14 days, roots were recovered and the length of cells in the root elongation zone was examined using confocal laser scanning microscopy. Vertical bars indicate standard error of the mean.

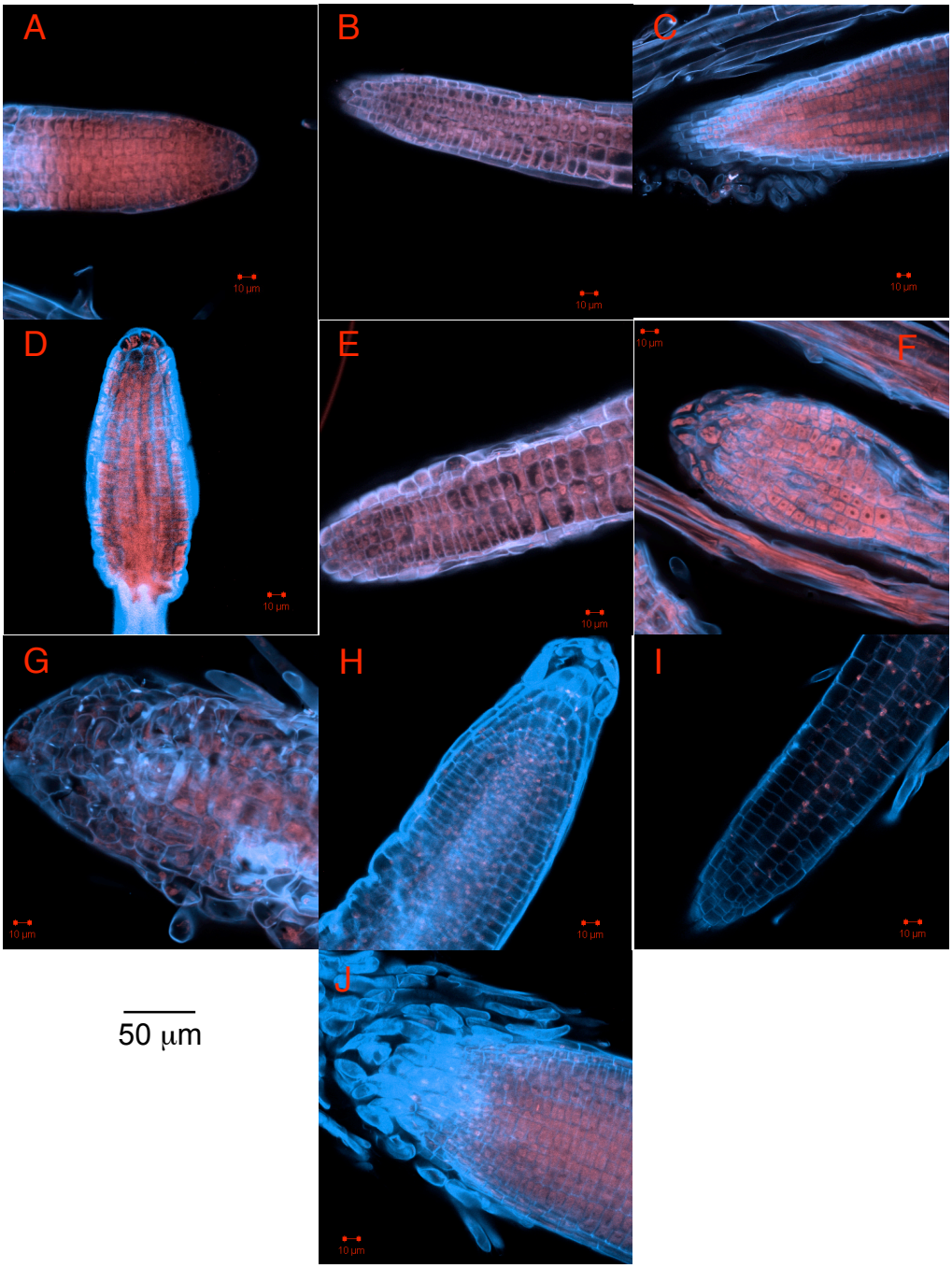

Figure 3.5: Representative images showing the effects of CaM inhibitors upon the morphology and length of cells in the *A. thaliana* root elongation zone.

Roots from fourteen-day old *A. thaliana* seedlings germinated on 0.5 X MS agar containing 0 to 200 μM W7, 0 to 200 μM W5 or 0 to 4 μM CMZ were labelled with 7-AAD and calcofluor-white and analysed using confocal laser scanning microscopy to determine changes in changes in morphology and elongation-zone cell lengths. Representative roots shown were recovered from plants grown 0.5 X MS media containing A: 0.1% DMSO carrier-solvent, B: 50 μM W5, C: 100 μM W5, D: 200 μM W5 E: 50 μM W7, F: 100 μM W7, G: 200 μM W7, H: 1 μM CMZ, I: 2 μM CMZ, J: 4 μM CMZ.

Whilst roots exposed to 200 μM W5, showed significant increases in cell length (10.8 μm (SE = ± 0.3), $P < 0.01$), this increase was much smaller than that seen in seedlings exposed to 100 μM W7. Although cells appeared regularly packed and to have normal variability in cell shape, root diameter was still unusually pronounced in the region of the elongation zone. These data, together with the root-length and root-number dose-response curves, enabled selection of concentrations of CMZ (1 μM), and W7 / W5 (50 μM), for further experiments.

3.2.4 Acclimation of Arabidopsis thaliana *to selected concentrations of CaM inhibitors.*

Root gravitropism is closely linked with Ca^{2+}-CaM signalling (Moreau, 1987; Zhang, 2003). Consequently a gravitropism assay was chosen as a means to determine the ability of *A. thaliana* to acclimate to constant exposure to CaM inhibitors.

A. thaliana were germinated on 0.5 X MS agar containing either 50 μM W7, 50 μM W5, 1 μM CMZ, a carrier-solvent control or 0.5 X MS medium only. After seven days, plates were either rotated 90° and changes in root growth and gravitropic root angle (Δ GRA) recorded. In parallel, seedlings were germinated on control medium and, after seven days, were transferred to fresh plates containing either CaM inhibitor, or control media. Gravitropism was again assayed.

Untransplanted seedlings germinated on plates containing CaM inhibitors showed no statistical difference in root elongation compared to those grown on control medium (at 24 hours, $P = 0.71$ for carrier-solvent controls; $P = 0.303$ for W5; $P = 0.695$ for W7; $P = 0.646$ for CMZ). Likewise no significant differences in Δ GRA were observed between seedlings germinated on control medium and those germinated on media containing carrier-solvent or CaM inhibitors (at 24 hours, $P = 0.947$ for carrier-solvent control; $P = 0.706$ for W5; $P = 0.957$ for W7; $P = 0.827$ for CMZ).

Root elongation for all treatments was greatest in the first 12 hours, however elongation also continued in the following 12-hour period (figure 3.6 A). A similar pattern was observed for Δ GRA (figure 3.6 B).

Seedlings transferred from control medium exhibited minimal growth for the first four hours regardless of whether the new media contained CaM inhibitors.

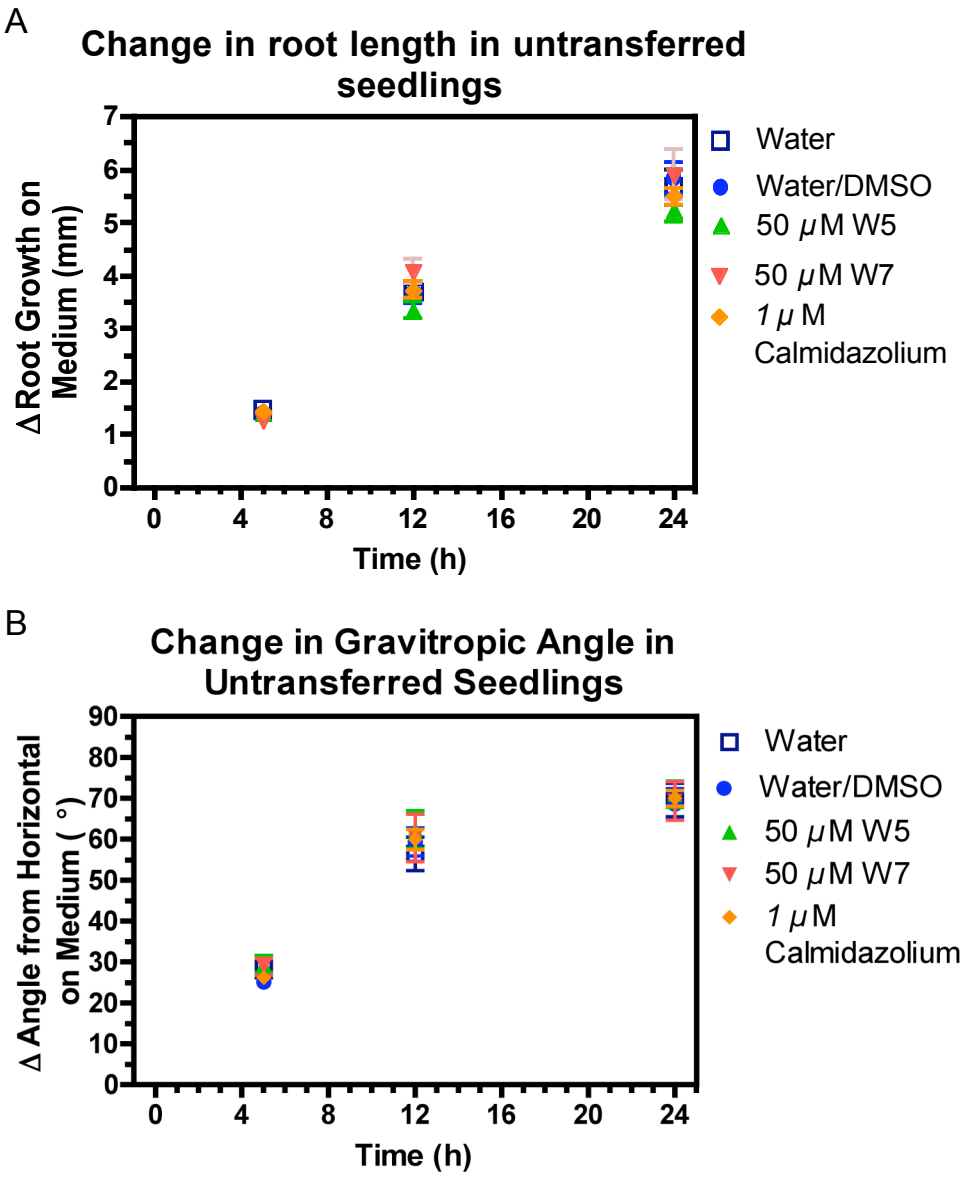

Figure 3.6: The effects of germination on media containing the calmodulin inhibitors W7, W5 and calmidazolium on gravitropic root responses in *A. thaliana* seedlings.

A. thaliana were vertically germinated either on 0.5 X MS media alone (unfilled squares) or on media containing 50 μM W7 (inverted red triangles), 50 μM W5 (green triangles), 1 μM CMZ (orange diamonds) or a DMSO carrier solvent (blue circles). After seven days, plates were rotated 90° and root elongation (Fig. 3.6 A) and gravitropic root angle (Fig. 3.6 B) recorded.

Between four and 48 hours, all seedlings displayed linear growth. No significant difference was found between W5 and control seedlings (P = 0.90), which displayed root elongation of approximately 10 mm over the 48-hour time-course. No significant difference was observed between seedlings transferred to media containing W7 or CMZ (P = 0.154), which gained approximately 2 to 3 mm in root length over 48 hours (figure 3.7 A).

Similar patterns were observed for Δ GRA, with plants under all treatments exhibiting minimal Δ GRA over the first four hours.

No significant difference in subsequent Δ GRA was observed between W5 and control seedlings over the course of the experiment (P = 0.46), with maximal Δ GRA (approximately 70°) occurring between four and 24 hours. The rate of change decreased between 24 and 48 hours, reaching a final Δ GRA of approximately 85°. Both W7 and CMZ treatments substantially decreased the rate at which Δ GRA occurred (figure 3.7 B). No significant difference in Δ GRA was observed between W7 and CMZ for the first 12 hours (P = 0.177). After 12 hours, the apparently linear Δ GRA for roots transferred to medium containing W7 exceeded that observed for CMZ treated roots. Final Δ GRA for W7 was approximately 50°, whilst for CMZ a final change of only approximately 20° was recorded.

In summary, following an assessment of the effects on W7, W5 and CMZ on various physiological traits, including root growth, cell expansion and gravitropic signalling, the optimum inhibitor concentrations for all subsequent experiments were set at 50 µM for W7 and W5 and 5 µM for CMZ.

3.3 Discussion

3.3.1 Avoiding unwanted side-effects of chemical calmodulin inhibitors.

The concentrations of pharmacological CaM inhibitors utilised in the literature differ according to procedure. However, the CaM inhibitor dose-response experiments performed here largely concurred with previous conclusions concerning effective working concentrations (Ali *et al.*, 2007; Hidaka *et al.*, 1979; Jan & Tseng, 2000b; Wetzel *et al.*, 2004). Increasing concentrations of CMZ and W7 did not produce linear changes in either root length or number. Rather, at lower concentrations (0 to 1 µM CMZ; 0 to 50 µM W7) little effect was observed. However, a sudden transition to a significantly 'inhibited' phenotype

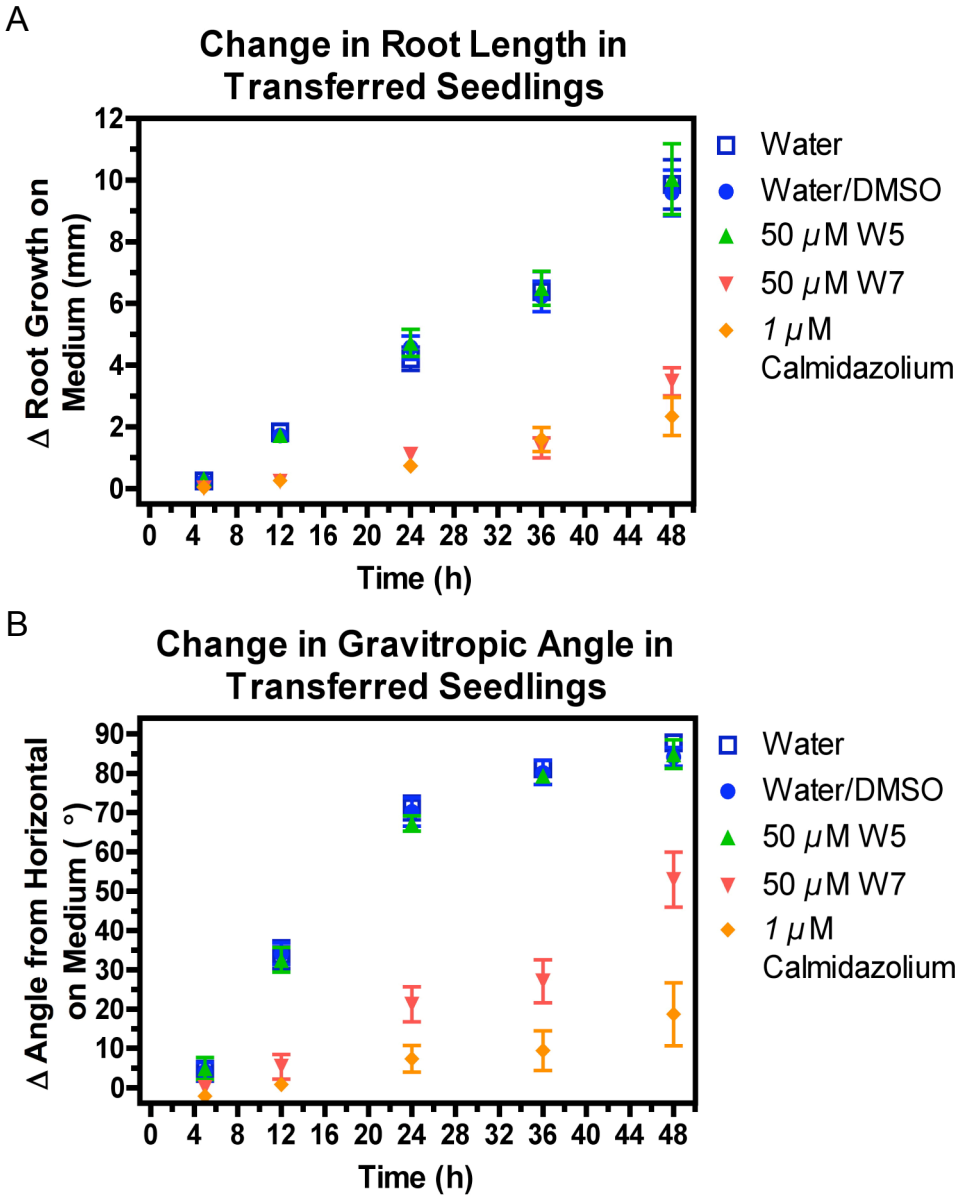

Figure 3.7: The effects of transplantation to media containing the calmodulin inhibitors W7, W5 and calmidazolium on gravitropic root responses in *A. thaliana* seedlings.

Seven day old *A. thaliana* seedlings vertically grown on 0.5 X MS media were transferred to either media alone (unfilled squares) or media containing 50 μM W7 (inverted red triangles), 50 μM W5 (green triangles), 1 μM CMZ (amber diamonds) or a DMSO carrier-solvent (blue circles). Plates were rotated 90° from original seedling orientation and root elongation (Fig. 3.7 A) and gravitropic root angle (Fig. 3.7 B) recorded.

occurred as the inhibitor concentration increased. Such lags in measured effect have been observed previously (Biden *et al.*, 1987; Jan & Tseng, 2000b; Love *et al.*, 1997a).

These observations support the notion that although CaM exists at 'sub-saturating' levels compared to total potential intracellular binding partners, it is normally present at levels slightly in excess of those required at any given timepoint (Zielinski, 1998).

As CaM is involved in mitosis (Vos & Hepler, 1998), it was considered valuable to investigate whether CaM inhibition generated unwanted changes in morphology at the cellular level. At the concentrations selected for aerial application, CMZ and W7 induced only small increases in cell length within the elongation zone and no other morphological changes were apparent. However, further increases in concentration led to increased cell length, increased variation in cell shape, altered cell packing morphology and uneven width along the body of the root. Disordered packing and increased variability in root cell shape may be due to disruption of anisotropic cellular expansion (Keith *et al.*, 1983). Normal expansion of root cells is regulated by the correct polymerisation of microtubules. Pharmacological agents inhibiting this process lead to microtubule depolymerisation and swelling of mitotic root tissue. Microinjection of CaM results in similar depolymerisation, therefore indicating that CaM is involved in controlling this polymerisation process in the mitotic spindle (Keith *et al.*, 1983). The changes observed across the inhibitor dose-response curves indicated that application of CaM inhibitors at concentrations higher than those selected would be unwise. Dissection of molecular networks requires discrete levels of disruption, with extensive systemic disruption likely overshadowing the true effects of inhibition upon a pathway.

3.3.2 Acclimation of Arabidopsis thaliana *to calmodulin inhibitors.*

The sudden transfer of seedlings from control medium to media containing W7 or CMZ resulted in continued and severe reduction in Δ GRA and root elongation.

No significant difference in root elongation was observed between CMZ and W7 treatments. Inhibition of Δ GRA due to the transfer of seedlings to W7 was

severe. However, especially at later points in the time-course, the effect of CMZ was more pronounced.

The concentrations of CMZ and W7 utilised were selected to be of similar CaM inhibitory activity. However, quantifying exact inhibitory effects is difficult in biological systems. As total root elongation under these treatments was minimal (2 to 3 mm), any variation in inhibitory potency between the two inhibitors may only be discernable by examination of Δ GRA. Alternatively gravitropic elongation and Δ GRA may be controlled by partially independent mechanisms. The occurrence of similar inhibitory effects for W7 and CMZ, but not for W5 strongly supports the idea that the effects observed were directly due to CaM inhibition and not to secondary pharmacological effects.

3.4 Conclusions

It has been demonstrated that dose response curves measuring root number and root growth are an effective method for selecting appropriate concentrations of CaM inhibitors for use in inhibition assays in *A. thaliana*. Confocal microscopy of treated roots confirmed that macroscopic changes induced by exposure to inhibitors were represented at the cellular level. The potency of W5 was dramatically reduced in comparison to W7. Consequently, W5 was considered a suitable control for W7. Gravitropic root assays, demonstrated that whilst acute application of inhibitors modulates CaM-dependent processes, sustained application of these agents results in rapid acclimation. These experimental data indicated that optimal levels of CaM inhibition in *A. thaliana* would be achieved via daily, pulsed application of inhibitors at the concentrations 1 μM CMZ and 50 μM W7 / W5.

CHAPTER 4: TRANSCRIPT PROFILING AND FLOWERING TIME ANALYSIS

4.1 Introduction

4.1.1 Pharmacological inhibition of Ca^{2+}-calmodulin signalling.

As previously discussed in chapter one, cytoplasmic free calcium (Ca^{2+}_{cyt}) acts as a powerful second messenger, encoding information in stimulus-specific Ca^{2+} signatures. As well as transducing information regarding environmental parameters, [Ca^{2+}_{cyt}] undergoes day-length specific circadian oscillations of abundance (Johnson *et al*, 1995; Love *et al.*, 2004). Two questions therefore arise. Firstly, are these [Ca^{2+}_{cyt}] oscillations are decoded, either as a feedback to the core oscillator or as regulators of circadian controlled processes such as photoperiodic flowering? Secondly, if circadian [Ca^{2+}_{cyt}] oscillations are indeed decoded, what are the cellular mechanisms that transduce accurate information processing?

Calmodulin (CaM) acts as the predominant sensor of calcium in plants. It is therefore an excellent candidate for a molecular mechanism by which circadian [Ca^{2+}_{cyt}] oscillations may be decoded. Limited work in *Robinia pseudoacacia* (Black-locust tree) and *Agave lophantha* (Thorn-crested Agave) supports a role for CaM in clock-influenced processes such as diurnal leaflet movement (Gomez & Simon, 1995). However, these studies did not focus on the molecular mechanisms behind the effects caused by disruption of CaM.

A number of strategies exist to investigate the molecular mechanisms involved in clock-related processes. Reverse genetic screens of known signal-transduction mutants may be undertaken to identify components involved in regulation of physiological or molecular outputs from the clock (Robertson *et al*., 2007). However, analysis of mutants may be of limited value when an organism contains multiple genes coding for closely related isoforms of proteins such as CaM. In the future it may be necessary to try and differentiate the roles of individual CaM isoforms in regulating the circadian clock and clock-dependent outputs, however it is first necessary to determine whether CaMs in general are involved in such processes. Pharmacological CaM inhibitors are not isoform-specific and may be applied at selected times and at selected concentrations. It was therefore decided to focus on a pharmacological approach in mapping the involvement of CaM in circadian signalling networks. Identifying which effects

direct result from targeted inhibition of CaM may be difficult, as drugs often deliver unwanted secondary effects (Suzuki *et al*., 1996). Three approaches were used to counter these difficulties. Firstly, as secondary effects appear to be specific to individual families of CaM inhibitors (Jan & Tseng, 2000a, 2000b), plants were treated with either of two structurally unrelated classes of CaM inhibitors. Secondly, where available, a reduced potency analogue of a strong CaM inhibitor was used as a control. Thirdly, inhibitors were applied at the maximum concentrations experimentally verified as not causing gross changes in root growth.

A. thaliana is highly phenotypically plastic and showed clear acclimation to chronic application of CaM inhibitors (section 3.2.4). In order to dissect any role CaM may play in circadian timekeeping or photoperiodic flowering, it was necessary that these compounds generate continued inhibition over the course of the experiment. Consequently, it was judged that pulsed daily application of 50 μM W7, 50 μM W7 and 1 μM CMZ would be necessary in order to minimise the likelihood of such acclimation occurring over the experimental timeframe.

4.1.2 Potential nodes of CaM interaction in the photoperiodic flowering pathway.

An earlier pilot experiment on a limited number of *A. thaliana* plants had provided an indication that application of pharmacological CaM inhibitors was capable of affecting amplitude of expression of the *A*. *thaliana* clock gene *TOC1* and flowering time gene *FT*. An expanded experiment was therefore performed in order to expand upon the precise nature the effects of CaM inhibition conferred upon transcription of clock and flowering-time genes

As CaM could potentially act anywhere in the photoperiodic flowering pathway, expression patterns of circadian regulated *CALMODULIN1* (*CAM1*) (Harmer, 2000), and key genes involved in the central oscillator and flowering output pathways was analysed. Quantitative Real Time-PCR (qRT-PCR) was used to quantify changes in gene expression induced due to treatment with CaM inhibitors.

The core circadian oscillator acts as a series of feedbacks and changes in one element of the oscillator therefore cascade to, and affect, the other elements (Brunner & Merrow, 2008). Such changes have been well described in numerous studies of core clock component mutants (Somers *et al*., 1998;

Yanovsky & Kay, 2002; Gardner *et al*., 2006; McClung, 2006). The core oscillator components CIRCADIAN CLOCK ASSOCIATED 1 (CCA1) and 'LATE ELONGATED HYPOCOTYL' (LHY) are homologous to each other and show partial redundancy. *TIMING OF CAB EXPRESSION 1* (*TOC1*), which has no homologues within the core oscillator, was therefore selected as representative of the *A. thaliana* clock in qRT-PCR expression studies (Alabadí *et al.*, 2001; Hayama & Coupland, 2003).

CONSTANS (CO), functions as the first output in to the photoperiodic flowering pathway which is not also involved with the functioning of the central oscillator. *CO* transcription shows photoperiod-specific circadian regulation and changes in phase and amplitude of expression have been clearly mapped to changes in flowering time (Suárez-López *et al.*, 2001; Valverde, 2006). In *A. thaliana*, the circadian clock regulates expression of *CO* mRNA and incident light stabilises CO protein. Unlike the central oscillator, the photoperiodic flowering pathway is not therefore represented as a single unit. *FLOWERING LOCUS T* (*FT*) is expressed in response to accumulation of light-stabilised CO (Yanovsky & Kay, 2002). FT activates transcription of floral meristem identity genes triggering floral transition (Wigge *et al.*, 2005). *CO* and *FT* were therefore selected to represent upstream and downstream nodes of the photoperiodic flowering pathway in qRT-PCR expression studies. The effects upon flowering time of modulating the expression of *TOC1*, *CO* and *FT* have been well studied (Simpson, 2003; Mizoguchi *et al*., 2005; Wigge *et al.*, 2005). It was therefore decided to investigate whether qRT-PCR-verified changes in gene expression led to corresponding alterations in flowering time in *A. thaliana*.

4.1.3 Bioinformatic analysis indicates SUPPRESSOR OF PHYA-105 as a potential calmodulin interaction partner.

Bioinformatic sequence analysis indicated that SUPPRESSOR OF PHYA-105 (SPA1) was a possible interaction target for CaM. Members of the SPA family share homology with the E3 ligase CONSTITUTIVE PHOTOMORPHOGENIC 1 (COP1), and together are involved in the targeted degradation of several proteins including the positive regulator of photomorphogenic development ELONGATED HYPOCOTYL 5 (HY5) and the flowering-time protein CO. Although each protein individually retains residual function, a SPA1/COP1

heterodimer is required for full activity (Jang *et al.*, 2008; Lin & Wang, 2007; Parks *et al.*, 2001). Plants carrying a null *cop1* mutation show photomorphogenic development, including flowering and accumulation of anthocyanin. In wild-type plants, such phenotypes are strictly light-dependant responses (Bowler *et al.*, 1994) (McNellis *et al.*, 1994; Nakagawa & Komeda, 2004). Unlike *cop1* mutants, dark-grown *spa1* and *spa2* single mutants show wild-type photomorphogenic responses including the absence of pigmentation. The differences in photomorphogenic phenotypes found between *spa* and *cop1* mutants is believed to be due to partial redundancy between members of the *SPA* family (Laubinger *et al.*, 2006; Lin & Wang, 2007). This hypothesis is supported by the observation that *spa1/spa2* double mutants show a similar pattern of anthocyanin accumulation to *cop1* mutants (Hoecker *et al.*, 1998; Laubinger, 2004; McNellis *et al.*, 1994).

Unlike *cop1* mutants, which flower after several weeks in darkness, studies examining dark-grown *spa* mutants have exclusively focused on seedlings (average age three to four days old). However, levels of SPA2 continually decrease as *A. thaliana* matures (Laubinger *et al.*, 2006; Lin & Wang, 2007). Consequently, it was considered that any *spa1*-phenotype that was initially masked by the presence of functional SPA2 may surface as *A. thaliana* matures. Additionally, as bioinformatic analysis suggested that SPA1 activity may be dependent on CaM, the possibility was raised that application of CaM inhibitors may generate partial phenocopying of *spa1* mutants. Wild-type plants and *spa1* mutants were therefore germinated in darkness on media containing either CaM inhibitors or carrier-solvent controls and resultant phenotypes compared at maturity.

4.2 Results

4.2.1 Quantitative Real Time-PCR primers produce single amplicons.

In order to precisely quantify changes in gene expression it was necessary to use primers that are specific for a single cDNA. Prior to qRT-PCR, primer sets specific for *CAM1*, the core clock gene *TOC1*, the photoperiodic-flowering time genes *CO* and *FT* and the housekeeping gene *GAPC* were checked to ensure specific amplification. Final PCR product was verified as a single band of the correct size by agarose gel electrophoresis (figure 4.1).

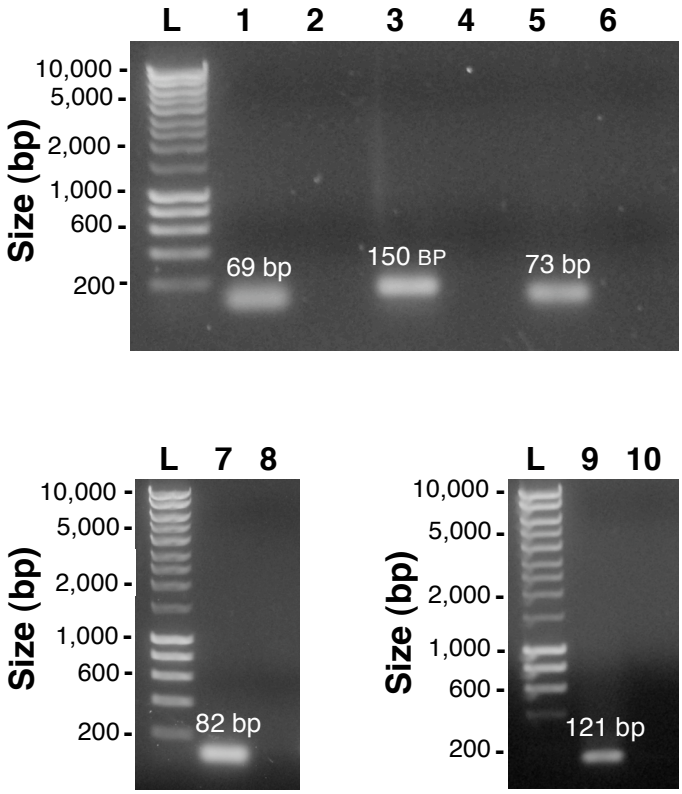

Figure 4.1: PCR-product generated using qRT-PCR primers.

PCR reactions using *A. thaliana* cDNA as the template were performed to verify that primers specific for *TOC1*, *FT*, *CO, CAM1* and *GAPC* produced correctly sized amplicons.
"L" represents DNA standards, for which fragment lengths are indicated. Lanes 1, 3, 5, 7 and 9 contain PCR product amplified from *Arabidopsis* cDNA using primer pairs specific for *TOC1*, *FT*, *CO, GAPC* and *CaM1* respectively. All primer pairs yielded bands of the expected size. No unexpected bands were visible, indicating that each primer set was specific to its target gene.
Lanes 2, 4, 6, 8, 10, contain PCR product following cycling of primers specific for *TOC1*, *FT*, *CO, GAPC* and *CaM1* respectively in the absence of target cDNA. No amplification was observed, indicating the primer sets were not prone to self - amplification.

End-point melt analysis verified only a single amplicon was present after completion of each qRT-PCR run (figure 4.2).

4.2.2 RNA extractions.

A. thaliana were grown under either long day or short day photoperiods and upon attaining ten true leaves were sprayed daily for 14 days with either the CaM inhibitors 50 µM W7, 50 µM W5 or 1 µM CMZ or with a 0.1% DMSO carrier-solvent control.

RNA was extracted from harvested *A. thaliana* aerial tissues. Denaturing agarose gel electrophoresis of randomly selected RNA samples confirmed that suitably non-degraded RNA free from genomic DNA contamination had been isolated (figure 4.3).

4.2.3 Expression of clock and flowering-time related genes in pharmacologically treated plants grown in 16L : 8D photoperiods.

At zero hours (dawn), abundance of *CAM1* transcript, as shown in figure 4.4, was low and non-significantly different in plants from all treatments (P = 0.406). Expression remained low until four hours. A rapid rise and peak, in *CAM1* transcript abundance was observed between four and eight hours. Expression from plants treated with W7 or CMZ was marginally greater than from those dosed with W5 or controls. *CAM1* transcript levels for control plants and those treated with W5 or CMZ steadily declined after eight hours. However, peak *CAM1* abundance from plants treated with W7 remained high for an additional four hours before rapidly diminishing. Between 16 hours (dusk) and 24 hours, levels of *CaM1* transcript diminished under all treatments except CMZ where it maintained a moderate plateau. Between 24 and 28 hours *CaM1* transcript in CMZ treated plants decreased to levels not significantly different than those observed under other treatments (P = 0.948). Relative total transcript, as determined by area under the curve and normalised to controls = 1, was W5 = 0.88, W7 = 1.23 and CMZ = 1.13.

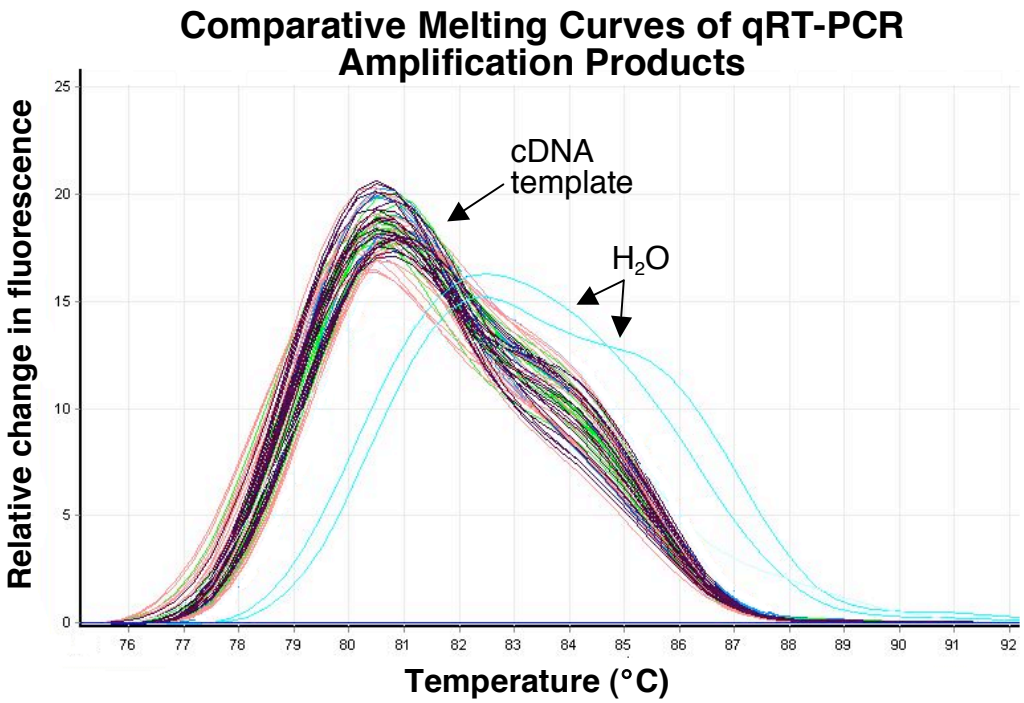

Figure 4.2: Melting curve analysis of product generated from representative qRT-PCR reactions.

Melting curve analysis serves to ensure that all amplification products have similar melting temperatures and that non-specific reaction products are not present.
H_2O controls lacking template showed melting curves with an 'inflection' (amplicon melting temperature) of 82.5 °C, most likely due to primer-dimer formation.
Reactions containing a cDNA template showed a higher inflection temperature than controls (80.6 °C) and the apparent absence of primer-dimer artifacts.

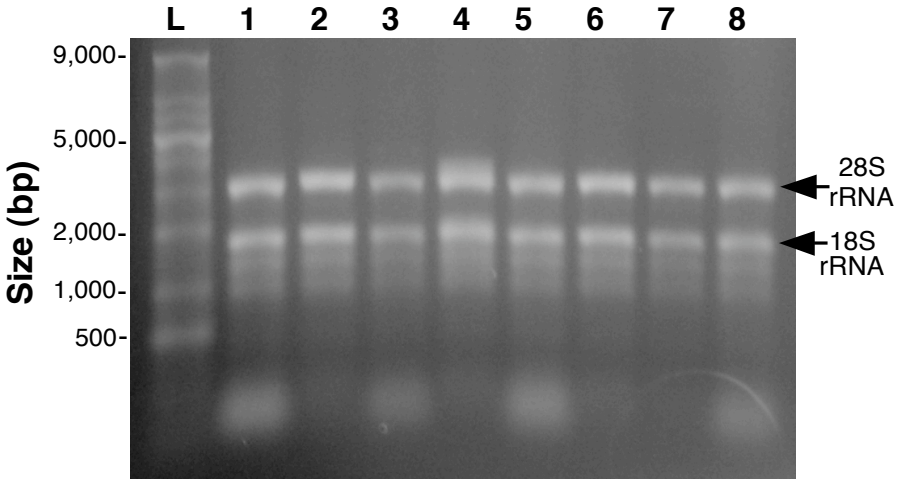

Figure 4.3: Agarose gel electrophoresis analysis of total RNA isolated from *Arabidopsis thaliana*.

.

"L" represents RNA standards for which fragment lengths are indicated. Lanes 1 to 8 represent 2 μg total RNA extracted from randomly selected pools of *A. thaliana* following treatment with the CaM inhibitors 50 μM W5, 50 μM W7 and 1 μM calmidazolium or a DMSO carrier-solvent control.

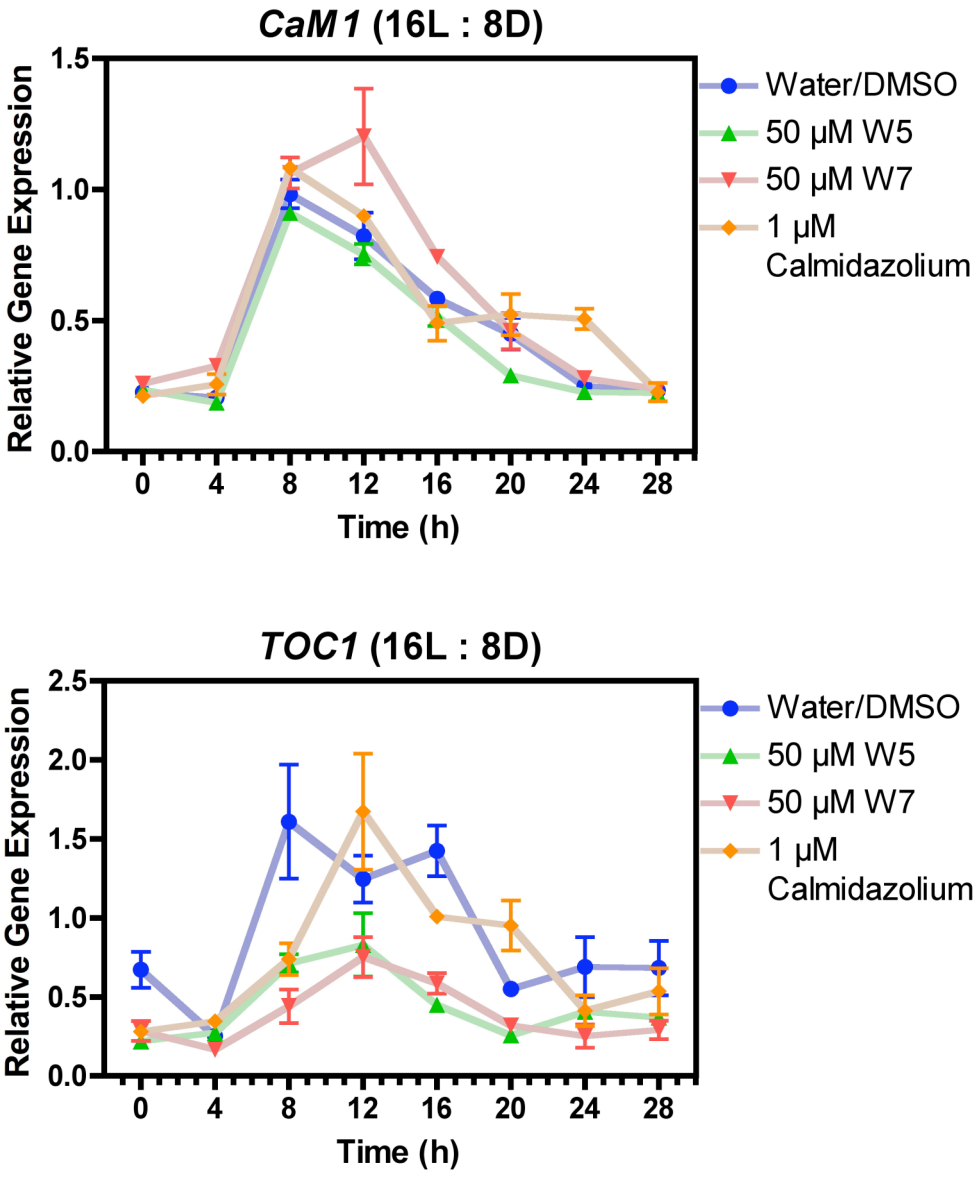

Figures 4.4 (top), 4.5 (bottom): The effects of pharmacological CaM inhibitors on *CaM1* and *TOC1* expression in *Arabidopsis thaliana* grown in long-day photoperiods.

A. thaliana ectopically treated daily for fourteen days with the CaM inhibitors 50 µM W5, 50 µM W7 and 1 µM calmidazolium or a DMSO carrier-solvent control. Samples were harvested every four hours for 28 hours and qRT-PCR was used to quantify changes in expression patterns.

In control plants, expression of the central oscillator component *TOC1* was reduced at dawn and showed a rapid increase between four and eight hours. *TOC1* transcript abundance remained high until dusk, before rapidly declining to basal levels. At dawn no significant difference in levels of *TOC1* mRNA was observed between plants treated with W5, W7 and CMZ (P = 0.530), with transcript levels marginally lower than in controls. As with control treatments, W5, W7 and CMZ plants showed increased levels of *TOC1* expression between four and eight hours; at this time-point, transcript abundance peaked in W5 treated plants (figure 4.5). In plants treated with W5, *TOC1* expression plateaued between eight and 12 hours. However, W7 and CMZ treatments led to a transcript peak at 12 hours; a four-hour phase delay compared to controls. Whilst peak abundance of *TOC1* mRNA in CMZ treated plants was non-significantly different to that observed in controls, peak expression in W5 and W7 treated plants was reduced by approximately 60%. In both controls and plants treated with W7, peak *TOC1* expression was maintained between 12 and 16 hours. However, in plants treated with CMZ or W5 termination of peak *TOC1* expression displayed a phase advance of four-hours. *TOC1* abundance in controls or plants treated with W5 or W7 returned to basal between 16 and 20 hours. In plants treated with CMZ, this decrease in transcript was less pronounced and was delayed by four hours. Total relative transcript over the experimental timeframe as normalised to controls was W5 = 0.50, W7 = 0.44 and CMZ = 0.75.

No obvious oscillations in levels of *CO* transcript were observed in control plants, (figure 4.6). *CO* transcript abundance was variable but high at zero hours, rapidly declining between until four hours. A slight, but significant, increase was observed from four hours to dusk (P = 0.045). During the scotophase (dark period), transcript abundance returned to basal levels. Unlike control plants, those treated with W5 displayed rhythmic *CO* expression. In these plants, levels of *CO* expression were low and non-significantly different at dawn and four hours (P = 0.205). Expression greatly increased and peaked at eight hours. *CO* remained high at 12 hours, returning to basal levels at dusk and remaining low until 28 hours. *CO* expression patterns in W7 treated plants were similar to those previously observed in untreated seedlings (Oda *et al.*, 2004; Suárez-López *et al.*, 2001).

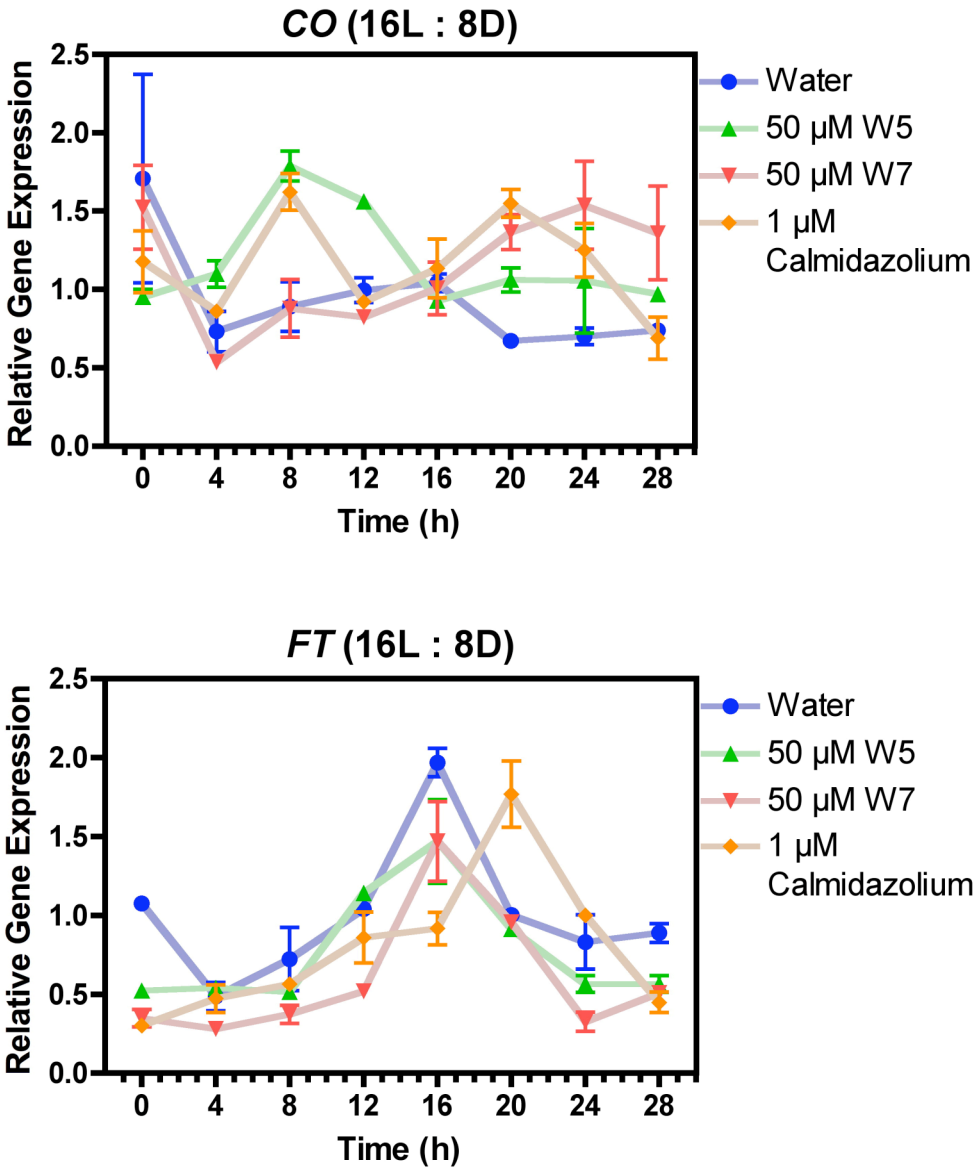

Figures 4.6 (top), 4.7 (bottom): The effects of pharmacological CaM inhibitors on *CO* and *FT* expression in *Arabidopsis thaliana* grown in long-day photoperiods.

A. thaliana ectopically treated daily for fourteen days with the CaM inhibitors 50 µM W5, 50 µM W7 and 1 µM CMZ or a DMSO carrier-solvent control. Samples were harvested every four hours for 28 hours and qRT-PCR was used to quantify changes in expression patterns.

However, a somewhat less pronounced rise in transcript level between eight and 16 hours was observed. Levels of *CO* mRNA were raised at dawn and fell sharply between zero and four hours. Following a small increase between four and eight hours, levels of *CO* transcript rose steadily, peaking at dawn. Plants treated with CMZ displayed a bi-modal pattern of *CO* expression. Dawn expression was moderate and decreased between four and eight hours. In plants treated with CMZ, *CO* levels increased greatly after four hours and showed a peak at eight hours which was non-significantly different that observed following W5 treatments (P = 0.338). *CO* returned to basal levels between eight and 12 hours before again increasing to a second peak at 20 hours. Relative total transcript over the course of the experiment, as normalised to controls = 1, was W5 = 1.35, W7 = 1.21 and CMZ = 1.32.

In control plants, *FT* expression declined from zero to four hours. Between four and 12 hours, *FT* transcript rose steadily, before increasing sharply to peak at dusk. Between dusk and 20 hours transcript declined to levels non-significantly different than those observed at 12 hours (P = 0.359) and remained low for the remainder of the time-course (figure 4.7).

In plants treated with W5, the overall pattern of *FT* expression was similar to that observed in control plants, however transcript abundance was reduced both at dawn and dusk. As with controls, *FT* abundance increased from eight hours to peak at dusk. Unlike controls, *FT* expression in plants treated with W5 declined between 20 and 24 hours, indicating a possible phase shift in *FT* expression. Plants treated with W7 showed a similar *FT* expression profile to those treated with W5. *FT* transcript abundance was very low at dawn and stayed at basal levels until eight hours. The increase in *FT* transcript observed between eight and 12 hours in W7 plants was less pronounced in those treated with W5. Between 12 hours and dusk, expression increased to a peak, non-significantly different to that of W5 loaded plants (P = 1.0), before immediately declining. At 20 hours, *FT* abundance was non-significantly different in control, W5 and W7 treated plants (P = 0.240). *FT* levels in CMZ treated plants increased steadily from a basal low at dawn, Unlike other treatments, in which *FT* peaked at 16 hours, CMZ treatment led to an expression plateau between 12 and 16 hours. Peak *FT* expression occurred at 20 hours; a phase delay of four hours. *FT* expression then rapidly decreased for the remainder of the time-

course. Total expression as calculated over the course of the experiment and normalised to controls =1 was W5 = 0.81, W7 = 0.62 and CMZ = 0.85.

4.2.4 Expression of clock and flowering-time related genes in pharmacologically treated plants grown in 8L : 16D photoperiods.

Under short days, as under long days, expression of *CaM1* expression at dawn was low and non-significantly different between all treatments (P = 0.341). *CAM1* mRNA remained low until 12 hours, when transcript abundance peaked under all treatments. Whilst a moderate peak in transcript abundance occurred in control plants, peak *CAM1* levels were approximately 80% higher in plants treated with W5, W7 and CMZ (figure 4.8). Following control treatments, *CAM1* expression remained stable between 12 and 16 hours, declining sharply at 20 hours. In plants treated with W5, CMZ and to a lesser degree W7, *CAM1* transcript levels began to decline rapidly between 12 and 16 hours. A phase advance of four hours was therefore evident in pharmacologically treated plants. In all treatments, levels of *CAM1* transcript continued to decline between 16 hours and dawn. Total *CAM1* transcript abundance as normalised against control treatments = 1 was calculated as W5 = 1.12, W7 = 1.36 and CMZ = 1.14.

In controls, expression of *TOC1* was low at dawn and declined until eight hours. At four hours, no significant difference in the abundance of *TOC1* transcript was observed between any of the treatments (P = 0.093). Levels of *TOC1* mRNA rose sharply for all treatments between eight and 12 hours, peaking for the control plants and for those treated with W5 and W7. At 12 hours, levels of *TOC1* in CMZ, W7 and W5 treated plants were non-significantly different (P = 0.609), and were approximately half that of controls. Levels of *TOC1* transcript declined between 12 and 16 hours in both W5 and W7 dosed plants, but maintained a plateau following control and CMZ treatments (figure 4.9). Between 16 and 28 hours *TOC1* abundance rapidly declined in controls. Levels of *TOC1* remained stable between 16 and 20 hours in plants treated with W7, whilst transcript increased in both W5 and CMZ plants.

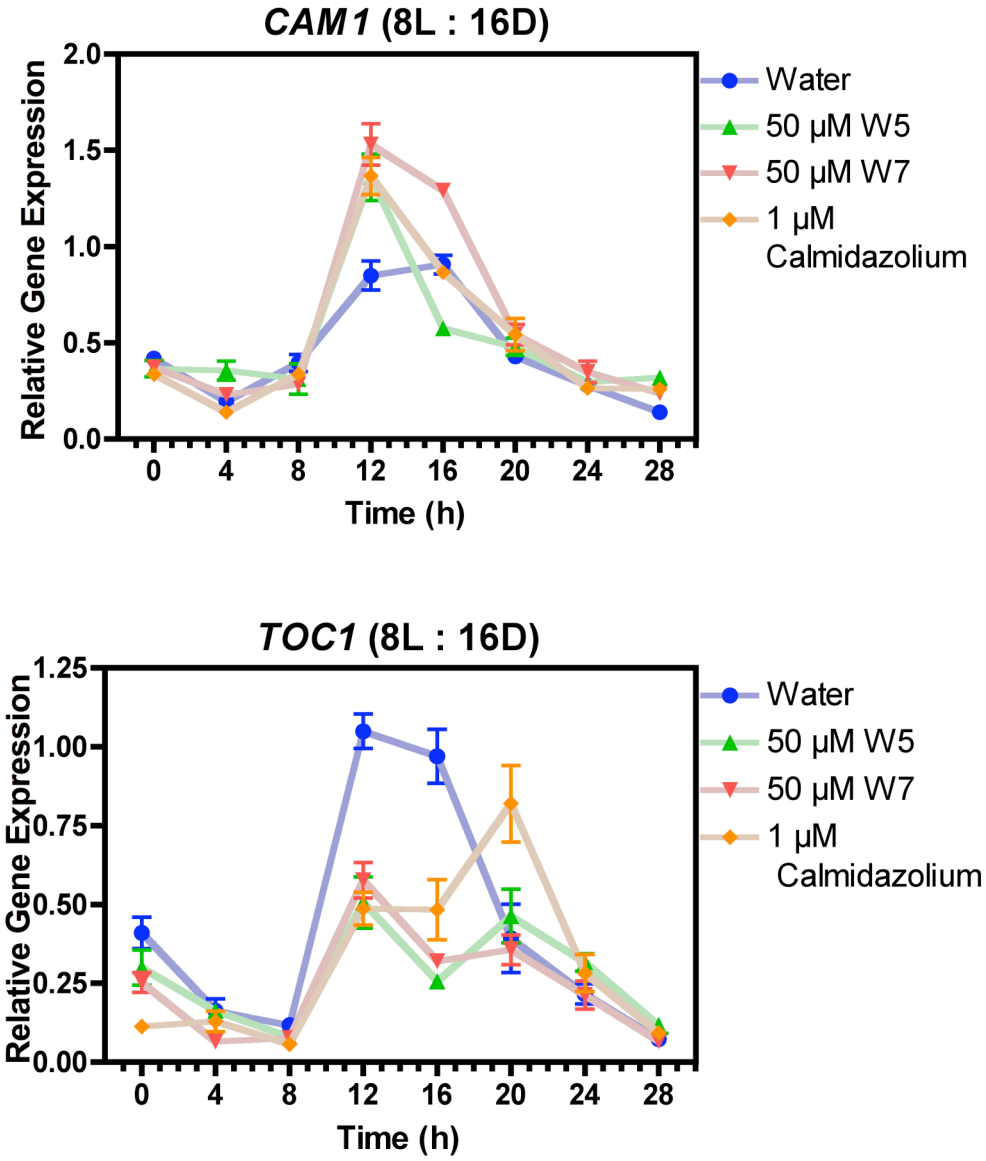

Figures 4.8 (top), 4.9 (bottom): The effects of pharmacological CaM inhibitors on *CaM1* and *TOC1* expression in *Arabidopsis thaliana* grown in short-day photoperiods.

A. thaliana ectopically treated daily for fourteen days with the CaM inhibitors 50 µM W5, 50 µM W7 and 1 µM calmidazolium or a DMSO carrier-solvent control. Samples were harvested every four hours for 28 hours and qRT-PCR was used to quantify changes in expression patterns.

A second expression peak was observed at 20 hours in W5 treated plants of an amplitude non-significantly different than the first peak (P = 0.731). At this time-point (20 hours), *TOC1* expression also peaked in CMZ treated plants, generating an eight-hour phase delay compared to control plants. Under all treatments, expression of *TOC1* declined between 20 and 28 hours and was not significantly different at either 24 or 28 hours (P= 0.30 at 24 hours; P = 0.153 at 28 hours). Total *TOC1* transcript as normalised against control treatments was calculated as W5 = 0.63, W7 = 0.56 and CMZ = 0.75.

In control plants, levels of *CO* transcript were low at dawn and diminished over the subsequent four hours. *CO* transcript abundance increased steadily from four hours, peaking between 12 and 16 hours before returning to basal. In W5 treated plants, levels of *CO* mRNA were elevated at dawn, then declined rapidly.

CO expression rose rapidly between 12 and 16 hours, revealing an apparent eight-hour phase delay compared to controls. No significant difference in *CO* expression was observed between control and W5 treated plants between 16 and 24 hours. (P = 0.130 at 16 hours; P = 0.396 at 20 hours; P = 0.480 at 24 hours). Whilst there appeared to be a clear oscillatory component to *CO* expression in control and W5 treated plants, no such oscillations were apparent in plants treated with W7 or CMZ (figure 4.10). In CMZ treated plants, *CO* abundance remained low throughout the experiment. In W7 treated plants, levels of *CO* were low at dawn and declined slightly between zero and eight hours, before slowly increasing again during the night. Overall transcript levels as normalised to controls were W5 = 1.24, W7 = 0.65 and CMZ = 0.69.

FT expression in control plants grown under short-day photoperiods was low at dawn and stayed at basal levels until dusk, when *FT* abundance increased by approximately 80% (figure 4.11). Levels of *FT* remained elevated until 24 hours, before returning to basal at 28 hours. In W5 treated plants, *FT* transcript abundance was greater than in controls at zero hours and remained relatively stable throughout the time-course, with a minor decrease in transcript at 24 hours. In W7 treated plants, *FT* abundance at dawn was not significantly different to that found following W5 treatments (P = 0.50). Between four and 12 hours, *FT* expression fluctuated at a low level before sharply increasing at 16 hours and remaining high.

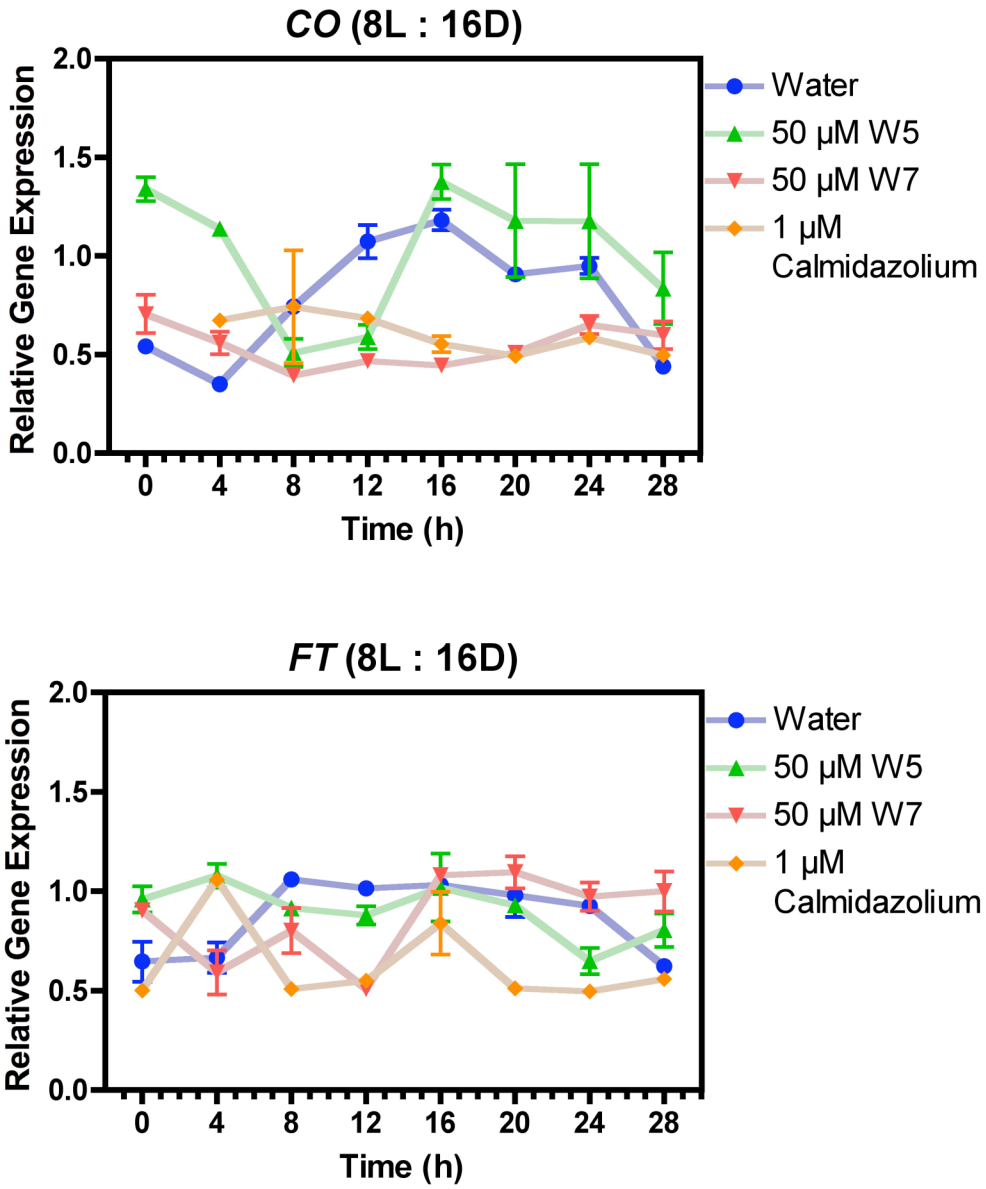

Figures 4.10 (top), 4.11 (bottom): The effects of pharmacological CaM inhibitors on *CO* and *FT* expression in *Arabidopsis thaliana* grown in short-days photoperiods.

A. thaliana ectopically treated daily for fourteen days with the CaM inhibitors 50 μM W5, 50 μM W7 and 1 μM calmidazolium or a DMSO carrier-solvent control. Samples were harvested every four hours for 28 hours and qRT-PCR was used to quantify changes in expression patterns.

In CMZ treated plants, levels of *FT* transcript were non-significantly different from controls at zero hours, however a transient expression peak was observed at four hours. *FT* abundance returned to basal at eight and 12 hours. A second transient peak in *FT* mRNA was observed at 16 hours before basal expression levels were again restored. No peak in *FT* expression was seen at 28 hours (one day plus four hours), where, due to the peak observed at four hours, one may have been expected. Consequentially, it is uncertain whether the variations in *FT* expression observed under short days are true regulated transcription events or just natural variation. Total normalised *FT* expression over the time-course was determined to be W5 = 1.0, W7 = 0.95 and CMZ = 0.71.

4.2.5 The effects on flowering time of pharmacological CaM inhibition.

The application of CaM inhibitors was found to affect both transcript abundance and the phase of expression of clock and flowering time genes. Consequently it was considered of interest whether such changes influenced photoperiodic flowering time.

Several criteria have been reported for the measurement of flowering time. However, the two most commonly employed are chronological flowering time (*i.e.* the age of the plant at bolting), and total rosette leaf number (RLN) at bolting. Chronological flowering time is easily measured, however it is highly sensitive to environmental conditions. Whilst RLN is less sensitive to environmental variability, under short days leaves may be hard to accurately count and older leaves may have undergone senescence (Koornneef *et al*., 1991). Consequently, both chronological flowering time were utilised in the experiments presented here

4.2.5.1 Chemical CaM inhibition affects photoperiodic flowering time on a developmental but not temporal level in Arabidopsis thaliana *grown under 16L : 8D photoperiods.*

The mean chronological flowering time for control plants grown under a 16L : 8D photoperiod was 23.47 days (SE = ± 0.281). Student's t-test indicated that no significant differences in chronological flowering time occurred between water-controls and plants treated with W5 (23.74 days (SE = ± 0.322), P =

0.525); W7 (23.58 days (SE = ± 0.31), P = 0.787) and CMZ (23.40 days (SE = ± 0.283), P = 0.880; figure 4.12 A).

Flowering time as a function of RLN at flowering was 16.84 (SE = ± 0.336) for controls. No significant difference in RLN was observed between controls and plants treated with W5 (RLN = 16.53 (SE = ± 0.379), P = 0.543). Although mean flowering time was slightly increased by application of W7 (RLN = 17.66 (SE = ± 0.405)), this increase was not statistically significant (P = 0.126). Plants treated with CMZ, however, were found to exhibit a small but significant increase in RLN at initiation of flowering (RLN =18.18 (SE = ± 0.416), P = 0.014; figure 4.12 B).

No obvious morphological differences between plants subjected to different treatments were observed during the experiment. Harvested seed were also found to be fertile regardless of treatment.

4.2.5.2 Photoperiodic flowering time in Arabidopsis thaliana *grown under 8L : 16D photoperiods is unaffected by chemical CaM inhibition.*

Under 8L : 16D, mean flowering time for control plants as measured by chronological age was 47.93 days (SE = ± 0.86). No significant difference in chronological age at flowering was observed between control plants and those treated with W5 (48.47 days (SE = ± 0.87), P= 0.663), W7 (47.13 days (SE = ± 0.618), P = 0.07) or CMZ (45.86 days (SE = ± 0.727), P = 0.07; figure 4.13 A). In controls, RLN at flowering was 41.37 (SE = ± 0.94). No significant difference in RLN at flowering was observed between control plants and those treated with W5 (RLN = 41.79 (SE = ± 1.093), P = 0.773) or W7 (RLN = 40.2 (SE = ± 1.186, P = 0.435)). Whereas in long-days application of CMZ led to an increase in RLN, under short days CMZ had no significant effect (RLN = 39.73 (SE = ± 1.524), P = 0.337; figure 4.13 B).

Seed harvested from plants from all treatments were found to be fertile and no obvious morphological differences were observed during the experiment.

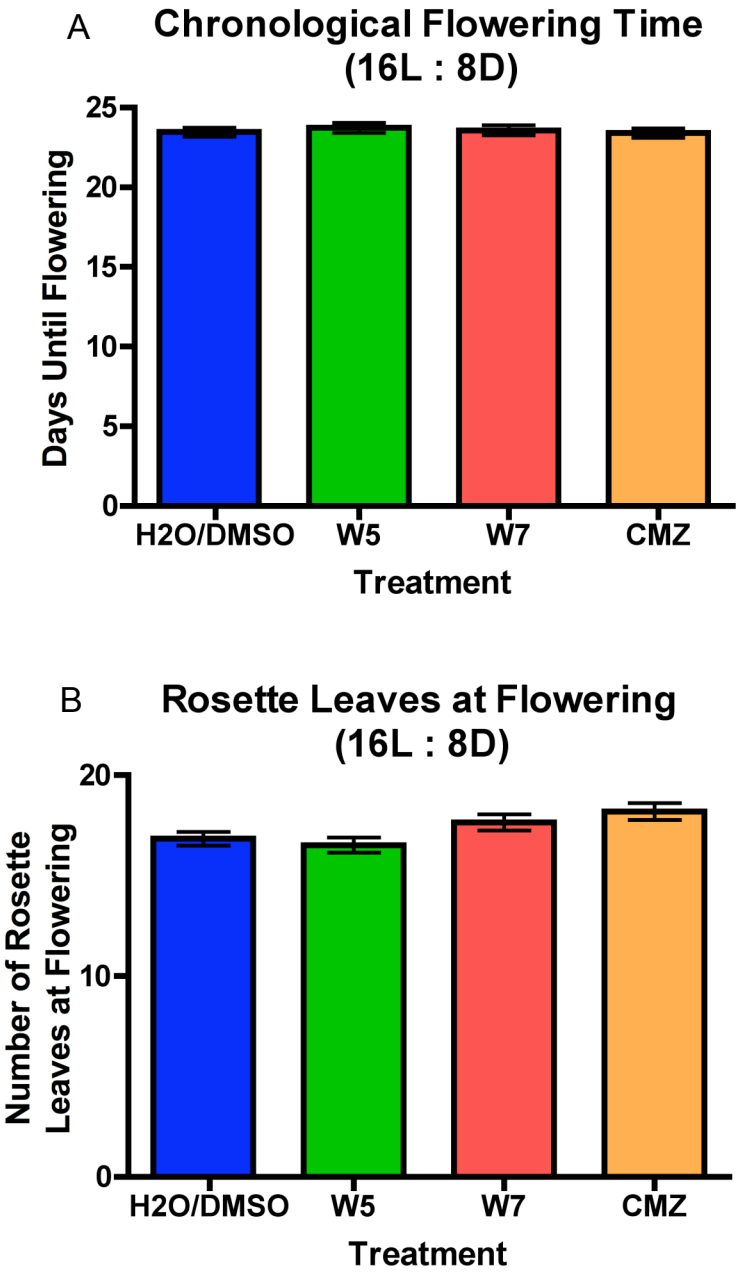

Figure 4.12: The effects of ectopic application of pharmacological CaM inhibitors on flowering time in *Arabidopsis thaliana* plants grown in long days.

Upon developing 3 true-leaves, *A. thaliana* were treated daily with either 50 μM W7, 50 μM W5, 1 μM CMZ or a 0.1% DMSO carrier-solvent control. Flowering time was recorded as a function of age (Fig: 4.12 A) and by number of rosette leaves at bolting (Fig: 4.12 B). Vertical bars indicate standard error of the mean.

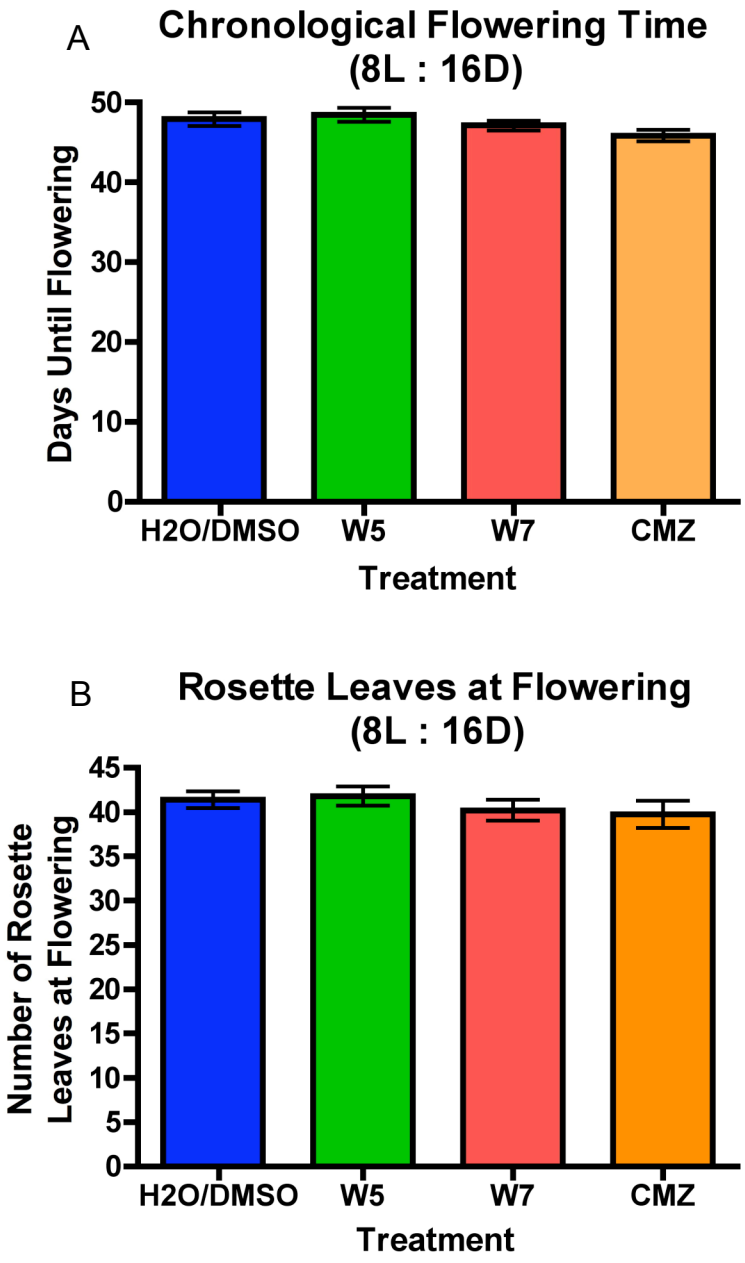

Figure 4.13: The effects of ectopic application of pharmacological CaM inhibitors on flowering time in *Arabidopsis thaliana* plants grown in short days.

Upon developing 3 true-leaves, *A. thaliana* were treated daily with either 50 μM W7, 50 μM W5, 1 μM CMZ or a 0.1% DMSO carrier-solvent control. Flowering time was recorded as a function of age (Fig: 4.13 A) and by number of rosette leaves at bolting (Fig: 4.13 B). Vertical bars indicate standard error of the mean.

4.2.6 Chronic pharmacological CaM inhibition releases inhibition of flowering in darkness, weakly mimicking a newly observed spa1-3 phenotype.

Wild-type Col 0 or Col 0 *spa1-3* mutants were germinated on 0.5 X MS agar containing either 50 µM W5, 50 µM W7, 1 µM CMZ or a carrier-solvent control. After 70 days in total darkness, dark-grown plants were recovered for observation.

All wild-type plants had developed true leaves and were approximately one to two cm in height and had normal root development (figure 4.14). Whilst plants grown on control or W5 media did not show signs of floral development, approximately half of the plants grown on W7 or CMZ displayed evidence of bolting, generally showing a maximum of two flowers on stubby bolts. Floral morphology ranged from partially developed to fully formed flowers (figure 4.15 A, B). *spa1-3* mutants developed true leaves and a small rosette under all treatments. Mutants displayed a well-developed root system and inflorescences were mostly erect. Each plant displayed multiple bolts, which were elongated compared to rosette size and stood approximately 6 to 10 cm in height. Each inflorescence had little secondary branching, three to six cauline leaves per bolt, and contained between twelve and twenty-five flowers. Flowers usually consisted of unopened buds, however some were partially opened (figure 4.16). Although analysing floral organs proved difficult, most flowers did not display significant morphological abnormalities. However, following CMZ exposure a minority of opened flowers displayed altered morphology included reduced petal number and elongated stigmas (figure 4.15 C to F). Development of siliques was not observed under any treatment. Brightfield and epifluorescence microscopy revealed no evidence of pigmentation.

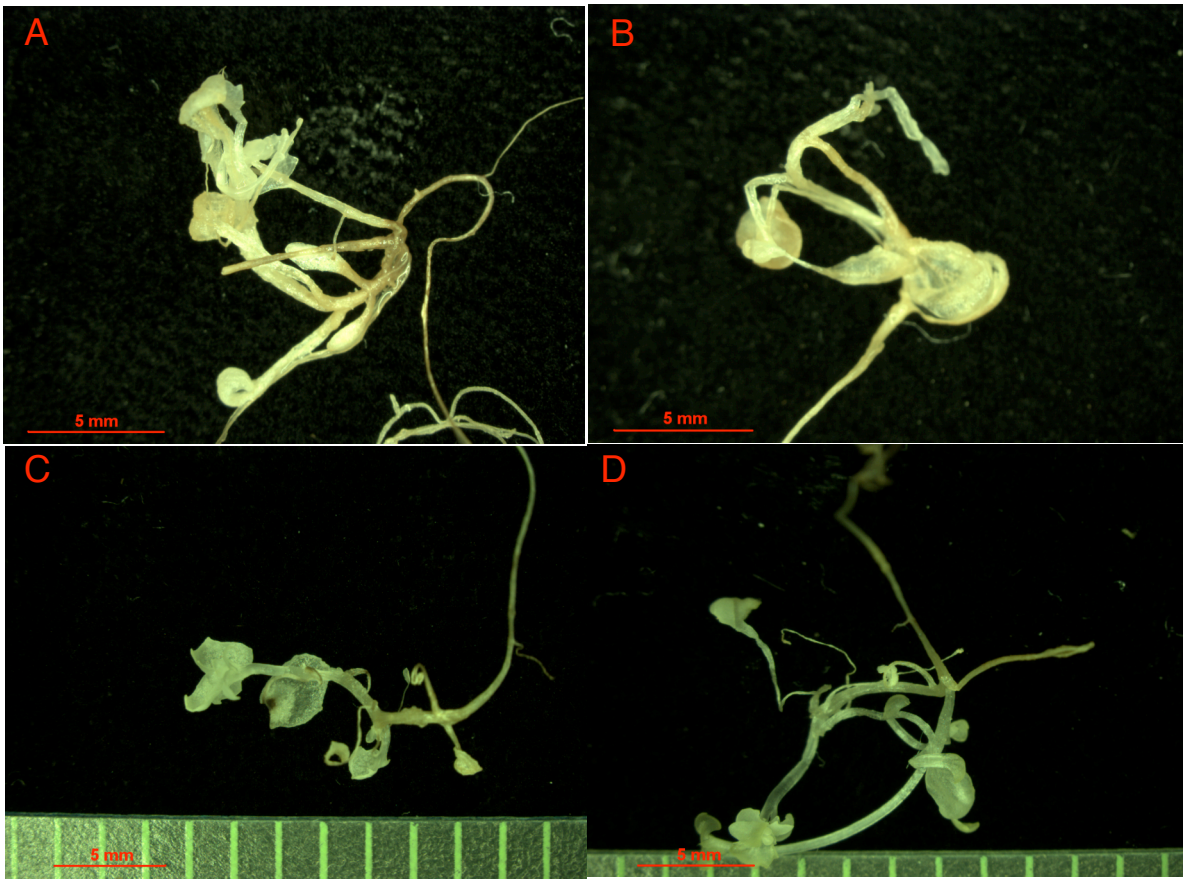

Figure 4.14: Representative examples of the developmental effects of continued exposure to calmodulin inhibitors on dark-grown wild-type *A. thaliana*.

Wild-type *A. thaliana* (ecotype Col 0) were grown in darkness for 70 days on 0.5 X MS agar containing 5% sucrose (w/v) and either or a carrier-solvent control (Fig 4.14 A), 50 μM W5 (Fig. 4.14 B), 50 μM W7 (Fig. 4.14 C), 1 μM CMZ (Fig. 4.14 D). Following recovery, plants were examined for signs of floral development.
Under all treatments, recovered plants showed poorly developed rosettes and were approximately 1 to 2 cm in length. Plants grown on control or W5 agar (A and B respectively), displayed no signs of floral initiation. Approximately 50% of plants grown on W7 or CMZ media agar (C and D respectively), displayed floral organ development.

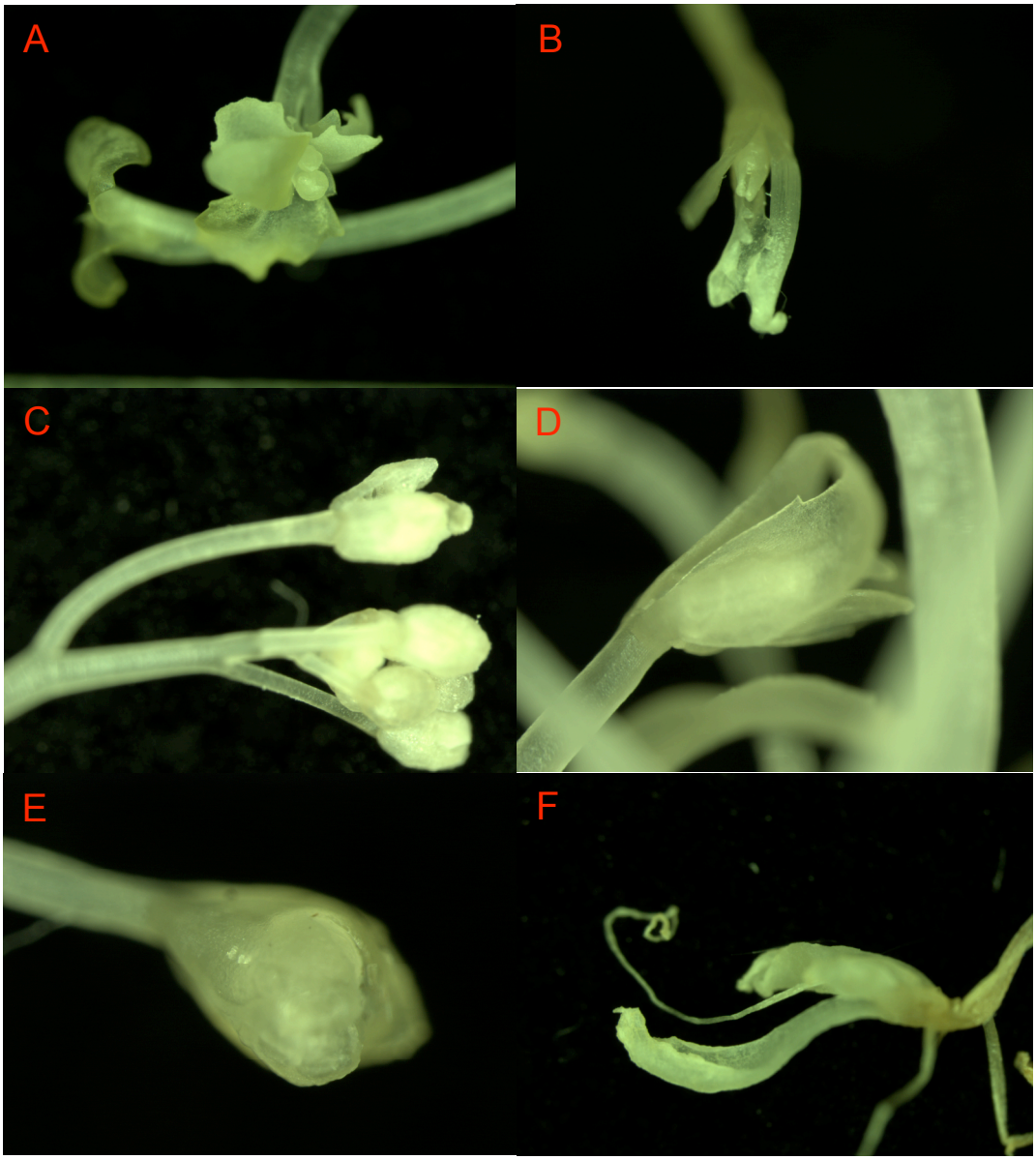

Figure 4.15: Representative examples of the floral development observed in dark-grown wild-type and *spa1-3* mutant *A. thaliana*.

Col 0 wild-type and *spa1-3* mutants were grown in darkness for 70 days on 0.5 X MS agar containing 5% sucrose (w/v) and either 50 μM W7, 50 μM W5, 1 μM CMZ or a 0.1% DMSO carrier-solvent control. Following recovery, plants were examined for signs of floral development.

Flowers were not observed in wild-type plants grown on control or W5 media. However, approximately 50% of those grown on W7 or CMZ media (Fig 4.15 A and B respectively), showed floral development. Floral organs however, appeared incompletely formed.

spa1-3 mutants grown on control, W5, W7 (Fig. 4.15 C, D and E respectively), produced multiple flowers with apparently normal morphology. Mutants grown on CMZ media (Fig. 4.15 F), also produced numerous flowers, however a number of these showed altered morphology including reduced numbers of petals and elongated stigmas.

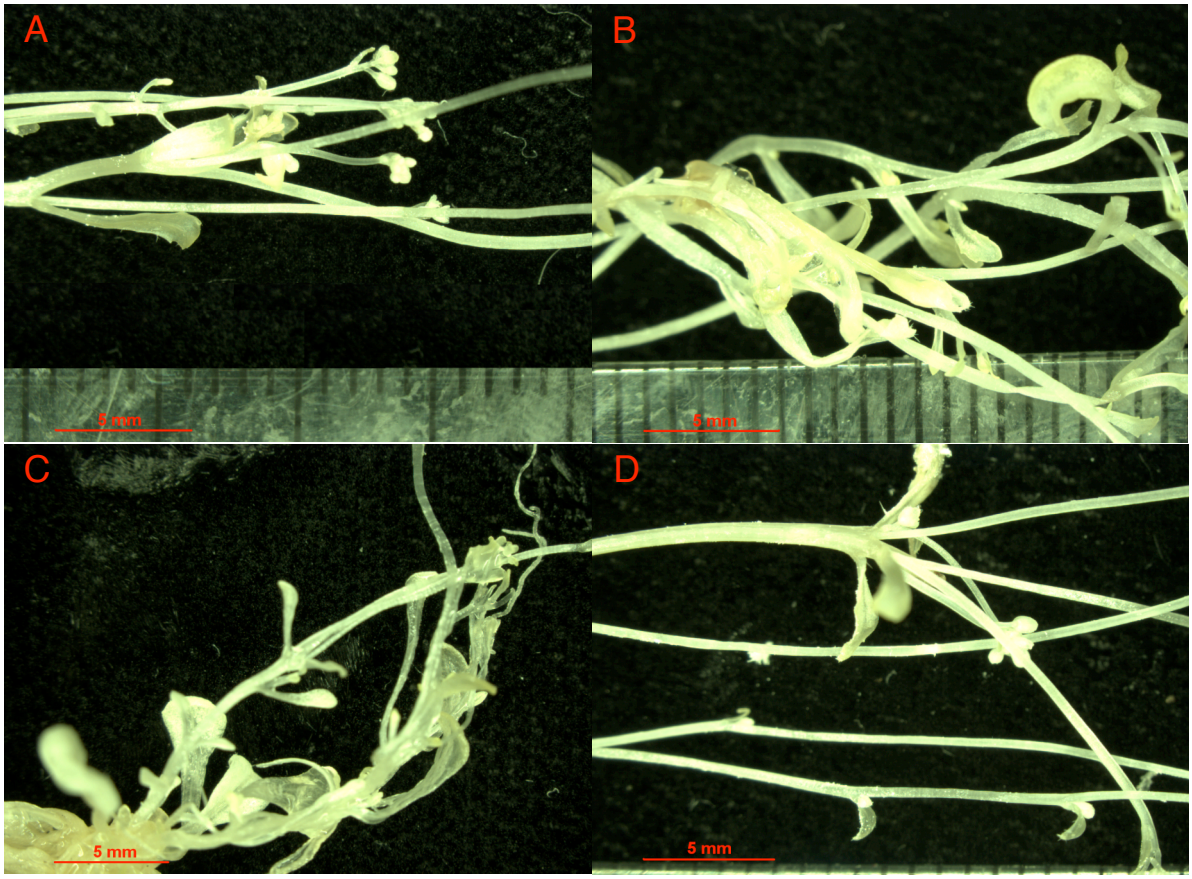

Figure 4.16: Representative examples of the developmental effects of continued exposure to calmodulin inhibitors on dark-grown *A. thaliana spa1-3* mutants.

spa1-3 mutants were grown in darkness for 70 days on 0.5 X MS agar containing 5% sucrose (w/v) and either 50 μM W7, 50 μM W5, 1 μM CMZ or a 0.1% DMSO carrier-solvent control. Following recovery, plants were examined for signs of floral development. Mutants grown on carrier-solvent control, 50 μM W5, 50 μM W7 or 1 μM CMZ agar (Fig. 4.16 A, B, C and D respectively), displayed small rosettes, multiple bolts and usually showed several flowers mostly consisting of unopened buds.

4.3 Discussion

4.3.1 Inhibition of CaM modulates expression of circadian clock and flowering-time associated genes in Arabidopsis thaliana.

In order that CaM inhibitors could be applied for a sufficient period, it was necessary plants used in this thesis were both grown on a different medium (compost) and significantly older than the seedlings normally used in circadian expression studies. Comparisons between the data presented here and earlier work are therefore limited to being qualitative in nature.

Published and unpublished microarray data have previously shown that, in agar-grown *A. thaliana* seedlings, *CAM1* transcript is both under circadian control and possibly day length responsive. These data indicated that *CAM1* transcript abundance was minimal at dawn, peaking at eight to 12 hours under 12L : 12D and 16L : 8D photoperiods and at 12 hours under 8L : 16D photoperiods (Harmer *et al.*, 2000; Winter *et al.*, 2007). The control plants used in this thesis displayed *CAM1* expression profiles broadly similar to those recorded in previous microarray data Winter *et al.*, 2007), with peak expression occurring during the night in short days and mid-photophase during long days. These data also confirm the diurnal, and possibly circadian, nature of *CAM1* transcript oscillations.

The changes in *CAM1* expression generated by CMZ, W7 or W5 were distinct between long days and short days and the possibility remains that the total degree of CaM inhibition conferred is dependent upon daylength. Care must therefore be taken in comparing changes in expression of a single gene across different day-lengths. Plants at the ten-leaf stage grown under short days were chronologically older than plants with a similar number of leaves grown under long days, having been exposed to a greater number of cycles of photoperiodic entrainment. Other factors, such as differences in cuticle thickness may also affect the permeability of the applied pharmacological agent. As many metabolic processes are day-length regulated (Herrera, 1999; Lu *et al.*, 2005), differential degradation of pharmacological agents under short days and long days is also likely to occur.

Under short day photoperiods, the *CAM1* expression peak was narrowed by four hours following all pharmacological treatments. Total *CAM1* transcript also increased following pharmacological applications. Under long days, treatment

with W5 led to a transcription signature almost identical to that of controls, however W7 led to a four-hour extension of the *CAM1* transcription peak. Interestingly, although CaM inhibitors affected the transcription patterns and overall abundance of *CAM1* transcript, the magnitude of these effects varied across the 28-hour timecourse. In both short days and long days no significant difference in *CAM1* transcript abundance was observed between any of the treatments at dawn. Such observations are consistent with previous *CAM1* expression data in seedlings (Harmer *et al.*, 2000).

As discussed previously, TOC1 forms an integral part of the *A. thaliana* circadian oscillator (Alabadí *et al.*, 2001; McClung *et al.*, 2002), and mis-expression leads to severe changes in flowering time (Más *et al.*, 2003b; McClung, 2006; Strayer *et al.*, 2000). Expression of *TOC1* in control plants grown under short days was broadly consistent with that predicted by recent models (Locke *et al.*, 2006), with transcript peaking between 12 and 16 hours and declining until dawn. Likewise, *TOC1* signatures in long day grown controls were broadly consistent with previously published experimental data (Strayer *et al*., 2000). Although a broader transcription peak was observed in the study presented here, it is again necessary to consider that differences in age, media and ecotype will contribute to the expression signatures recorded.

Under both photoperiods, application of W5 or W7 led to similar reductions in total *TOC1* transcript abundance. This effect was unexpected, as in gravitropic and flowering-time assays W5 had produced responses statistically similar to those seen following control treatments. However, these assays recorded physiological and cellular changes and not the molecular changes indicated by qRT-PCR. At the molecular level, *TOC1* may be extremely sensitive to inhibition of CaM, enabling even a weak inhibitor such as W5 to generate a significant effect. However, naphthalene-sulphonamide CaM inhibitors are not as specific for CaM as would be desired and the possibility remains that unintended secondary effects were present (Tanaka *et al.*, 1982). Due to large reductions in *TOC1* transcript abundance following treatment with either W7 or W5, it is impossible to say with sufficient confidence that this effect is primarily due to inhibition of CaM or a secondary effect unrelated to CaM inhibition. Further studies employing a greater diversity of CaM inhibitors would therefore

be necessary to clarify the exact nature of the observed reduction in *TOC1* transcript.

Under short days, application of CMZ resulted in a four-hour delay in peak *TOC1* expression and a narrowed expression peak. Under long days, plants treated with CMZ or W7 showed a four-hour delay in peak *TOC1* transcript abundance. Unlike the pharmacologically induced reductions in *TOC1* transcript, these phase-shifts in *TOC1* expression were not present in plants treated with W5 and are therefore highly likely to be solely due to inhibition of CaM. Such phase shifts in expression of an integral component of the central oscillator indicate that CaM is able to directly modulate expression of at least one core clock gene.

Unlike TOC1, CONSTANS (CO) is not implicated in circadian timekeeping.

In long days, *CO* abundance is high at dawn before declining, and remaining low until approximately eight hours before dusk when it rapidly rises and remains high until daybreak (Suárez-López *et al.*, 2001). Under short days, *CO* abundance remains low throughout the day and rapidly rises following dusk, remaining high until daybreak (Mizoguchi *et al.*, 2005; Suárez-López *et al.*, 2001). The *CO* expression signature is critical for normal induction of flowering and the only noted phenotype in plants misexpressing *CO* is altered flowering time (Suárez-López *et al.*, 2001). In short days, mutants in which *CO* transcript peaks before dusk undergo an accelerated transition to flowering similar to that normally found under long days (Yanovsky & Kay, 2002). As discussed, the plants used in the current study were of a different ecotype (Col 0), than those studied previously (Landsberg erecta (Ler)), and were considerably older. Given these differences, expression patterns of *CO* in short day controls were mostly consistent with published data. The increase in transcript between four and eight hours was unexpected, however similar increases are recorded in unpublished microarray data accessible at the Arabidopsis eFP browser (http://bbc.botany.utoronto.ca/efp/cgi-bin/efpWeb.cgi) and may be related to age or the regulation of *CO* by a putative 'light-quality pathway' (Cerdán & Chory, 2003). Although the rise in *CO* expression observed in controls was delayed in plants treated with W5, transcript levels followed a similar pattern. Application of either CMZ or W7 led to a dramatic decrease in overall *CO*

transcript and an almost total suppression of rhythmicity, indicating a significant role for CaM in the maintenance of circadian *CO* signatures.

In long days, *CO* expression signatures in control plants deviated from those previously published, with no strong oscillations in transcript abundance being observed (Suárez-López *et al.*, 2001; Tseng *et al.*, 2004). This discrepancy may be due to the relative proximity of the plants to flowering compared to the three to ten day-old seedlings used in previous studies.

Unusually, each pharmacological agent appeared to generate distinct *CO* transcription profiles, likely, in part, to the inherent arrhythmicity observed in untreated plants. W5 treated plants appeared to show rhythmic *CO* expression, however the transcript signature observed was almost precisely the inverse of that normally found under long day photoperiods with transcript abundance peaking mid-photophase, quickly falling and remaining basal throughout the night. Treatment with W7 generated a distinct *CO* signature whereby transcript abundance increased from a basal low during the light to a high during the night. Unlike plants treated with W7, plants treated with CMZ displayed bi-modal *CO* expression peaks, with expression increasing between 12 and 20 hours and remaining high until dawn.

Under non-inductive photoperiods, *FT* expression in *A. thaliana* seedlings is minimal (Yanovsky & Kay, 2002). Although the plants used in the investigation conducted here were significantly more mature, *FT* expression did not track *CO* expression under short days and is strongly supportive of the hypothesis that *FT* was expressed at low levels (Valverde *et al.*, 2004). It is therefore uncertain whether the differences in expression observed between treatments are due to changes in transcription or merely background variation. However, treatments that reduced total *CO* abundance also led to reduced overall *FT* transcript as would be expected.

Under 16L : 8D, *FT* expression followed a pattern similar to that previously reported, slowly rising between eight and 12 hours and then increasing rapidly to a peak at dusk before immediately declining. Such an *FT* expression signature would normally occur due to rising levels of light-stablised CO between eight hours and dusk followed by targeted degradation of CO throughout the night (Laubinger *et al.*, 2006; Liu *et al.*, 2008; Valverde, 2006).

As with *TOC1*, W7 generated a *FT* signature broadly similar to that found following treatment with W5. Dusk peaks were observed, but occurred at a much-reduced degree to those seen after control treatments. These similarities between changes induced by W5 and W7 again prevent clear determination of whether effects are primarily CaM related or due to secondary effects. Plants treated with CMZ expressed *FT* in a pattern mostly similar to that observed in controls. However overall *FT* transcript was reduced under the CMZ regimen and the transcript peak delayed by four hours in a manner similar to the observed phase shift in *TOC1* expression. As the clock is responsible for both the level and timing of *CO* expression it is consequently involved in the control of *FT* expression (Mizoguchi *et al.*, 2002; Mizoguchi *et al.*, 2005). The observed *FT* transcript signature therefore corresponds well with the changes in *TOC1* expression induced by treatment with CMZ and indicates that CaM-based modulation of the clock is able to cascade throughout the photoperiodic flowering pathway.

Unfortunately, neither of the *CO* expression peaks observed for CMZ treated, plants satisfactorily correspond to the observed phase shifted *FT* peak. The latter *CO* peak occurred during the night when CO is not stabilised and therefore unable to induce *FT* expression, whilst the earlier matched the peak observed in W5 treated plants. However, unlike in CMZ treated plants, no phase-shift in the *FT* peak was observed in plants treated with W5. Equally as problematic is that whilst a strong *FT* peak is observed in water controls, there is no corresponding *CO* peak to explain its induction.

It has already been speculated that the age of the plants investigated may contribute to the unusual *CO* signature. It is possible that once the phase of *FT* expression is established, the reported rhythms of *CO* expression are no longer required and become less pronounced. However, to verify this it would be essential to study *CO* expression across *A. thaliana* at a broad range of life stages.

4.3.2 Inhibition of CaM modulates photoperiodic flowering time on a developmental level.

Changes in the expression of clock and photoperiodism related genes, as recorded under circadian conditions, are known to have significant effects on

photoperiodic flowering time (Somers *et al*., 1998; Valverde, 2006). The expression studies in this thesis were necessarily recorded under diurnal conditions. However, changes in transcription patterns induced by CaM inhibitors would likely be represented at the circadian level and may therefore influence photoperiodic flowering time.

Under short day photoperiods, aerial application of W5, W7 or CMZ did not significantly affect either chronological or developmental flowering time. Given that under non-inductive photoperiods timing of flowering is controlled by pathways other than the photoperiodic pathway, this is not necessarily unexpected. Under the inductive photoperiod, CMZ generated a small but significant increase in flowering time as measured by rosette leaf number (RLN). These data appear to imply that, at least at the conservative concentrations utilised, pharmacological CaM inhibition affects photoperiodic flowering time on a developmental but not temporal level.

Although the extension in RLN flowering time following application of CMZ was not found for W7, this may be due to differences in the relative potency of CaM inhibition. Differential metabolism of inhibitors may occur *in planta* and although the concentrations utilised were chosen by empirical root assays, more quantitative methods may be found to exist. It is interesting however that although plants treated with CMZ had a greater overall *FT* abundance and a higher expression peak under long days, they flowered later (as measured by RLN) than those treated with W7. Phase delays as observed under CMZ treatments, whereby peak *FT* expression is shifted into the night, may therefore elicit a greater effect than an overall reduction in transcript. Such an effect may conceivably be due to reduced vascular transport of translated FT to the shoot apical meristem under darkness (Corbesier *et al.*, 2007).

4.3.3 The presence of CAM appears necessary for SPA1 mediated repression of flowering in darkness.

SPA1 is involved in the repression of photomorphogenesis in darkness, however three to four day-old seedlings of *spa1* mutants show wild-type photomorphogenic development due to the partial redundancy between SPA1 and SPA2. As levels of SPA2 diminish with age (Laubinger, 2004), it was conjectured that *spa1* phenotypes, normally masked by the presence of SPA2,

may surface in sufficiently mature dark-grown plants. The bioinformatic prediction of a CaM binding site in SPA1 raised the possibility that such unmasked *spa1* phentoypes may be reproducible in wild-type plants via addition of CaM inhibitors to the growth medium.

As expected, neither wild-type plants grown on control medium nor those grown on medium containing W5 underwent floral induction. However, the formation of flowers on wild-type plants treated with W7 or CMZ strongly indicates that CaM acts to positively repress photomorphogenic flowering under darkness. Inhibition of CaM is apparently sufficient to relieve this inhibition and allow floral induction.

Dark-grown *spa1* mutants flowered following both control and pharmacological treatments. Unlike wild-type plants, *spa1* mutants displayed multiple elongated meristems each containing numerous flowers, but no siliques. No obvious changes in plant size or number of flowers were observed between untreated *spa1* mutants and mutants treated with 50 W5, W7 50 μM or 1 μM CMZ. This suggests that, when supplied with a suitable carbon source, *spa1* mutants flower naturally in darkness and are not strongly affected by the concentrations of inhibitors used in this study, although altered floral morphology was observed in plants treated with CMZ. As no similar changes were observed following W7 treatment it is likely these effects are not related to CaM inhibition.

Though only a partial phenocopy of the *spa1* mutant, the simplest explanation for the flowering of wild-type plants treated with CMZ and W7 is that CaM is necessary in order for SPA1 to fully suppress flowering in darkness. At the concentrations of pharmacological agents employed it is unlikely that CaM would be fully inhibited. Consequently, activation of at least some CaM-binding proteins would still occur. It is therefore logical that reproduction of any mutant phenotype in wild-type lines would, at best, be partial in nature.

It is interesting to note that the concentrations of inhibitors utilised in this experiment were identical to those to which seedlings adapted in the earlier gravitropism assay. As continued CaM inhibition generated a clear phenotype under extended darkness this would suggest that, at least at the concentrations utilised in this thesis, *A. thaliana* does not fully acclimate to the presence of CaM inhibitiors. It is also be possible that plasticity may vary between different systems. While gravitropic responses acclimated to the presence of CaM

inhibitors, such adaptation may be less pronounced in other systems. Alternatively the presence of sucrose in the medium or the absence of light may also contribute to differences in acclimation threshold. Indeed, recent evidence indicates the light-dependency of at least some acclimation processes in plants (Kangasjärvi *et al.*, 2009).

4.4 Conclusions

It has been demonstrated that CaM appears to be intricately involved in the regulation of flowering in *A. thaliana* under both light-dark cycles and under constant darkness. It's role in photoperiodic flowering, however appears distinct from its influence on floral induction under darkness.

Under normal light-dark cycles, the effects of CaM inhibition appear to cascade from the central-oscillator gene *TOC1* to the terminal flowering-time gene *FT* and are best evidenced by phase-shifts, most often delays, in peak expression. The ability of CaM to modulate the photoperiodic flowering pathway is supported by the effect of CaM-inhibition upon flowering time. However under long days, where the photoperiodic pathway is the dominant determinant of flowering time, CaM inhibition leads to delayed flowering on a developmental level. It therefore appears that CaM is involved in the promotion of flowering under inductive photoperiods.

Under darkness, flowering in wild-type lines is naturally repressed. However, such repression is inhibited in plants treated with CaM antagonists. Such de-repression mimics a newly discovered phenotype observed in lines lacking the putative CaM-binding protein SPA1 and strongly supports the hypothesis that SPA1-based suppression of dark flowering is dependent on the presence of CaM.

CHAPTER 5: DETERMINATION OF THE SPECIFICITY AND BINDING KINETICS OF CA^{2+}-CALMODULIN-CALSPERMIN USING SURFACE PLASMON RESONANCE AND AFFINITY CHROMATOGRAPHY

5.1 Published work

The following paper has been previously published as:

Murphy, A. J., Kemp, F., Love, J., (2008). Surface Plasmon Resonance Characterization of Calspermin-Calmodulin Binding Kinetics. *Analytical Biochemistry,* **376**; 61-72.

The authors of the paper made the following contributions:
Andrew J. Murphy:

- *Ab initio* modelling and structural characterisation of *Rattus norvegicus* calspermin.
- Cloning of the fusion constructs *smGFP* (soluble-modified Green Fluorescent Protein) and *smGN* (soluble-modified GFP/calspermin) in to the expression vector PRSETA.
- Expression, isolation and analysis of all recombinant proteins via nickel-affinity chromatography and SDS-PAGE.
- Determination of the inhibitory activity (*Ki*), of smGN (and smGFP controls) toward calmodulin using the calmodulin-phosphodiesterase (CaM-PDE) assay.
- Determination of the specificity of smGN for CaM using smGN affinity chromatography against *A. thaliana* protein extracts and subsequent SDS-PAGE 'band-shift' assays.
- General experimental design of Surface Plasmon Resonance (SPR) experiments, overall running of experimental procedures and subsequent data analysis.
- Co-preparation of figures for publication.
- Primary authorship of all drafts of paper, including final version as published.

Fred Kemp:

- Refining experimental design to accommodate constraints of the system and to maximise quality of gathered data.
- Provision of training for the BIACORE 3000 SPR machine.
- Provision of training for BIAevaluation data analysis package.
- Fact checking paper prior submission for publication

John Love:

- Provision of *smGN* and *smGFP* in pBluescript.
- Contributed to experimental design of CaM-PDE and band-shift assays.
- Co-preparation of figures for publication.
- Proofread and edited each draft of the paper prior to submission.
- Supervised the research.

5.2 Additional Experimental Work Unpublished in the Article

Additional experimental work relating to the characterisation of smGN and not presented in Murphy *et al*. (2008) is provided below.

5.3 Introduction

The research published in Murphy *et al*. (2008) described the development of the chimaeric GFP/calspermin fusion protein, labelled smGN, and the analysis of its properties as a selective CaM inhibitor. It was shown that smGN inhibits CaM-dependent phosphodiesterase activity with a K_i of 1.97 nM, a value 3,800 times lower than that of the pharmacological CaM inhibitor W7 (K_i = 7.5 μM) (Hidaka & Tanaka, 1983). smGN also displayed a K_D of $4.42^{\bullet}10^{-9}$ M towards CaM, which represents an affinity 2,500 times greater than that displayed by W7 (Hidaka *et al.*, 1981). smGN affinity chromatography indicated that, if expressed in *A. thaliana*, smGN would be highly specific toward only true CaMs and not related proteins. Bioinformatic analyses largely supported earlier studies regarding the identities of key amino acid residues within the calspermin CaM-binding motif. However two additional residues, Met 143 and Leu 166, were also predicted as being components of the CaM-binding pocket.

In addition to the work presented in Murphy *et al*. (2008), further investigations were undertaken to better validate the structural properties of the smGN chimaera. Additional bioinformatic analyses were also utilised in order to both verify the quality of the modelled structure of smGN and to provide insights in to how the activity of calspermin may be regulated *in vivo*.

5.4 Materials and Methods

5.4.1 Analysis of the spectral characteristics of the smGN chimaera.

In order to examine the excitation and emission spectra of smGN, 50 μg smGN was diluted in 1.5 ml 25 mM Tris-HCl buffer (pH 7.4) and a three-dimensional emission / excitation scan was performed using a AMINCO-Bowman Series 2 spectrofluorometer (AMINCO, USA).

Photomultiplier tube sensitivity (detector high voltage) was configured to auto-range and was automatically set at 700 V. Excitation was set from 300 to 600 nm using a 5 nm gap and emission recorded from 350 to 650 nm also with 5 nm gap.

5.4.2 Assessment of the quality of ab initio *modelled calspermin.*

Protein data bank (PDB) coordinate files generated using the PROTINFO *ab initio* modelling server (Hung *et al.*, 2005), were submitted to the WebMol server hosted at the University of California, San Francisco (http://www.cmpharm.ucsf.edu/~walther/webmol.html) for analysis of stereochemical quality and rendered using default parameters.

5.4.3 Hydrophobic Cluster Analysis.

The primary amino acid sequence of calspermin was submitted to the HCA server hosted at the Ressource Parisienne en Bioinformatique Structurale (http://bioserv.rpbs.jussieu.fr), for plotting using default parameters.

5.4.4 Simulating the effects of phosphorylation of Ser 27 on the CaM binding region of calspermin.

A 50 amino acid region centring on the CaM-binding domain of calspermin and containing substitutions of Ser 27 for the phosphoserine mimics Asp or Glu was modelled *ab initio* using the Protinfo AB CM program (Hung *et al.*, 2005; Hung & Samudrala, 2003). PyMol software (Delano, 2002), was used to visualise conformational alterations of the CaM-binding motif induced by simulated phosphorylation of Ser 27.

5.5 Results and Discussion

5.5.1 Spectral characteristics of the smGN chimera are identical to smGFP.

It was shown in Murphy *et al*. (2008) that smGN retained the ability to interact with CaM with high specificity and high affinity, strongly indicating that fusion with GFP had not adversely affected the tertiary structure of the calspermin subunit. However, further verification that alternative folding had not occurred was sought. To help determine whether altered folding may have occurred due to interactions between calspermin and GFP, the excitation and emission spectra of smGN were quantified by spectrofluorometry.

The spectral characteristics of smGN were found to be in accordance those published for smGFP (Davis & Vierstra, 1996, 1998). The GFP moiety of smGN

was most strongly excited by irradiance at 395 nm, with a secondary moderate excitation peak at 488 nm (figure 5.1). Peak emission occurred at 510 nm, whilst the secondary 540 nm emission 'shoulder' characteristic of smGFP was also observed. No other excitation or emission peaks were found. As the observed spectral signature matched that published for smGFP, it is highly unlikely that unwanted interactions between the chimaeric domains of smGN had resulted in altered peptide folding.

5.5.2 Ab initio *modelled calspermin is of high stereochemical quality.*

Murphy *et al*. (2008), describes bioinformatic analyses that were undertaken in order to better elucidate the structure of calspermin in general and its CaM-binding motif specifically and to ascertain the orientation of the CaM binding motif of calspermin in relation to the GFP fusion. 3-D topology models largely supported previous conclusions regarding residues believed to form the putative CaM-binding motif of calspermin. However the models also indicated that Met 143 and Leu 166 form part of the CaM-binding pocket and therefore may contribute to interaction with CaM.

The validity of inferences drawn from a protein topology model are directly dependent upon the quality of that model. As the analyses of calspermin presented in Murphy *et al.* (2008) indicated a novel structural feature not previously predicted, it was considered important to further validate and extend upon these predictions. An important indicator of the quality of a modelled protein structure is the distribution of main-chain phi (Φ) and psi (Ψ) torsion angles. The stereochemical quality of calspermin topology model was assessed by a Ramachandran plot (figure 5.2), whereby the distributions of these torsion angles are graphically mapped (Morris *et al.*, 1992). The overall quality of the modelled structure was classified as high. 82.9% of residues lie in 'most favoured' regions, 15.7% in 'allowed' and only 1.4% of residues are in 'generous' zones. No residues lie in 'disallowed' regions. Residues in the putative CaM binding domain (coloured green), are all located in an area of the plot corresponding to right-hand α-helices, a conformation common to CaM-binding motifs (O'Neil & Degrado, 1990), and all are in most favoured orientations.

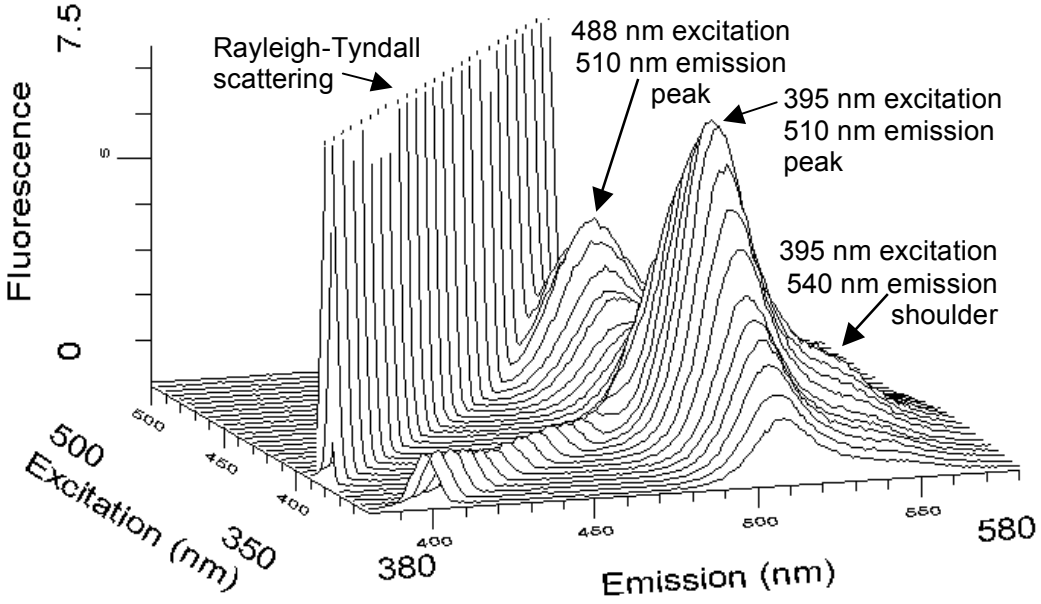

Figure 5.1: Three-dimensional plot of the spectral characteristics of smGN.

Spectral characteristics observed for smGN were identical to those published for smGFP. Maximum excitation was observed at 395 nm and a secondary, more moderate, excitation peak was observed at 488 nm
The emission maxima occurred at 510 nm, whilst a secondary emission 'shoulder' characteristic of smGFP was observed 540 nm.

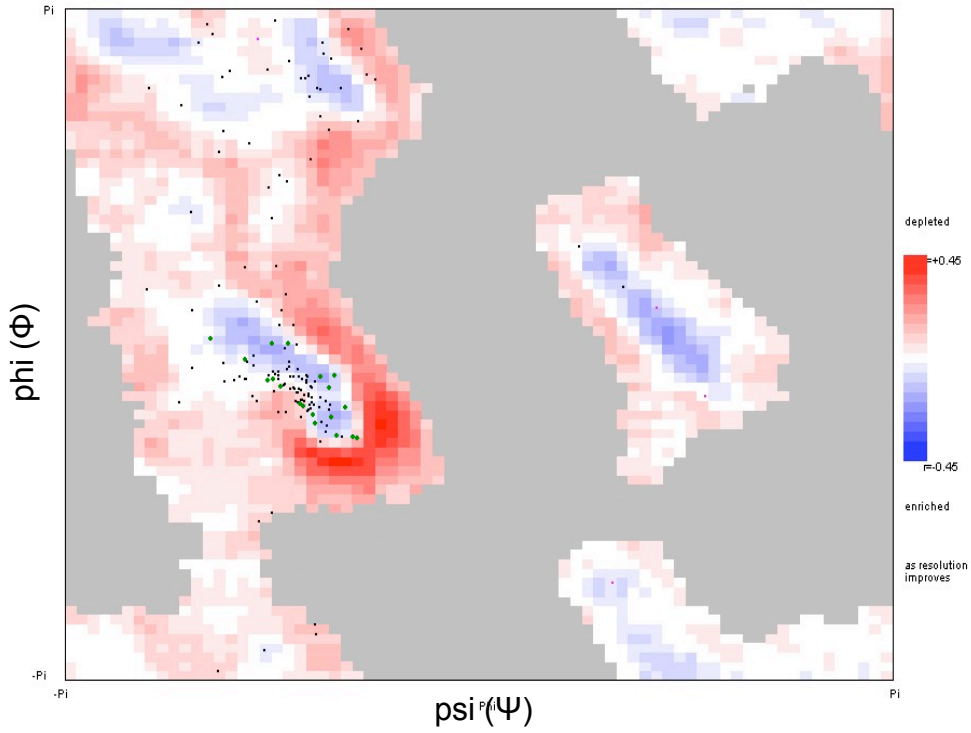

Figure 5.2: Ramachandran plot of the modelled calspermin structure.

A Ramachandran plot was performed on the calspermin model was in order to assess the overall stereochemical quality of the structure.
82.9% of residues lie in 'most favoured' regions (shown in blue and white), 15.7% in 'allowed' and only 1.4% of residues are in 'generous' zones (shown in red). No modelled residues were found to lie in 'disallowed' regions.
All residues within the putative CaM binding domain (highlighted in green), are in most favoured orientations and are found in the area of the plot corresponding to right-hand α-helices.

The high quality of the model supports the hypothesis that the localisation of amino acids within calspermin conforms closely to those modelled. The quality of the model is of particular relevance when considering the unexpected localisation of Met 143 and Leu 166 within the CaM-binding pocket. It was previously hypothesised that Met 143 and Leu 166 may play a role in either the stability of this region or directly in the binding of CaM (Murphy *et al*., 2008), and a model of inferior quality may have indicated that the position of these residues was artifactual.

5.5.3 Hydrophobic Cluster Analysis supports helical wheel projections.

Residues Leu 17, Val 21, Val 24 and Leu 30 had previously been predicted to form the core hydrophobic residues within the CaM-binding domain of calspermin (Rhoads & Friedberg, 1997). The JPRED analysis and helical-wheel projection presented in Murphy *et al*. (2008), supported the positioning of Leu 17, Val 21, Val 24 within an amphipathic helix characteristic of the majority of CaM binding domains (O'Neil & Degrado, 1990; Rhoads & Friedberg, 1997). However Val 25 was predicted to form a key component of the hydrophobic hemicylinder, whilst Leu 30 was shown to lie outside this region. Hydrophobic Cluster Analysis (HCA) was therefore undertaken in order to further examine the likelihood of Val 25 or Leu 30 contributing to the amphipathic helix.

Whereas helical-wheel projections begin with an initial assumption that that a peptide sequence forms an α-helix and then derive the properties of that helix, HCA identifies structural features across entire protein sequences by analysis of clusters of hydrophobic residues (Gaboriaud *et al.*, 1987). The HCA projection lends support to Val 25 being localised within the hydrophobic region of the α-helix at the heart of the CaM-binding motif. Leu 30 is again predicted to lie outside the hydrophobic hemicylinder, being structurally separated from the other core hydrophobic residues by cluster-breaking serine residues (figure 5.3).

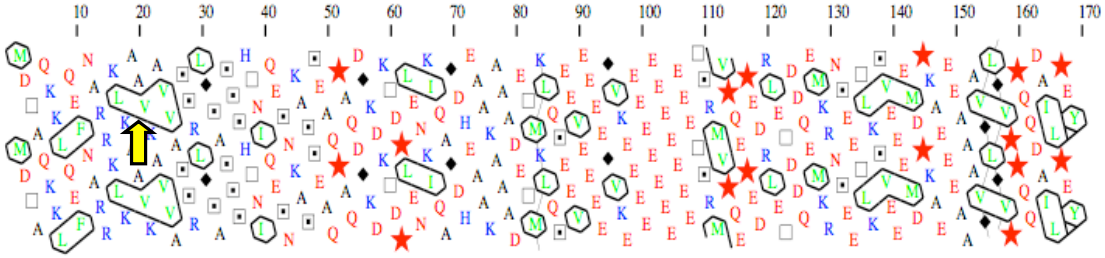

Figure 5.3: **H**ydrophobic cluster analysis of secondary structure components of the calspermin amino acid sequence.

Hydrophobic cluster analysis was used to verify residues within the hydrophobic hemicylinder of the calspermin CaM-binding motif.
Together with Leu 17, Val 21 and Val 24, Val 25 forms a cluster typical of hydrophobic components of α-helices (indicated by yellow arrow). This clustering supports the involvement of Val 25 as a possible component of the core hydrophobic CaM-binding motif. Analysis also predicts that Leu 30, which forms the final residue of the CaM-binding motif lies outside of the predicted α-helix, being separated from the other core residues by cluster-breaking serine residues.

Though perhaps unexpected, the location of Leu 30 outside of the core amphipathic helix is not without precedent. At only 12 amino acid residues in length, the predicted helical component of the calspermin CaM-binding domain is relatively short. 1-5-8-14 motifs associated with such short helices have previously been observed to have the the fourth key hydrophophobic residue localised outside of the core helix, whilst in longer helices (14 to 16 residues), the fourth key residue is located within the helix (Aoyagi *et al.*, 2003).

5.5.4 Phosphorylation as a modulator of calspermin activity.

Phosphorylation of serine residues affects the conformation of the CaM binding domains of a number of peptides including human protein 4.1, by creating favourable electrostatic interactions between the phosphate group and the helix backbone (Vetter & LeClerc, 2001). These interactions alter, and most often stabilise, the adoption of α-helical conformations (Andrew *et al.*, 2002; Smart & McCammon, 1999; Vetter & LeClerc, 2001). Calspermin is transcribed from an internal promoter within an intron of Ca^{2+}-CaM-dependent protein kinase IV (CaMKIV) (Sun & Means 1995) and is homologous to the CaMKIV CaM binding C-terminal domain (Means *et al.*, 1991). Phosphorylation of CaMKIV Ser 332 (corresponding to calspermin Ser 27), leads to total inactivation of Ca^{2+}/CaM-dependent activity. However, phosphorylation of its immediate neighbour, Ser 333, has no such effect (Watanabe *et al.*, 1996). The possibility that calspermin's affinity toward CaM may be modulated by phosphorylation has been raised previously (Ono *et al.*, 1989). However, even though calspermin Ser 27 lies within the putative CaM binding domain, the effects of its phosphorylation have not been experimentally investigated. Analysis of the topology model of calspermin presented in Murphy *et al*. (2008), indicated that, in its native state, calspermin Ser 27 is surface localised and forms the terminal residue in the CaM binding domain α-helix. Conversely, Ser 28 lies outside the α-helical region and is partially buried. The model therefore suggests that phosphorylation of Ser 27, but not Ser 28, may regulate calspermin/Ca^{2+}-CaM binding (Andrew *et al.*, 2002; Smart & McCammon, 1999; Vetter & LeClerc, 2001).

Given the development of smGN for use as a 'CaM sponge' it was of interest to determine whether phosphorylation of Ser 27 may lead to alterations in the

ability of calspermin to interact with CaM. Substitution of Ser residues with Asp or Glu is routinely used to mimic the effect of Serine phosphorylation (Wong *et al.*, 2005), and substitution of CaMKIV Ser 332 for Asp has previously been shown to mimic phosphorylation of the Ser residue and induce insensitivity to activation by Ca^{2+}-CaM (Watanabe *et al.*, 1996). Bioinformatic topology models of calspermin substituting Ser 27 for Asp and Glu were therefore generated.

Ramachandran analysis of the calspermin model indicated all residues within the putative CaM binding site remained in most favoured geometry, suggesting that modifications in relative positioning of residues were not due to poor modelling. JPRED analysis of the CaM binding moiety of calspermin had previously predicted α-helical secondary structure from Arg 15 to Ala 26. However A*b initio* modelling of native calspermin indicated that the α-helix maintained a coiled aspect from Arg 15 to Lys 22 (figure 5.4 A shown in blue and labelled). The model also indicated that Ser 27 (figure 5.4 A shown in red) was the terminal residue in the α-helical region of the CaM binding domain. Between Arg 14 and Arg 15 there was also a significant increase in the reflex angle of the helical structure.

Mutation of Ser 27 to either Asp (figure 5.4 B) or Glu (figure 5.4 C) resulted in stabilisation of the α-helix from Arg 15 to Lys 22. Such stabilisation of the α-helix is a hallmark of phosphorylation-based regulation of CaM-binding proteins (CaMBPs) (Smart & McCammon, 1999; Vetter & LeClerc, 2001), and suggests that regulation of calspermin may occur by modulation of its phosphorylation state. It has been questioned whether phosphorylation-generated stearic and electrostatic interactions or changes in secondary structure modulate the ability of CaMBPs to bind CaM (Vetter & LeClerc, 2001). Mutation of Ser 27 to either Asp or Glu resulted in altered geometry between Arg 14 and Arg 15. In both models, the mutated Ser 27 also no longer forms part of the helix, whilst substitution with Glu also results in Ala 26 (shown in yellow) no longer being a helical component. Such significant alteration in the modelled conformation of the CaM-binding motif upon mimicking phosphorylation of Ser 27 indicates that CaM binding ability may, at least partially, be modulated through direct alteration of peptide secondary structure. However, experimental point-mutation studies would be required to accurately quantify the effects of Ser 27 phosphorylation in calspermin and to elucidate any mechanism of action.

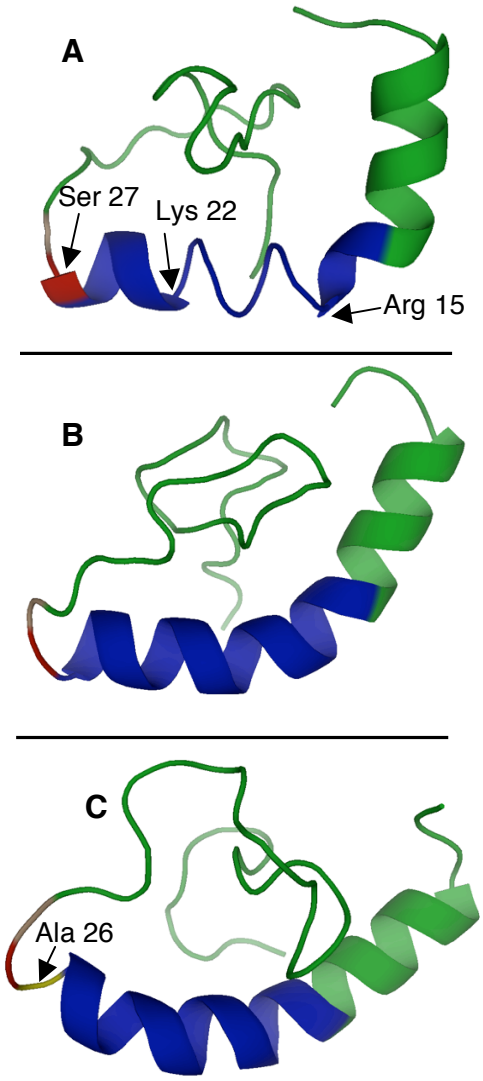

Figure 5.4: Modelling the effects of phosphorylation of calspermin Ser 27.

Fig. 5.4 A: *Ab initio* model of a 50 bp region surrounding the CaM binding moiety of calspermin. Although predicted to form a stable α-helix, a coiled aspect is evident in the helical region from Arg 15 to Lys 22 (shown in blue and labelled). Ser 27 (in red) is found to be the terminal residue in the α-helical region of the CaM binding domain. Between Arg 14 and Arg 15 there is also a significant increase in the reflex angle of the helical structure.

Fig. 5.4 B: Substitution of Ser 27 to the phosphoserine-mimic Asp results in altered geometry, reduced reflex angle between Arg 14 and Arg 15 and stabilisation of the α-helix. In this model the terminal helical residue is Ala 26 with the mutated residue 27 no longer a component of the helix.

Fig. 5.4 C: Simulated mutation of Ser 27 to Glu produces a similar effect as substitution with Asp; there is stabilisation of the α-helix from Arg 15 to Lys 22 and reduced reflex angle between Arg 14 and Arg15. In this model, neither the mutated Ser 27 nor the preceding Ala 26 (shown in yellow and labelled) are constituents of the helix.

5.6 Conclusions

The work presented in Murphy *et al*. (2008), was undertaken in order to elucidate the structure of calspermin and the kinetics of its binding with CaM. The additional analyses presented in this thesis were performed to validate and further expand upon the published work.

Spectrofluorometry further validated that the tertiary structure of the smGN chimaera was correctly folded. This validation supports the view that the data presented in Murphy *et al*. (2008), was representative of native calspermin.

Bioinformatic analyses extended the available information regarding the structure / function relationship of calspermin. These analyses supported the conclusion that calspermin residues Met 143 and Leu 166 lie within the CaM-binding pocket and that Val 25 is a key hydrophobic component of the core CaM-binding motif, whilst Leu 30 likely lies outside this region. Additionally, simulated-mutagenesis studies have provided novel insights in to possible *in vivo* regulation of calspermin, with phosphorylation of Ser 27 predicted to induce structural changes within calspermin and likely modulate its CaM-binding affinity. Future experimental validation of this finding could conceivably lead to mechanisms for more closely regulating the activity of recombinant calspermin during *in vivo* CaM-inhibition studies.

CHAPTER 6: THE SMGN CHIMAERA AS AN INDUCIBLE CALMODULIN SPONGE IN *ARABIDOPSIS THALIANA*

6.1 Introduction

Several classes of pharmacological agents, including phenothiazines, naphthalene-sulphonamides, dihydropyridines and diphenylalkylamines have been used in CaM inhibition studies. Although valuable, non of these agents are without significant disadvantages (Zimmer & Hofmann, 1987). Permeability of inhibitors differ according to cell type and homogenous or targeted application is often difficult (Ito & Hidaka, 1984; Athari & Jungermann, 1991; Jan & Tseng, 2000a, 2000b; Love et al., 1997). Severe side effects including disruption of the plasmalemma, disruption of neuronal conductance pores, and induction of nitric-oxide release occur below concentrations routinely used in inhibition studies (Gonzalez-Daros *et al.*, 1993; Lin & Rydqvist, 2000; Osawa *et al.*, 1998; Sengupta *et al.*, 2007). Some pharmacological CaM inhibitors including mebeverine and aprindine have even been found to have higher affinities for other enzymes than for CaM itself (Zimmer & Hofmann, 1987). In chapter four of this thesis it was reported that, in *A. thaliana*, daily application of pharmacological CaM inhibitors affected both flowering-time and the expression of circadian clock and photoperiodic-flowering genes. Plants were treated with structurally unrelated inhibitors and, where available, low affinity analogues were also used to help discriminate between the effects of CaM inhibition and secondary non-CaM related effects. However, no pharmacological inhibitor of CaM is available with a completely inactive structural analogue. Even if such an analogue were identified, it is likely that differential rates of metabolism between the two molecules would still affect determination of which effects are related to true CaM inhibition. An alternative means of CaM inhibition, free of the multiple unwanted effects of pharmacological agents, would therefore be of great use.

We reported in Murphy *et al*. (2008), that the chimaeric fusion protein soluble-modified GFP/calspermin (smGN), was determined to be an extremely specific and very high affinity CaM binding agent. As calspermin lacks enzymatic activity, a peptide agent such as this would be expected to elicit far fewer side effects during *in vivo* CaM inhibition studies than pharmacological equivalents. In order to initially assess the ability of smGN to act as an *in vivo* CaM-sponge,

A. thaliana were transformed with *smGN* under the control of the glucocorticoid-inducible transcription factor GVG and expression of the transgene was determined.

6.2 Results

6.2.1 Engineering and expression of soluble-modified GFP/calspermin in Arabidopsis thaliana.

The *smGN* chimaera consists of a plant expressible GFP in frame with the rat calspermin coding sequence. Following cloning of the chimaera in to pINDEX3, *E. coli* strain DH5-α was transformed with the construct. Six bacterial colonies were selected, of which two possessed the desired insert. *A. tumefaciens* carrying with the pINDEX3-*smGN* construct was used to transform *A. thaliana*. In order to confirm the presence of *smGN*, transgene-specific PCR was performed on genomic DNA isolated from transformed *A. thaliana*. Six *A. thaliana* lines were verified as positive for the construct. Each produced a single amplicon matching that observed from a pBlueScript-*smGN* positive control (figure 6.1). These six lines were then treated for three days with either 10 μM of the glucocorticoid dexamethasone or a carrier-solvent control, RNA extracted and cDNA synthesis performed. Active transcription of the transgene was then verified via PCR (sections 2.2.32).

Strong PCR amplification from the cDNA template was observed for four of the glucocorticoid treated lines. cDNA from a further line resulted in moderate amplification, whilst template from the final line generated a very faint DNA band. No secondary bands were observed and all amplicons were of the size expected for *smGN* (~1250 bp). In five lines, plants treated with the control treatment displayed no uninduced expression, however in the sixth line, a very faint band was observed (figure 6.2).

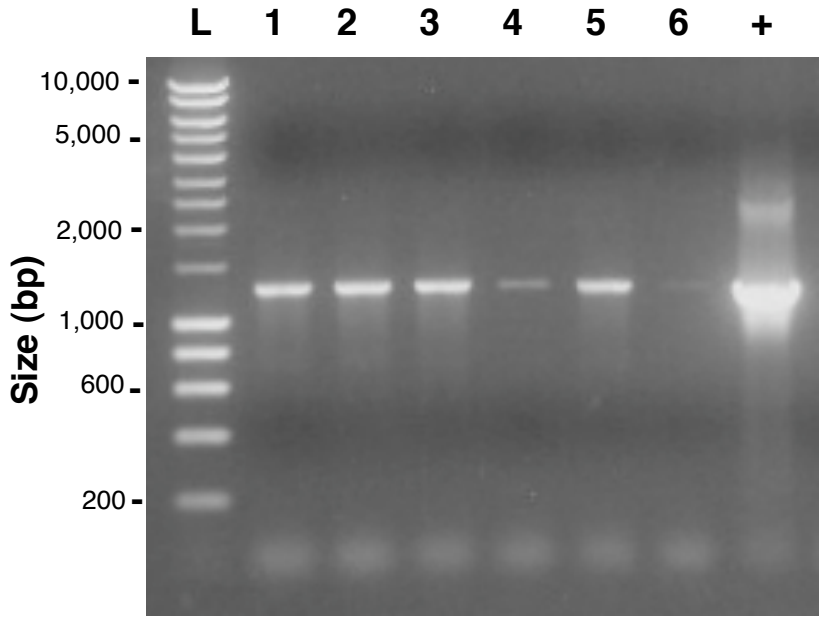

Figure 6.1: Agarose gel electrophoresis of bands generated by *smGN*-specific PCR performed on genomic DNA from putatively transformed *A. thaliana*.

Genomic DNA from *A. thaliana* lines putatively transformed with the *smGN* transgene was used as a template for *smGN*-specific PCR. Resulting PCR product was resolved by agarose gel electrophoresis.
"L" DNA standards, for which fragment lengths are indicated. Lanes 1 to 6 indicate each of the six lines putatively transformed with the *smGN* transgene. "+" represents a *smGN* positive control. Strong amplification of *smGN* was observed in reactions utilising genomic DNA template from lines one, two, three and five. Fainter bands were observed using template from lines four and six.

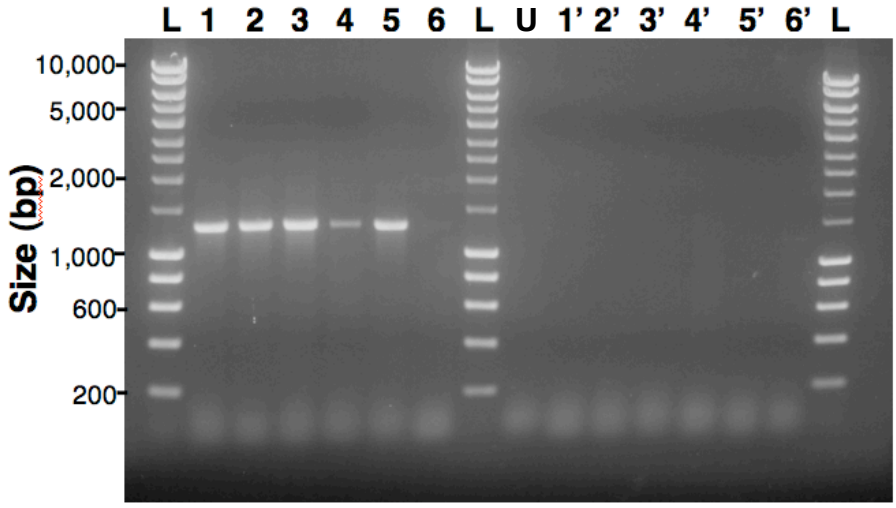

Figure 6.2: Agarose gel of bands generated by *smGN*-specific PCR performed on cDNA synthesised from induced and uninduced *A. thaliana* transformants.

cDNA was synthesised from individual lines transformed with *smGN* which had been treated with either 10 μM dexamethasone or a carrier-solvent control. Transcription of the transgene was verified via *smGN*-specific PCR.
"L" represents DNA standards for which fragment lengths are indicated. Lanes 1 to 6 indicate each of the six transformant-lines following induction with 10 μM dexamethasone. Strong amplification of *smGN* cDNA was observed in lines one to five, however only a faint band was observed from line six.
"U" indicates a cDNA template from an untransformed line and for which no amplification was observed. Lanes 1' to 6' indicate each of the six transformant lines following treatment with a carrier-solvent. No visible bands were visible for lines one to five. A faint band corresponding to the expected size for *smGN* (1,242 bp) was observed for line six.

6.2.2 Arabidopsis thaliana *lines containing the smGN chimaera displayed no GFP fluorescence under either induced or uninduced conditions.*

Seedlings from each verified transformant line, together with controls in which the *smGN* transgene was not present, were grown on 0.5 X MS agar plates containing 5 μM, 10 μM, or 30 μM dexamethsone or similar concentrations of triamcinolone to induce transgene expression. 0.5 X MS agar containing 0.1% DMSO served as a control. Soil-grown plants at the ten-leaf stage were also sprayed with either dexamethasone or triamcinolone for three days.

Epifluorescence microscopy indicated that functional GFP was not present in any line under either induced or non-induced conditions (figures 6.3 and 6.4). Background fluorescence was low and similar between all lines and across all treatments and was attributed to pigment and necrotic autofluorescence. Lack of obvious fluorescence strongly indicated the absence of the fusion protein at levels great enough to visualise.

6*.2.3 Translation of* smGN *is undetectable by SDS-PAGE and immunodetection.*

To determine whether smGN was expressed, but not fluorescent, protein was extracted from transformant lines treated with 0 μM, 10 μM or 30 μM dexamethasone or similar concentrations of triamcinolone. Protein extract from untransformed plants served as a negative control.

Following all treatment regimens, SDS-PAGE failed to resolve differences between protein extracted from untransformed controls and *smGN* transformants (figure 6.5). The absence of bands corresponding to the expected molecular weights of smGN, calspermin or GFP (as shown in Murphy *et al*. (2008)), suggested that the chimaera was either not actively translated or was being translated at levels below the resolution of SDS-PAGE. Western blotting using GFP-specific primary antibody was therefore undertaken to determine whether smGN was present at levels insufficient for detection by other means.

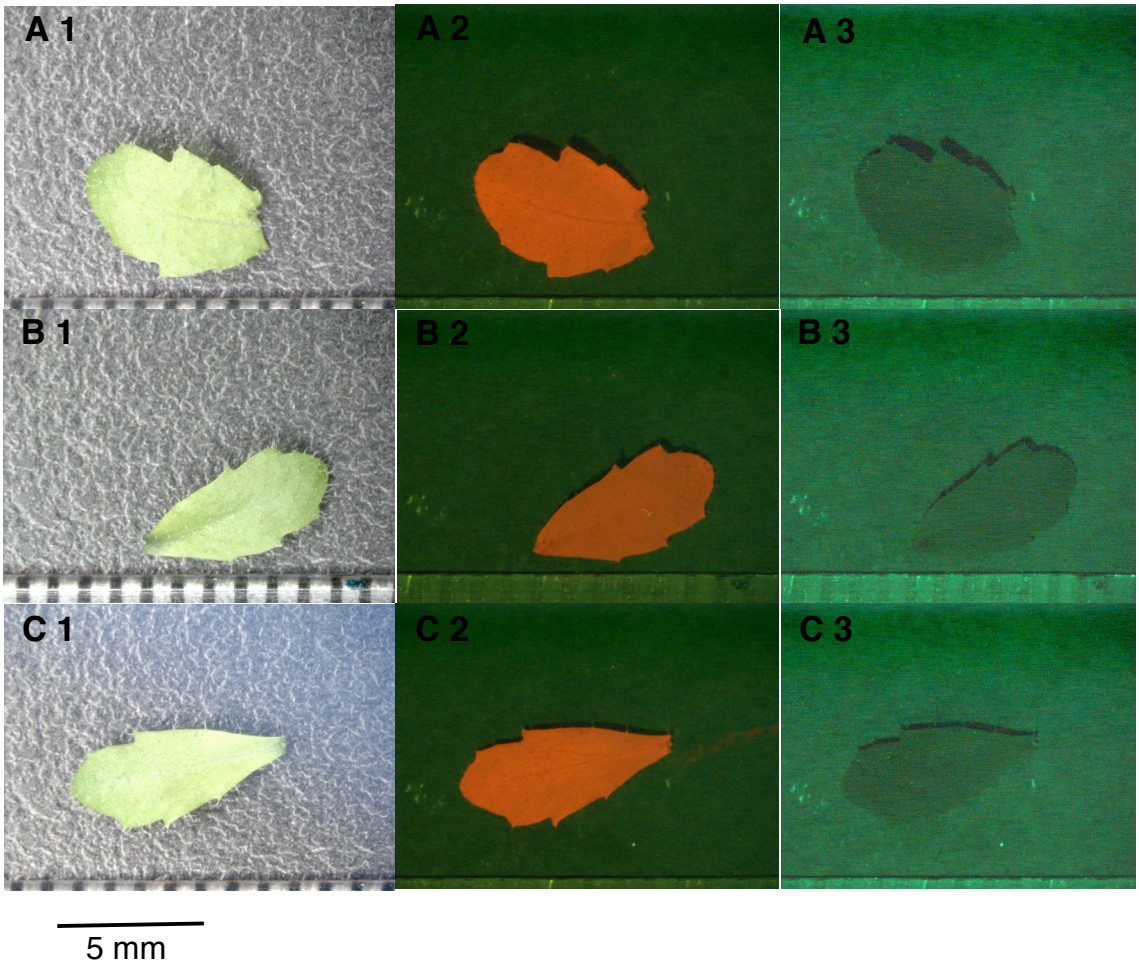

Figure 6.3: Brightfield and epifluorescence microscopy of representative leaves from untransformed *A. thaliana* following glucocorticoid or control treatments.

Upon developing ten true leaves *A. thaliana* negative for the *smGN* transgene were treated with either a carrier-solvent control (A1, A2, A3) 30 μM dexamethasone (B1, B2, B3) or 30 μM triamcinolone (C1, C2, C3). Leaves were imaged using brightfield microscopy (A1, B1, C1) and further examined by epifluorescence microscopy to distinguish between background autofluorescence (A2, B2, C2) and GFP fluorescence (C1, C2, C3). Strong autofluorescence was observed following all treatments and no GFP fluorescence was present in untransformed plants.

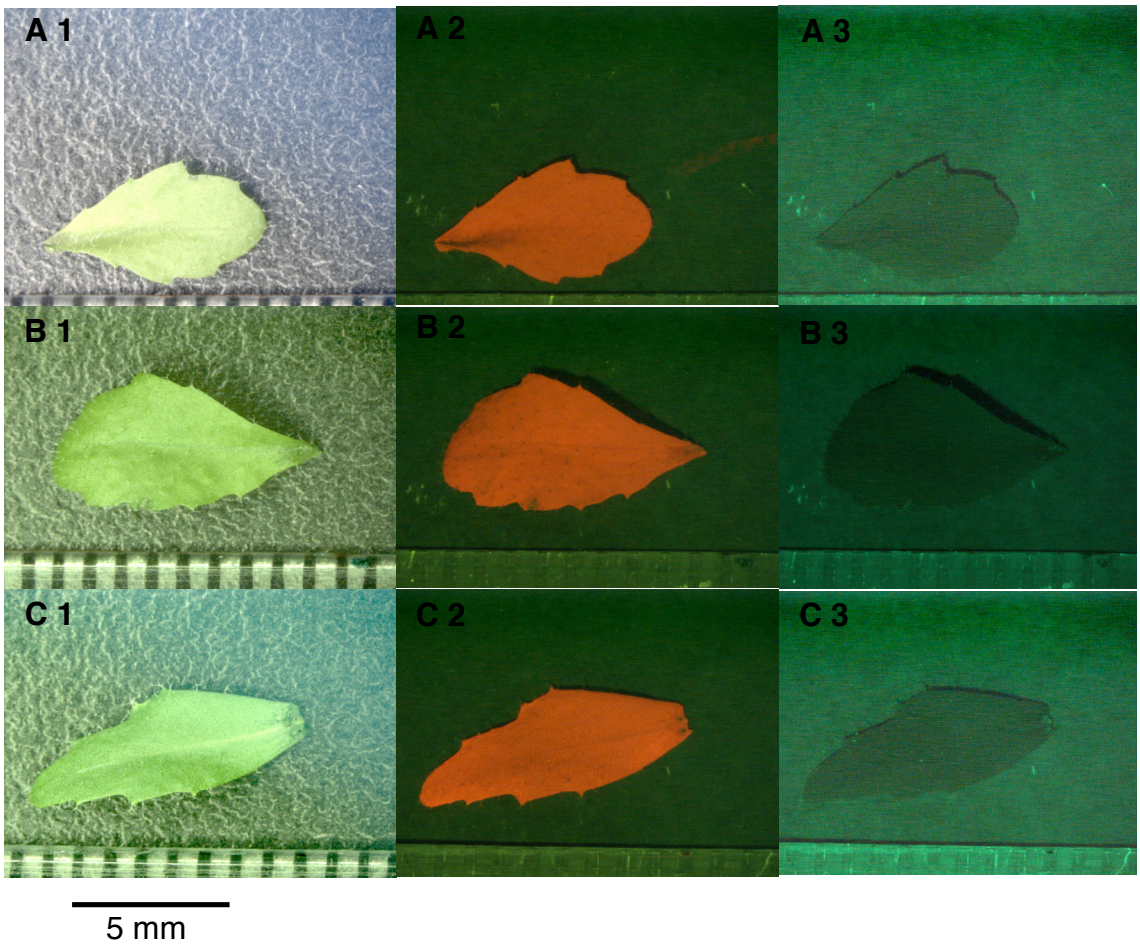

Figure 6.4: Brightfield and epifluorescence microscopy of leaves from the smGN-three line, representative of plants transformed with the *smGN* chimaera following glucocorticoid or solvent-control treatments.

Upon developing ten true leaves *A. thaliana* were sprayed with either a carrier-solvent control (A1, A2, A3) 30 μM dexamethasone (B1, B2, B3) or 30 μM triamcinolone (C1, C2, C3). Leaves were imaged using brightfield microscopy (A1, B1, C1) and further examined by epifluorescence microscopy to distinguish background autofluorescence (A2, B2, C2) and GFP fluorescence (C1, C2, C3). Whereas strong autofluorescence was observed following all treatments, no GFP fluorescence was observed in any transformant line.

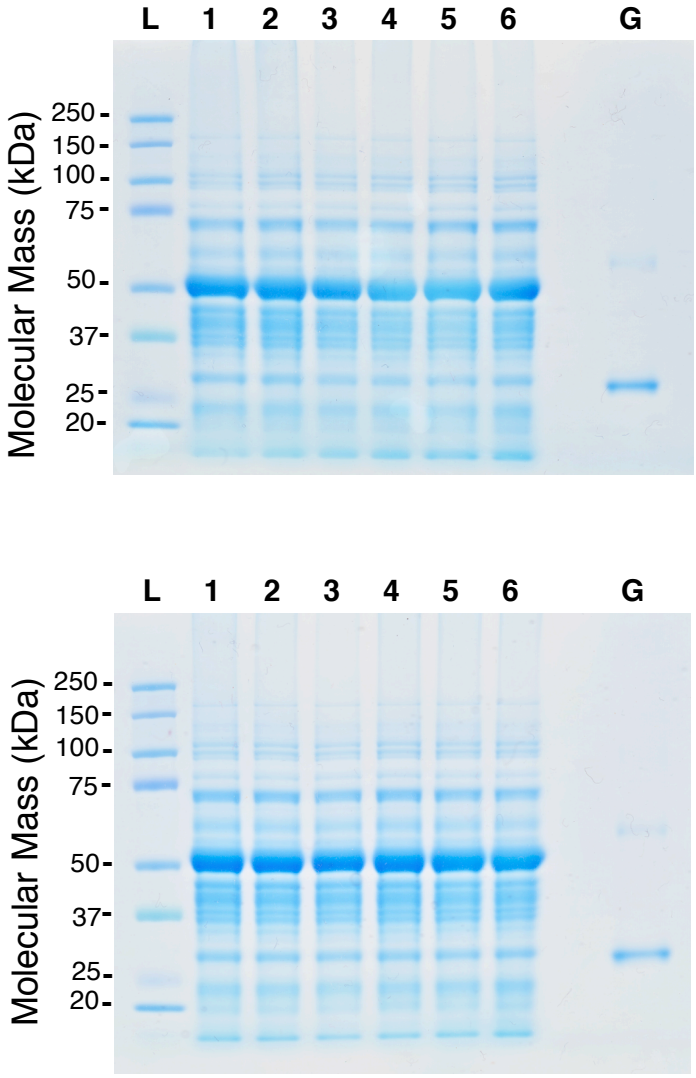

Figure 6.5: SDS PAGE of protein fractions from two representative lines of *Arabidopsis thaliana* transformed with the *smGN* chimaera.

A. thaliana lines containing the *smGN* transgene were treated with 10 μM or 30 μM dexmethsone, 10 μM or 30 μM triamcinolone or a carrier-solvent control.
Protein extracts were prepared from harvested plants and subjected to SDS PAGE. Protein extracted from plants lacking the *smGN* transgene served as a negative control.
"L" represents protein standards, for which the molecular masses are indicated. Lane 1 represents protein from *A. thaliana* lacking the *smGN* transgene. Lane 2 represents protein from plants treated with a solvent-control. Lanes 3 and 4 represent proteins from the transformant line treated with 10 μM or 30 μM dexamethsone respectively. Lanes 5 and 6 contained protein from plants treated with 10 μM or 30 μM triamcinolone respectively. Lane "G" represents purified recombinant GFP.

A reversible Ponceau S stain indicated complete and even transfer of *A. thaliana* protein and GFP to the PVDF membrane (figure 6.6).

In the GFP-control lane, four bands were visualised by immunodetection (figure 6.7). The predominant band migrated with an apparent molecular weight of approximately 29 kDa and was taken as corresponding to the dominant population of monomeric GFP. A secondary band at approximately 58 kDa appeared to correlate with dimeric GFP. Two fainter bands migrated with apparent molecular masses of 100 kDa and 130 kDa and may correlate with multimeric or incompletely denatured GFP.

A faint band denoting interaction between the anti-GFP antibody and a constituent of the *A. thaliana* protein extract is visible at approximately 52 kDa. However, this band was present at equal intensity in untransformed controls and lines containing the *smGN* transgene and is believed to be an artefact of cross-reactivity between the anti-GFP antibody and the large subunit of *A. thaliana* Rubisco (Sullivan, 2007). No unique bands were observed in any of the transformant populations, reinforcing the view that translated smGN was not present.

6.3 Discussion

6.3.1 Expression of smGN mRNA in Arabidopsis thaliana.

Gene-specific qRT-PCR confirmed that five of the six lines did not display uninduced transcription of the *smGN* chimaera. This broadly confirms earlier reports that the glucocorticoid-inducible GVG system allows relatively tight regulation of transgene expression (Aoyama & Chua, 1997; Ouwerkerk *et al.*, 2001). Following addition of 10 μM dexamethasone, four lines appeared to show high levels of *smGN* transcript. Interestingly, the line showing weakest amplification (line six) was also the line that generated the weakest amplification from genomic DNA and from which uninduced transcript was detected.

Variation in expression levels can be accounted for by a number of factors. Primarily, the naturally low rate of homologous recombination in plants allows gene insertion to occur at almost any locus within the genome (Butaye, 2005). The chromatin status at the insertion locus affects expression levels by determining the accessibility of DNA binding factors and the presence of nearby

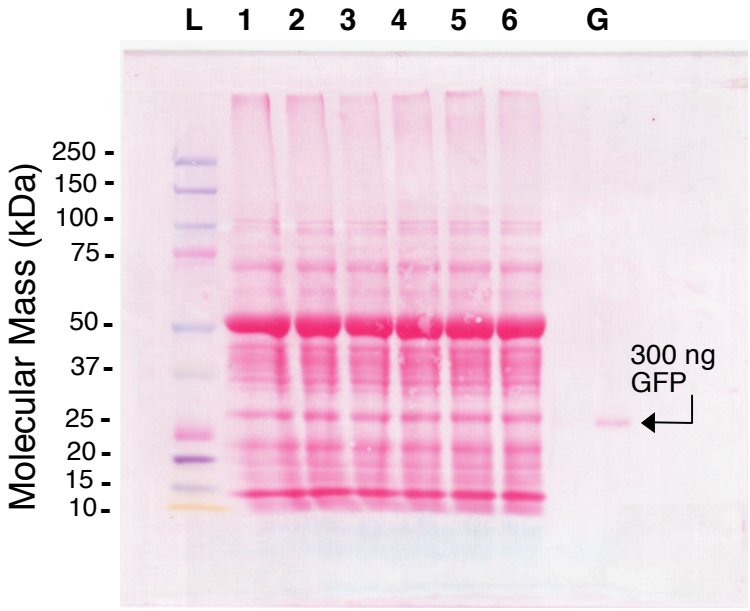

Figure 6.6: Transfer of proteins to a PVDF membrane as revealed by the Ponceau S stain.

Following SDS PAGE of *A. thaliana* protein extract, separated proteins were transferred to PVDF membrane. To verify that the protocol used resulted in lossless transfer of protein to the membrane, a representative membrane was stained with Ponceau S solution.
Lane "G" represents 300 ng of purified recombinant GFP, which was clearly revealed by the stain. As Ponceau S has a detection sensitivity approximating 250 to 500 ng protein per band, the visibility of the GFP band indicated complete transfer of protein to the membrane.

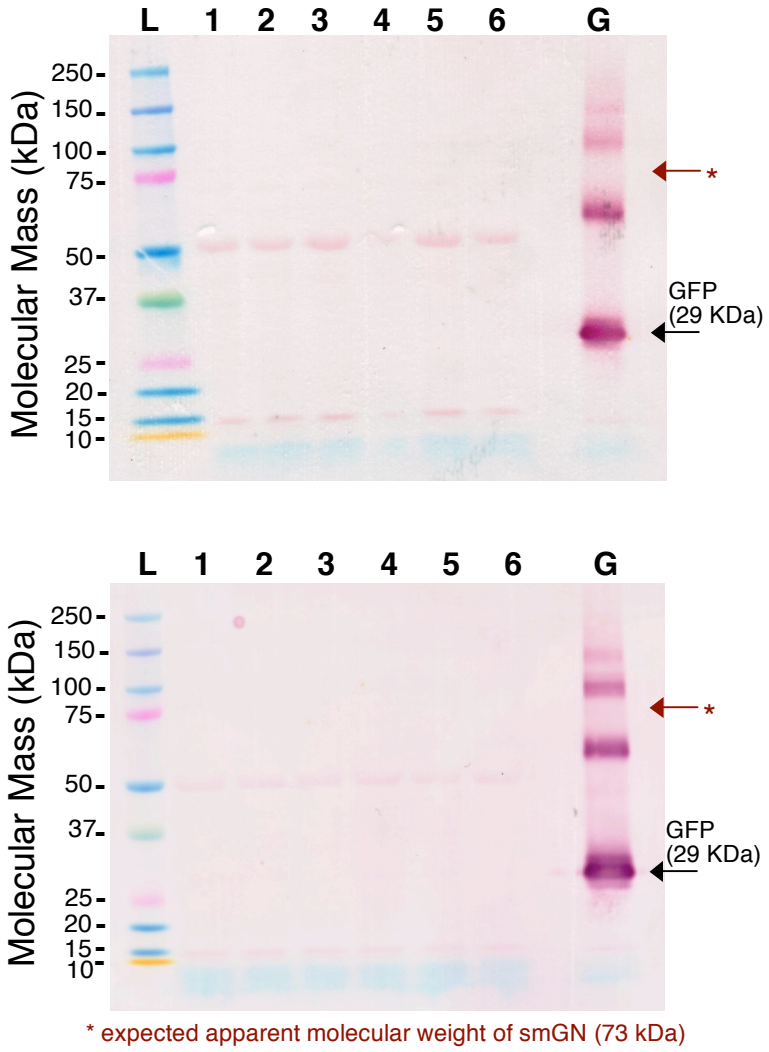

Figure 6.7: Western blot of protein fractions from two representative lines of *A. thaliana* transformed with the *smGN* chimaera.

"L" represents protein standards for which the molecular masses are indicated. Lane 1 represents protein from untransformed *A. thaliana* lacking the *smGN* transgene. Lane 2 represents protein from transformants treated with a carrier-solvent control. Lanes 3 and 4 represent proteins from transformants treated with 10 μM or 30 μM dexmethasone respectively. Lanes 5 and 6 represent protein from plants treated with 10 μM or 30 μM triamcinolone respectively. Lane "G" represents purified recombinant GFP. No unique bands were observed in any of the transformant populations.

transcriptional enhancers or suppressors can also have strong effects on the levels at which a gene is expressed (Butaye *et al.*, 2005; Grewal & Moazed, 2003).

6.3.2 Translation of the smGN chimaera in planta.

As well as serving as an effective anchor for the determination of SPR based smGN-CaM binding kinetics (Murphy *et al*., 2008), the GFP moiety served in epifluorescence-microscopy based tracking of the smGN chimaera. Whilst no GFP fluorescence was observed following control treatments, neither was it seen following treatment with up to 30 μM dexamethasone. This was unexpected given that gene transcription had already been found to be induced at a glucocorticoid concentration of only 10 μM. Whilst dexamethasone has been reported as the standard steroid for activating transcription from the GVG system (Aoyama & Chua, 1997; Ouwerkerk *et al.*, 2001), other studies have indicated that triamcinolone acts as a much more potent inducer (Tang & Newton, 2004). Treatment of each line with triamcinolone at similar concentrations to those used for dexamethasone also failed to generate the expected GFP-fluorescence signature. smGN had earlier been found to fold correctly when expressed in *E. coli*; having normal fluorescence and activity as a functional CaM inhibitor (Murphy *et al*., 2008). Due to the divergent isoelectric points of the smGN domains (smGFP = 6.04, calspermin = 3.9), together with differences in protein synthesis between prokaryotes and eukaryotes, the presence of smGN containing misfolded, and therefore inactive, GFP could not be discounted.

Apparent molecular weights of smGN and its individual GFP and calspermin domains, as determined by SDS-PAGE, were already known from experimental data and the literature (Ono *et al*., 1989; Murphy *et al*., 2008). Total protein extracts from transgenic *A. thaliana* lines treated with dexamethasone or triamcinolone failed to reveal the presence of intact smGN when analysed by SDS-PAGE and Western blot. Only 300 ng GFP was used per control lane, however the Ponceau S stain clearly revealed the presence of GFP. This stain has previously been demonstrated as having a sensitivity threshold approximating 250 to 500 ng protein per band for both PVDF and nitrocellulose membranes (Gentile *et al.*, 1997; Salinovich & Montelaro, 1986). The efficiency

of the transfer argues strongly that poor transfer was not responsible for negative immunoblots. Likewise, given the strong visualisation of the GFP controls on the immunoblots the reagents utilised were not responsible.

A number of possibilities exist regarding the absence of translated protein. It is possible that transcript was produced at levels insufficient to produce detectable protein. This is however unlikely, as expression of the GVG transcription factor is driven by the strong 35S promoter and although *smGN* transcription was not directly quantified, it was present in sufficient quantity to be easily detectable by *smGN* specific PCR.

Given levels of expression normally sufficient for detectable levels of protein, lack of protein product may occur due to inefficient translation of mRNA or rapid degradation of translated protein. As SDS-PAGE and immunodetection yielded no novel bands from induced or uninduced transformant lines, protein degradation appears unlikely.

Translation efficiency varies greatly between different classes of proteins, with kinases often amongst those poorly translated from mRNA (Karagyozov *et al.*, 2008). Although lacking kinase activity, calspermin is, as previously discussed, homologous with the final 169 residues of CaMKIV. Gene fusions can result in mRNA secondary structures considerably divergent from either unfused gene (Hughes & McElwaine, 2006). Although, in eukaryotes, the relationship between mRNA secondary-structure and translation efficiency is not clearly defined, a number of features have been recognised which appear to influence this process. The presence of stable stem and hairpin loops close to the 5' end of the transcript has been shown to interfere with binding and entry to the ribosome. Destabilisation of such features strongly enhances translation (Cameron *et al.*, 2008; Kawaguchi & Bailey-Serres, 2005; Wang & Wessler, 2001). Bioinformatic analysis of smGN mRNA using the 'RNA Analyzer' package (Bengert & Dandekar, 2003), subsequently suggested *smGN* forms a highly stable structure (-370.10 kcal mol^{-1}) containing a putative structural hairpin close to the 5' end. Although merely indicative, such structure may go some way to explain the lack of translated protein.

6.4 Conclusions

Although smGN protein successfully expresses in *E. coli*, similar expression was not obtainable in *A. thaliana*. Given that *smGN* transcript was detectable in *A. thaliana*, the failure to detect smGN protein indicates that it is translation rather than transcription of *smGN* mRNA which limits its accumulation *in planta*. Though GFP serves as a useful intracellular tag it is not necessary for inhibition studies. Given its high specificity and affinity for CaM, its lack of catalytic activity and its proven ability to fold correctly in eukaryotic cells (Della Rocca *et al.*, 1999; Ono *et al.*, 1984), calspermin still holds much promise as a potential research tool. Should further work show untagged calspermin to express to suitable a level in *A. thaliana*, then its utility as a peptide-based inhibitor of CaM is assured.

CHAPTER 7: GENERAL DISCUSSION

7.1 Background and Objectives

In *Arabidopsis thaliana,* photoperiodic flowering is mediated by outputs from the circadian clock (Sawa *et al.,* 2008). Circadian and diurnal oscillations in cytoplasmic [Ca^{2+}] ([Ca^{2+}_{cyt}]) are a feature of *A. thaliana* circadian rhythms. In plants Ca^{2+} acts as a powerful and versatile second messenger that activates numerous cellular and physiological responses (Malhó, 1999). Although it has not yet been established what, if any, role circadian [Ca^{2+}_{cyt}] oscillations play in cellular signalling, they appear to encode information regarding both photoperiod and light-quality; [Ca^{2+}_{cyt}] peaks just prior to dusk in short-day photoperiods and during the day under long-day photoperiods (Love *et al.*, 2004). Circadian [Ca^{2+}_{cyt}] rhythms have therefore been implicated in day-length signalling and floral timing, but the relationship between the molecular triggers of flowering and photoperiodic sensing is unknown.

Calmodulin (CaM) is both the most abundant and most intensively studied of the Ca^{2+}-sensing proteins found in plants. Ca^{2+}-CaM is known to regulate the activity of over 150 structural and enzymatic proteins that regulate diverse cellular processes (Hoeflich & Ikura, 2002; Popescu *et al.*, 2007). Importantly, CaM has been linked to the regulation of flowering-time; in *Pharbitis nil*, the application of CaM inhibitors leads to delayed photoperiodic flowering (Friedman *et al.*, 1989). Such observations strongly suggest that, were circadian [Ca^{2+}_{cyt}] oscillations to play a role in modulation of daylength-regulated responses, CaM would be a strong candidate for transducing these signals.

The objective of this thesis was therefore to test the hypothesis that CaM is involved in the transduction of photoperiod-specific information encoded within circadian [Ca^{2+}_{cyt}] rhythms, either by regulating inputs to the core circadian oscillator or more directly by altering the regulation of essential proteins and genes involved in the photoperiodic-flowering pathway. To achieve these aims, both pharmacological and peptide based approaches were undertaken for the inhibition of CaM signalling.

7.2 Discussion and Conclusions

7.2.1 Untagged calspermin is likely to be a highly effective in vitro CaM inhibitor.

Traditionally, CaM inhibition studies have almost exclusively relied upon pharmacological inhibitors. However, difficulty of application combined with non-specific binding and secondary effects, such as disruption of the plasmalemma, make such inhibitors less than ideal tools for dissecting CaM signalling pathways (Jan & Tseng, 2000a, 2000b; Lin & Rydqvist, 2000).

In an attempt to more precisely target CaM inhibition, a new peptide inhibitor of CaM, labelled smGN, was developed and characterised (Murphy *et al*., 2008). smGN is a chimaeric fusion of the CaM-binding peptide calspermin and a plant-specific GFP. Affinity chromatography demonstrated the highly specific nature of smGN. Combined with a lack of enzymatic activity (Sun et al., 1995), this specificity means that smGN should only modulate CaM-signalling pathways. Additionally, surface plasmon resonance (SPR) analysis showed that, *in vitro*, smGM binds CaM with $K_D = 4.42\ 10^{-9}$ M; an affinity for CaM 2,500 times greater than that of the commonly deployed pharmacological inhibitor W7 (Hidaka *et al.,* 1981; Murphy *et al*., 2008). High levels of the peptide should not therefore be required for effective inhibition of CaM signalling.

A. thaliana plants were transformed with the *smGN* sequence under control of the dexamethasone-inducible GAL4/*UAS* promoter and six independent transformant lines were selected. Whilst all lines showed transcription of the transgene following addition of dexamethasone, no evidence for transcription was obtained, either by GFP fluorescence or western-blot analysis. Although attempts at deploying smGN *in planta* have been, to date, unsuccessful, this may be due in part to the presence of the GFP moiety. This moiety acted as an effective means of anchoring and orienting the protein to the SPR sensor chip and, significantly, offers a method by which other acidic polypeptides may be anchored for kinetic analysis (Murphy *et al*., 2008). However, bioinformatic analysis indicated that, in eukaryotes, translation of *smGN* mRNA may be inhibited by its stability. Although the GFP moiety of smGN would be useful in tracking protein expression and localisation, it is not required for the sequestration of CaM. Calspermin could therefore, in future, be deployed untagged as an effective *in vivo* inhibitor of CaM.

7.2.2 Optimal CaM inhibition requires timed application of inhibitors at carefully determined concentrations.

Given that it proved impractical to deploy smGN *in planta*, it was necessary to rely on pharmacological inhibitors for investigating the role of CaM as a regulator of circadian-clock function and photoperiodic-flowering in *A. thaliana*.

The literature reveals that the concentration of chemical CaM inhibitors utilised varies relatively broadly between studies (Jan & Tseng, 2000a, 2000b; Osuna *et al.*, 2004; Sengupta *et al*., 2007; Si & Olds-Clarke, 2000). As such, there are no universally accepted concentrations of CaM inhibitors for deployment in plant-based studies. In order to determine the most suitable concentrations of inhibitors to deploy *in planta*, a protocol was therefore developed whereby the effects of varying concentrations each inhibitor on *A. thaliana* root growth were determined.

Dose-response curves revealed that arithmetic increases in inhibitor concentration did not produce linear changes in root length or root number, thus supporting the hypothesis that that CaM is normally present at concentrations slightly in excess of those required by its interaction partners (Zielinski, 1998). Microscopic inspection of recovered roots linked inhibitor-induced changes in root growth with morphological changes at the cellular level and confirmed root-based dose-response curves to be a useful tool in assessing optimal concentrations of inhibitors in studies involving *A. thaliana*.

Combined with the observation that gravitropic responses readily acclimate to continued exposure to CaM inhibitors, the non-linearity observed in dose-response curves strongly support the hypothesis that, in *A. thaliana*, CaM signalling networks are inherently robust. In order to account for these observations, it was determined that optimal concentrations in studies involving *A. thaliana* would be achieved at the concentrations 1 μM CMZ and 50 μM W7 / W5. It was also concluded that daily, pulsed application of each inhibitor was necessary to maintain inhibition of CaM during subsequent experiments.

7.2.3 Inhibition of CaM disrupts CO *expression primarily via modulation of GI.*

To determine the effect of CaM inhibition on the photoperiodic pathway, we determined the levels of expression of genes that are known to be critical nodes in floral timing and in the circadian clock. Transcript levels of *CALMODULIN 1* (*CAM1*), *TIMING OF CAB* (*TOC*), *CONSTANS* (*CO*), *FLOWERING LOCUS T*

(*FT*) were analysed by qRT-PCR over 8L : 16D and 16L : 8D diurnal cycles and standardised to the expression of the house-keeping gene *GLYCERALDEHYDE-3-PHOSPHATE DEHYDROGENASE C SUBUNIT* (*GAPC*). It was determined that daily treatment with either W7 or CMZ induced phase delays in expression of the core clock component *TOC1* under both short and long days. Under circadian conditions, defects in core oscillator components often lead to alterations in free running period (FRP) (Park *et al*., 1999; Mizoguchi et al., 2002; Harmer & Kay, 2005). Under the diurnal conditions utilised in the work described here, plants are subject to the clock resetting conditions of a light / dark photoperiod. Any extension in FRP may therefore be visualised as a constant phase delay (Covington *et al*., 2001).

ZEITLUPE (ZTL) acts upon the central oscillator by the targeted degradation of TOC1 and is therefore influential in clock maintenance (Jarillo *et al.*, 2001; Kiba *et al.*, 2007; Más *et al.*, 2003a). Although *ztl* mutants belonging to the C24 ecotype exhibit lengthened clock-periods, in the Col 0 ecotype -which was utilised in the experiments presented in this thesis-, no such period lengthening is apparent (Somers *et al.*, 2004). It is therefore unlikely that expression patterns in CMZ and W7 treated plants are due to direct CaM mediated modulation of ZTL alone.

Mutations of most core elements of the clock lead to shortened rather than extended clock periods, with *TOC1* expression advanced by up to four-hours in *late elongated hypocotyl* (*lhy*) and *circadian clock associated 1* (*cca1*) mutants (Mizoguchi *et al.*, 2002; Mizoguchi *et al.*, 2005). This stands in marked contrast to the delayed *TOC1* expression generated by CaM inhibitors. Unlike with other clock components, plants either over-expressing or showing lesions in *GIGANTEA* (*GI*), display a four-hour delay in expression of clock-controlled genes (Mizoguchi *et al.*, 2005). Such expression patterns are consistent with those recorded in this study. In addition, both *gi* mutants and *GI* over-expressers display a reduction in the amplitude of clock-controlled outputs consistent with those observed in the pharmacologically treated plants studied here (Mizoguchi *et al.*, 2005).

As with *TOC1*, *CO* expression was strongly affected by application of CMZ or W7, with severe decreases in total *CO* transcript and repression of rhythmicity under short days. CaM therefore appears to play a significant role in the

maintenance of circadian *CO* signatures. Unlike its light-stabilised protein product, CO transcript abundance is almost entirely regulated by the core oscillator (Lin & Wang, 2007; Suárez-López *et al*., 2001; Yakir *et al*., 2007). Considered in this context, suppression of transcript is most explainable by interference with a CaM mediated component of the core oscillator.

As discussed, inhibition of CaM induced phase delays in the pattern of *TOC1* expression. However, direct disruption of *TOC1* expression is unlikely to be responsible for such a dramatic suppression of *CO*. The short period *toc1*-1 mutant exhibits a phase-shift in *CO* expression under 24-hour photoperiods, but total *CO* expression levels remain unchanged. Likewise, wild-type plants grown in photoperiods significantly shorter than their, approximately 24-hour, FRPs (thus mimicking a long period mutation), show no alteration in total *TOC1* transcript abundance (Yanovsky & Kay, 2002).

As well as being a putative component of the core oscillator, GI acts as the primary initiator of *CO* expression. *gi* mutants show suppressed expression of *CO* and inhibition of rhythmicity similar to that observed following treatment with strong CaM inhibitors (Mizoguchi et al., 2005). As *GI* transcription is repressed by LHY/CCA1 (Fowler et al., 1999; Locke et al., 2005b), it is possible that expression characteristics seemingly mediated by GI in fact result from modulation of LHY/CCA1. However, unlike plants treated with CaM inhibitors, *lhy/cca1* mutants display extremely high levels of rhythmic *CO* transcript, which peaks before dusk and induces early flowering in short days (Mizoguchi et al., 2002; 2005). Taken together, these results strongly indicate that inhibition of CaM leads to disruption of *CO* primarily through interference with GI or an interacting partner (figure 7.1). GI interacts with SPINDLY (SPY) in promotion of *CO* expression and subsequent induction of photoperiodic flowering. However, in contrast to the *CO* signatures observed in *gi* mutants and plants treated with strong CaM inhibitors, *spy* mutants maintain robust circadian *CO* rhythms with increased peak amplitude (Tseng *et al*., 2004). It is therefore unlikely that SPY is directly affected by inhibition of CaM.

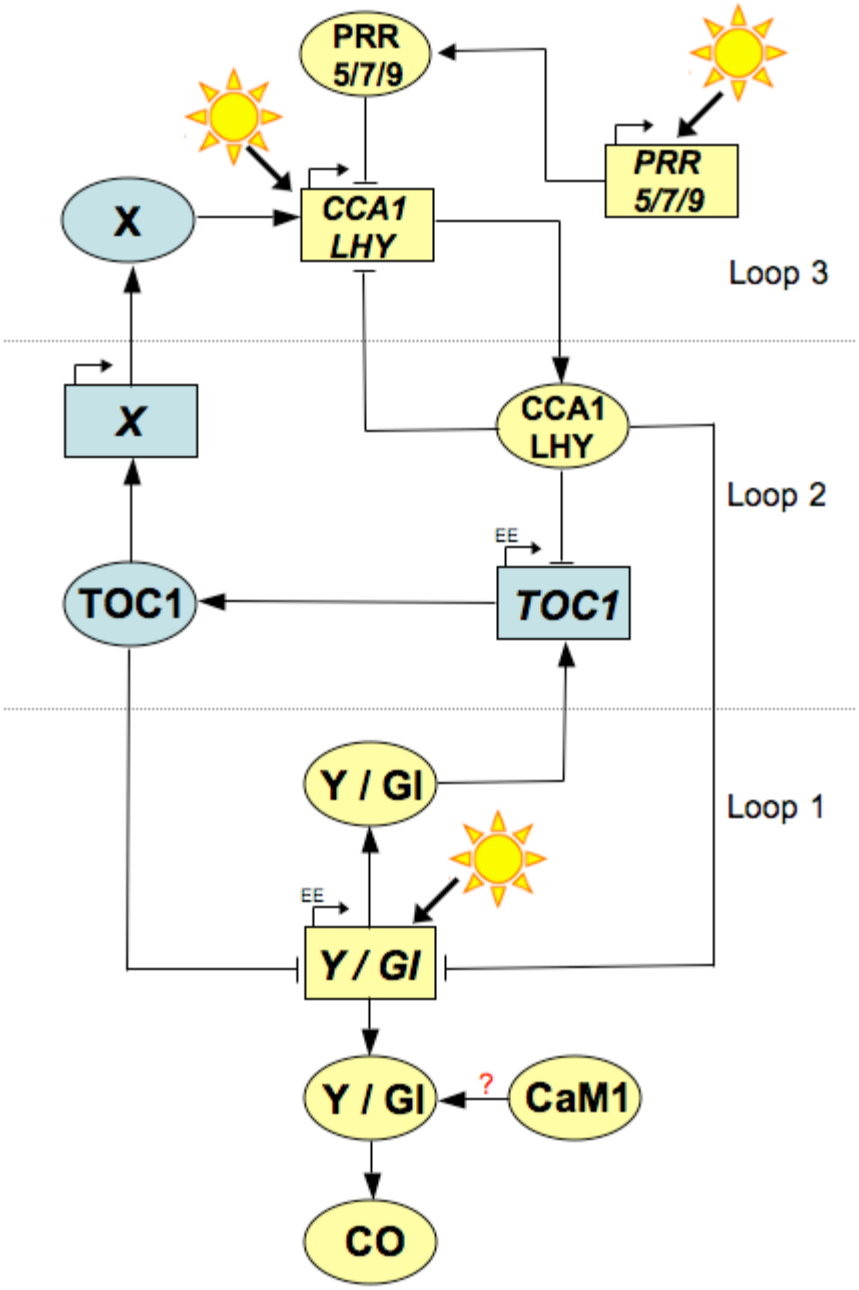

Figure 7.1: An extension of the three-loop model representing a possible interaction by which CaM may influence the circadian clock and the photoperiodic flowering pathway in *A. thaliana*.

Expression studies and flowering-time experiments utilising CaM inhibitors indicated that CaM plays a previously unpredicted role in the regulation of photoperiodic flowering in *A. thaliana*. In this model, CaM activates GI, which in turn acts to promote photoperiodic flowering via the action of CO.

Under long days, control plants lacked obvious oscillations in *CO* transcript, a feature likely arising due to the maturity of the harvested plants and their proximity to flowering. CMZ treated subjects displayed bi-modal *CO* expression, with peaks at eight and 20 hours. Such a signature does not closely correspond with previously recorded patterns of *CO* expression in plants exhibiting lesions in core clock components. Unexpectedly, the pattern of *CO* expression observed in plants treated with W7 differed from that seen in plants treated with CMZ. Application of W7 led to a *CO* signature, which, like controls, showed reduced rhythmicity. However, *CO* transcript levels were found to increase from a basal low during the light to a high during the night. This shallow-curve is an almost exact match for the *CO* signature found in *gi* mutants grown under long days (Suárez-López *et al.*, 2001). Together with the data from the corresponding short-day experiments, these results support the hypothesis that inhibition of CaM leads to disruption of *CO* transcription primarily through modulation of GI (figure 7.1).

The low abundance of *FT* transcript present under short days make it difficult to clearly attribute changes in expression to application of pharmacological agents. Under long days however, clear differences in *FT* expression profiles were apparent between control and pharmacologically treated plants. The similarities between *FT* transcript-profiles of plants treated with W7 or its low affinity analogue W5, prevented determination of whether the effects were related to CaM inhibition or due to secondary effects. However, plants treated with CMZ displayed a clear four-hour delay in peak *FT* transcript abundance.

A phase-shift in peak *TOC1* expression in plants treated with CMZ was described here previously and was associated with CaM modulating the activity of GI. As the clock (and therefore TOC1), is involved in the timing of *FT* expression (Mizoguchi *et al.*, 2005), the corresponding delay in peak *FT* transcript found in CMZ treated plants remains consistent with the hypothesis that GI acts as a node for CaM signalling to the clock (figure 7.1).

In combination, the effect of CMZ on flowering times under both long and short days builds upon the previously described qRT-PCR data in supporting the conclusion that CaM mediates the *A. thaliana* circadian clock and photoperiodic flowering pathways through modulation and activation of GI. This model (figure

7.1), remains consistent with our current understanding of the circadian oscillator as a system of interlocking feedback loops (Locke *et al.*, 2005b). However, this model also offers the possibility that CaM acts to modulate a key element of the clock in a previously unforeseen manner.

In plants, CaM regulates an impressive list of cellular and physiological processes including gene expression, acclimation, gravitropism and apoptosis (Park *et al*., 2008; Zielinski, 1998; White & Broadley, 2003). Direct regulation of the activity of a core oscillator component would be a significant addition to CaM's known functions and, if correct, extend our understanding of the already complex nature of the *A. thaliana* circadian clock. Moreover, given that the circadian clock is involved in the regulation of numerous biological processes, future research investigating individual CaM signalling pathways should ensure that any observed transcriptional or developmental changes are not merely mediated by unforeseen modulation of the central oscillator.

7.2.4 SPA1 requires functional CaM in order to suppress dark flowering.

Unlike under inductive photoperiods where CaM appears to be involved in the promotion of flowering, inhibition experiments indicated that under darkness CaM acts to repress flowering via modulation of SUPPRESSOR OF PHYA-105 (SPA1). Both pharmacological inhibition of CaM and lesions in *spa1* relieved this inhibition, allowing flowering in darkness. Previous data have indicated partial redundancy amongst members of the four-member SPA family, with seedlings carrying a *spa1* null-mutation showing wild-type characteristics when grown for a few days in darkness (Laubinger *et al.*, 2006; Lin & Wang, 2007). The results obtained here show that over larger time-scales this observation does not hold true. These results would therefore strongly counsel against drawing conclusions regarding mature *A. thaliana* based solely on gene expression and developmental data that have been obtained in immature seedlings.

The newly observed dark-flowering phenotype of *spa1* mutants is in itself an interesting and significant characteristic. SPA1 is believed to suppress flowering via heterodimerisation with COP1 and subsequent targeted degradation of CO (Laubinger et al., 2006). It is therefore highly likely that flowering in *spa1* mutants is the result of the accumulation of CO and subsequent induction of *FT*.

Unfortunately; undegraded RNA was not obtainable from any of the dark-grown samples to enable evaluation of this hypothesis. However, if true, this would confirm that residual COP1 activity is insufficient to constitutively block flowering.

The simplest model accounting for flowering of *spa1* mutants and wild-type plants treated with CaM inhibitors is that CaM is required in order for SPA1 to fully suppress dark flowering. In this model, presented in figure 7.2, SPA1 is activated following either transient interaction with, or continued binding to, CaM. Following binding, SPA1 or the SPA1/CaM1 complex then interacts with COP1. This complex then targets CO for proteasomal degradation and thus prohibits flowering. Until now, no experimental data have suggested that CaM may perform an integral function in the targeting of proteins for proteasomal degradation. Were the accuracy of this model to be verified, the possibility is raised that, due to the numerous interaction partners of SPA1 (Laubinger *et al*., 2004; 2006), CaM may be involved in regulating the degradation of many significant proteins.

7.2.5 SPA1-mediated degradation of GI may allow CaM to regulate both photoperiodic flowering and flowering under darkness via a single interaction.

The proposed role of CaM in the activation of SPA1 and subsequent degradation of CO (figure 7.2), would appear to run counter to its predicted role in activation of GI (figure 7.1). However, recent evidence indicates that, although *GI* transcript is regulated by the circadian clock, GI protein is post-transcriptionally regulated, showing diurnal oscillations in abundance even when constitutively expressed (David *et al*., 2006). Moreover, it was a similar observation which led to the discovery that SPA1 targets CO for degradation (Jang *et al*., 2008). Although the mechanism by which GI is targeted for proteasomal degradation has not yet been experimentally determined, the possibility is presented that, like CO, GI may undergo similar SPA1-mediated targeting. Targeted degradation of GI in this manner would necessarily suggest the possibility of an additional model to explain the observations made in this thesis. In this model (figure 7.3), CaM again activates SPA1, in turn leading to the degradation of CO. However, in addition to CO, GI is also targeted for proteasomal degradation. Application of CaM inhibitors would therefore affect

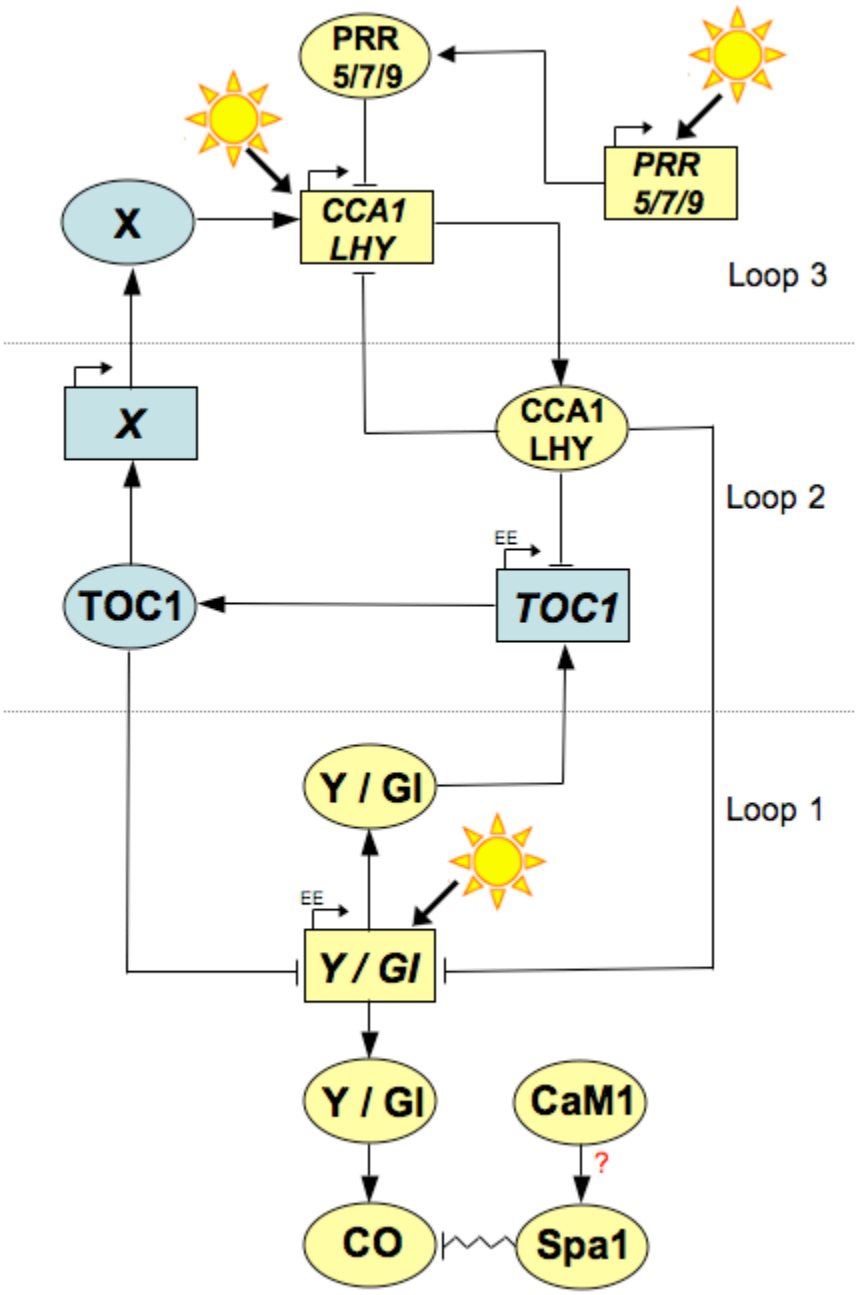

Figure 7.2: An extension of the three-loop model representing a possible interaction by which CaM may repress flowering in darkness in *A. thaliana*.

Plants showing a lesion for the putative CaM-binding protein SPA1 were found to flower on sucrose-supplemented media when grown in darkness. Chronic pharmacological CaM inhibition was found to partially mimic this phenotype in wild-type plants indicating that CaM acts to repress dark-flowering in *A. thaliana* via the activation of SPA1 which in turn leads to degradation of CO.

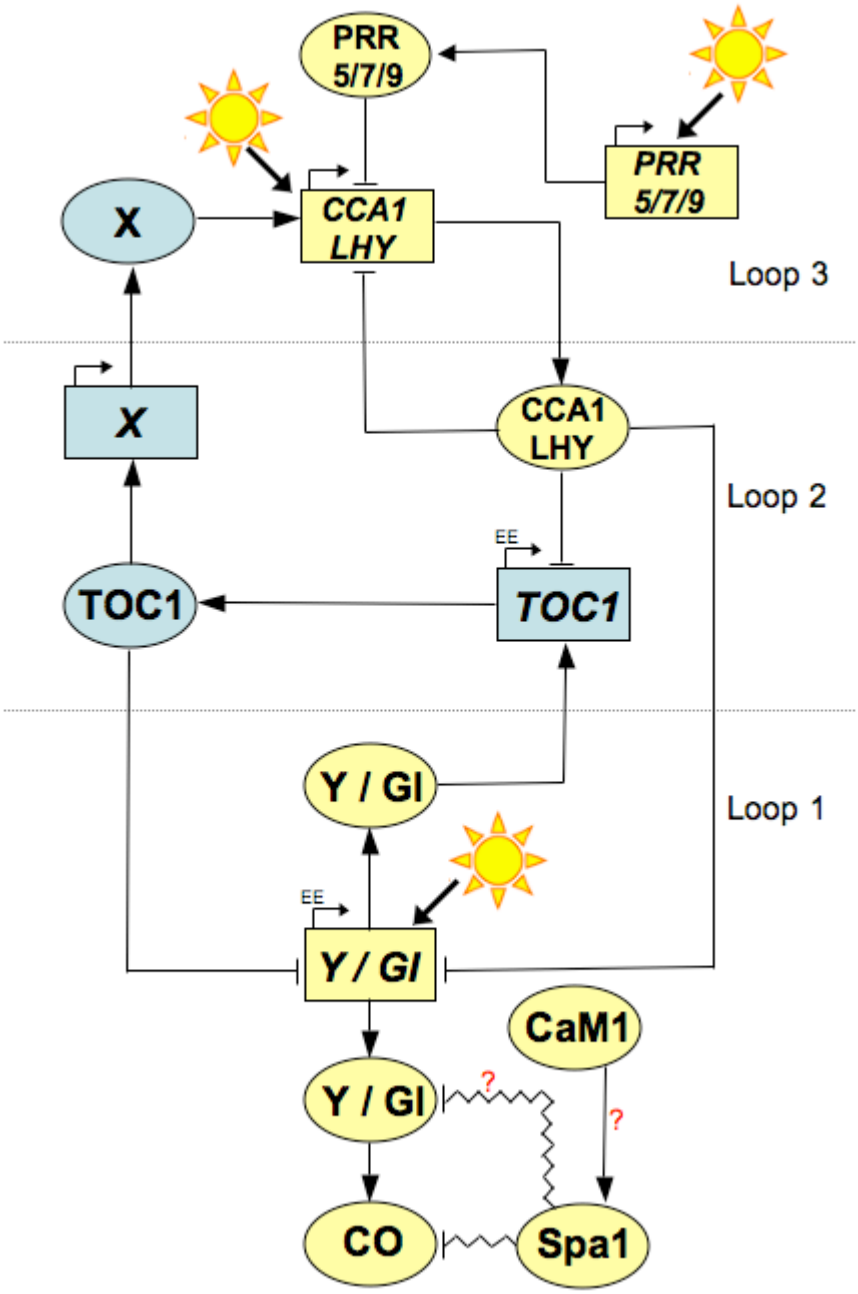

Figure 7.3: A possible mechanism by which CaM may influence both photoperiodic and dark flowering in *A. thaliana*.

In this model, CaM interacts with and activates SPA1. In a known interaction, SPA1 then targets CO for proteasomal degradation. In addition, SPA1 is also predicted to act in the targeted degradation of GI.

both the circadian clock and the photoperiodic flowering pathway via a singular reduction in SPA1 activity.

If, as the model predicts, SPA1 targets GI for degradation, reduced levels of SPA1 activity would logically lead to elevations in GI. Such an increase may, at first hand, appear to run counter to qRT-PCR evidence suggesting that inhibition of CaM mimics reduced levels of GI. However, there is a degree of evidence to suggest that transcription of, at least some, clock-regulated genes may be affected by elevations in GI in a manner similar to those seen in lines with *gi* lesions (Mizoguchi *et al*., 2005).

7.3 Summary and Future Work

This thesis has demonstrated that CaM mediates photoperiodic signalling in *A. thaliana*; most probably by interaction with GI or SPA1. Each of the models presented here (figures 7.1; 7.2; 7.3) serve to explain the developmental and transcriptional changes that occur following application of CaM inhibitors. However, further evidence will be required in order to distinguish which of these models is most representative of the full range of circadian and photoperiodic changes induced by inhibition of CaM.

Although qRT-PCR offered accurate quantitation of gene expression (Sherlock, 2005), it was necessary to limit the number of target genes studied. Given the data presented here, it would be of interest to quantify the expression of additional genes; with *GI* and *SPA1* being principle targets. Additionally, an unfortunate dichotomy currently exists as, whilst normal flowering occurs only when *A. thaliana* has reached sufficient maturity, studies involving expression of circadian clock-related genes have traditionally been undertaken using seedlings (Covington et al., 2001; Yanovsky & Kay, 2002; Salomé *et al*., 2008). One approach which would help to resolve this dichotomy as well as highly complementing the data presented in this thesis would be to generate a series of transgenic lines containing promoter::*luciferase* fusions for genes including *CHLOROPHYLL A/B BINDING PROTEIN* 2 (*CAB2)*, *CAM1*, *TOC1*, *SPA1*, *PHYTOCHROME A* (*PHYA*), *GI*, *CO* and *FT*. Such fusions would enable the promoter activity of target genes to be visualised in real-time across all life-stages and under a wide range of treatments and return data that would be time consuming and difficult to obtain using qRT-PCR.

Additionally, microarray assays of CaM inhibitor treated plants would allow whole-transcriptome modelling not possible using qRT-PCR. Thirdly, as both CaM and [Ca^{2+}_{cyt}] show circadian regulation and, as demonstrated in this thesis, CaM mediates photoperiodic signalling, it is conceivable that CaM may influence the form of circadian [Ca^{2+}_{cyt}] rhythms as well as decoding information contained within them. If this is the case, then application of CaM inhibitors may induce phase-delays in circadian [Ca^{2+}_{cyt}] rhythms similar to those observed in the expression patterns of *CAM1*, *TOC1* and *FT*. It would therefore be of interest to undertake aequorin-based [Ca^{2+}_{cyt}] quantification in whole plants in order to address this possibility.

The data generated by this series of experiments would ideally enable refinement and extension of the models presented here, allow the generation of experimentally testable predictions and further expand our understanding of the relationships between [Ca^{2+}_{cyt}], CaM, circadian-clock function and photoperiodic-flowering in *A. thaliana*.

BIBLIOGRAPHY

Ahmad, M., Jarillo, J. A.*, et al.* (1998a). Chimeric Proteins between CRY1 and CRY2 *Arabidopsis* Blue Light Photoreceptors Indicate Overlapping Functions and Varying Protein Stability. *Plant Cell,* **10**; (2): 197-208.

Ahmad, M., Jarillo, J. A.*, et al.* (1998b). The CRY1 Blue Light Photoreceptor of *Arabidopsis* Interacts with Phytochrome A *in vitro*. *Mol Cell,* **1**: 939-948.

Alabadí, D., Oyama, T.*, et al.* (2001). Reciprocal Regulation between TOC1 and LHY/CCA1 within the *Arabidopsis* Circadian Clock. *Science,* **293**; (5531): 880-883.

Ali, R., Ma, W.*, et al.* (2007). Death Don't Have No Mercy and Neither Does Calcium: *Arabidopsis* Cyclic Nucleotide Gated Channel2 and Innate Immunity. *Plant Cell Online,* **19**; (3): 1081-1095.

Allen, G. J., Kwak, J. M.*, et al.* (1999). Cameleon Calcium Indicator Reports Cytoplasmic Calcium Dynamics in *Arabidopsis* Guard Cells. *Plant J,* **19**: 735-747.

Allen, G. J., Chu, S. P.*, et al.* (2000). Alteration of Stimulus-Specific Guard Cell Calcium Oscillations and Stomatal Closing in *Arabidopsis det3* Mutant. *Science,* **289**: 2338-2342.

Allen, G. J., Chu, C. L.*, et al.* (2001). A Defined Range of Guard Cell Calcium Oscillation Parameters Encodes Stomatal Movements. *Nature,* **441**: 1053-1057.

Andretic, R. and Hirsch, J. (2002). Circadian Modulation of Dopamine Receptor Responsiveness in *Drosophila Melanogaster*. *Proc Natl Acad Sci U S A,* **97**: 1873-1878.

Andrew, C. D., Warwicker, J.*, et al.* (2002). Effect of Phosphorylation on Alpha-Helix Stability as a Function of Position. *Biochemistry,* **41**: 1897-1905.

Anthony, A. R. (2006). *Signal Transduction Regulating Floral Development*. The Molecular Biology and Biotechnology of Flowering. B. R. Jordan. Wallingford, CABI.

Antoine, A. F., Faure, J.*, et al.* (2000). A Calcium Influx Is Triggered and Propagates in the Zygote as a Wavefront During in Vitro Fertilisation of Flowering Plants. *Proc Natl Acad Sci U S A,* **97**: 10643-10648.

Aoyagi, M., Arvai, A. S.*, et al.* (2003). Structural Basis for Endothelial Nitric Oxide Synthase Binding to Calmodulin. *EMBO J,* **22**; (4): 766-775.

Aoyama, T. and Chua, N. H. (1997). A Glucocorticoid-Mediated Transcriptional Induction System in Transgenic Plants. *Plant J,* **11**; (3): 605-612.

Athari, A. and Jungermann, K. (1991). Unspecific Inhibition by the Calmodulin Antagonist Calmidazolium and the Intracellular Calcium Antagonist TMB-8 of the Actions of Sympathetic Hepatic Nerves and Noradrenaline on Glucose Balance and Flow in Perfused Rat Liver. *Biochem Int,* **23**: 203-213.

Babu, Y. S., Bugg, C. E.*, et al.* (1988). Structure of Calmodulin Refined at 2.2 Å Resolution. *J Mol Biol,* **204**: 191-204.

Baird, G. S., Zacharias, D. A.*, et al.* (1999). Circular Permutation and Receptor Insertion within Green Fluorescent Proteins. *Proc Natl Acad Sci U S A,* **96**: 11241-11246.

Barbieri, M. (2003). The Organic Codes. Cambridge, Cambridge University Press.

Baskin, T. I. and Bivens, N. J. (1995). Stimulation of Radial Expansion in *Arabidopsis* Roots by Inhibitors of Actomyosin and Vesicle Secretion but Not by Various Inhibitors of Metabolism. *Planta,* **197**; (3): 514-521.

Bengert, P. and Dandekar, T. (2003). A Software Tool-Box for Analysis of Regulatory RNA Elements. *Nucleic Acids Res,* **31**; (13): 3441-3445.

Berger, J. (2004). Regulation of Circadian Rhythms. *J Appl Biomed,* **2**: 131-140.

Björkman, T. and Leopold, A. C. (1987). Effect of Inhibitors of Auxin Transport and of Calmodulin on a Gravisensing-Dependent Current in Maize Roots. *Plant Physiol,* **84**: 847-850.

Bjorn, L. O. (2002). Photobiology. Amsterdam, Springer.

Block, G. D. (2006). *Drosophila* and Mammalian Circadian Systems: Similarities on the Surface, Some Differences at the Core. *Sleep Biol Rhyth,* **4**: 235-239.

Blázquez, M. (2005). Illuminating Flowers: Constans Induces Leafy Expression. *Bioessays,* **19**: 277-279.

Bognár, L. K., Hall, A.*, et al.* (1999). The Circadian Clock Controls the Expression Pattern of the Circadian Input Photoreceptor, Phytochrome B. *Proc Natl Acad Sci USA,* **96**; (25): 14652-14657.

Boss, P., Bastow, R. M.*, et al.* (2004). Multiple Pathways in the Decision to Flower: Enabling, Promoting, and Resetting. *The Plant CELL ONLINE,* **16**; (suppl_1): S18-S31.

Biden, T. J., Comte, M.*, et al.* (1987). Calcium-Calmodulin Stimulates Inositol 1,4,5-Trisphosphate Kinase Activity from Insulin-Secreting RINm5F Cells. *J Biol Chem,* **262**; (20): 9437-9440.

Block, M and Zucker, I. (1976). Circadian Rhythms of Rat Locomotor Activity after Lesions of the Midbrain Raphe Nuclei. *J. Comp. Physiol*, **109**; 235-247.

Bothwell, J. H., Brownlee, C.*, et al.* (2006). Biolistic Delivery of Ca2+ Dyes into Plant and Algal Cells. *Plant J,* **46**: 327-335.

Bothwell, J. H., Kisielewska, J.*, et al.* (2008). Ca2+ Signals Coordinate Zygotic Polarization and Cell Cycle Progression in the Brown Alga *Fucus Serratus*. *Development,* **135**: 2173-2181.

Boulos, Z., Macchi, M.*, et al.* (1996). Twilight Transitions Promote Circadian Entrainment to Lengthening Light-Dark Cycles. *Am J Physiol,* **271**: 813-818.

Boulos, Z., Macchi, M.*, et al.* (2002). Twilights Widen the Range of Photic Entrainment in Hamsters. *J Biol Rhythms,* **17**: 353-363.

Bowler, C., Yamagata, H.*, et al.* (1994). Phytochrome Signal Transduction Pathways Are Regulated by Reciprocal Control Mechanisms. *Genes Dev,* **8**; (18): 2188-2202.

Bradford, M. M. (1976). A Rapid and Sensitive Method for the Quantitation of Microgram Quantities of Protein Utilizing the Principle of Protein-Dye Binding. *Anal Biochem,* **72**: 248-254.

Brady, J. (1982). Biological Timekeping. London, Society for Experimental Biology.

Brewbaker, J. L. and Kwack, B. H. (1963). The Essential Role of Calcium Ion in Pollen Germination and Pollen Tube Growth. *Am J Bot,* **50**: 859-865.

Brunner, M. and Merrow, M. (2008). The Green Yeast Uses Its Plant-Like Clock to Regulate Its Animal-Like Tail. *Genes Dev,* **22**; (7): 825-831.

Butaye, K., Cammue, B.*, et al.* (2005). Approaches to Minimize Variation of Transgene Expression in Plants. *Mol Breeding,* **16**: 79-91.

Cameron, A. D., Volar, M.*, et al.* (2008). RNA Secondary Structure Regulates the Translation of sxy and Competence Development in *Haemophilus Influenzae*. *Nucleic Acids Res,* **36**; (1): 10-20.

Carre, I. A. (1995). Multiple DNA–Protein Interactions at a Circadian-Regulated Promoter Element. *Plant Cell,* **7**: 3039-3051.

Carre, I. A. (2002). ELF3: A Circadian Safeguard to Buffer Effects of Light *Trends Plant Sci.,* **7**: 4-6.

Casal, J., Luccioni, L.*, et al.* (2003). Light, Phytochrome Signalling and Photomorphogenesis in *Arabidopsis*. *Photochem. Photobiol. Sci.,* **2**; (6): 625.

Casal, J. (2007). GIGANTEA Regulates Phytochrome A Mediated Photomorphogenesis. *Plant Physiol,* **144**: 495-502.

Cerdán, P. D. and Chory, J. (2003). Regulation of Flowering Time by Light Quality. *Nature,* **423**; (6942): 881-885.

Chen, W. (2008). A Mathematical Analysis of Second Messenger Compartmentalization. *Phys Biol,* **5**: 46006-46012.

Clack, T., Mathews, S.*, et al.* (1994). The Phytochrome Apoprotein Family in *Arabidopsis* Is Encoded by Five Genes: The Sequences and Expression of PHYD and PHYE. *Plant Mol Biol,* **25**: 413-427.

Corbesier, L., Vincent, C.*, et al.* (2007). FT Protein Movement Contributes to Long-Distance Signaling in Floral Induction of *Arabidopsis*. *Science,* **316**; (5827): 1030-1033.

Correa, A. and Bell-Pederson, D. (2002). Distinct Signaling Pathways from the Circadian Clock Participate in Regulation of Rhythmic Conidiospore Development in *Neurospora Crassa*. *Eukaryotic Cell,* **1**: 273-280.

Correa-Aragunde, N., Graziano, M.*, et al.* (2006). Nitric Oxide Modulates the Expression of Cell Cycle Regulatory Genes During Lateral Root Formation in Tomato. *J Exp Bot,* **57**: 581-588.

Cousson, A. and Vavasseur, A. (1998). Two Potential Ca^{2+} -Dependent Transduction Pathways in Stomatal Closing in Response to Abscisic Acid. *Plant Physiol,* **36**: 257-262.

Daan, S. (1977). Tonic and Phasic Effects of Light in the Entrainment of Circadian Rhythms. *Ann NY Acad Sci,* **290**: 51-59.

Daan, S. (2000). Colin Pittendrigh, Jurgen Aschoff, and the Natural Entrainment of Circadian Systems. *J Biol Rhythms,* **15**: 195-207.

Daan, S., Gerkema, M. P.*, et al.* (2001). Circadian Timing: A Molecular Clock for All Seasons? Behavioural Performance. F. Zwarts, BCN**:** 150-151.

David, K. M., Armbruster, U.*, et al.* (2006). *Arabidopsis* GIGANTEA Protein Is Post-Transcriptionally Regulated by Light and Dark. *FEBS Lett,* **580**; (5): 1193-1197.

Davis, S. J. and Vierstra, R. D. (1996). Soluble Derivatives of Green Fluorescent Protein (GFP) for Use in *Arabidopsis thaliana*. *Weeds World,* **3**: 43-48.

Davis, S. J. and Vierstra, R. D. (1998). Soluble, Highly Fluorescent Variants of Green Fluorescent Protein (GFP) for Use in Higher Plants. *Plant Mol Biol,* **36**; (4): 521-528.

DeLano, W. L. (2002). The PyMOL User's Manual. Palo Alto, DeLano Scientific.

Della Rocca, G. J., Mukhin, Y. V.*, et al.* (1999). Serotonin 5-HT1A Receptor-Mediated Erk Activation Requires Calcium/Calmodulin-Dependent Receptor Endocytosis. *J Biol Chem,* **274**; (8): 4749-4753.

Demaurex, N. and Frieden, M. (2003). Measurements of the Free Luminal Er Ca^{2+} Concentration with Targeted “CaMeleon” Fluorescent Proteins. *Cell Calcium,* **34**: 109-119.

Demaurex, N. (2005). Calcium Measurements in Organelles with Ca^{2+}-Sensitive Fluorescent Proteins. *Cell Calcium,* **38**: 213-222.

Demidchik, V., Davenport, R. N.*, et al.* (2002). Non-Selective Cation Channels in Plants. *Annu Rev Plant Mol Biol,* **53**: 67-107.

Devlin, P. F. and Kay, S. A. (2000). Cryptochromes Are Required for Phytochrome Signaling to the Circadian Clock but Not for Rhythmicity. *Plant Cell,* **12**; (12): 2499-2510.

Di Capite, J., Ng, S. W.*, et al.* (2009). Decoding of Cytoplasmic Ca^{2+} Oscillations through the Spatial Signature Drives Gene Expression. *Curr Biol,* **19**: 853-858.

Dieter, P. and Marme, D. (1983). The Effect of Calmodulin and Far-Red Light on the Kinetic Properties of the Mitochondrial and Microsomal Calcium-Ion Transport System from Corn *Planta,* **159**: 277-281.

Dodd, A., Love, J.*, et al.* (2005a). The Plant Clock Shows Its Metal: Circadian Regulation of Cytosolic Free Ca^{2+}. *Trends Plant Sci,* **10**; (1): 15-21.

Dodd, A. N., Salathia, N.*, et al.* (2005b). Plant Circadian Clocks Increase Photosynthesis, Growth, Survival, and Competitive Advantage. *Science,* **309**; (5734): 630-633.

Dodd, A. N., Gardner, M. J.*, et al.* (2007). The *Arabidopsis* Circadian Clock Incorporates a CADPR-Based Feedback Loop. *Science,* **318**: 1789-1791.

Edwards, K. D., Lynn, J. R.*, et al.* (2005). Natural Allelic Variation in the Temperature-Compensation Mechanisms of the *Arabidopsis thaliana* Circadian Clock. *Genetics,* **170**; (1): 387-400.

Elvin, M. (2005). The PAS/LOV Protein Vivid Supports a Rapidly Dampened Daytime Oscillator That Facilitates Entrainment of the *Neurospora* Circadian Clock. *Genes Dev,* **19**; (21): 2593-2605.

Endo, M., Nakamura, S.*, et al.* (2005). Phytochrome B in the Mesophyll Delays Flowering by Suppressing Flowering Locus T Expression in *Arabidopsis* Vascular Bundles. *Plant Cell,* **17**; (7): 1941-1952.

Endo, M. (2006). Calcium Ion as a Second Messenger with Special Reference to Excitation-Contraction Coupling. *Plant Cell,* **11**: 691-706.

Endo, T., Tanaka, T.*, et al.* (1981). Calcium-Dependent Affinity Chromatography of S-100 and Calmodulin on Calmodulin Antagonist-Coupled Sepharose. *J Biol Chem,* **256**; (23): 12485-12489.

Fankhauser, C. and Staiger, D. (2002). Photoreceptors in *Arabidopsis thaliana*: Light Perception, Signal Transduction and Entrainment of the Endogenous Clock. *Planta,* **216**; (1): 1-16.

Franklin-Tong, V. E., Droback, B. K.*, et al.* (1996). Growth of Pollen Tubes of Papaver Rhoeas Is Regulated by a Slow-Moving Calcium Wave Propagated by Inositol 1,4,5-Trisphosphate. *Plant Cell,* **8**: 1305-1321.

Friedman, H., Goldschmidt, E. E.*, et al.* (1989). Involvement of Calcium in the Photoperiodic Flower Induction Process of *Pharbitis nil*. *Plant Physiol,* **89**; (2): 530-534.

Gaboriaud, C., Bissery, V.*, et al.* (1987). Hydrophobic Cluster Analysis: An Efficient New Way to Compare and Analyse Amino Acid Sequences. *FEBS Lett,* **224**; (1): 149-155.

Gardner, M. J., Hubbard, K. E.*, et al.* (2006). How Plants Tell the Time. *Biochem J,* **397**: 15-24.

Garner, W. W. and Allard, H. A. (1920). Effect of the Relative Length of Day an Night and Other Factors of the Environment on Growth and Reproduction in Plants. *J. Agric. Res.,* **18**: 553-606.

Garofalo, R. S., Gilligan, D. M.*, et al.* (1983). Calmodulin Antagonists Inhibit Secretion in Paramecium. *J Cell Biol,* **96**; (4): 1072-1081.

Geddes, C. D. (2005). Advanced Concepts in Fluorescence Sensing. New York, Springer Science.

Geisler, M., Axelsen, K. B.*, et al.* (2000). Molecular Aspects of Higher Plant P-Type Ca^{2+}-ATPases. *Biochim Biophys Acta,* **2**: 52-78.

Gentile, F., Balì, E., *et al.* (1997). Sensitivity and Applications of the Nondenaturing Staining of Proteins on Polyvinylidene Difluoride Membranes with Amido Black 10b in Water Followed by Destaining in Water. *Anal Biochem,* **245**; (2): 260-262.

Gilroy, S., Read, N., *et al.* (1990). Decoding of Cytoplasmic Ca^{2+} Oscillations through the Spatial Signature Drives Gene Expression. *Nature,* **343**: 769-771.

Gilroy, S., Bethke, P., *et al.* (1993). Calcium Homeostasis in Plants *J Cell Sci,* **106**: 453-462.

Gomez, L. A. and Simon, E. (1995). Circadian Rhythm of Robinia Pseudoacacia Leaflet Movements: Role of Calcium and Phytochrome. *Photochem Photobiol Sci,* **61**: 210-215.

Gonzalez-Daros, F., Carrasco-Luna, J., *et al.* (1993). Effects of Calmodulin Antagonists on Auxin-Stimulated Proton Extrusion in Avena Sativa Coleoptile Segments. *Physiol Plantarum,* **87**: 68-76.

Goosey, L., Palecanda, L., *et al.* (1997). Differential Patterns of Expression of the *Arabidopsis* PHYB, PHYD, and PHYE Phytochrome Genes. *Plant Physiol,* **115**; (3): 959-969.

Grewal, S. I. S. and Moazed, D. (2003). Heterochromatin and Epigenetic Control of Gene Expression. *Science,* **301**: 798-802.

Guse, A. H. and Lee, C. H. (2008). Naadp: A Universal Ca^{2+} Trigger. *Sci Signal,* **4**: 10.

Halberg, F. (1959). Physiologic 24 Hour Periodicity; General and Procedural Considerations with Reference to the Adrenal Cycle. *Z Vitam Homl Fermentforsch,* **10**: 225-296.

Hall, A. and Mcwatters, H. G. (2006). Endogenous Plant Rhythms. London, Wiley.

Hardie, G. (1991). Biochemical Messengers: Hormones, Neurotransmitters and Growth Factors. Amsterdam, Springer.

Harmer, S. L., Hogenesch, J. B., *et al.* (2000). Orchestrated Transcription of Key Pathways in *Arabidopsis* by the Circadian Clock. *Science,* **290**; (5499): 2110-2113.

Hartmann, K. M. (1966). A General Hypothesis to Interpret 'High Energy Phenomena' of Photomorphogenesis on the Basis of Phytochrome. *Photochem Photobiol Sci.,* **5**: 349-366.

Hayama, R. and Coupland, G. (2003). Shedding Light on the Circadian Clock and the Photoperiodic Control of Flowering. *Curr Opin Plant Biol,* **6**: 13-19.

Heilbrunn, L. V. (1940). The Action of Calcium on Muscle Protoplasm. *Physiol Zool,* **13**: 88-94.

Helfrich-Forster, C. (2002). The Circadian System of *Drosophila Melanogaster* and Its Light Input Pathways. *Zoology,* **105**: 297-312.

Helfrich-Forster, C., Yoshii, T.*, et al.* (2007). The Lateral and Dorsal Neurons of Drosophila Melanogaster: New Insights About Their Morphology and Function. Cold Spring Harbor Symposia on Quantitative Biology. Cold Spring Harbor Cold Spring Harbor Press.

Henderson, I. and Dean, C. (2004). Control of *Arabidopsis* Flowering: The Chill before the Bloom. *Development,* **131**; (16): 3829-3838.

Hepler, P. K. (2005). Calcium: A Central Regulator of Plant Growth and Development. *Plant Cell,* **17**: 2142-2155.

Hepworth, S., R., Valverde, F.*, et al.* (2002). Antagonistic Regulation of Flowering-Time Gene Soc1 by Constans and Flc Via Separate Promoter Motifs. *EMBO J,* **21**: 4327-4337.

Herrera, A. (1999). Effects of Photoperiod and Drought on the Induction of Crassulacean Acid Metabolism and the Reproduction of Plants of *Talinum triangulare*. *Can J Bot,* **77**: 404-409.

Hicks, K. A., Albertson, T. M.*, et al.* (2001). EARLY FLOWERING 3 Encodes a Novel Protein That Regulates Circadian Clock Function and Flowering in *Arabidopsis*. *Plant Cell,* **13**; (6): 1281-1292.

Hidaka, H., Yamaki, T.*, et al.* (1979). Selective Inhibitors of Ca^{2+}-Binding Modulator of Phosphodiesterase Produce Vascular Relaxation and Inhibit Actin-Myosin Interaction. *Mol Pharmacol,* **15**: 49-59.

Hidaka, H., Inagaki, M.*, et al.* (1981). Selective Inhibitors of Calmodulin - Dependent Phosphodiesterase and Other Enzymes. *Methods Enzymol*, 652-660.

Hidaka, H. and Tanaka, T. (1983). Naphthalenesulfonamides as Calmodulin Antagonists. *Methods Enzymol,* **102**: 185-194.

Hirschfeld, M., Tepperman, J. M.*, et al.* (1998). Coordination of Phytochrome Levels in *phyB* Mutants of *Arabidopsis* as Revealed by Apoprotein-Specific Monoclonal Antibodies. *Genetics,* **149**; (2): 523-535.

Hirschi, K. D. (1999). Expression of *Arabidopsis CAX1* in Tobacco: Altered Calcium Homeostasis and Increased Stress Sensitivity. *Plant Cell,* **11**: 2113-2122.

Hoecker, U. (1999). SPA1, a WD-Repeat Protein Specific to Phytochrome A Signal Transduction. *Science,* **284**; (5413): 496-499.

Hoeflich, K. P. and Ikura, M. (2002). Calmodulin in Action: Diversity in Target Recognition and Activation Mechanisms. *Cell,* **108**; (6): 739-742.

Hoeflich, K. P., Truong, K.*, et al.* (2009). Ca^{2+} as a Second Messenger: New Reporters for Calcium (Cameleons and Camgaroos) Cell Biology Assays: Essential Methods E. Julio, Elsevier.

Hofer, A. M. and Lefkimmiatis, K. (2007). Extracellular Calcium and cAMP: Second Messengers As "Third Messengers"? *Physiology,* **22**: 320-327.

Holdaway-Clarke, T. L., Feijo, J. A.*, et al.* (1997). Pollen Tube Growth and the Intracellular Cytosolic Calcium Gradient Oscillate in Phase While Extracellular Calcium Influx Is Delayed. *Plant Cell,* **9**: 1999-2010.

Hong, S. W., Jon, J. H.*, et al.* (1997). Identification of a Receptor-Like Protein Kinase Gene Rapidly Induced by Abscisic Acid, Dehydration, High Salt, and Cold Treatments in *Arabidopsis thaliana*. *Plant Physiol,* **113**; (4): 1203-1212.

Hua W, Zhang L, Liang S, Jones RL, Lu YT. A tobacco calcium/calmodulin-binding protein kinase functions as a negative regulator of flowering. *J Biol Chem.* 2004;279:31483–31494.

Hubbard, K. E., Hotta, C.*, et al.* (2007). *Circadian Rhythms in Stomata: Physiological and Molecular Aspects* Rhythms in Plants. Berlin, Springer**:** 157-177.

Hughes, T. A. and McElwaine, J. N. (2006). Mathematical and Biological Modelling of RNA Secondary Structure and Its Effects on Gene Expression. *Comp & Math. Meth in Med.,* **7**; (1): 37-43.

Hung, L. H. and Samudrala, R. (2003). Protinfo: Secondary and Tertiary Protein Structure Prediction. *Nucleic Acids Res,* **31**; (13): 3296-3299.

Hung, L. H., Ngan, S. C.*, et al.* (2005). Protinfo: New Algorithms for Enhanced Protein Structure Predictions. *Nucleic Acids Res,* **33**; (e): W77-80.

Huq, E., Tepperman, J. M.*, et al.* (2000). GIGANTEA Is a Nuclear Protein Involved in Phytochrome Signaling in *Arabidopsis*. *Proc Natl Acad Sci USA,* **97**; (17): 9789-9794.

Imaizumi, T. and Kay, S. A. (2006). Photoperiodic Control of Flowering: Not Only by Coincidence. *Trends Plant Sci,* **11**; (11): 550-558.

Ishikawa, M., Kiba, T.*, et al.* (2006). The *Arabidopsis* SPA1 Gene Is Required for Circadian Clock Function and Photoperiodic Flowering. *Plant J,* **46**; (5): 736-746.

Ito, H. and Hidaka, H. (1984). Direct Interaction of Calmodulin Antagonists with Ca^{2+}/Calmodulin-Dependent Cyclic Nucleotide Phosphodiesterase. *J Biochem,* **96**: 1721-1726.

Iwano, M., Entani, T.*, et al.* (2009). Fine-Tuning of the Cytoplasmic Ca^{2+} Concentration Is Essential for Pollen Tube Growth. *Plant Physiol,* **150**: 1322-1334.

Jarillo, J. A., Capel, J.*, et al.* (2001). An *Arabidopsis* Circadian Clock Component Interacts with Both CRY1 and PHYB. *Nature,* **410**; (6827): 487-490.

Jan, C. R. and Tseng, C. J. (2000a). Calmidazolium-Induced Rises in Cytosolic Calcium Concentrations in Madin Darby Canine Kidney Cells. *Toxicology Appl Pharmacol,* **162**; (2): 142-150.

Jan, C. R. and Tseng, C. J. (2000b). W-7 Induces [Ca^{2+}](I) Increases in Madin-Darby Canine Kidney (MDCK) Cells. *J Pharmacol Exp Ther,* **292**; (1): 358-365.

Jang, S., Marchal, V.*, et al.* (2008). *Arabidopsis* COP1 Shapes the Temporal Pattern of CO Accumulation Conferring a Photoperiodic Flowering Response. *EMBO J,* **27**; (8): 1277-1288.

Jaworski, K. (2003). Biochemical Evidence for a Calcium-Dependent Protein Kinase from Pharbitis Nil and Its Involvement in Photoperiodic Flower Induction. *Phytochemistry,* **62**; (7): 1047-1055.

Johnson, B. C. (1992). Nutrient Intake as a Time Signal for Circadian Rhythm. *Am Inst Nutr*: 1753-1759.

Johnson, C. H. (1990). An Atlas of Phase Response Curves for Circadian and Circatidal Rhythms. Nashvile, Vanderbilt University.

Johnson, C. H., Knight, M. R.*, et al.* (1995). Circadian Oscillations of Cytosolic and Chloroplastic Free Calcium in Plants. *Science,* **269**: 1863-1865.

Johnson, C. H. (1999). Forty Years of PRCs - What Have We Learned. *Chronobiol Int,* **16**: 711-743.

Johnson, C. H., Elliott, J. A.*, et al.* (2003). Entrainment of Circadian Programs. *Chronobiol Int,* **20**; (5): 741-774.

Johnson, C. H., Elliott, J. A.*, et al.* (2004). *Fundamental Properties of Circadian Rhythms*. Chronobiology. P. J. Decoursey. Sunderland, Sinauer Asociates, Inc.**:** 67-107.

Johnson, E., Bradley, M.*, et al.* (1994). Photoresponses of Light-Grown *phyA* Mutants of *Arabidopsis* (Phytochrome A Is Required for the Perception of Daylength Extensions). *Plant Physiol,* **105**; (1): 141-149.

Jung, J., Seo, Y.*, et al.* (2007). The GIGANTEA-Regulated MicroRNA172 Mediates Photoperiodic Flowering Independent of CONSTANS in *Arabidopsis*. *Plant Cell Online,* **19**; (9): 2736-2748.

Kamada, T. and Kinoshita, H. (1943). Disturbances Initiated from the Naked Surface of Muscle Protoplasm. *Jpn J Zool,* **10**: 469-493.

Kangasjärvi, S., Nurmi, M.*, et al.* (2009). Cell-Specific Mechanisms and Systemic Signalling as Emerging Themes in Light Acclimation of C3 Plants. *Plant, Cell Environ,* (32): 1230-1240.

Kaplan, B., Davydov, O.*, et al.* (2006). Rapid Transcriptome Changes Induced by Cytosolic Ca^{2+} Transients Reveal ABRE-Related Sequences as Ca^{2+}-Responsive Cis Elements in *Arabidopsis*. *Plant Cell Online,* **18**; (10): 2733-2748.

Karagyozov, L., Godfrey, R.*, et al.* (2008). The Structure of the 5'-End of the Protein-Tyrosine Phosphatase PTPRJ mRNA Reveals a Novel Mechanism for Translation Attenuation. *Nucleic Acids Res,* **36**; (13): 4443-4453.

Kato, R., Arashida, M.*, et al.* (2003). Inhibitions of Growth and Lateral Branch Development by Calmodulin Antagonists in Hairy Roots of Lithospermum Erythrorhizon, *Atropa Belladonna* and *Daucus Carota Bull. Yamagata Univ Nat Sci,* **15**: 79-88.

Kawaguchi, R. and Bailey-Serres, J. (2005). mRNA Sequence Features That Contribute to Translational Regulation in *Arabidopsis*. *Nucleic Acids Res,* **33**; (3): 955-965.

Kawamura, M., Ito, S.*, et al.* (2008). The Function of the Clock-Associated Transcriptional Regulator CCA1 (Circadian Clock-Associated 1) in *Arabidopsis thaliana*. *Biosci. Biotechnol. Biochem.,* **72**; (5): 1307-1316.

Kiegle, E., Moore, C. A.*, et al.* (2000). Cell-Type-Specific Calcium Responses to Drought, Salt and Cold in the *Arabidopsis* Root. *Plant J,* **23**: 267-278.

Keith, C., Dipaola, M.*, et al.* (1983). Microinjection of Ca^{2+}-Calmodulin Causes a Localized Depolymerization of Microtubules. *J Cell Biol,* **97**; (6): 1918-1924.

Kendrick, R. E. (1994). Photomorphogenesis in Plants. Amsterdam, Springer.

Kiba, T., Henriques, R., *et al.* (2007). Targeted Degradation of PSEUDO-RESPONSE REGULATOR5 by an SCFZTL Complex Regulates Clock Function and Photomorphogenesis in *Arabidopsis thaliana*. *Plant Cell,* **19**; (8): 2516-2530.

Kim, J., Park, J., *et al.* (2005a). Phytochrome Phosphorylation in Plant Light Signaling. *Photochem Photobiol Sci,* **4**: 681-687.

Kim, W. Y., Hicks, K. A., *et al.* (2005b). Independent Roles for EARLY FLOWERING 3 and ZEITLUPE in the Control of Circadian Timing, Hypocotyl Length, and Flowering Time. *Plant Physiol,* **139**; (3): 1557-1569.

Kim, W., Fujiwara, S., *et al.* (2007). ZEITLUPE Is a Circadian Photoreceptor Stabilized by GIGANTEA in Blue Light. *Nature,* **449**; (7160): 356-360.

Knight, H. (1996). Cold Calcium Signaling in *Arabidopsis* Involves Two Cellular Pools and a Change in Calcium Signature after Acclimation. *Plant Cell Online,* **8**; (3): 489-503.

Knight, H., Trewavas, A., *et al.* (1997). Calcium Signaling in *Arabidopsis thaliana* Responding to Drought and Salinity. *Plant J,* **12**: 1067-107.

Knight, H., Brandt, S., *et al.* (1998). A History of Stress Alters Drought Calcium Signalling Pathways in *Arabidopsis*. *Plant J,* **16**: 681-687.

Knight, M. R., Campbell, A. K., *et al.* (1991). Transgenic Plant Aequorin Reports the Effects of Touch and Cold-Shock and Elicitors on Cytoplasmic Calcium. *Nature,* **352**: 524-526.

Krinke, O., Novotná, Z., *et al.* (2007). Inositol Trisphosphate Receptor in Higher Plants: Is It Real? *J Exp Bot,* **58**: 361-376.

Kuhlman, S. J., Mackey, S. R., *et al.* (2007). *Introductory Workshop: Chronobiology Concepts & Nomenclature*. 72nd Cold Spring Harbor Laboratories Symposium: Clocks & Rhythms, Cold Spring Harbor Laboratories, Cold Spring Harbor Laboratories Publications.

Kolosova, N., Gorenstein, N., Kish, C. M., Dudreva, N. (2001). Regulation of Circadian Methyl Benzoate Emission in Diurnally and Nocturnally Emitting Plants. *Plant cell*, **13**; 2333-2347.

Komeda, Y. (2004). Genetic Regulation of Time to Flower in *Arabidopsis thaliana*. *Annu. Rev. Plant. Biol.,* **55**; (1): 521-535.

Koornneef, M., Hanhart, C. J., *et al.* (1991). A Genetic and Physiological Analysis of Late Flowering Mutants in *Arabidopsis thaliana*. *Mol Gen Genet,* **229**: 57-66.

Koukkari, W. L. and Sothern, R. B. (2006). Introducing Biological Rhythms. Amsterdam, Springer.

Kurdyukov, S., Faust, A., *et al.* (2006). The Epidermis-Specific Extracellular Bodyguard Controls Cuticle Development and Morphogenesis in *Arabidops*is. *Am Soc Plant Biol,* **18**: 321-339.

Larkindale, J. and Knight, M. R. (2002). Protection against Heat Stress-Induced Oxidative Damage in *Arabidopsis* Involves Calcium, Abscisic Acid, Ethylene, and Salicylic Acid. *Plant Physiol,* **128**; (2): 682-695.

Laubinger, S. (2004). The SPA Quartet: A Family of WD-Repeat Proteins with a Central Role in Suppression of Photomorphogenesis in *Arabidopsis*. *Plant Cell Online,* **16**; (9): 2293-2306.

Laubinger, S., Marchal, V., *et al.* (2006). *Arabidopsis* SPA Proteins Regulate Photoperiodic Flowering and Interact with the Floral Inducer CONSTANS to Regulate Its Stability. *Development,* **133**; (16): 3213-3222.

Leckie, C. P., Mcainsh, M. R., *et al.* (1998). Visualizing Changes in Cytosolic-Free Ca^{2+} During the Response of Stomatal Guard Cells to Abscisic Acid. *Proc Natl Acad Sci U S A,* **95**: 15837-15842.

Li, J., Wang, D. Y., *et al.* (2004a). PPF1 Inhibits Programmed Cell Death in Apical Meristems of Both G2 Pea and Transgenic *Arabidopsis* Plants Possibly by Delaying Cytosolic Ca^{2+} Elevation. *Cell Calcium,* **35**; (1): 71-77.

Li, Y., Wang, G., *et al.* (2004b). The Parameters of Guard Cell Calcium Oscillation Encodes Stomatal Oscillation and Closure in Vicia Faba. *Plant Science,* **166**: 415-421.

Lin, J. H. and Rydqvist, B. (2000). Inhibition of Mechanotransducer Currents in Crayfish Sensory Neuron by Cgs 9343b, a Calmodulin Antagonist. *Eur J Pharmacol,* **397**; (1): 11-17.

Lin, R. and Wang, H. (2007). Targeting Proteins for Degradation by *Arabidopsis* COP1: Teamwork Is What Matters. *J Int Plant Biol,* **49**; (1): 35-42.

Liu, L., Zhang, Y., *et al.* (2008). COP1-Mediated Ubiquitination of CONSTANS Is Implicated in Cryptochrome Regulation of Flowering in *Arabidopsis*. *Plant Cell Online,* **20**; (2): 292-306.

Locke, J. C., Millar, A. J., *et al.* (2005a). Modelling Genetic Networks with Noisy and Varied Experimental Data: The Circadian Clock in *Arabidopsis thaliana*. *J Theor Biol,* **234**; (3): 383-393.

Locke, J. C., Southern, M.*, et al.* (2005b). Extension of a Genetic Network Model by Iterative Experimentation and Mathematical Analysis. *Mol Syst Biol,* **1**: 2005.0013.

Locke, J., Kozma-Bognár, L.*, et al.* (2006). Experimental Validation of a Predicted Feedback Loop in the Multi-Oscillator Clock of *Arabidopsis thaliana*. *Mol Syst Biol,* **2**: 59.

Love, J., Brownlee, C.*, et al.* (1997). Ca^{2+} and Calmodulin Dynamics During Photopolarization in *Fucus Serratus* Zygotes. *Plant Physiol,* **115**; (1): 249-261.

Love, J., Dodd, A. N.*, et al.* (2004). Circadian and Diurnal Calcium Oscillations Encode Photoperiodic Information in *Arabidopsis*. *Plant Cell,* **16**; (4): 956-966.

Lu, Y., Gehan, J. P.*, et al.* (2005). Daylength and Circadian Effects on Starch Degradation and Maltose Metabolism. *Plant Physiol,* **138**; (4): 2280-2291.

Maathuis, F. J. (2006). cGMP Modulates Gene Transcription and Cation Transport in *Arabidopsis* Roots. *Plant J.,* **45**: 700-711.

Mackey, S. R. (2007). Molecular Basis of Rhythms Generation 72nd Cold Spring Harbor Laboratories Symposium:

Clocks & Rhythms. Cold Spring Harbor Laboratories, Cold Spring Harbor Laboratories Publications.

MacRobbie, E. (2000). Aba Activates Multiple Ca^{2+} Fluxes in Stomatal Guard Cells, Triggering Vacuolar $K^+(Rb^+)$ Release. *Proc Natl Acad Sci U S A,* **97**: 12361-12368.

Makino, S., Matsushika, A.*, et al.* (2001). Light Response of the Circadian Waves of the APRR1/TOC1 Quintet: When Does the Quintet Start Singing Rhythmically in *Arabidopsis*? *Cell Physiol,* **42**: 334-339.

Malhó, R. (1999). Coding Information in Plant Cells: The Multiple Roles of Ca^{2+} as a Second Messenger. *Plant Biol,* **1**: 487-494.

Martin-Tryon, E. L., Kreps, J. A.*, et al.* (2007). GIGANTEA Acts in Blue Light Signaling and Has Biochemically Separable Roles in Circadian Clock and Flowering Time Regulation. *Plant Physiol,* **143**; (1): 473-486.

Martinez-Garcia, J. F., Huq, E., Quail, P. H. (2000). Direct Targeting of Light Signals to a Promoter Element-Bound Transcription Factor. *Science*, **288**; 859-863.

Más, P., Kim, W.*, et al.* (2003a). Targeted Degradation of TOC1 by ZTL Modulates Circadian Function in *Arabidopsis thaliana*. *Nature,* **426**; (6966): 567-570.

Mathews, S. and Sharrock, R. (1997). Phytochrome Gene Diversity. *Plant Cell Environ,* **20**: 666-671.

Means, A. R., Cruzalegui, F.*, et al.* (1991). A Novel Ca^{2+}/Calmodulin-Dependent Protein Kinase and a Male Germ Cell-Specific Calmodulin-Binding Protein Are Derived from the Same Gene. *Mol Cell Biol,* **11**; (8): 3960-3971.

McAinsh, M. R., Webb, A.*, et al.* (1995). Stimulus-Induced Oscillations in Guard Cell Cytosolic Free Calcium. *Plant Cell,* **7**: 1207-1219.

McClung, C. R., Salomé, P.*, et al.* (2002). The *Arabidopsis* Circadian System. *The Arabidopsis Book,* **15**; (1): 1.

McCormack, E. and Braam, J. (2003). Calmodulins and Related Potential Calcium Sensors of *Arabidopsis*. *New Phytol,* **159**; (3): 585-598.

McCormack, E., Tsai, Y. C.*, et al.* (2005). Handling Calcium Signaling: *Arabidopsis* CaMs and CMLs. *Trends Plant Sci,* **10**; (8): 383-389.

McGraw-Hill (2009). McGraw-Hill Concise Encyclopedia of Science and Technology. New York, McGraw Hill

McNellis, T. W., Von Arnim, A. G.*, et al.* (1994). Genetic and Molecular Analysis of an Allelic Series of *cop1* Mutants Suggests Functional Roles for the Multiple Protein Domains. *Plant Cell,* **6**; (4): 487-500.

Millar, A. J. and Kay, S. A. (1996). Integration of Circadian and Phototransduction Pathways in the Network Controlling CAB Gene Transcription in *Arabidopsis*. *Proc Natl Acad Sci USA,* **93**; (26): 15491-15496.

Mitsutake, S. and Igarashi, Y. (2005). Calmodulin Is Involved in the Ca^{2+}-Dependent Activation of Ceramide Kinase as a Calcium Sensor. *J Biol Chem,* **280**; (49): 40436-40441.

Miyamoto, Y. and Sancar, A. (1998). Vitamin B2-Based Blue-Light Photoreceptors in the Retinohypothalamic Tract as the Photoactive Pigments for Setting the Circadian Clock in Mammals. *Proc Natl Acad Sci USA,* **95**; (11): 6097-6102.

Miyawaki, A., Llopis, J.*, et al.* (1997). Fluorescent Indicators for Ca^{2+} Based on Green Fluorescent Proteins and Calmodulin. *Nature,* **388**; (882-7).

Mizoguchi, T., Wheatley, K.*, et al.* (2002). LHY and CCA1 Are Partially Redundant Genes Required to Maintain Circadian Rhythms in *Arabidopsis*. *Dev Cell,* **2**; (5): 629-641.

Mizoguchi, T., Wright, L.*, et al.* (2005). Distinct Roles of GIGANTEA in Promoting Flowering and Regulating Circadian Rhythms in *Arabidopsis*. *Plant Cell,* **17**; (8): 2255-2270.

Mockler, T. C., Guo, H.*, et al.* (1999). Antagonistic Actions of *Arabidopsis* Cryptochromes and Phytochrome B in the Regulation of Floral Induction. *Development,* **126**; (10): 2073-2082.

Moreau, R. A. (1987). Calcium-Binding Proteins in Fungi and Higher Plants. *J Dairy Sci,* **70**; (7): 1504-1512.

Morris Structure Coordinates. *Proteins,* **12**: 345-364., A. L., Hutchinson, E. G.*, et al.* (1992). Stereochemical Quality of Protein.

Murphy, A. J., Kemp, F.*,* Love, J., (2008). Surface Plasmon Resonance Characterization of Calspermin-Calmodulin Binding Kinetics. *Analytical Biochemistry,* **376**; 61-72.

Muto, S. and Hirosawa, T. (1987). Inhibition of Adventitious Root Growth in Tradescantia by Calmodulin Antagonists and Calcium Inhibitors. *Plant Cell Phys,* **28**: 1569-1574.

Nagai, T., Sawano, N. T.*, et al.* (2001). Circularly Permuted Green Fluorescent Proteins Engineered to Sense $Ca^{2+.}$ *Proc Natl Acad Sci U S A,* **98**: 3197-3202.

Nagata, T., Lizumi, S.*, et al.* (2004). Comparative Analysis of Plant and Animal Calcium Signal Transduction Element Using Plant Full-Length cDNA Data. *Mol Biol Evol,* **21**: 1855-1870.

Navazio, L., Bewell, M. A.*, et al.* (2000). Calcium Release from the Endoplasmic Reticulum of Higher Plants Elicited by the Nadp Metabolite Nicotinic Acid Adenine Dinucleotide Phosphate. *Proc Natl Acad Sci U S A,* **97**: 8693-8698.

Ng, C., McAinsh, M. R.*, et al.* (2003). Encoding Specificity in Plant Calcium Signalling: Hot-Spotting the Ups and Downs and Waves. *Ann Bot,* **92**: 477-485.

Nelson, M. R. and Chazin, W. J. (1998). An Interaction-Based Analysis of Calcium-Induced Conformational Changes in Ca^{2+} Sensor Proteins. *Protein Sci,* **7**; (2): 270-282.

Nemerow, G. R. and Cooper, N. R. (1984). Infection of B Lymphocytes by a Human Herpesvirus, Epstein-Barr Virus, Is Blocked by Calmodulin Antagonists. *Proc Natl Acad Sci USA,* **81**; (15): 4955-4959.

Nozue, K., Covington, M.*, et al.* (2007). Rhythmic Growth Explained by Coincidence between Internal and External Cues. *Nature,* **448**; (7151): 358-361.

Oda, A., Fujiwara, S.*, et al.* (2004). Antisense Suppression of the *Arabidopsis PIF3* Gene Does Not Affect Circadian Rhythms but Causes Early Flowering and Increases *FT* Expression. *FEBS Lett,* **557**; (1-3): 259-264.

O'Neil, K. T. and Degrado, W. F. (1990). How Calmodulin Binds Its Targets: Sequence Independent Recognition of Amphiphilic Alpha-Helices. *Trends Biochem Sci,* **15**: 59-64.

Ono, T. Slaughter, G. R.*, et al.* (1989). Molecular Cloning Sequence and Distribution of Rat Calspermin, a High Affinity Calmodulin-Binding Protein. *J Biol Chem,* **264**; (4): 2081-2087.

Osawa, M., Swindells, M. B.*, et al.* (1998). Solution Structure of Calmodulin-W-7 Complex: The Basis of Diversity in Molecular Recognition. *J Mol Biol,* **276**; (1): 165-176.

Osuna, L., Coursol, S.*, et al.* (2004). A Ca^{2+}-Dependent Protein Kinase with Characteristics of Protein Kinase C in Leaves and Mesophyll Cell Protoplasts from *Digitaria Sanguinalis*: Possible Involvement in the C_4-Phosphoenolpyruvate Carboxylase Phosphorylation Cascade. *Biochem Biophys Res Commun,* **314**; (2): 428-433.

Ouwerkerk, P. B., De Kam, R. J.*, et al.* (2001). Glucocorticoid-Inducible Gene Expression in Rice. *Planta,* **213**; (3): 370-378.

Park, D. H., Somers, D. E.*, et al.* (1999). Control of Circadian Rhythms and Photoperiodic Flowering by the *Arabidopsis* GIGANTEA Gene. *Science,* **285**; (5433): 1579-1582.

Park, H. Y., Kim, S. A.*, et al.* (2008). Conformational Changes of Calmodulin Upon Ca^{2+} Binding Studied with a Microfluidic Mixer. *Proc Natl Acad Sci USA,* **105**; (2): 542-547.

Parks, B. M., Hoecker, U.*, et al.* (2001). Light-Induced Growth Promotion by SPA1 Counteracts Phytochrome-Mediated Growth Inhibition During De-Etiolation. *Plant Physiol,* **126**; (3): 1291-1298.

Pei, Z. M., Ward, J.*, et al.* (1999). Magnesium Sensitizes Slow Vacuolar Channels to Physiological Cytosolic Calcium and Inhibits Fast Vacuolar Channels in Fava Bean Guard Cell Vacuoles. *Plant Physiol,* **121**: 977-986.

Persson, S., Wyatt, S. E.*, et al.* (2001). The Ca^{2+} Status of the Endoplasmic Reticulum Is Altered by Induction of Calreticulin Expression in Transgenic Plants. *Plant Physiol,* **126**; (3): 1092-1104.

Peterson, E. L. and Saunders, D. S. (1980). The Circadian Eclosion Rhythm in *Sarcophaga argyrostoma*: A Limit Cycle Representation of the Pacemaker. *J Theor Biol,* **86**: 265-277.

Pfaffl, M. W., Horgan, G. W.*, et al.* (2002) Relative Expression Software Tool (REST) for Group-Wise Comparison and Statistical Analysis of Relative Expression Results in Real-Time PCR. Nucleic Acids Res **30**, e36

Pittendrigh, C. S. (1954). On Temperature Independence in the Clock System Controlling Emergence Time in *Drosophila*. *Proc Natl Acad Sci U S A,* **40**: 1018-1029.

Pittendrigh, C. S. and Minnis, D. H. (1964). The Entrainment of Circadian Oscillations by Light and Their Role as Photperiodic Clocks. *Am Nat,* **118**: 261-285.

Pittendrigh, C. S. and Daan, S. (1976a). A Functional Analysis of Circadian Pacemakers in Nocturnal Rodents. IV. Entrainment: Pacemaker as Clock. *J Comp Physiol,* **106**: 291-331.

Pittendrigh, C. S. and Daan, S. (1976b). A Functional Analysis of Circadian Pacemakers in Nocturnal Rodents. V. Pacemaker Structure: A Clock for All Seasons. *J Comp Physiol,* **106**: 333-355.

Pittendrigh, C. S. (1981). *Circadian Systems: Entrainment*. Handbook of Behavioral Neurobiology. J. Aschoff. New York, Plenum Press**:** 95-124.

Plieth, C. (2001). Plant Calcium Signaling and Monitoring: Pros and Cons and Recent Experimental Approaches. *Protoplasma,* **218**; (1-2): 1-23.

Polisensky, D. H. and Braam, J. (1996). Cold-Shock Regulation of the *Arabidopsis* TCH Genes and the Effects of Modulating Intracellular Calcium Levels. *Plant Physiol,* **111**; (4): 1271-1279.

Poovaiah, B. W., McFadden, J. J.*, et al.* (1987). The Role of Calcium Ions in Gravity Signal Perception and Transduction. *Physiol Plant,* **71**: 401-407.

Popescu, S. C., Popescu, G. V.*, et al.* (2007). Differential Binding of Calmodulin-Related Proteins to Their Targets Revealed through High-Density *Arabidopsis* Protein Microarrays. *Proc Natl Acad Sci USA,* **104**; (11): 4730-4735.

Provenzano, M. and Mocellin, S. (2007). Complementary Techniques: Validation of Gene Expression Data by Quantitative Real Time Pcr. *Adv Exp Med Biol,* **593**: 66-73.

Putterill, J., Robson, F., *et al.* (1995). The CONSTANS Gene of *Arabidopsis* Promotes Flowering and Encodes a Protein Showing Similarities to Zinc Finger Transcription Factors *Cell,* **80**: 847-857.

Putterill, J., Laurie, R., *et al.* (2004). It's Time to Flower: The Genetic Control of Flowering Time. *Bioessays,* **26**; (4): 363-373.

Quail, P. H., Boylan, M. T., *et al.* (1995). Phytochromes: Photosensory Perception and Signal Transduction. *Science,* **268**: 675-680.

Rashid, A. (2004). Modeling the Mutational Effects on Calmodulin Structure: Prediction of Alteration in the Amino Acid Interactions. *Biochem Biophys Res Comm,* **317**; (2): 363-369.

Rea, E., Di Monte, G., *et al.* (1995). Inhibition of Root Growth by Spermidine Is Not Due to Enhanced Production of Ethylene. *Plant Sci,* **108**: 121-124.

Reed, J. W. (1999). Phytochromes Are Pr-Ipatetic Kinases. *Curr Opin Plant Biol,* **2**: 393-397.

Rhoads, A. R. and Friedberg, F. (1997). Sequence Motifs for Calmodulin Recognition. *FASEB J,* **11**; (5): 331-340.

Rieger, D., Fraunholz, C., *et al.* (2007). The Fruit Fly Drosophila Melanogaster Favors Dim Light and Times Its Activity Peaks to Early Dawn and Late Dusk. *J Biol Rhythm,* **22**: 387-399.

Robertson, F., Briggs, H. M., *et al.* (2007). Identification of Regulators and Targets of Circadian Calcium Targets. Soc Exp Biol. Glasgow, Elsevier.

Roenneberg, T. and Merrow, M. (2002). “What Watch?... Such Much!” Complexity and Evolution of Circadian Clocks. *Cell Tiss Res,* **309**: 3-9.

Roenneberg, T. and Merrow, M. (2005). Circadian Clocks - the Fall and Rise of Physiology. *Nar Rev Mol Cell Biol,* **6**: 965-971.

Rushton, H. and Knight, H. (2006). An Unbiased Approach to the Question of Specificity in Calcium Signalling Society for Experimental Biology Annual Main Meeting Canterbury, SEB.

Sachs, M. M. and Ho, T. H. D. (1986). Alteration of Gene Expression During Environmental Stress in Plants. *Annu Rev Plant Physiol,* **37**: 363-376.

Sai, J. and Johnson, C. H. (2002). Dark-Stimulated Calcium Ion Fluxes in the Chloroplast Stroma and Cytosol. *Plant Cell,* **14**; (6): 1279-1291.

Saijo, Y., Zhu, D., *et al.* (2008). *Arabidopsis* COP1/SPA1 Complex and FHY1/FHY3 Associate with Distinct Phosphorylated Forms of Phytochrome a in Balancing Light Signaling. *Mol Cell,* **31**; (4): 607-613.

Salinovich, O. and Montelaro, R. C. (1986). Reversible Staining and Peptide Mapping of Proteins Transferred to Nitrocellulose after Separation by Sodium Dodecylsulfate-Polyacrylamide Gel Electrophoresis. *Anal Biochem,* **156**: 341-347.

Salomé, P. A., Xie, Q.*, et al.* (2008). Circadian Timekeeping During Early *Arabidopsis* Development. *PLANT PHYSIOLOGY,* **147**; (3): 1110-1125.

Sanders, D., Brownlee, C.*, et al.* (1999). Communicating with Calcium. *Plant Cell,* **11**: 691-706.

Sanders, D., Pelloux, J.*, et al.* (2002). Calcium at the Crossroads of Signaling. *Plant Cell,* **14**: 401-417.

Sawa, M., Nusinow, D.*, et al.* (2008). Fkf1 and Gigantea Complex Formation Is Required for Day-Length Measurement in *Arabidopsis*. *Science,* **318**; (5848): 261-265.

Schafer, E. and Bowler, C. (2002). Phytochrome-Mediated Photoperception and Signal Transduction in Higher Plants. *EMBO Rep,* **3**; (11): 1042-1048.

Scrase-Field, S. and Knight, M. R. (2003). Calcium: Just a Chemical Switch? *Current Opinion in Plant Biology,* **6**: 500-506.

Searle, I. and Coupland, G. (2004). Induction of Flowering by Seasonal Changes in Photoperiod. *EMBO J,* **23**; (6): 1217-1222.

Sengupta, P., Ruano, M.*, et al.* (2007). Membrane-Permeable Calmodulin Inhibitors (e.g. W-7/W-13) Bind to Membranes, Changing the Electrostatic Surface Potential: Dual Effect of W-13 on Epidermal Growth Factor Receptor Activation. *J Biol Chem,* **282**; (11): 8474-8486.

Seo, H. S., Watanabe, E.*, et al.* (2004). Photoreceptor Ubiquitination by COP1 E3 Ligase Desensitizes Phytochrome a Signaling. *Gene Dev,* **18**; (6): 617-622.

Sharma, V. K. (2003). Adaptive Significance of Circadian Clocks. *Chronobiol Int,* **20**: 901-919.

Sharma, V. K. and Chandrashekaran, M. K. (2005). Zeitgebers (Time Cues) for Biological Clocks. *Curr Sci,* **89**; (7): 1136-1146.

Sheremet, Y. A., Yemets, A. I.*, et al.* (2008). The Effect of Okadaic Acid on *Arabidopsis Thaliana* Root Morphology and Microtubule Organization in Its Cells. *Cyt Genet,* **43**: 1-8.

Sherlock, G. (2005). Of Fish and Chips. *Nat Methods,* **2**; (329-30).

Si, Y. and Olds-Clarke, P. (2000). Evidence for the Involvement of Calmodulin in Mouse Sperm Capacitation. *Biol Reprod,* **62**; (5): 1231-1239.

Simpson, G. (2003). Evolution of Flowering in Response to Day Length: Flipping the CONSTANS Switch. *Bioessays,* **25**; (9): 829-832.

Sinclair, W., Oliver, I.*, et al.* (1996). The Role of Calmodulin in the Gravitropic Response of the *Arabidopsis thaliana agr-3* Mutant. *Planta,* **199**; (3): 343-351.

Smart, J. L. and McCammon, J. A. (1999). Phosphorylation Stabilizes the N-Termini of Alpha-Helices. *Biopolymers,* **49**; (3): 225-233.

Snedden, W. A. and Fromm, H. (2001). Calmodulin as a Versatile Calcium Signal Transdudcer in Plants. *New Phytologist,* **151**: 35-66.

Somers, D. E., Devlin, P. F.*, et al.* (1998a). Phytochromes and Cryptochromes in the Entrainment of the *Arabidopsis* Circadian Clock. *Science,* **282**; (5393): 1488-1490.

Somers, D. E., Webb, A. A.*, et al.* (1998b). The Short-Period Mutant, *toc1-1*, Alters Circadian Clock Regulation of Multiple Outputs Throughout Development in *Arabidopsis thaliana. Development,* **125**; (3): 485-494.

Somers, D., Kim, W.*, et al.* (2004). The F-Box Protein ZEITLUPE Confers Dosage-Dependent Control on the Circadian Clock, Photomorphogenesis, and Flowering Time. *Plant Cell,* **16**; (3): 769-782.

Stokkan, K. A., Yamazaki, S.*, et al.* (2001). Entrainment of the Circadian Clock in the Liver by Feeding. *Science,* **291**: 490-493.

Strayer, C. A., Oyama, T.*, et al.* (2000). Cloning of the Arabidopsis Clock Gene TOC1, an Autoregulatory Response Regulator Homolog. *Science,* **289**: 768-771.

Suárez-López, P., Wheatley, K.*, et al.* (2001). CONSTANS Mediates between the Circadian Clock and the Control of Flowering in *Arabidopsis*. *Nature,* **410**; (6832): 1116-1120.

Sullivan, M., Rubisco Crossreactivity, Available at http://www.bio.net/bionet/mm/methods/2007-July/102355.html, (2007).

Sun, Z. and Means, A. R. (1995). An Intron Facilitates Activation of the Calspermin Gene by the Testis-Specific Transcription Factor Crem Tau. *J Biol Chem,* **270**; (36): 20962-20967.

Suzuki, S., Katagiri, S.*, et al.* (1996). Mutants with Altered Sensitivity to a Calmodulin Antagonist Affect the Circadian Clock in *Neurospora Crassa*. *Genetics,* **143**: 1175-1180.

Swade, R. H. (1969). Circadian Rhythms in Fluctuating Light Cycles: Toward a New Model of Entrainment. *J Theor Biol,* **24**: 227-239.

Tanaka, T., Ohmura, T.*, et al.* (1982). Two Types of Calcium-Dependent Protein Phosphorylations Modulated by Calmodulin Antagonists.

Tang, W. and Newton, R. J. (2004). Regulated Gene Expression by Glucocorticoids in Cultured Virginia Pine (*Pinus virginiana Mill*.) Cells. *J Exp Bot,* **55**: 1499-1508.

Thain, S., Hall, A.*, et al.* (2000). Functional Independence of Circadian Clocks That Regulate Plant Gene Expression. *Curr Biol,* **10**: 951-956.

Thain, S. (2004). Circadian Rhythms of Ethylene Emission in *Arabidopsis*. *Plant Physiol,* **136**; (3): 3751-3761.

Thion, L., Mazars, C.*, et al.* (1998). Plasma Membrane Depolarization-Activated Calcium Channels, Stimulated by Microtubule-Depolymerizing Drugs in Wild-Type *Arabidopsis thaliana* Protoplasts, Display Constitutively Large Activities and a Longer Half-Life in *ton2* Mutant Cells Affected in the Organization of Cortical Microtubules. *Plant J,* **13**: 603-610.

Tóth, R., Kevei, E.*, et al.* (2001). Circadian Clock-Regulated Expression of Phytochrome and Cryptochrome Genes in Arabidopsis. *Plant Physiol,* **127**; (4): 1607-1616.

Townley, H. (2002). Calmodulin as a Potential Negative Regulator of *Arabidopsis COR* Gene Expression. *Plant Physiol,* **128**; (4): 1169-1172.

Trewavas, A. and Malho, R. (1998). Ca^{2+} Signalling in Plant Cells: The Big Network! *Curr Opin Plant Biol,* **1**: 428-433.

Tseng, T. S., Salomé, P. A.*, et al.* (2004). Spindly and GIGANTEA Interact and Act in *Arabidopsis thaliana* Pathways Involved in Light Responses, Flowering, and Rhythms in Cotyledon Movements. *Plant Cell,* **16**; (6): 1550-1563.

Tuteja, N. and Mahajan, S. (2007). Calcium Signaling Network in Plants an Overview. *Plant Signal Behav,* **2**: 79-85.

Ueda, H. (2006). Systems Biology Flowering in the Plant Clock Field. *Mol Syst Biol,* **2**: 60.

Valverde, F., Mouradov, A.*, et al.* (2004). Photoreceptor Regulation of CONSTANS Protein in Photoperiodic Flowering. *Science,* **303**; (5660): 1003-1006.

Valverde, F. V. (2006). Time to Flower, the Control of Flowering Time by Photoperiod. *MCFA Annals,* **4**.

Véry, A. and Davies, J. M. (2000). Hyperpolarization-Activated Calcium Channels at the Tip of *Arabidopsis* Root Hairs *PNAS,* **97**: 9801-9806.

Vetter, S. W. and LeClerc, E. (2001). Phosphorylation of Serine Residues Affects the Conformation of the Calmodulin Binding Domain of Human Protein 4.1. *Eur J Biochem,* **268**; (15): 4292-4299.

Vos, J. W. and Hepler, P. K. (1998). Calmodulin Is Uniformaly Distributed During Cell Division in Living Stamen Hair Cells of *Tradescantia virginiana*. *Protoplasma,* **201**: 158-171.

Wang, L. and Wessler, S. R. (2001). Role of mRNA Secondary Structure in Translational Repression of the Maize Transcriptional Activator Lc. *Plant Physiol,* **125**; (3): 1380-1387.

Wang, D., Xu, Y.*, et al.* (2003). Transgenic Expression of a Putative Calcium Transporter Affects the Time of *Arabidopsis* Flowering. *Plant J,* **33**; (2): 285-292.

Wang, Z. Y. and Tobin, E. M. (1998). Constitutive Expression of the *CIRCADAN CLOCK ASSOCIATED1* (*CCA1*) Gene Disrupts Circadian Rhythms and Suppresses Its Own Expression. *Cell,* **93**; (7): 1207-1217.

Ward, J. and Schroeder, J. I. (1994). Calcium-Activated K^+ Channels and Calcium-Induced Calcium Release by Slow Vacuolar Ion Channels in Guard Cell Vacuoles Implicated in the Control of Stomatal Closure. *Plant Cell,* **6**: 669-683.

Watanabe, S., Okuno, S.*, et al.* (1996). Inactivation of Calmodulin-Dependent Protein Kinase IV by Autophosphorylation of Serine 332 within the Putative Calmodulin-Binding Domain. *J Biol Chem,* **271**; (12): 6903-6910.

Webb, A. A. (2003). The Physiology of Circadian Rhythms in Plants. *New Phytol,* **160**: 281-303.

Wetzel, D. M., Chen, L. A.*, et al.* (2004). Calcium-Mediated Protein Secretion Potentiates Motility in *Toxoplasma gondii*. *J Cell Sci,* **117**; (Pt 24): 5739-5748.

Williams, J. P., Blair, H. C.*, et al.* (1996). Regulation of Avian Osteoclastic H^+ - ATPase and Bone Resorption by Tamoxifen and Calmodulin Antagonists. Effects Independent of Steroid Receptors. *J Biol Chem,* **271**; (21): 12488-12495.

Whippo, C. W. and Hangarter, R. P. (2004). Phytochrome Modulation of Blue-Light-Induced Phototropism. *Plant, Cell Environ,* **27**: 1223-1228.

White, P. J. (1993). Characterization of High-Conductance, Voltage-Dependent Cation Channel from the Plasma Membrane of Rye Roots in Planar Lipid Bilayers. *Planta,* **191**: 541-551.

White, P. J. (2000). Calcium Channels in Higher Plants. *Biochim Biophys Acta,* **1465**: 171-189.

White, P. J. and Davenport, R. J. (2002). The Voltage-Independent Cation Channel in the Plasma Membrane of Wheat Roots Is Permeable to Divalent Cations and May Be Involved in Cytosolic Ca^{2+} Homeostasis. *Plant Physiol,* **130**: 1386-1395.

White, P. J. and Broadley, M. R. (2003). Calcium in Plants. *Ann Bot,* **92**; (4): 487-511.

Wigge, P. A., Kim, M. C.*, et al.* (2005). Integration of Spatial and Temporal Information During Floral Induction in *Arabidopsis*. *Science,* **309**; (5737): 1056-1059.

Williamson, R. E. and Ashley, C. C. (1982). Free Ca^{2+} and Cytoplasmic Streaming in the Alga Chara. *Nature,* **296**: 647-651.

Winter, D., Vinegar, B.*, et al.* (2007) An "Electronic Fluorescent Pictograph" Browser for Exploring and Analyzing Large-Scale Biological Data Sets. *PLoS ONE* **2**, 718.

Woelfle, M., Ouyang, Y. *et al.* (2004). The Adaptive Value of Circadian Clocks an Experimental Assessment in Cyanobacteria. *Curr Biol,* **14**; (16): 1481-1486.

Wood, N. T., Haley, A.*, et al.* (2001). The Calcium Rhythms of Different Cell Types Oscillate with Different Circadian Phases. *Plant Physiol,* **125**; (2): 787-796.

Woodland Hastings, J. (2006). *Resonance,* **11**: 81-86.

Wong, S. E., Bernacki, K.*, et al.* (2005). Competition between Intramolecular Hydrogen Bonds and Solvation in Phosphorylated Peptides: Simulations with Explicit and Implicit Solvent. *J Physical Chem B,* **109**; (11): 5249-5258.

Xu, X., Hotta, C.*, et al.* (2007). Distinct Light and Clock Modulation of Cytosolic Free Ca^{2+} Oscillations and Rhythmic CHLOROPHYLL A/B BINDING PROTEIN2 Promoter Activity in *Arabidopsis*. *Plant Cell Online,* **19**; (11): 3474-3490.

Xue, H.-W., Hosaka, K.*, et al.* (2004). Cloning of *Arabidopsis thaliana* Phosphatidylinositol Synthase and Functional Expression. *Plant Mol Biol,* **42**: 1573-1528.

Yakir, E., Hilman, D.*, et al.* (2007). Regulation of Output from the Plant Circadian Clock. *FEBS J,* **274**; (2): 335-345.

Yang, T. and Poovaiah, B. W. (2003). Calcium/Calmodulin-Mediated Signal Network in Plants. *Trends Plant Sci,* **8**; (10): 505-512.

Yanovsky, M. J. and Kay, S. A. (2002). Molecular Basis of Seasonal Time Measurement in *Arabidopsis*. *Nature,* **419**; (6904): 308-312.

Yap, K. L., Kim, J.*, et al.* (2000). Calmodulin Target Database. *J Struct Funct Genom,* **1**; (1): 8-14.

Yoshida, Y. and Hasunuma, K. (2003). Reactive Oxygen Species Affect Photomorphogenesis in *Neurospora Crassa*. *J Biochem,* **279**: 6986-6993.

Yu, H. J., Ito, T.*, et al.* (2004). Repression of Agamous-Like 24 Is a Crucial Step in Promoting Flower Development. *Nat Genet,* **36**: 157-161.

Zalejski, C., Zhang, Z.*, et al.* (2005). Diacylglycerol Pyrophosphate Is a Second Messenger of Abscisic Acid Signaling in *Arabidopsis thaliana* Suspension Cells. *Plant J,* **42**: 145-152.

Zeilinger, M. N., Farre, E.*, et al.* (2006). A Novel Computational Model of the Circadian Clock in *Arabidopsis* That Incorporates PRR7 and PRR9. *Mol Syst Biol,* **2**: 58.

Zhang, L. (2003). Calmodulin-Binding Protein Kinases in Plants. *Trends Plant Sci,* **8**; (3): 123-127.

Zielinski, R. E. (1998). Calmodulin and Calmodulin-Binding Proteins in Plants. *Annu Rev Plant Physiol Plant Mol Biol,* **49**: 697-725.

Zimmer, M. and Hofmann, F. (1987). Differentiation of the Drug-Binding Sites of Calmodulin. *Eur J Biochem,* **164**; (2): 411-420.

Zivkovic, B. (2009) Clock Tutorial #16: Photoperiodism - Models and Experimental Approaches. A Blog Around the Clock. http://scienceblogs.com/clock/2009/07/clock_tutorial_16_photoperiodi_3.php